Synthetic Scaffolds Based on Biodegradable, Functionalized Polyesters for Tissue Engineering Applications

Hajar Seyednejad

2012

The printing of this thesis was financially supported by:

Utrecht Institute for Pharmaceutical Sciences (UIPS)
J. E. Jurriaanse Stichting, Rotterdam, The Netherlands
Nederlandse vereniging voor Biomaterialen en Tissue Engineering (NBTE)

Synthetic scaffolds based on biodegradable, functionalized polyesters for tissue engineering applications

By: Hajar Seyednejad

ISBN: 978-90-39357347
Cover design and manuscript layout by Hajar Seyednejad
Back cover: Several steps of scaffolds preparation for tissue engineering applications; from synthesis to *in vivo*.
Printed by: GVO drukkers & vormgevers B.V. | Ponsen & Looijen

Synthetic scaffolds based on biodegradable, functionalized polyesters for tissue engineering applications

Synthetische scaffolds gebaseerd op biodegradeerbare gefunctionaliseerde polyesters voor TE toepassingen
(met een samenvatting in het Nederlands)

داربست‌های مصنوعی زیست تخریب پذیر بر پایه پلی استرهای عامل دار شده
جهت کاربرد در مهندسی بافت (همراه با چکیده فارسی)

Proefschrift

ter verkrijging van de graad van doctor aan de Universiteit Utrecht op gezag van de rector magnificus, prof. dr. G. J. der Zwaan, ingevolge het besluit van het college voor promoties in het openbaar te verdedigen op woensdag 7 maart 2012 des middags te 2.30 uur

door

Hajar Seyednejad
geboren op 28 juni 1981 te Tehran, Iran

Promotoren:	Prof. dr. ir. W. E. Hennink
	Prof. dr. W. J. A. Dhert
Co-promotoren:	Dr. ir. T. Vermonden
	Dr. C. F. van Nostrum

This thesis was (partly) accompanied with financial support from the Dutch Program for Tissue Engineering (DPTE) (project number 6731).

A man without **ambition** is dead.
A man with ambition but no **love** is dead.
A man with ambition and love for his blessings here on earth
is ever so alive.

Pearl Bailey
1918-1990

To my beloved family

Table of Contents

To engineer is to create:

The link between engineering and regeneration

"The reason why there is the word 'engineering' in the term 'tissue engineering' is not intuitively obvious. The majority of definitions of engineering invoke the use of scientific knowledge to solve practical problems and/or the systemic analysis of practical data to yield tangible end-products. Although not entirely unconnected, neither of these concepts is readily translated into the paradigms that are now represented by tissue engineering. Tissue engineering does have end products but the underlying science is far more related to cell, molecular and developmental biology, and to pharmacology, that to the physical sciences that normally underpin classical engineering. There is, however, another meaning of engineering, appreciated best when we consider that the origin of the term is the Latin 'ingenium', from which we can see that it is ingenuity, or creativeness, that is really at the heart of the subject."

David F. Williams
TRENDS in Biotechnology
2006, 24 (1), 4-8.

Chapter 1

General Introduction

1.1 Tissue engineering

Aging, disease, and trauma frequently lead to damage and/or degeneration of tissues and organs in the human body. Possible treatments to help patients suffering from organ or tissue failure are mainly based on transplanting tissue from one site to another in the same patient (an autograft) or from one individual to another (a transplant or an allograft)[1]. However, organ transplantation is limited by the number of available donors, risk of immune rejection, high processing costs, and donor site morbidity[2, 3]. These limitations lead thousands of patients to the long waiting lists to find a suitable organ donor, and unfortunately many of them die before a suitable organ becomes available. In order to find an alternative way to help these patients, the term "tissue engineering" (which is often interchangeably used with regenerative medicine) was introduced in 1993 by Langer and Vacanti[4] as "an interdisciplinary field that applies the principles of engineering and life sciences toward the development of biological substitutes that restore, maintain, or improve tissue function". The clinical applications of tissue engineering (TE) are huge, with vast therapeutic potential in the ageing and lifestyle diseases prevalent in Western populations- such as heart disease, diabetes, and osteoarthritis- as well as other major afflictions, including spinal cord injury and disfigurement[5]. The classical process of tissue engineering starts with harvesting the relevant cells, and ends with preparation of a hybrid graft for implantation into the host to allow for tissue regeneration. The pathway between these two points can follow different routes but essentially consists of three major elements: cells, biomaterials, and bioactive molecules. TE typically involves seeding of cells into some form of supporting structural device- termed a scaffold- and allowing the cells to remodel the scaffold into natural tissue, before implanting it into a patient's body (Figure 1, traditional TE). The cells can be triggered to do this by molecular signals provided by growth factors, or other bioactive molecules that are loaded into the scaffold. In some cases, the scaffolds are seeded with the cells of patient shortly before implantation, and the regeneration relies on the subsequent deposition of an extracellular matrix (ECM) inside the body utilizing a compartment of the host's own body as a bioreactor[5] (Figure1, scaffold seeded with cells at the time of implantation). In some other cases, the scaffold is prepared without cells and implanted inside the body as such (Figure 1, acellular scaffold). Whatever approach is taken, the scaffold is critical to the success of the implant and in several cases actively directs the behavior of the seeded and/or infiltrated cells within.

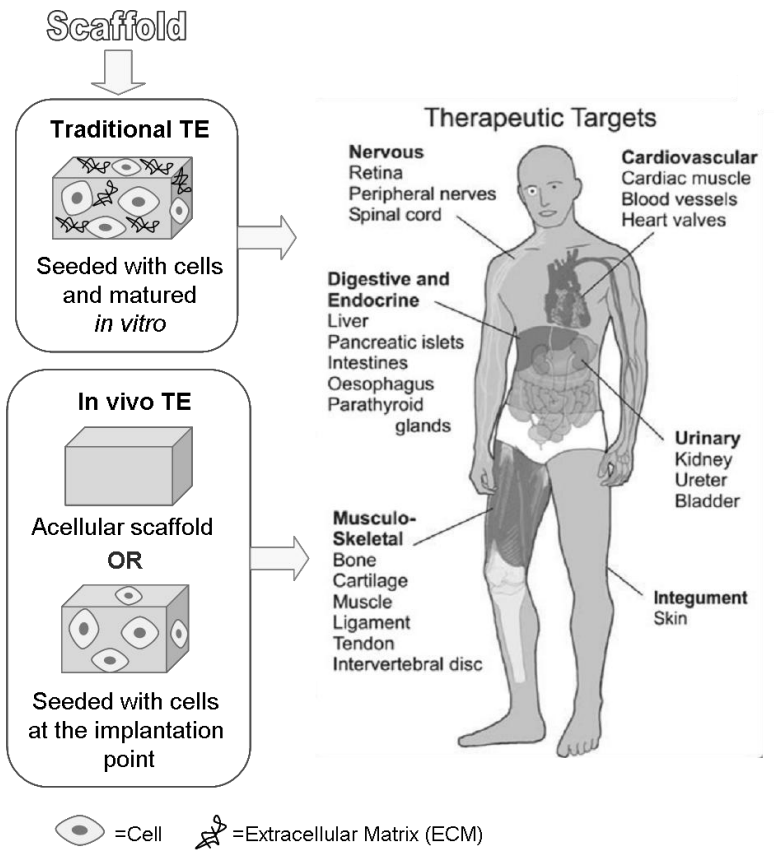

Fig.1. Tissue engineering approaches. In traditional TE, the scaffold is seeded with cells *in vitro*, and implanted in the body when a hybrid graft is formed. For *in vivo* TE, the scaffold is implanted in the body with/without cells. Reproduced from Ref.[5].

1.2 Scaffolds

A basic concept in tissue engineering is that the scaffold performs as a transient architecture and is 'foreign' to the natural environment. In other words, it ideally disappears once its function has been fulfilled, leaving behind a viable and functional biological system[6]. In the first consensus Conference of the European Society for Biomaterials (ESB) in 1976, a biomaterial was defined as a "nonviable material used in a medical device, intended to interact with biological systems"; however, the ESB's current definition is a "material intended to interact with biological systems to evaluate, treat, augment or replace any tissue, organ or function of the body"[1]. This subtle change in definition shows how the field of

biomaterials has evolved over the years, from the use of materials that are merely interacting with the body to the materials that actively modulate biological processes toward the goal of tissue regeneration. Three major classes of biomaterials which are generally used for the preparation of scaffolds can be distinguished: polymers, ceramics, and metals. Also hybrid systems (e.g., combination of polymer and ceramic) can be used. Broadly speaking, the main demands on scaffolds for TE applications are that they serve the bulk mechanical and structural requirements of the target tissue, and importantly, allow for tissue healing. In general, the biomechanical properties of the construct should match those of the surrounding tissue (e.g. relatively tough in bone, softer in pliable tissues). Last but not least, the main key elements of scaffolds are biocompatibility and biodegradation.

1.2.1 Biocompatibility of scaffolds

Biocompatibility is defined by Dr. David Williams as "the ability of a scaffold or matrix to perform as a substrate that will support the appropriate cellular activity, including the facilitation of molecular and mechanical signaling systems, in order to optimize tissue regeneration, without eliciting any undesirable local or systemic responses in the eventual host"[7]. In fact, the key to understand biocompatibility is the understanding of the mechanisms (chemical, biochemical, physiological, physical or other types) which become operative under the highly specific conditions associated with contact between biomaterials and tissues of the body and what are the consequences of these interactions[7]. Several natural as well as synthetic polymers with good biocompatibility are known and FDA approved for certain applications within the body and therefore frequently used for TE applications. However, there is a need for improving the physical/chemical properties of these polymers.

1.2.2 Biodegradability of scaffolds

The use of non-permanent scaffold materials that over time are completely replaced by natural extracellular matrix is an important theme in TE. The objective is to create a scaffold that can persist in a robust state for sufficient time to allow for the formation of new tissue, but that ultimately will degrade and be replaced by this tissue[5]. The most widely used synthetic degradable polymers are poly(α-hydroxy acids) such as poly(lactic acid) (PLA), poly(glycolic acid) (PGA), poly(ε-caprolactone) (PCL) and their copolymers. These aliphatic polyesters degrade by hydrolysis, eventually releasing water-soluble oligomers and monomers that feed

into natural metabolic pathways[8, 9]. These polymers have been particularly prevalent as they already had a range of medical applications (e.g. in degradable sutures, stents, wound dressings)[5] and have FDA approval for those applications. However, these polymers are hydrophobic and have consequently poor wettability characteristics resulting in poor cellular interaction and attachment[5]. The rate of hydrolytic degradation of ester linkages of the aliphatic polyesters is affected by a multitude of factors, such as the type of polyester used and the size of the device[10-12]. The degradation rate also depends on the glass transition temperature (T_g) and crystallinity of the polymeric material, because both factors have effect on the water access of the polymer matrix.

A high T_g is associated with relatively limited molecular motion and low free volume within the polymer matrix, meaning that water molecules have difficulties to penetrate into the material. Similarly, a high degree of crystallinity limits hydration because of the tight and ordered packing of polymer chains. Crystallinity is reduced by actions which disrupt packing, for instance inclusion of short side chains or random copolymerization. Further, degradation can be accelerated by blending with a more hydrophilic polymer which increases the water penetration and water-absorbing capacity of the polymer matrix[13, 14].

1.3 Preparation methods

The physical properties of scaffolds, as well as the polymer choice, are very relevant with respect to final application of the graft. The scaffold is meant to provide the appropriate chemical, physical, and mechanical properties required for cell survival and tissue formation[15]. Material chemistry together with processing route determine to a large extent the maximum functional properties that a scaffold can achieve as well as how cells interact with the scaffold[16]. Several requirements have been identified as crucial for the production of tissue engineering scaffolds[17]: the scaffold should (1) possess interconnecting pores of appropriate scale to favor tissue integration and vascularization, (2) be made from a material with controlled biodegradability and bioresorbability so that regenerated tissue will eventually replace the scaffold, (3) have appropriate surface chemistry to favor cellular attachment, proliferation, and differentiation, (4) possess adequate mechanical properties to match the intended site of implantation and handling, (5) should not induce any adverse response, and (6) be easily fabricated into a variety of shapes and sizes. Bearing these requirements in mind, several approaches have been employed to fabricate

scaffolds for TE applications that can be divided into conventional and advanced methods of scaffolds fabrication.

1.3.1 Conventional scaffold fabricating techniques

- Solvent casting/ particulate leaching (SCPL)

This is the oldest and still a commonly used technique to fabricate scaffolds. This technique is based on the principle that porogens (most commonly salt particles) are dispersed into a polymer solution and that after evaporation of the solvent, followed by solidification of the polymer, and dissolution of the porogens, a highly (for high volume fractions of salt particles) porous scaffold (also known as a foam) is created as depicted in Figure 2. This technique is characterized by its simple operation and adequate control over the pore size and the porosity is tailored by the particle size and the amount of added salt particles, respectively.

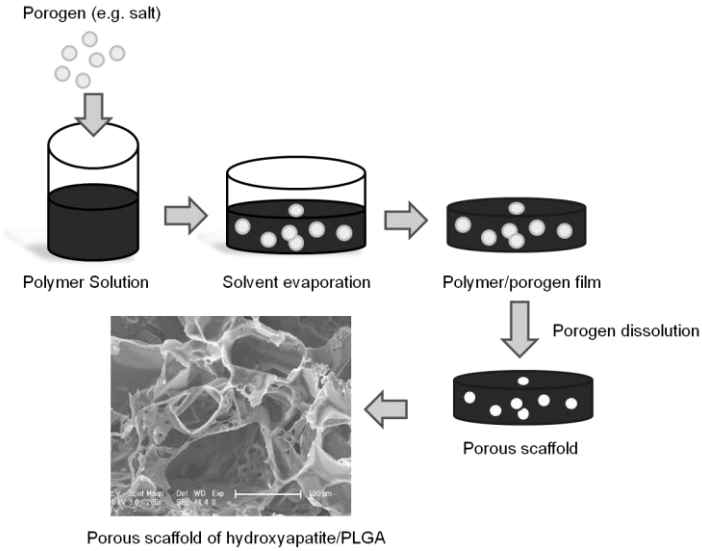

Fig.2. Schematic representation of solvent casting/particulate leaching (SCPL) method. The SEM image illustrates the morphology of a porous hydroxyapatite/PLGA scaffold obtained using this method[20].

However, the distribution of the salt particles is often not uniform within the polymer solution. This is because the density of the liquid polymer solution and the solid salt are substantially different, and the degree of direct contact between the salt particles is not well controlled. As a result, the interconnectivity of the

pores in the final scaffold can not be modulated well. Moreover, the polymer solution and the salt particles are mixed in such a way that salt particles tend to be wrapped completely by the polymer solution. These wrapped salt particles can not be easily leached out with water. Thus, most porous scaffolds prepared by SCPL method are limited to thickness of maximum 4 mm[18] and contain a porosity of up to 90% with a pore size ranging from 5 to 600 µm[19].

- **Melt molding**

Melt molding is another method that uses the principles of solvent casting and particulate leaching. A polymer powder is mixed with hydrated gelatin microspheres, placed into a Teflon mold and heated above the polymer glass transition temperature. PLGA is generally preferred over other biodegradable polyesters such as PLA or PGA because it can be processed at low temperatures. Elevated temperatures preclude the incorporation of bioactive molecules and may result in structural changes in gelatin that adversely affect its aqueous solubility. After heating, the composite is placed in water, which dissolves the water-soluble microspheres yielding a porous structure. This technique is similar to SCPL in that pore size and porosity are determined by the porogen diameter and concentration, respectively. Also, like other leaching methods, pores do not have uniform diameters and incomplete porogen removal is probable. In favor of the method, melt molding does avoid the use of (toxic) solvents.

- **Gas foaming**

This method to fabricate porous scaffolds was first introduced by Mooney et al[21]. In this technique, a foaming agent such as sodium bicarbonate is added into the polymer phase to generate an inert gas such as N_2 or CO_2 when exposed to acidic solutions[22]. A porous structure is formed when the dispersed particles are converted into a gas due to the exposure to an acidic aqueous solution. During the formation of the polymeric foam, however, the liquid phase tends to drain downwards while the gas tends to move upwards, which leads to the formation of an inhomogeneous foam with a non-porous bottom layer and highly porous top surface.

- Emulsification/ Freeze drying

Using this technique, first a polymer is dissolved into a suitable, water-immiscible organic solvent and then a small volume of water is added to the polymeric

solution and the two liquids are mixed in order to obtain a w/o emulsion (Figure 3). Before macroscopic phase separation occurs, the emulsion is cast into a mold and quickly frozen (i.e. by immersion into liquid nitrogen). The frozen emulsion is subsequently freeze-dried to remove the dispersed water and organic solvent, yielding a solidified, porous polymeric structure[23]. The pore sizes obtained with this method are relatively small and the porosity is often irregular.

- Phase separation

Phase separation is another means of scaffold processing designed with the intent of incorporating bioactive molecules. A liquid-liquid phase separation technique has been employed to produce foams with the potential for drug delivery[25, 26]. As an example, PLLA and solid naphthalene are mixed in a flask, heated, and stirred to obtain a homogenous solution. The solution is then poured or sprayed (using an atomizer) into a cooled mold resulting in the formation of a polymer-rich and a polymer-poor phase. Naphthalene is subsequently removed by vacuum drying. The foam morphology and pore distribution depend on the kinetics of phase separation. This technique creates scaffolds with a relatively uniform pore distribution with diameters of 50-100 µm and porosities up to 87% can be achieved depending on the polymer concentration in the solution. However, the use of organic solvents might have detrimental effects on cells.

- Electrospinning

As the primary role of the scaffolds is to serve as a temporary artificial matrix, it is useful to mimic certain characteristics of the native extracellular matrix (ECM) while designing a scaffold. Fabricating nanofibrous scaffolds with appropriate pore geometry via electrospinning method has gained wide attention in recent years[27]. Electrospinning is a straightforward, versatile, and cost-effective technique employing electrostatic forces to produce polymer fibers, ranging from a few microns to tens of nanometers in diameter (Figure 4). This technique was first introduced by Zelency[28] in the beginning of this century, but it was not developed for tissue-engineering applications at the time of invention. The uniqueness of this technique over other conventional methods is its ability to spin continuous nano-featured scaffolds with a large surface area-volume ratio and an interconnected porous geometry with spatial orientation. A basic apparatus for electrospinning consists of three essential elements: a spinneret, a fiber collector, and a high-voltage power supply. The spinneret is directly connected to a syringe, which acts as a reservoir for the polymer solution to be electrospun. This polymer

solution can be fed through the spinneret at a steady and controllable feed rate with the help of a syringe pump. The fiber collector is positioned right beneath the spinneret within an appropriate distance. Typically, high voltage is required for the conversion of polymer solution into an electrified polymer jet. This voltage (usually up to 30 kV) is applied across the spinneret and the ground metallic target (collector) during electrospinning. The scaffolds obtained using this method contain up to 90% porosity and the pore size is in range of 1-10 μm[19].

Bioactive scaffolds which can release biomolecules in a controlled manner and aim to induce proliferation and differentiation of seeded cells *in vitro.* It is also aimed that such scaffolds continue to release the growth factors once implanted *in vivo,* thereby, promoting tissue regeneration in the defect area[29]. Optimizing the electrospinning set-up can provide bioactive scaffolds by coaxial electrospinning of two solutions simultaneously through different feeding capillary channels in one needle. This type of scaffolds has gained wide attention recently as the core-shell structure of fibers preserves the bioactivity of loaded proteins[30].

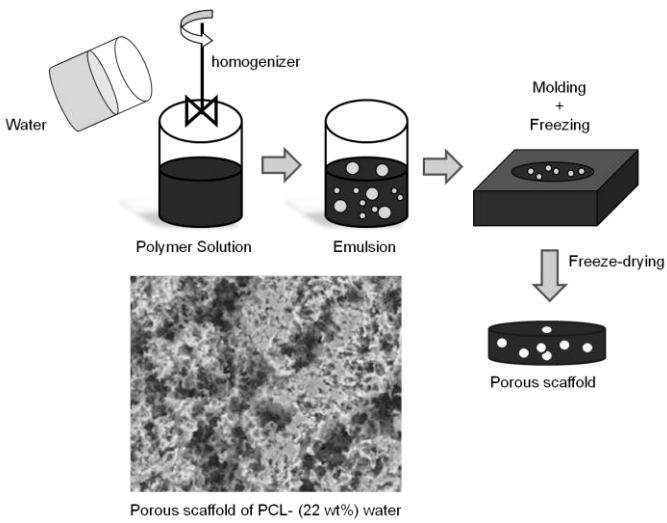

Fig.3. Schematic representation of emulsion/freeze drying technique. The SEM image illustrates the morphology of PCL scaffolds obtained using this method[24].

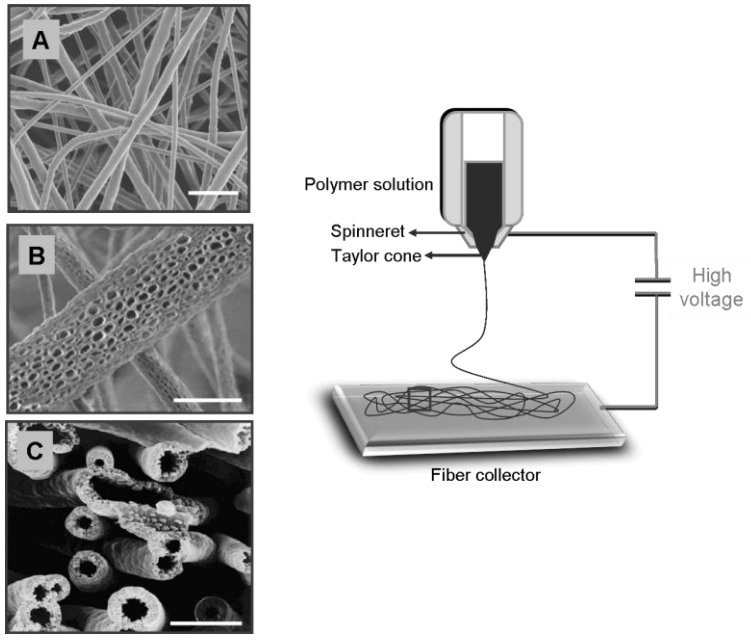

Fig.4. Schematic representation of electrospinning technique. Electrical potential is applied to the polymer solution at the tip of capillary tube, yielding a charged solution, which is then elongated to form a Taylor cone. An increase in the electrical potential results in ejection of a jet from the tip of this cone, which gradually thins in the air due to elongation and solvent evaporation, and results in formation of randomly oriented fibers on the metallic collector[31]. The SEM images illustrate the morphologies of variety of fibers obtained by this method. (A) morphology of pHMGCL/PCL electrospun fibers, described in **Chapter 6** (scale bar is 3 µm). (B) morphology of porous PLA fibers spun on a solution of 5 M sodium chloride in water to ensure the conductivity of the collector[32] (scale bar is 3 µm), and (C) the inner surface of rough PLA fibers coated with polyparaxylylene[32] (scale bar is 5 µm).

1.3.2 Advanced scaffold fabricating techniques

There has been a growing realization of the importance of three-dimensionality in engineered tissue constructs. This interest is largely driven by considerations such as complex issues of nutrients and oxygen delivery and waste removal in engineered organs (i.e. need for vascularization)[6]. Advanced mouldless manufacturing techniques, commonly known as solid freeform fabrication (SFF), rapid prototyping (RP), or more colloquially *art to part* technology have recently been used for fabricating complex shaped scaffolds[33]. SFF builds parts by selectively adding materials, layer-by-layer, as specified by a computer program.

Each layer represents the shape of a cross-section of the mold at a specific level[34] (Figure 5).

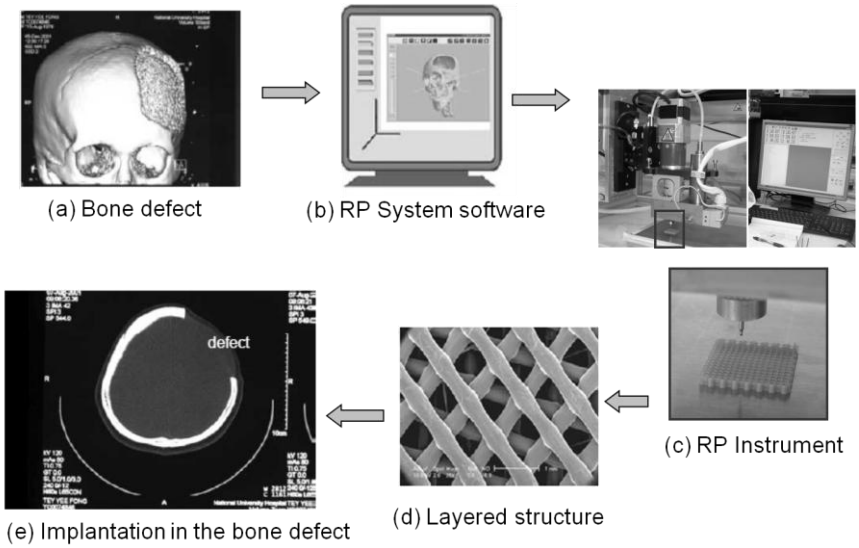

Fig.5. Tissue engineering of patient-specific implant (e.g.bone graft) via SFF technique. CT scan data of patient's bone defect (a) are used to generate a computer based 3D model (b) which is then sliced into layers using rapid prototyping (RP) software. This software controls a dispensing system (c) to deposit the polymer in a layer-by-layer fashion (d), resulting in a well-defined 3D-structre, which will be implanted into patient's bone defect (e). Reproduced from Ref[33].

Today, SFF is considered as an efficient way of reproducibly generating scaffolds of desired properties on a large scale[17]. Additionally, one of the potential benefits of SFF technology is the ability to create parts with highly reproducible architecture and compositional variation. RP techniques (as a subgroup of SFF techniques) used in tissue engineering field can be automated and integrated with imaging techniques to produce scaffolds that are customized in size and shape, allowing tissue-engineered implants to be tailored for specific applications or individual patients. RP methods can be divided into different categories: a) systems based on laser technology, that either photopolymerize a liquid resin (i.e., stereolithography (SLA)) or sinter powdered materials (i.e., selective laser sintering), b) systems based on print technology including printing a chemical binder onto a powdered material (3D-printing) or directly printing wax (wax

printing), and c) systems based on extrusion (also defined as nozzle-based systems[35]) that process a material either thermally or chemically as it passes through a nozzle such as 3D-bioplotting, fused deposition modeling, and precise extrusion manufacturing. In the following section, one example from each category is described in more detail.

a) Laser-based technology

- Stereolithography

This method is based on spatially controlled solidification of a liquid photo-polymerizable resin. Using a computer-controlled laser beam or a digital light projector with a computer-driven building stage, a solid, three-dimensional object can be constructed in a layer-by-layer fashion. Spatial control is one of the advantages of photo-initiated polymerization, besides short polymerization times, temporal control and the ability to carry out the polymerization under mild conditions[36]. Photo-initiated networks can be prepared in any shape using stereolithography with high precision and accuracy. However, the limited number of resins that are commercially available is often considered the main limitation of the technique. The porosity and pore size of scaffolds obtained by this method are up to 90% and in the range of 20-1000 µm, respectively.

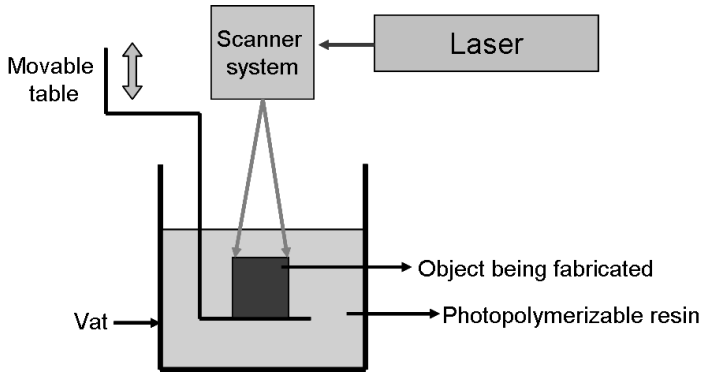

Fig.6. Schematic representation of stereolithography technique. Using a computer-controlled laser beam, a pattern is illuminated on the surface of resin. Therefore, the resin in the pattern is solidified to a defined depth, causing it to adhere to the support platform. After photopolymerization of the first layer, the platform is moved down and the built layer is recoated with liquid resin. The second layer is then cured and this process is repeated until the 3D object is ready. Image is reproduced from Ref[35].

b) Printing-based technology

- 3D-printing

This technique is based on conventional inkjet printing technology. In this method, the inkjet head prints droplets of a binder fluid on a powder bed. This fluid binds the powder and thus builds up part of model's cross section. This procedure is repeated for every layer until the 3D structure is printed and the remaining powder is removed[37]. This is a versatile method from a materials point of view as almost any powder, provided that it is combined with an adequate binder, can be used in this method. However, the flowability of the powdered material is an important factor for building up thin layers and to remove the printed part from the powder. The porosity of scaffolds obtained with this method is approximately 45 to 60% and the pore size can be tuned from 45 to 1600 µm[19].

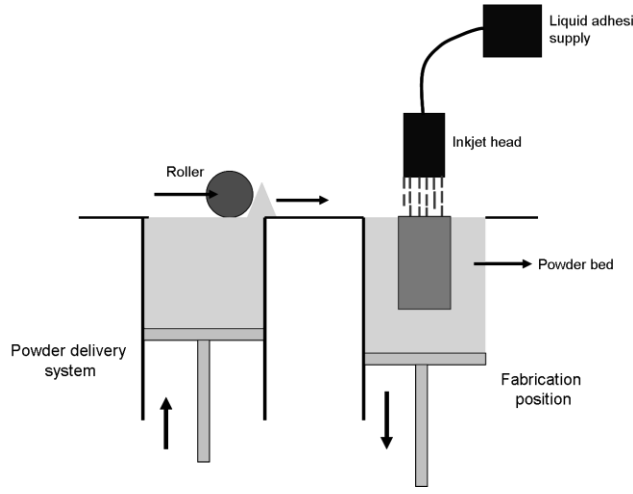

Fig.7. Schematic representation of 3D-printing technique. The inkjet head prints droplets of a binder into a powder bed, which results in the binding of powder and building up parts of an object. This process is repeated for every layer, and when the 3D structure is ready, the remaining powder is removed. The image is reproduced from Ref[35].

c) Extrusion-based technology

- 3D-melt plotting

3D-melt plotting is a technique based on extrusion of polymer fibers on a stationary stage, yielding layered 3D structures. Using this technique, first a

model of the required implant is created on a computer, and the dispensing material is subsequently loaded into the 3-axis robot arm and the material is extruded layer-by-layer enabling formation of 3D structures of defined external shape and internal morphology[38]. This technology is an attractive method to fabricate scaffolds for tissue engineering applications since it does not use possible toxic solvents. The pore size of scaffolds obtained can be tuned by varying the nozzle size used to deposit the polymer fibers. The porosity of scaffold obtained by this method is normally up to 80% and the pore size is within the range of 100-2000 µm[19].

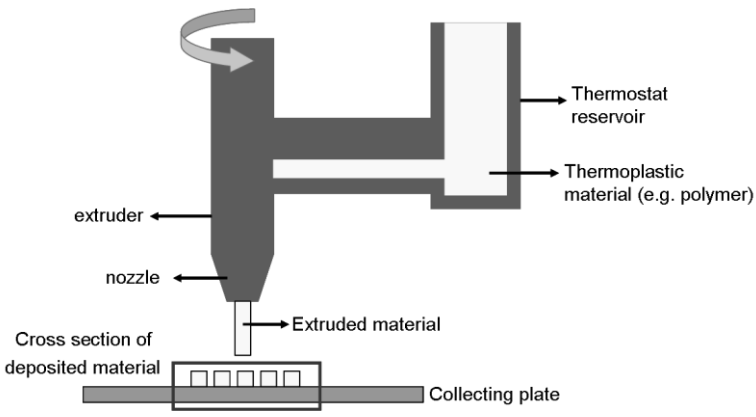

Fig.8. Schematic representation of 3D-melt plotting. In this method, a thermoplastic material (e.g. polymer) is introduced into a reservoir in which the material is heated above its melting temperature. The molten material is then passed through a channel and enters an extruder. The extruder is rotated and the material fibers are deposited on a surface in a layer-by-layer fashion.

1.4 Aim of the thesis

The aim of this thesis was to investigate the possibility of using a novel hydroxyl-functionalized polyester [poly(hydroxymethylglycolide-co-ε-caprolactone), pHMGCL] (Fig.9) to fabricate scaffolds for tissue engineering applications. Degradable polymers that are frequently used for tissue engineering applications are 'normal' aliphatic polyesters such as PCL, PLA and PLGA. One of the drawbacks of these polyesters is their hydrophobicity and lack of functional groups, which limits cell adhesion which is an important factor when constructing polymeric scaffolds[39, 40]. Another drawback is their slow hydrolytic degradation (in case of PCL[41] and PLA) due to high extent of crystallinity and hydrophobicity,

which makes these materials only suitable for long term implantable devices. Although several functionalized polyesters have been synthesized in recent years (described in **Chapter 2**), only a limited number has been evaluated for tissue engineering applications so far. Thus, there is a strong need for development of novel materials with improved physical, chemical, and biological properties for tissue engineering applications.

In this thesis we reasoned that increased hydrophilicity of the hydroxyl-functionalized polyester (pHMGCL) in comparison with its counterpart polyester (PCL) will result in improved cell-interaction properties as well as faster degradation times, which are both desired properties for scaffolds applied in tissue engineering field. Therefore, random pHMGCL polyesters with different molar ratios of HMG/CL were prepared and characterized. This polyester was further processed into different types of scaffolds and evaluated *in vitro* and *in vivo* for cell and tissue compatibility.

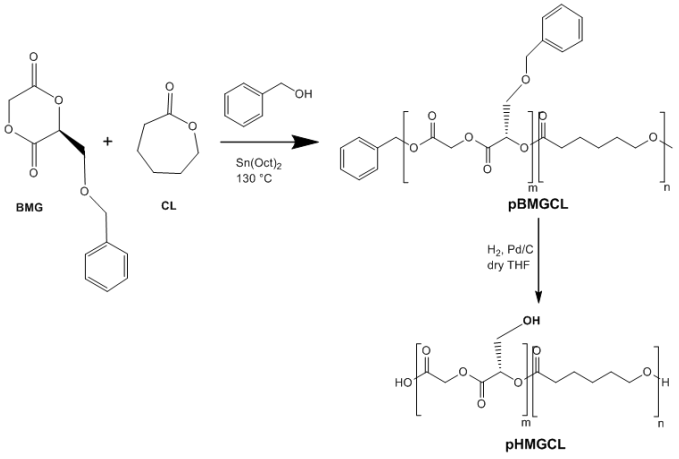

Fig.9. Synthesis scheme of poly(benzyloxymethylglycolide-co-ε-caprolactone) [pBMGCL] via ring opening melt polymerization at 130 °C, and poly(hydroxymethylglycolide-co-ε-caprolactone) [pHMGCL], via hydrogenation at room temperature using Pd/C catalyst.

1.5 Outline of thesis

Whereas this first chapter presents a general overview of scaffolds in tissue engineering, **Chapter 2** gives a detailed literature overview of recent trends in synthesis of functionalized polyesters for biomedical applications, including tissue engineering. Topics discussed are their synthesis via a) polycondensation polymerization, b) ring opening polymerization, and c) enzymatic polymerization.

Additionally, the application of these functionalized polyesters in protein/gene delivery and tissue engineering is discussed.

In **Chapter 3**, the synthesis of functionalized polyesters based on two monomers, (benzyloxymethyl glycolide [BMG]) and ε-caprolactone (CL), via melt polymerization is presented. It is shown that deprotection of the obtained polymers (poly(benzyloxymethylglycolide-co-ε-caprolactone), pBMGCL) yields copolymers with pendant hydroxyl groups (poly(hydroxymethyl glycolide-co-ε-caprolactone) [pHMGCL]. The physical characteristics of pHMGCL of varying monomer compositions are studied and the effect of hydroxyl group density on the hydrophilicity of polymeric films (prepared by solvent casting method) is shown. Moreover, the correlation between the wettability of these polymeric films and the adhesion, proliferation, and differentiation of human mesenchymal stem cells (hMSCs) is investigated.

The possibility of fabricating 3D-structures based on these polymers by using a Bioscaffolder is studied in **Chapter 4**. These scaffolds are based on pHMGCL containing 8% hydrophilic units and compared with PCL scaffolds as control. The physical and mechanical properties of these scaffolds are evaluated and the cell-scaffold interactions are investigated by dynamically seeding hMSCs into these constructs and studying cell proliferation and osteogenic differentiation. Additionally, the metabolic activity of seeded cells is measured and the possibility to use these highly porous constructs with well-defined structure for bone tissue engineering is discussed.

To asses the biocompatibility and biodegradation of the aforementioned scaffolds, an *in vivo* study is presented in **Chapter 5**. The scaffolds as described in chapters 3 and 4 are implanted subcutaneously in Balb/c mice for a duration of 12 weeks. After 4 and 12 weeks, the scaffolds are harvested and investigated for biodegradation of the polymers (pHMGCL and PCL) by investigating changes in the copolymer composition, thermal properties, and molecular weight as well as changes in the morphology of the scaffolds. Furthermore, the biocompatibility of the scaffolds is evaluated by studying the presence of inflammatory cells in the infiltrated and adjacent tissue of the scaffolds.

In **Chapter 6**, another scaffolding technique (electrospinning) is employed and the possibility of fabricating nanofibers based on pHMGCL using this technique is presented. The functionalized polyester containing 8% hydrophilic units is processed into nanofibers with a diameter of approximately 900 nm and the scaffolds are seeded with chondrocytes to evaluate the possibility for cartilage tissue engineering. Moreover, the *in vitro* degradation of polymeric films based on pHMGCL and PCL in PBS for a duration of 70 weeks is shown.

In order to demonstrate the possibility of loading bioactive molecules into these fibers, a variation of the conventional electrospinning technique (i.e. coaxial electrospinning) is used and the obtained scaffolds are presented in **Chapter 7**. These scaffolds are based on blends of pHMGCL with 25% of hydrophilic units and PCL (with varied ratios). The miscibility of these two polymers is shown by means of differential scanning calorimetry and the fibrous scaffolds are characterized morphologically. A model protein, bovine serum albumin (BSA), is loaded into these fibers and its release is investigated for 35 days. To demonstrate that the bioactivity of incorporated protein is preserved during the electrospinning process and release afterwards, a bioactive protein, vascular endothelial growth factor (VEGF), is loaded into these fibers and the effect of released growth factor on adhesion and proliferation of human endothelial cells is studied.

Finally, **Chapter 8** summarizes the work described in this thesis together with the major findings and it provides future perspectives for the scaffolds designed in this work.

References

[1] O'Brien, F. J., Biomaterials & scaffolds for tissue engineering. *Materials Today* **2011**, 14, (3), 88-95.

[2] Vats, A.; Tolley, N. S.; Polak, J. M.; Gough, J. E., Scaffolds and biomaterials for tissue engineering: A review of clinical applications. *Clinical Otolaryngology and Allied Sciences* **2003**, 28, (3), 165-172.

[3] Dvir, T.; Timko, B. P.; Kohane, D. S.; Langer, R., Nanotechnological strategies for engineering complex tissues. *Nature Nanotechnology* **2011**, 6, (1), 13-22.

[4] Langer, R.; Vacanti, J. P., Tissue Engineering. *Science* 1993, 260, (5110), 920-926.

[5] Place, E. S.; George, J. H.; Williams, C. K.; Stevens, M. M., Synthetic polymer scaffolds for tissue engineering. *Chemical Society Reviews* **2009**, 38, (4), 1139-1151.

[6] Kohane, D. S.; Langer, R., Polymeric biomaterials in tissue engineering. *Pediatric Research* **2008**, 63, (5), 487-491.

[7] David F, W., On the mechanisms of biocompatibility. *Biomaterials* 2008, 29, (20), 2941-2953.

[8] Platel, R. H.; Hodgson, L. M.; Williams, C. K., Biocompatible initiators for lactide polymerization. *Polymer Reviews* **2008**, 48, (1), 11-63.

[9] Amass, W.; Amass, A.; Tighe, B., A review of biodegradable polymers: Uses, current developments in the synthesis and characterization of biodegradable polyesters, blends of biodegradable polymers and recent advances in biodegradation studies. *Polymer International* **1998**, 47, (2), 89-144.

[10] Vert, M.; Li, S. M.; Spenlehauer, G.; Guerin, P., Bioresorbability and biocompatibility of aliphatic polyesters. *Journal of Materials Science: Materials in Medicine* **1992**, 3, (6), 432-446.

[11] Vert, M.; Li, S.; Garreau, H.; Mauduit, J.; Boustta, M.; Schwach, G.; Engel, R.; Coudane, J., Complexity of the hydrolytic degradation of aliphatic polyesters. *Angewandte Makromolekulare Chemie* **1997**, 247, 239-253.

[12] Grizzi, I.; Garreau, H.; Li, S.; Vert, M., Hydrolytic degradation of devices based on poly(DL-lactic acid) size dependence. *Biomaterials* **1995**, 16, (4), 305-311.

[13] Chen, C. C.; Chueh, J. Y.; Tseng, H.; Huang, H. M.; Lee, S. Y., Preparation and characterization of biodegradable PLA polymeric blends. *Biomaterials* **2003**, 24, (7), 1167-1173.

[14] Cai, Q.; Bei, J.; Wang, S., In vitro study on the drug release behavior from polylactide-based blend matrices. *Polymers for Advanced Technologies* **2002**, 13, (7), 534-540.

[15] Shoichet, M. S., Polymer scaffolds for biomaterials applications. *Macromolecules* **2010**, 43, (2), 581-591.

[16] Hollister, S. J., Porous scaffold design for tissue engineering. *Nat Mater* **2005**, 4, (7), 518-524.

[17] Hutmacher, D. W., Scaffold design and fabrication technologies for engineering tissues - State of the art and future perspectives. *Journal of Biomaterials Science, Polymer Edition* **2001**, 12, (1), 107-124.

[18] Sin, D.; Miao, X.; Liu, G.; Wei, F.; Chadwick, G.; Yan, C.; Friis, T., Polyurethane (PU) scaffolds prepared by solvent casting/particulate leaching (SCPL) combined with centrifugation. *Materials Science and Engineering,* **2010**, *C* 30, (1), 78-85.

[19] Dalton, P. D.; Woodfield, T.; Hutmacher, D. W., Snapshot: Polymer scaffolds for tissue engineering. *Biomaterials* **2009**, 30, (4), 701-702.

[20] Zhang, P.; Hong, Z.; Yu, T.; Chen, X.; Jing, X., In vivo mineralization and osteogenesis of nanocomposite scaffold of poly(lactide-co-glycolide) and hydroxyapatite surface-grafted with poly(l-lactide). *Biomaterials* **2009**, 30, (1), 58-70.

[21] Mooney, D. J.; Baldwin, D. F.; Suh, N. P.; Vacanti, J. P.; Langer, R., Novel approach to fabricate porous sponges of poly(d,l-lactic-co-glycolic acid) without the use of organic solvents. *Biomaterials* **1996**, 17, (14), 1417-1422.

[22] Dehghani, F.; Annabi, N., Engineering porous scaffolds using gas-based techniques. *Current Opinion in Biotechnology* **2011**, 22, (5), 661-666.

[23] Sultana, N.; Wang, M., Fabrication of HA/PHBV composite scaffolds through the emulsion freezing/freeze-drying process and characterisation of the scaffolds. *Journal of Materials Science: Materials in Medicine* **2008**, 19, (7), 2555-2561.

[24] Baker, S. C.; Rohman, G. r.; Southgate, J.; Cameron, N. R., The relationship between the mechanical properties and cell behavior on PLGA and PCL scaffolds for bladder tissue engineering. *Biomaterials* **2009**, 30, (7), 1321-1328.

[25] Gutsche, A. T.; Lo, H.; Zurlo, J.; Yager, J.; Leong, K. W., Engineering of a sugar-derivatized porous network for hepatocyte culture. *Biomaterials* **1996**, 17, (3), 387-393.

[26] Lo, H.; Kadiyala, S.; Guggino, S. E.; Leong, K. W., Poly(L-lactic acid) foams with cell seeding and controlled-release capacity. *Journal of Biomedical Materials Research* **1996**, 30, (4), 475-484.

[27] Murugan, R.; Ramakrishna, S., Nano-featured scaffolds for tissue engineering: A review of spinning methodologies. *Tissue Engineering* **2006**, 12, (3), 435-447.

[28] Zeleny, J., The electrical discharge from liquid points, and a hydrostatic method of measuring the electric intensity at their surfaces. *Physical Review* **1914**, 3, (2), 69-91.

[29] Dahlin, R. L.; Kasper, F. K.; Mikos, A. G., Polymeric nanofibers in tissue engineering. *Tissue Engineering - Part B: Reviews* **2011**, 17, (5), 349-364.

[30] Ji, W.; Sun, Y.; Yang, F.; Van Den Beucken, J. J. J. P.; Fan, M.; Chen, Z.; Jansen, J. A., Bioactive electrospun scaffolds delivering growth factors and genes for tissue engineering applications. *Pharmaceutical Research* **201**1, 28, (6), 1259-1272.

[31] Venugopal, J.; Low, S.; Choon, A. T.; Ramakrishna, S., Interaction of cells and nanofiber scaffolds in tissue engineering. *Journal of Biomedical Materials Research - Part B Applied Biomaterials* **2008**, 84, (1), 34-48.

[32] Agarwal, S.; Greimer, A.; Wendorff, J. H., Electrospinning of manmade and biopolymer nanofibers - Progress in techniques, materials, and applications. *Advanced Functional Materials* **2009**, 19, (18), 2863-2879.

[33] Hutmacher, D. W.; Sittinger, M.; Risbud, M. V., Scaffold-based tissue engineering: Rationale for computer-aided design and solid free-form fabrication systems. *Trends in Biotechnology* **2004**, 22, (7), 354-362.

[34] Pham, D. T.; Gault, R. S., A comparison of rapid prototyping technologies. *International Journal of Machine Tools and Manufacture* **1998**, 38, (10-11), 1257-1287.

[35] Hollister, S. J., Porous scaffold design for tissue engineering. *Nature Materials* **2005**, 4, (7), 518-524.

[36] Melchels, F. P. W.; Feijen, J.; Grijpma, D. W., A review on stereolithography and its applications in biomedical engineering. *Biomaterials* **2010**, 31, (24), 6121-6130.

[37] Butscher, A.; Bohner, M.; Hofmann, S.; Gauckler, L.; Müller, R., Structural and material approaches to bone tissue engineering in powder-based three-dimensional printing. *Acta Biomaterialia* **2011**, 7, (3), 907-920.

[38] Fedorovich, N. E.; Alblas, J.; Hennink, W. E.; Oner, F. C.; Dhert, W. J. A., Organ printing: the future of bone regeneration? *Trends in Biotechnology*, **2011**, 29 (12), 601-606.

[39] Noga, D. E.; Petrie, T. A.; Kumar, A.; Weck, M.; Garcia, A. J.; Collard, D. M., Synthesis and modification of functional poly(lactide) copolymers: Toward biofunctional materials. *Biomacromolecules* **2008**, 9, (7), 2056-2062.

[40] Wang, S.; Cui, W.; Bei, J., Bulk and surface modifications of polylactide. *Analytical and Bioanalytical Chemistry* **2005**, 381, (3), 547-556.

[41] Gan, Z.; Liang, Q.; Zhang, J.; Jing, X., Enzymatic degradation of poly(ε-caprolactone) film in phosphate buffer solution containing lipases. *Polymer Degradation and Stability* **1997**, 56, (2), 209-213.

Chapter 2

Functionalized Polyesters for Biomedical and Pharmaceutical Applications

Hajar Seyednejad
Amir H. Ghassemi
Cornelus F. van Nostrum
Tina Vermonden
Wim E. Hennink

Journal of Controlled Release
2011, 152 (1), 168- 176

Functional aliphatic polyesters are biodegradable polymers with many possibilities to tune physico-chemical characteristics such as hydrophilicity and degradation rate as compared to traditional polyesters (e.g. PLLA, PLGA and PCL), making the materials suitable for drug delivery or as scaffolds for tissue engineering. Lately, a large number of polyesters have been synthesized by homopolymerization of functionalized monomers or co-polymerization with other monomers mainly via ring-opening polymerization (ROP) of cyclic esters. This review presents the recent trends in the synthesis of these materials and their application for protein delivery and tissue engineering.

1. Introduction

Aliphatic polyesters belong to the category of biodegradable polymers and have been broadly used in medical products such as sutures, bone screws, tissue engineering scaffolds and drug delivery systems [1-3]. With the advancement of biotechnology that has resulted in increased number of available therapeutic peptides/proteins, traditional aliphatic polyesters such as poly(lactic acid) (PLA), poly(lactic-co-glycolic acid) (PLGA) and poly(ε-caprolactone) (PCL) have been exploited for the development of controlled release systems for peptides/proteins [4, 5]. Polyesters used for biomedical applications are mainly derived from glycolide (GA), lactide (LA), β-butyrolactone (β-BL), ε-caprolactone (ε-CL), 1,5-dioxepan-2-one (DXO) and trimethyl carbonate (TMC) [2, 6]. There are three major routes for the synthesis of aliphatic polyesters. The first route is by polycondensation of a hydroxy acid or of a diol and a diacid [1]. However, this method has some drawbacks including the low degree of polymerization resulting in low molecular weight polymers [1, 7] and block copolymers can not be synthesized. The second route is via ring opening polymerization (ROP) of lactones and other cyclic diesters such as lactide and glycolide which under proper conditions can result in polyesters with high molecular weights and ROP is associated with limited side reactions such as racemization [8, 9]. Moreover, it has been shown that block copolymers can be obtained by living ROP [10, 11]. Enzymatic polymerization is the third route to obtain polyesters and is carried out under mild conditions avoiding the use of toxic reagents and with the possibility to recycle the catalyst [12]. Additionally, regional and stereo selectivity of enzymes provides attractive possibilities for the direct synthesis of functional polyesters avoiding the use of protected monomers and block copolymers can be synthesized by using enzymatic polymerization [13]. However, the major drawback of the enzymatic synthesis of polyesters is the relatively low molecular weight of the obtained polymers [2, 12].

The degradation of aliphatic polyesters generally proceeds via hydrolysis of main chain ester bonds and the rate and extent of degradation depends on the character of polymer (e.g. hydrophilicity and crystallinity). They degrade either by bulk erosion or surface erosion [1, 14, 15]. Although aliphatic polyesters have been used for many years for biomedical and pharmaceutical applications, there is still need for improvements. To illustrate, PLGA has been extensively investigated for development of microspheres with the aim to get a controlled release of the entrapped therapeutic agent (e.g. a low molecular weight drug, a pharmaceutical protein or pDNA) for a prolonged time. Particularly, emphasis has been given in the last two decades on the development of protein loaded PLGA

formulations. However, instability, aggregation and chemical modification of the loaded proteins due to a pH drop in the microspheres upon their degradation has been reported [16-20]. Importantly, the resulting aggregates can cause unwanted immunogenic reactions [21-23]. Another example of an aliphatic biodegradable polyester is PCL which has been extensively used for the development of biomedical devices and tissue engineering scaffolds. Its slow degradation (2 to 4 years) and intrinsic hydrophobicity are major drawbacks for use in tissue engineering [24]. The introduction of functional groups into commonly used polyesters such as PLA and PCL provides polymers with tunable degradation behavior by suppression of crystallinity and enhanced hydrophilicity which favors cell adhesion to the surfaces important for tissue engineering purposes [25]. Further, an increasing hydrophilicity results in a greater water absorbing capacity of the polymers, thereby increasing the degradation rate and probably preventing a pH drop inside the degrading matrices and hence prevent aggregation and incomplete release of encapsulated proteins [26]. Moreover, coupling peptide ligands with the RGD (Arg-Gly-Asp) sequence to functionalized polymers improves cell adhesion which in turn will trigger cell growth and proliferation [27, 28].

Many functionalized polyesters have been synthesized in recent years [29-32]. However, despite their obvious advantages over their non-functionalized counterparts, applications of these polymers have been rarely studied in the biomedical and pharmaceutical areas. This article reviews recent developments of functionalized aliphatic polyesters and discusses their applications for tissue engineering and protein/pDNA delivery.

2. Synthesis of functional polyesters

2.1. General aspects

Functional polyesters can be synthesized by post-polymerization functionalization. This can be established by abstraction of protons from the polyester by treatment with a base, such as lithium diisopropyl amide (LDA), followed by subsequent addition of an electrophilic reagent, such as a halogen- or a carbonyl-containing compound [33, 34]. The main drawback of this method is the possibility of side reactions, such as chain scission and racemization. Besides, the preparation of block copolymers using this strategy is not straightforward. Therefore post-polymerization functionalization is not the preferred route to obtain functional polyesters. A more frequently used route to functional polyesters is to homopolymerize functional (protected) monomers or

copolymerize such monomers with commercially available non-functionalized monomers which can be performed via three major polymerization routes as pointed out in the introduction section. The functional groups in the monomers are normally protected to avoid side reactions and consequently a deprotection step after polymerization has to be carried out to obtain polymers bearing functional groups [32, 35].

The most frequently studied functional monomers are based on lactones [8, 36-39]. Highly pure monomers are the key factor to tailor the molecular weight of aliphatic polyesters from these monomers and to obtain high molecular weight polymers [38]. The main advantage of lactones for polyester synthesis is the possibility to purify them by recrystallization or distillation prior to polymerization. Recent reviews on the different synthesis routes to functionalized lactones can be found elsewhere [8, 40].

2.2. Polycondensation polymerization

Step-growth polymerization refers to the condensation of hydroxyl-acids or mixtures of diacids and diols. The major drawbacks of this method are the high temperatures and long reaction times which may lead to side reactions, such as racemization [38]. The molecular weight of polycondensates is indeed usually limited to a few tens of thousands (M_n < 30 kDa), because completion of the reaction is a (kinetic) problem and deviation of the stoichiometry of diacids and diols detrimentally affects the chain length [7, 38].

There are only a few publications on the synthesis of functionalized polyesters via polycondensation. For instance, Brown et al. [41] reported on the synthesis of amorphous aliphatic polyesters containing unsaturated double bonds which were in a subsequent reaction converted to ether or amine functional groups. They used Diels-Alder reactions to synthesize new difunctional monomers via the reaction of fumaric acid or maleic anhydride and a variety of dienes (Fig.1).

The resulting unsaturated dicarboxylate monomers were incorporated into aliphatic polyesters (M_n ranging from 11-18 kDa) by step growth polycondensations with di-alcohols (e.g. 1,8-octanediol). In a subsequent reaction, thermal crosslinking of these polymers was performed by mixing the polyesters with AIBN and heating at 130 °C for 24h, to yield degradable elastomers. Since these materials are intended for biomedical applications, the cured elastomers were tested for their cytotoxic response, using L-929 mouse fibroblast cells and it was shown that these materials were non-toxic.

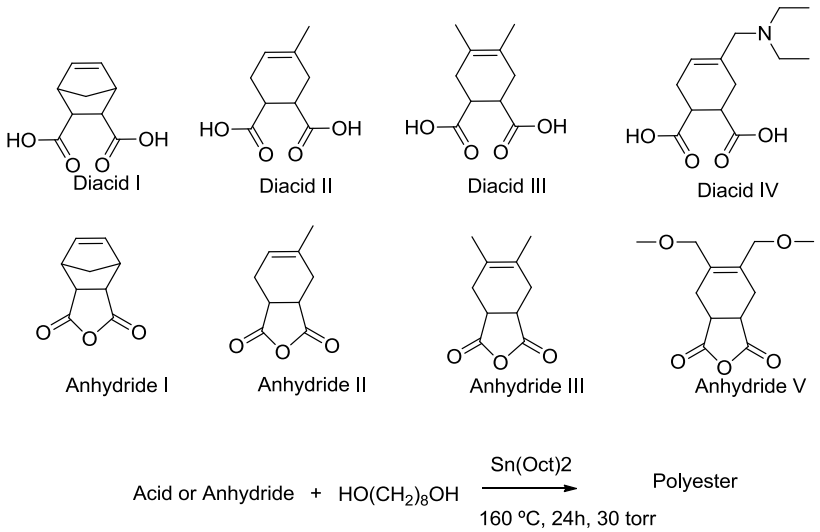

Fig.1. Synthesis of unsaturated aliphatic polyesters via polycondensation [41].

Wang et al. [42] synthesized an elastomer through polycondensation of glycerol and sebacic acid (Fig.2) in which the molar ratio of glycerol/sebacic acid was 1:1. This reaction resulted in a colorless elastomer, featuring small number of crosslinks (crosslink density of 38.3 ± 3.4 mol/m^3) in which the hydroxyl groups were directly attached to the network backbone.

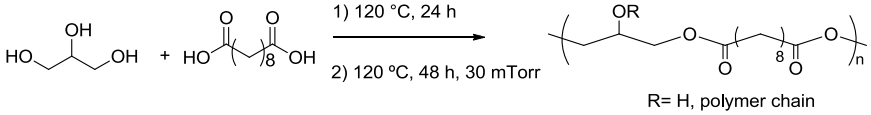

Fig.2. Synthesis of poly(glycerol-sebacate) [42].

Yang et al. reported on the synthesis of a biodegradable elastomer, i.e. poly(1,8-octanediol-co-citric acid), with a controllable number of crosslinks, tailorable elasticity and biodegradability [43]. They first prepared a low molecular weight (M_w ~1100) pre-polymer by a controlled condensation reaction between 1,8-octanediol and citric acid (citric acid:1,8-octanediol molar ratio of 1:1), and then crosslinked the formed polymer under various conditions. They showed that the polymer that was crosslinked under mild conditions (low temperatures, e.g. 60 or 80 °C, no vacuum) had a significantly faster degradation rate than the polymer

crosslinked under relatively tougher conditions (high temperature, e.g. 120 °C, 2 Pa vacuum). The crosslinked polymers synthesized at 60 °C completely degraded within 6 months of incubation in phosphate buffered saline (PBS) at 37 °C, while the crosslinked polymers synthesized at higher reaction temperature were more stable and showed only 50 % weight loss during this time.

2.3. Ring opening polymerization

High-molecular weight aliphatic polyesters can be prepared by ring opening polymerization (either in melt or solution) of lactones of different ring-size, with or without (protected) functional groups [39, 40]. Many of the reported ROP reactions to synthesize functional polymers are based on ε-CL derivatives. This monomer can be derivatized at different CH_2 positions and with a variety of functional groups (Fig.3).

Halogen-bearing CL monomers are the most frequently used functional monomers in ROP reactions. As an example, a iodine-functionalized caprolactone monomer (Fig. 3A) was synthesized by Habnouni et al. through activation of caprolactone with a non-nucleophilic strong base (lithium diisopropyl amide), followed by an electrophilic substitution with iodine monochloride [29]. This monomer was copolymerized with ε-caprolactone at 100 °C in toluene, initiated by methanol and catalyzed by $SnOct_2$, to yield an iodine bearing copolymer. The authors suggested that these iodinated polyesters open the way to new functional polyesters by substitution of the iodine group by other functional groups and to yield polymers that can potentially be applied in temporary reconstruction materials or drug delivery systems.

Gautier et al. [30] synthesized random copolyesters by controlled ROP polymerization of ε-caprolactone with γ-bromo-ε-caprolactone (Fig. 3B) or γ-triethylsiloxy-ε-caprolactone (Fig. 3C) using aluminum triisopropoxide as initiator. The obtained copolyesters were quaternized by reaction of the γBrCL units with pyridine and deprotected by acidic hydrolysis of γEt_3SiOCL units to yield p(CL-co-γPyCL) and p(CL-co-γOHCL), respectively. Further, they prepared stable nanoparticles by co-precipitation of poly(D,L-lactide) with small amounts of PCL partly substituted with pyridinium, with the aim to obtain degradable colloidal carriers with ability to bind molecules of interest.

Lenoir et al. synthesized α-chloro-ε-caprolactone (Fig.3D), and copolymerized this monomer with ε-caprolactone [44]. They used the pendant

chlorides of this copolymer to graft poly(methyl methacrylate) or poly(butenyl benzoate) blocks by ATRP.

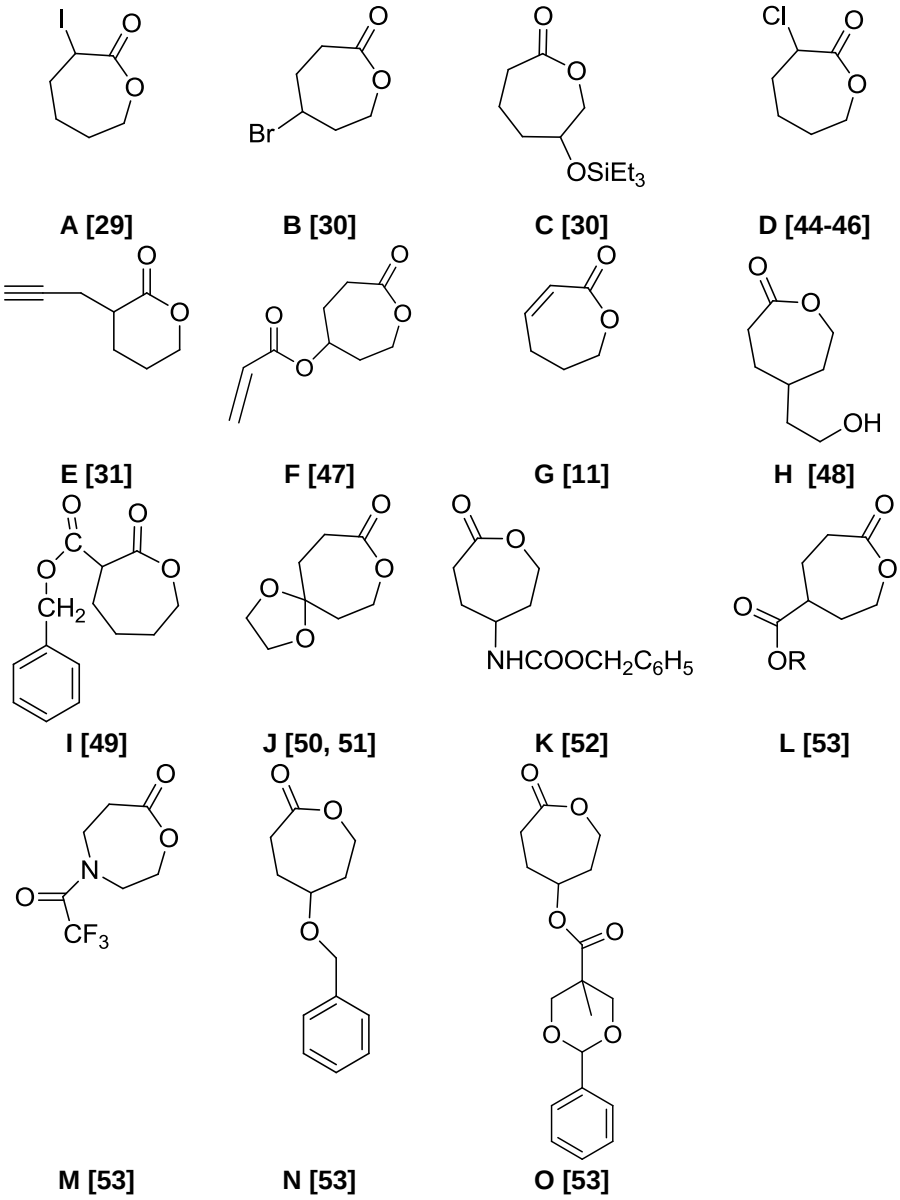

Fig.3. Functionalized monomers based on ε-CL derivatives (except E) suitable for ROP.

Riva et al. [45, 46] copolymerized the same monomer, α-chloro-ε-caprolactone Fig. 3D), with ε-CL and substituted the pendant chlorides by azide. These azide functionalized polymers were subsequently reacted under mild conditions by Huisgen's cycloaddition reaction [47] with alkyne functionalized reagents having ester, amine, and ammonium groups, as well as well with alkyne-derivatized PEO chains.

Parrish et al. [31] synthesized aliphatic polyesters with pendant acetylene groups by controlled ROP of α-propargyl-δ-valerolactone (Fig. 3E) with ε-caprolactone. They subsequently grafted azide-terminated PEG-1100 monomethyl ether and an azide functionalized GRGDS peptide to the polyester by click chemistry. They also showed that these polymers were biocompatible using in-vitro cytotoxicity assays.

Mecerreyes et al. [48] reported the synthesis of a functional lactone containing a pendant acrylate group (Fig. 3F). The homopolymers of 3F with different molecular weights (M_n of 7 kDa to 20 kDa) were synthesized via ROP at 25 °C in dry toluene and the polymers had a T_g of -60 °C. Random 6-arm star copolymers of 4-(acryloyloxy)-ε-caprolactone and ε-caprolactone were synthesized in bulk at 110 °C using the hydroxyl hexafunctional dendrimer of bis-MPA (2,2'-bis(hydroxymethyl)propionic acid) and $Sn(Oct)_2$, as initiator and catalyst, respectively. Poly(L,L-lactide$_{0.85}$-co-4-(acryloyloxy)-ε-caprolactone$_{0.15}$) was dissolved in dichloromethane in the presence of benzoin diethyl ether as radical photoinitiator followed by UV irradiation to yield degradable networks. Crosslinking was also established by dissolving the polymer in toluene and using AIBN as a thermal radical initiator. However, the characteristics (e.g. cell compatibility, degradation kinetics) of the obtained networks were not reported.

Another unsaturated cyclic ester, 6,7-dihydro-2(5H)-oxepinone (DHO) was synthesized by Lou et al. [11] (Fig. 3G). They copolymerized this monomer with ε-CL in toluene at room temperature, using $Al(O^iPr)_3$ as initiator to obtain unsaturated aliphatic polyesters. Thermal analysis of the copolymers showed that an increasing amount of DHO has a strong effect on the melting temperature of the polymer; T_m decreases from 57 to 29 °C at F_{DHO}=0.66, followed by an increase up to T_m of the homopolymer of DHO (35 °C). The unsaturated polyester backbone offers sites for crosslinking, which is useful for the synthesis of biodegradable networks.

Liu et al. reported a new approach for synthesis of hyperbranched polymers in which ring-opening polymerization is combined with some of the features of self-condensing vinyl polymerization (SCVP) [49]. They synthesized an AB type monomer, containing ε-caprolactone ring as well as an alcohol

initiating group (a so-called inimer (=initiator/monomer), i.e. 4-(2-hydroxyethyl)-ε-caprolactone, Fig.3H). This monomer was polymerized at 110 °C in bulk using stannous octoate ($SnOct_2$) as catalyst, yielding a hyperbranched polymer with a M_w of 65 - 85 kDa containing a large number of hydroxyl group chain ends. These hydroxyl groups can be used to attach biologically active molecules.

In a recent paper, Wolf et al. [50] described the synthesis of branched and hyperbranched poly(L-lactide) copolymers with hydroxyl end groups by ROP of L-lactide and a hydroxyl-functional lactone inimer, i.e. 5-hydroxymethyl-1,4-dioxane-2-on (5HDON). The polymerization was performed both in bulk and solution, and was catalyzed by either $Sn(Oct)_2$ or an organic base, 1,5,7-triazabicyclo[4.4.0]dec-5-ene (TBD). They showed that both the degree of branching and the molecular weight could be tailored by the monomer/inimir ratio. The authors suggested that these potentially biodegradable and biocompatible branched/dendritic structures are useful for polymer modification reactions and surface functionalization.

Different biodegradable PEO-b-poly(ester) block copolymers having functional pendant α-benzyl carboxylate or carboxyl groups were prepared by ROP of α-benzyl carboxylate-ε-caprolactone (Fig. 3I) with ε-caprolactone using methoxy poly(ethylene oxide) as initiator, to yield PEO-b-PBCL which after catalytic debenzylation yielded PEO-b-PCCL [51]. It was shown that these amphiphilic polyesters were able to form spherical micelles with nanoscopic dimension (average diameter of 62 and 20 nm for PEO-b-PBCL and PEO-b-PCCL, respectively) in water. These micelles are potentially suitable as delivery systems for controlled and /or targeted delivery of therapeutic agents.

5-Ethylene ketal ε-caprolactone (Fig. 3J) was synthesized by Tian et al. [52, 53] and they copolymerized this monomer with ε-caprolactone at 25 °C in toluene, using $Al(O^iPr)_3$ as initiator, to yield copolymers bearing acetal pendant groups. Deprotection of the copolymers was carried out with triphenylcarbenium tetrafluoroborate and the formed ketone groups were reduced to yield hydroxyl groups by sodium borohydride. They showed that these polymers form stable nanoparticles in water with a mean size below 100 nm potentially suitable for drug delivery.

An amine-functionalized PCL was synthesized by copolymerization of the functional monomer γ-(carbamic acid benzyl ester)-ε caprolactone (Fig. 3K) with ε-CL at 130 °C using $SnOct_2$ as catalyst [54]. Subsequently, the synthesized polymer was deprotection by hydrogenation using Pd/C as catalyst, to yield PCL with pendant amine groups (Fig. 4). Biotin (a model compound) was attached to

these amine groups to show the accessibility of these functional groups for further conjugation with bioactive molecules.

Trollsås et al. synthesized several functionalized caprolactone monomers (Fig. 3L, M, N, and O) which were synthesized by the Bayer-Villiger oxidation of the corresponding cyclohexanone derivatives [55]. Homopolymerization of these protected functionalized ε-caprolactone derivatives (hydroxyl-, bis-(hydroxyl)-, amino- and carboxyl-substituted) were performed either in bulk or in toluene as solvent (Fig. 5) at 110 °C to minimize possible transesterification reactions. They showed that the obtained polymers had a M_n close to their targeted molecular weights (5000-15000 g/mol) with narrow polydispersities (1.20-1.35).

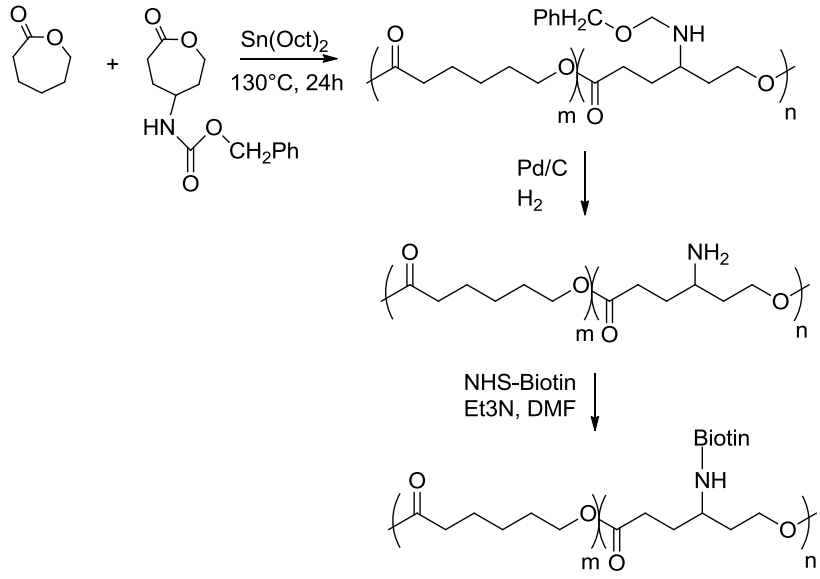

Fig.4. Synthesis and biotinylation of poly(CL-co-ACL) [54].

John et al. [56, 57] synthesized poly(ε-caprolactone-co-glycolic acid-co-L-serine) from the corresponding monomer, e.g. 3-(O-benzyl)-L-serinylmorpholine-2,5-dione (Fig. 6). First, copolymerization of ε-caprolactone and the aforementioned monomer was performed using $Sn(Oct)_2$ as initiator. The obtained copolymer was subsequently deprotected by catalytic hydrogenation and acrylic derivatives of the copolymer were synthesized by reacting the PCL(Glc-Ser) copolymer with acryloyl chloride. Crosslinked scaffolds and microspheres of this polymer were prepared by means of photopolymerization.

Protected functional glycolide-type monomers, i.e. 3S-(benzyloxymethyl)-6S-methyl-1,4-dioxane-2,5-dione and 3S-benzyloxymethyl-1,4-dioxane-2,5-dione, were synthesized by Leemhuis et al. [32, 58] (Fig. 7).

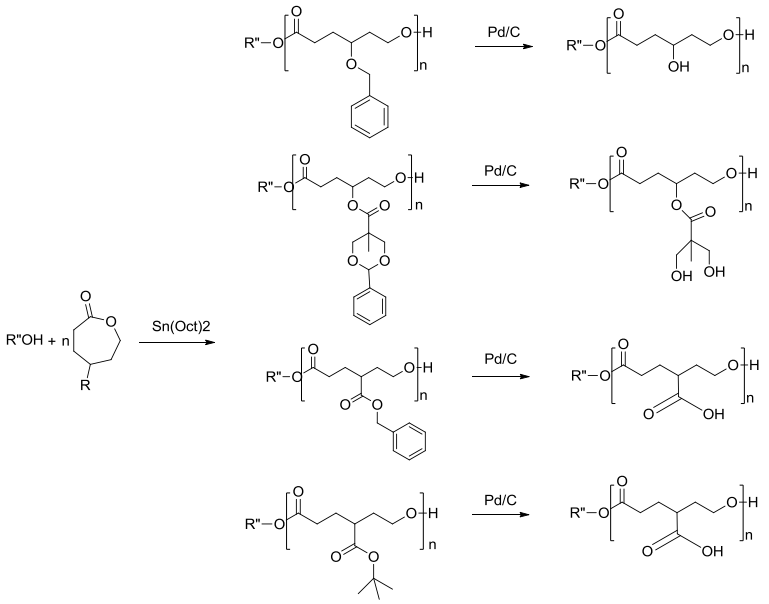

Fig.5. ROP of different functional lactones followed by deprotection [55].

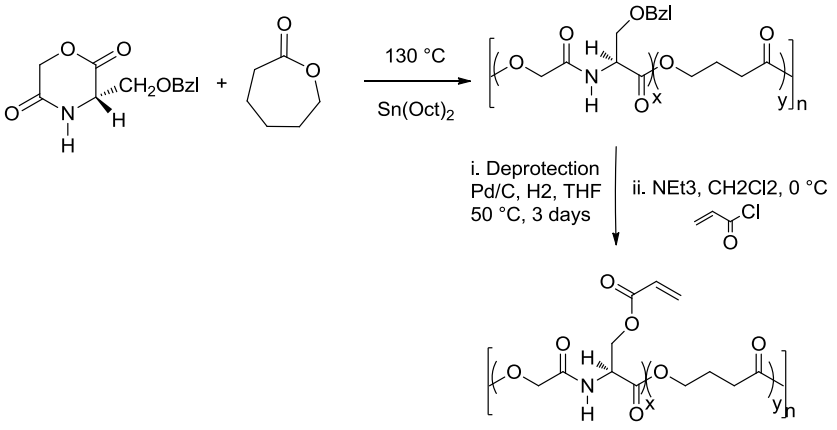

Fig.6. Synthesis of acrylated PCL(Glc-Ser) [56].

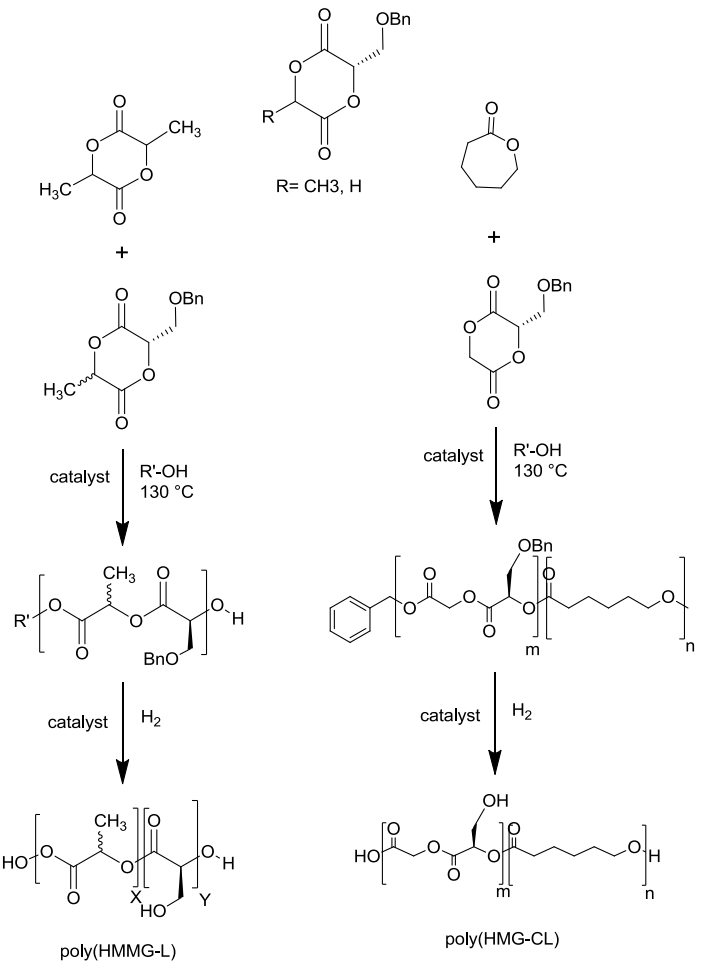

Fig.7. Synthesis of poly(HMMG-L) [26] and poly(HMG-CL) [59].

These functional monomers were copolymerized with L-lactide to form, after deprotection, the corresponding hydroxyl functionalized poly(lactide-co-hydroxymethyl methyl glycolide) (poly(HMMG-L)). In a follow-up paper [60], Leemhuis et al. studied the hydrolytic degradation of these functionalized polyesters of different copolymer compositions in phosphate buffer (174 mM, pH 7.4) at 37 °C. It was observed that the degradation times ranged from less than 1 day (for the homopolymers of hydroxymethyl methyl glycolide) to 2 months (copolymers with lactide containing 25% of functionalized monomer). The degradation rates increased with increasing hydroxyl density of the polymers, which was associated with a switch from bulk to surface erosion.

Loontjens et al. [61] showed that functional random copolymers of these monomers with ε-caprolactone (poly(BMG-co-CL)) synthesized at 110 °C, 130 °C and 150 °C (containing more than 40 mol % of the protected BMG monomer) had T_g's of -16, -29 and -28 °C, respectively. It was shown that at all these temperatures, ε-CL started to polymerize when BMG was almost fully converted. Deprotection of these copolymers resulted in a subtle increase in the T_g which indicates a decrease in the mobility of the polymer chains due to stronger interpolymer interactions of the hydroxyl groups.

Leemhuis et al. [62] synthesized an ally-functionalized glycolide monomer (i.e. 3-allyl-1,4-dioxane-2,5-dione) and copolymerized this monomer with L-lactide by ROP in the melt using benzyl alcohol and $Sn(Oct)_2$ as initiator and catalyst, respectively. They showed that the obtained polymers were amorphous materials and their T_g increased with increasing lactide content, ranging from 19 to 42 °C, when the lactide content increased from 25% to 75%. Further, the allyl groups of poly(allylglycolide) copolymers were oxidized using m-chloroperoxy benzoic acid (mCPBA) to yield the corresponding epoxidated polymers in high yield. These polymers were amorphous as well and their T_g varied from 21 to 24 °C, depending on their copolymer composition.

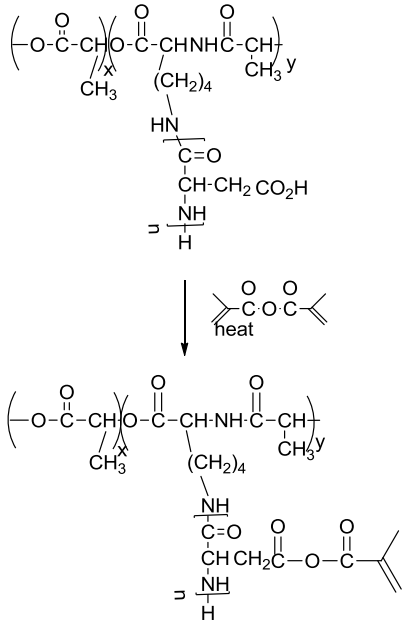

Fig.8. Synthesis of poly(lactic acid-co-lysine) grafted with poly(aspartic acid) and modified with methacrylate groups [63].

PLA-based polymers with ε-amine side groups (poly(lactic acid-co-lysine), PLAL) were synthesized by Elisseeff et al. [63] (Fig. 8). Poly(aspartic acid) side chains were grafted to the amine functionalities of the polymers to obtain PLAL-ASP. Different percentages of aspartic acid units of this polymer were partially converted to the methacrylate mixed anhydride by varying the duration of the substitution reaction at 37 and 60 °C. Hydrogels of these polymers were prepared by UV polymerization in bulk. The swelling degree of networks prepared from polymers containing 5-22% methacrylate groups, was ~5.5 in PBS. The compression moduli of these networks ranged from 1.4 to 3.1 kPa having mechanical characteristics suitable for biomaterials/tissue engineering applications.

Hu et al. [64] synthesized a functionalized polymer (PEG-b-P(LA-co-PTO)) via copolymerization of a functionalized/protected monomer, [9-phenyl-2,4,8,10-tetraoxapiro[5,5]undecan-3-one] (PTO) with LA, in the presence of monohydroxyl poly(ethyleneglycol) as macro initiator and $Sn(Oct)_2$ as catalyst (Fig. 9).

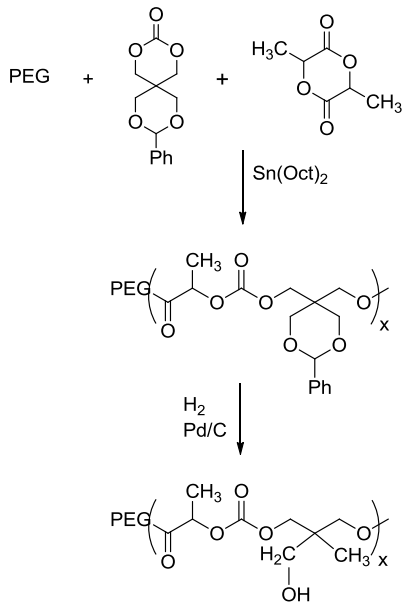

Fig.9. Synthesis of PEG-b-P(LA-co-PTO) block copolymers followed by deprotection [64].

The benzylidene protecting groups of this polymer were removed by catalytic hydrogenation to obtain PEG-b-P(LA-co-DHP). Micelles of the protected polymer

were formed in aqueous solution and it was shown that CMC decreased with increasing PTO content (from 12.3 to 1.0 mg/L when the PTO content increases from 5% to 20%). A cytocompatibility study was carried out by investigating the adhesion and spreading of Vero cells on films of both protected and deprotected polymers. After 24 hours, almost all cells adhered to the polymer films and they proliferated and covered the whole surfaces after 48 hours. They also studied the enzymatic degradation of these polymers in presence of proteinase K at 37 °C and compared that to PLA. After 40h, the weight loss was 89% for the deprotected polymer while it was 77% and 70% for the protected polymer and PLA, respectively. They derivatized the free hydroxyl groups with biotin to demonstrate the potential of this polymer for drug conjugation.

2.4. Enzymatic Polymerization

Enzymatic polymerization, particularly using lipase, is an efficient method for the synthesis of aliphatic polyesters [65]. The advantage of this polymerization method is its regioselectively and there is no need for protection/deprotection [66]. The mechanism of the lipase-catalyzed polymerization of a lactone is schematically shown in Fig. 10.

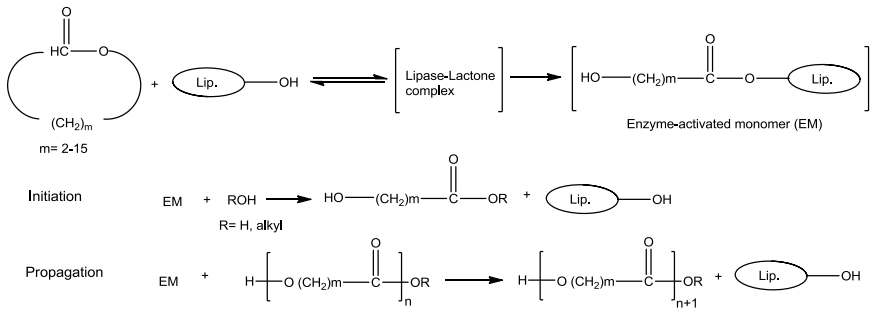

Fig.10. Schematic presentation of enzymatic polymerization by lipase [65].

Reaction of the lactone with lipase causes ring-opening to give an acyl-enzyme intermediate (enzyme-activated monomer, EM). Initiation is by nucleophilic attack of enzyme-absorbed water molecules onto the acyl carbon of the intermediate to yield an α-hydroxycarboxylic acid. In the propagation stage, the EM is nucleophilically attacked by the terminal hydroxyl group of a propagating polymer chain to yield a one-unit-more elongated chain. A kinetic investigation of the polymerization showed that the overall rate-determining step is the formation of

the EM and, therefore, the polymerization proceeds via a “monomer-activated mechanism” [65]. As an example of functionalized polyesters synthesized in this way, Al-Azemi et al.[67] reported on the lipase-catalyzed synthesis of a water-soluble polycarbonate having pendant carboxyl groups on the main chain using 5-methyl-5-benzyloxycarbonyl-1, 3-dioxin-2-one as monomer (Fig.11). They hypothesized that these polymers have enhanced biodegradability, but they have not reported the degradation data, yet.

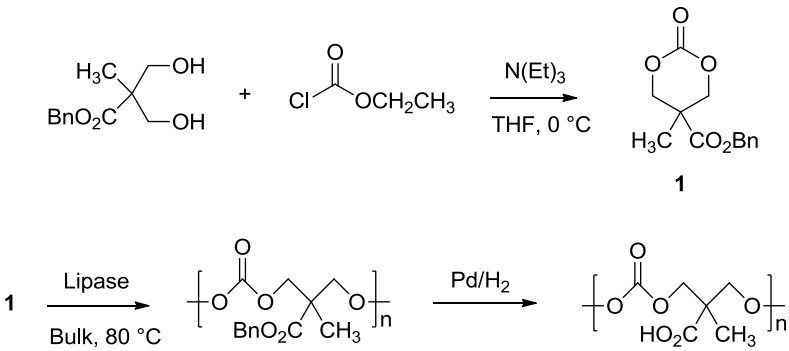

Fig.11. Synthesis of 5-methyl-5-benzyloxycarbonyl-1,3-dioxane-2-one and its enzymatic polymerization using lipase [67].

Veld et al. [68] synthesized two novel monomers, ambrettolide epoxide and isopropyl aleuriteate, containing functional groups. The homopolymers of ambrettolide epoxide were synthesized using Novozym 435 as catalyst to obtain a polymer of M_n = 9.7 kg/mol and PDI = 1.9, while the epoxide groups remained unaffected during the polymerization. Selective polymerization of isopropyl aleuriteate using Novozym 435 was performed as well and a polymer with moderate molecular weight (M_n = 5.6 kg/mol, PDI = 3.2) was obtained. Copolymerization of isopropyl aleuriteate with e-CL at different ratios resulted in soluble, hydroxy functional polymers with M_n’s ranging from 10. to 27 kg/mol in a good yield (~75 %). The secondary hydroxy groups of the polymer reacted easily with hexyl isocyanate, to demonstrate that these groups are assessable for post-polymerization modifications

3. Applications

3.1. Protein delivery

For the past two decades, non-functionalized aliphatic polyesters such as PLLA, PLDLA and PLGA have been extensively studied for the controlled delivery of therapeutic peptides/proteins [16, 69, 70]. However, due to the drawbacks associated with these systems (e.g. unfavourable protein-polymer interactions [71], acidification of the matrix during degradation [17], acylation of the encapsulated proteins [72] and difficult to tailor the release [73]), it is questionable whether the systems are generally applicable for the development of well-performing formulations. In recent studies, microspheres based on functionalized polyesters, i.e. the previously mentioned poly(L-lactide-co-hydroxymethyl glycolide) (poly(HMMG-L), (Fig. 7)), were investigated for encapsulation and release of a model protein(lysozyme) [26]. Poly(HMMG-L) microspheres were prepared by a multiple emulsion (w/o/w) solvent evaporation technique and, depending on the polymer concentration used for the preparation, 50 to 70% of lysozyme was released in a sustained manner from the microspheres. In comparison, PLGA microspheres showed hardly any sustained release of lysozyme after an initial small burst release (Fig.12). Importantly, the released lysozyme was fully enzymatically active and preserved its structural integrity (CD analysis). However, insoluble residues remained which as demonstrated by DSC and FTIR analysis contained lactic acid oligomers and aggregated lysozyme which likely explains the observed incomplete release of the protein.

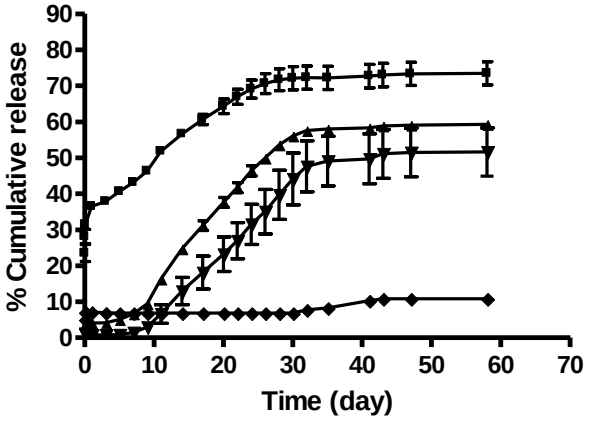

Fig.12. Lysozyme release from poly(HMMG-L) microspheres prepared with different polymer concentration (10 (■), 15 (▲) and 20 % (▼) in the organic phase). Also the release from PLGA microspheres is shown (♦) [26].

Replacing L-lactide by D,L-lactide in the copolymer prevented the formation of insoluble degradation products of crystalline oligomers of lactic acid. In this case, bovine serum albumin (BSA) was encapsulated with high efficiency (>85%) and was quantitatively released from microspheres of poly(D,L-lactide-co-hydroxymethyl glycolide). It was shown that the release from 2 weeks to 2 months was governed by degradation of the microspheres and depended on the copolymer composition (Fig. 13) and, importantly, no insoluble residues remained [74].

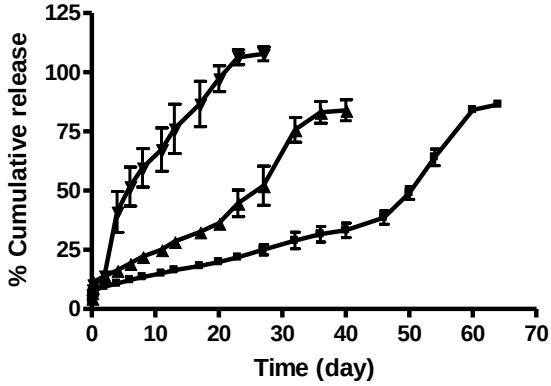

Fig.13. BSA release from poly(HMMG-L) microspheres prepared from copolymers with different copolymer composition; (▼) 50/50, (▲) 35/65 and (■) 25/75 [74].

In a recent study, Cristian et al. studied the encapsulation of BSA in microspheres of PCL bearing pendant acryloyloxy or methacryloyloxy groups [75]. Microspheres were prepared by a double emulsion evaporation method and the final emulsion was UV-irradiated in the presence of a photinitiator to crosslink the particles. They showed successful encapsulation of BSA in crosslinked polymer particles with raman spectroscopy. However, no data on either the loading efficiency nor the release and stability of the encapsulated BSA were reported, yet.

3.2. Tissue engineering

Degradable polymers that are frequently used for tissue engineering applications are 'normal' aliphatic polyesters such as PCL, PLA and PLGA. Drawbacks of these polyesters are their hydrophobicity and lack of functional groups, which limits cell adhesion that is an important factor when constructing polymeric scaffolds [76, 77]. Another drawback is their slow hydrolytic degradation [78].

Although several functionalized polyesters have been synthesized in recent year (described in section 2) only a limited number of functionalized polyesters has been evaluated for tissue engineering applications so far.

Wang et al. [42] evaluated both the *in vitro* and *in vivo* biocompatibility of a functionalized elastomer, (poly(glycerol-sebacate), PGS) (Fig.2), to get insight into the potential of this material for tissue engineering. They showed that NIH 3T3 fibroblast cells cultured on PGS-coated glass petri dishes were viable, showed normal morphology and had a higher growth rate in comparison with cells cultured on PLGA films as control. After subcutaneous implantation in rats it was shown thatPGS implants completely absorbed within 60 days without granulation or formation of scar tissues.

Yang et al. [43] investigated the suitability of poly(1,8-octanediol-co-citric acid) (POC) for cardiovascular tissue engineering applications. They showed that the water contact angles on POC films decreased from 76° to 38° after 30 minutes exposure to water, indicating that the surface becomes more hydrophilic in time. The adhesion and proliferation of human aortic smooth muscle cells and endothelial cells seeded on POC films was investigated as well and it was observed that growth and viability of both cell types was at least as good as or better than that observed on PLLA films.

Seyednejad et al. synthesized poly(hydroxymethylglycolide-co-caprolactone) (Figure 7) and investigated the suitability of this polymer for tissue engineering applications [59]. It was shown that the wettability of these polymers was tunable by the percentage of the functional monomer in the structure and they showed that incorporation of the functional monomer in the copolymer structure resulted in a decrease in receding contact angle from 64° to 40° after 20 min exposure to water, likely caused by exposure of the hydroxyl groups of the polymer at the water/polymer interface. Importantly, the increased hydrophilicity of copolymer films resulted in the improved adherence of human mesenchymal stem cells (hMSCs) along with the ability of the seeded cells to differentiate towards osteogenic lineage, when compared to hydrophobic PCL. In a follow up study [79], it was shown that three-dimensional scaffolds can be made from these functional polyesters by means of 3D-printing and the scaffolds showed superior properties in comparison with PCL scaffolds regarding mechanical properties as well as hMSCs adherence and proliferation.

3.3. Gene delivery

In recent years, gene therapy has become an important modality for the treatment of patients with acquired or inherited genetic diseases [80-82]. Viral gene delivery

systems including adenoviruses and retroviruses demonstrated high transfection efficiency [83-85], but their application is limited due to their side effects such as immunogenicity and mutagenesis caused by the cell-infected viruses [86]. Functional water-soluble cationic polyesters have been used as non-viral vectors for the binding and subsequent intracellular release of plasmid DNA [87]. For instance, poly(α-(4-aminobutyl)-L-glycolic acid) (PAGA) synthesized by Lim et al. [88, 89] is able to form PAGA/DNA polyplexes and it was shown that these polyplexes had a 3-fold higher transfection activity *in vitro* compared to the polyamide analogue of PAGA, i.e. poly-L-lysine (pLL). Importantly, PAGA showed no cytotoxicity at 100 μg/ml while pLL is highly cytotoxic at this concentration. In another study, Vromen et al.[90] investigated copolymers of ε-caprolactone and γ-bromo-ε-caprolactone quarternized by pyridine for gene delivery. They observed that the cytotoxicity and transfection efficiency was comparable to polyethylenimine 50 kDa [91-93] which is a non-biodegradable but commonly used polymer for gene delivery. A series of modified hyperbranched polymers based on 2,2-bis-(methylol)propionic acid (bis-MPA) with tertiary amines were synthesized by Reul et al.[94]. They showed that the toxicity of these hyperbranched polyesters was very low as compared to polyethyleneimine (PEI) and the transfection activity of the polymers increased with amine density. In a recent study, Liu et al. [95] synthesized degradable poly(β-aminoester)s with pendant aminoethyl groups and demonstrated that polyplexes of these polymers had higher transfection efficiencies than branched PEI 25 kDa in 293T cells.

4. Conclusions

In this contribution, the recent approaches to synthesize biodegradable and biocompatible functional aliphatic polyesters and their pharmaceutical and biomedical applications are reviewed. It is shown that functional polyesters with well-defined characteristics can be synthesized by homo- and copolymerization of (protected) functional monomers. Importantly, the characteristics of copolymers such as T_g, hydrophilicity, solubility and degradability can be tuned by the copolymer composition. Although a limited number of studies regarding the applications of functional aliphatic polyesters has been published, the results obtained so far encourage future investigations. The increasing number of accessible functional aliphatic polyesters provides the opportunity to study relationships between structure and functionality of these polymers such as degradability and cell adhesion *in vitro* and *in vivo* as well as to develop applications of these potential materials for drug delivery in the form of micro- and nanoparticles, implants, or scaffolds in tissue engineering.

References

[1] Albertsson, A. C.; Varma I., Aliphatic polyesters: synthesis, properties and applications. *Adv. Polym. Sci.*, **2002**, 157,1-40.

[2] Albertsson, A. C.; Varma I.K., Recent developments in ring opening polymerization of lactones for biomedical applications. *Biomacromolecules*, **2003**, 4 (6), 1466-1486.

[3] Jain, R., et al., Controlled drug delivery by biodegradable poly(ester) devices: different preparative approaches. *Drug Dev. Ind. Pharm.*, **1998**, 24 (8), 703-727.

[4] Saito, N., et al., Synthetic biodegradable polymers as drug delivery systems for bone morphogenetic proteins. *Adv. Drug Deliv. Rev.*, **2005**, 57 (7), 1037-1048.

[5] Zellin, G.R.; Hedner E.; Linde A., Bone regeneration by a combination of osteopromotive membranes with different BMP preparations: a review. *Connect. Tissue Res*., **1996**, 35 (1-4), 279-284.

[6] Buttafoco, L., et al., Porous hybrid structures based on P(DLLA-co-TMC) and collagen for tissue engineering of small-diameter blood vessels. *J. Biomed. Mater. Res. B*, **2006**, 79B (2), 425-434.

[7] Hyon, S. H.; Jamshidi K.; Ikada Y., Synthesis of polylactides with different molecular weights. *Biomaterials*, **1997**, 18 (22), 1503-1508.

[8] Pounder, R. J.; Dove A.P., Towards poly(ester) nanoparticles: recent advances in the synthesis of functional poly(ester)s by ring-opening polymerization. *Polym. Chem.*, **2010**, 1 (3), 260-271.

[9] Thomas, C.M., Stereocontrolled ring-opening polymerization of cyclic esters: synthesis of new polyester microstructures. *Chem. Soc. Rev.,* **2010**, 39 (1), 165-173.

[10] Velthoen W. I.; Dijkstra P. J.; Feijen J., AB_2 functional polyesters via ring opening polymerization: synthesis and characterization. *Macromol. Chem. Phys.,* **2009**, 210 (8), 689-697.

[11] Lou, X., et al., Living ring-opening (co)polymerization of 6,7-Dihydro-2(5H)-oxepinone into unsaturated aliphatic polyesters. *Macromolecules*, **2001**, 34 (17), 5806-5811.

[12] Kobayashi, S.; Uyama H.; Kimura S., Enzymatic Polymerization. *Chem. Rev.*, **2001**, 101 (12), 3793-3818.

[13] Loos, K.; Stadler R., Synthesis of amylose-block-polystyrene rod-coil block copolymers. *Macromolecules*, **1997**, 30 (24), 7641-7643.

[14] Kasperczyk, J., et al., Degradation of copolymers obtained by ring-opening polymerization of glycolide and ε-caprolactone: A high

resolution NMR and ESI-MS study. *Polym. Degrad. Stabil.,* **2008**, 93 (5), 990-999.

[15] Vert, M., et al., Something new in the field of PLA/GA bioresorbable polymers? *J. Control. Release*, **1998**, 53 (1-3), 85-92.

[16] Ye, M.; Kim S.; Park K., Issues in long-term protein delivery using biodegradable microparticles. *J. Control. Release*, **2010**, 146 (2), 241-260.

[17] Ding, A.; Schwendeman S., Acidic microclimate pH distribution in PLGA microspheres monitored by confocal laser scanning microscopy. *Pharm. Res.*, **2008**, 25 (9), 2041-2052.

[18] van de Weert, M.; Hennink W. E.; Jiskoot W., Protein instability in poly(lactic-co-glycolic acid) microparticles. *Pharm. Res.*, **2000**, 17 (10), 1159-1167.

[19] Lucke, A.; Göpferich A., Acylation of peptides by lactic acid solutions. *Eur. J. Pharm. Biopharm.,* **2003**, 55 (1), 27-33.

[20] Fu, K., et al., Visual evidence of acidic environment within degrading poly(lactic-co-glycolic acid) (PLGA) microspheres. *Pharm. Res.*, **2000**, 17 (1), 100-106.

[21] Hermeling, S., et al., Structure-immunogenicity relationships of therapeutic proteins. *Pharm. Res.,* **2004**, 21 (6), 897-903.

[22] Tia, E., et al., BSA degradation under acidic conditions: A model for protein instability during release from PLGA delivery systems. *J. Pharm. Sci.,* **2006**, 95 (7), 1626-1639.

[23] Jiskoot, W., et al., Immunological risk of injectable drug delivery systems. *Pharm. Res.*, **2009**, 26 (6), 1303-1314.

[24] Eda, D.Y., et al., Effect of dielectric barrier discharge plasma on the attachment and proliferation of osteoblasts cultured over poly(ε-caprolactone) scaffolds. *Plasma. Process. Polym.,* **2008**, 5 (1), 58-66.

[25] Ken, W.; Vladimir H.; Patrick A.T., Relative importance of surface wettability and charged functional groups on NIH 3T3 fibroblast attachment, spreading, and cytoskeletal organization. *J. Biomed. Mater. Res.*, **1998**, 41 (3), 422-430.

[26] Ghassemi, A.H., et al., Preparation and characterization of protein loaded microspheres based on a hydroxylated aliphatic polyester, poly(lactic-co-hydroxymethyl glycolic acid). *J. Control. Release,* **2009**, 138 (1), 57-63.

[27] Agrawal, C. M.; Robert B. R., Biodegradable polymeric scaffolds for musculoskeletal tissue engineering. *J. Biomed. Mater. Res.,* **2001**, 55 (2), 141-150.

[28] Fussell, G. W.; Cooper S. L., Synthesis and characterization of acrylic terpolymers with RGD peptides for biomedical applications. *Biomaterials*, **2004**, 25 (15), 2971-2978.

[29] Habnouni, S. E.; Darcos V.; Coudane J., Synthesis and ring opening polymerization of a new functional lactone, α-Iodo-ε-caprolactone: a novel route to functionalized aliphatic polyesters. *Macromol. Rapid. Comm.*, **2009**, 30 (3), 165-169.

[30] Gautier, S., et al., Amphiphilic copolymers of ε-caprolactone and γ-substituted ε-caprolactone. Synthesis and functionalization of poly(D,L-lactide) nanoparticles. *J. Biomat. Sci-polym. E.,* **2003**, 14, 63-85.

[31] Parrish, B.; Breitenkamp R. B.; Emrick T., PEG- and peptide-grafted aliphatic polyesters by click chemistry. *J. Am. Chem. Soc.,* **2005**, 127 (20), 7404-7410.

[32] Leemhuis, M., et al., Functionalized poly(α-hydroxy acid)s via ring-opening polymerization: toward hydrophilic polyesters with pendant hydroxyl groups. *Macromolecules*, **2006**, 39 (10), 3500-3508.

[33] Saulnier, B., et al., Lactic acid-based functionalized polymers via copolymerization and chemical modification. *Macromol. Biosci.*, **2004**, 4 (3), 232- 237.

[34] Ponsart, S.; Coudane J.; Vert M., A novel route to poly(ε-caprolactone)-based copolymers via anionic derivatization. *Biomacromolecules,* **2000**, 1 (2), 275- 281.

[35] Noga, D.E., et al., Synthesis and modification of functional poly(lactide) copolymers: toward biofunctional materials. *Biomacromolecules,* **2008**, 9 (7), 2056-2062.

[36] Lecomte, P., et al., Novel functionalization routes of poly(ε-caprolactone). *Macromol. Symp.,* **2000**, 157, 47-60.

[37] Lou, X.; Detrembleur C.; Jérôme R., Novel aliphatic polyesters based on functional cyclic (Di)esters. *Macroml. Rapid Comm.,* **2003**, 24 (2), 161-172.

[38] Jérôme, C.; Lecomte P., Recent advances in the synthesis of aliphatic polyesters by ring-opening polymerization. *Adv. Drug Deliver. Rev.,* **2008**, 60 (9), 1056-1076.

[39] Williams, C.K., Synthesis of functionalized biodegradable polyesters. *Chem. Soc. Rev.,* **2007**, 36 (10), 1573-1580.

[40] Xudong, L.; Christophe D.; Robert J., Novel aliphatic polyesters based on functional cyclic (di) esters. *Macromol. Rapid. Comm.,* **2003**, 24 (2), 161-172.

[41] Brown, A. H.; Sheares V. V., Amorphous unsaturated aliphatic polyesters derived from dicarboxylic monomers synthesized by diels-alder chemistry. *Macromolecules,* **2007**, 40 (14), 4848-4853.

[42] Wang, Y., et al., A tough biodegradable elastomer. *Nature Biotechnology*, **2002**, 20 (6), 602-606.

[43] Yang, J.; Webb A.; Ameer G., Novel citric acid-based biodegradable elastomers for tissue engineering. *Adv. Mater*., **2004**, 16 (6), 511-516.

[44] Lenoir, S., et al., Ring-opening polymerization of α-chloro-ε-caprolactone and chemical modification of Poly(α-chloro-ε-caprolactone) by atom transfer radical processes. *Macromolecules*, **2004**, 37 (11), 4055-4061.

[45] Riva, R., et al., Combination of ring-opening polymerization and "click chemistry": toward functionalization and grafting of poly(ε-caprolactone). *Macromolecules,* **2007**, 40 (4), 796-803.

[46] Riva, R., et al., Combination of ring-opening polymerization and "click" chemistry towards functionalization of aliphatic polyesters. *Chem. Commun.*, **2005**, 42, 5334-5336.

[47] Van Dijk, M., et al., Synthesis and applications of biomedical and pharmaceutical polymers via click chemistry methodologies. *Bioconjugate Chem,* **2009**, 20 (11), 2001-2016.

[48] Mecerreyes, D., et al., First example of an unsymmetrical difunctional monomer polymerizable by two living/controlled methods. *Macromol. Rapid Comm.,* **2000**, 21 (11), 779-784.

[49] Liu, M.; Vladimirov N.; Frechet J. M. J., A new approach to hyperbranched polymers by ring-opening polymerization of an AB monomer: 4-(2-hydroxyethyl)-ε-caprolactone. *Macromolecules,* **1999**, 32 (20), 6881-6884.

[50] Wolf, F. K.; Frey H., Inimer-Promoted synthesis of branched and hyperbranched polylactide copolymers. *Macromolecules*, **2009**, 42 (24), 9443-9456.

[51] Mahmud, A.; Xiong X. B.; Lavasanifar A., Novel self-associating poly(ethyleneoxide)-block-poly(ε-caprolactone) block copolymers with functional side groups on the polyester block for drug delivery. *Macromolecules*, **2006**, 39 (26), 9419-9428.

[52] Tian, D., et al., Poly(2-oxepane-1,5-dione): a highly crystalline modified poly(ε-caprolactone) of a high melting temperature. *Macromolecules,* **1998**, 31 (3), 924-927.

[53] Tian, D., et al., Ring-opening polymerization of 1,4,8-Trioxaspiro[4.6]-9-undecanone: a new route to aliphatic polyesters bearing functional pendent groups. *Macromolecules*, **1997**, 30 (3), 406-409.

[54] Yan, J., et al., Novel poly(ε-caprolactone)s bearing amino groups: synthesis, characterization and biotinylation. *React. Funct. Polym.*, **2010**, 70 (7), 400-407.

[55] Trollsås, M., et al., Hydrophilic aliphatic polyesters: design, synthesis, and ring-opening polymerization of functional cyclic esters. *Macromolecules,* **2000**, 33 (13), 4619-4627.

[56] John, G.; Morita M., Synthesis of polymer network scaffolds and microspheres based on poly(ε-caprolactone-co-glycolic acid-co-L-serine). *Mat. Sci. Eng. C- Bio. S.,* **2000**, 13 (1-2), 91-95.

[57] John, G.; Sakae T.; Mikio M., Synthesis and modification of new biodegradable copolymers: Serine/glycolic acid based copolymers. *J. Polym. Sci. Pol. Chem.,* **1997**, 35 (10), 1901-1907.

[58] Leemhuis, M., et al., A versatile route to functionalized dilactones as monomers for the synthesis of poly(α-hydroxy) acids. *Eur. J. Org. Chem.*, **2003** (17), 3344-3349.

[59] Seyednejad, H., et al., Synthesis and characterization of hydroxyl-functionalized caprolactone copolymers and their effect on adhesion, proliferation, and differentiation of human mesenchymal stem cells. *Biomacromolecules,* **2009**, 10 (11), 3048-3054.

[60] Leemhuis, M., et al., In vitro hydrolytic degradation of hydroxyl-functionalized poly(α-hydroxy acid)s. *Biomacromolecules,* **2007**, 8 (9), 2943-2949.

[61] Loontjens, C. A. M., et al., Synthesis and characterization of random and triblock copolymers of ε-caprolactone and (benzylated)hydroxymethyl glycolide. *Macromolecules*, **2007**, 40 (20), 7208-7216.

[62] Leemhuis, M., et al., Synthesis and characterization of allyl functionalized poly(α-hydroxy)acids and their further dihydroxylation and epoxidation. *Eur. Polym. J.,* **2008**, 44, 308-317.

[63] Elisseeff, J., et al., Synthesis and characterization of photo-cross-linked polymers based on poly(L-lactic acid-co-L-aspartic acid). *Macromolecules,* **1997**, 30 (7), 2182-2184.

[64] Hu, X., et al., Biodegradable amphiphilic block copolymers bearing protected hydroxyl groups: synthesis and characterization. *Biomacromolecules,* **2008**, 9 (2), 553-560.

[65] Kobayashi, S., Enzymatic polymerization: A new method of polymer synthesis. J*. Polym. Sci. Pol. Chem.,* **1999**, 37 (16), 3041-3056.

[66] Gross, R.A.; Kumar A.; Kalra B., Polymer Synthesis by In Vitro Enzyme Catalysis*. Chemical Reviews*, **2001**, 101 (7), 2097-2124.

[67] Al-Azemi, T. F.; Bisht K. S., Novel functional polycarbonate by lipase-catalyzed ring-opening polymerization of 5-methyl-5-benzyloxycarbonyl-1,3-dioxan-2-one. *Macromolecules*, **1999**, 32 (20), 6536-6540.

[68] Veld, M. A. J.; Palmans A. R. A.; Meijer E. W., Selective polymerization of functional monomers with novozym 435. *J. Polym. Sci. Pol. Chem.*, **2007**, 45 (24), 5968-5978.

[69] Péan, J. M., et al., NGF release from poly(D,L-lactide-co-glycolide) microspheres. effect of some formulation parameters on encapsulated NGF stability. *J. Control. Release*, **1998**, 56 (1-3), 175-187.

[70] Boury, F., et al., Bovine serum albumin release from poly(α-hydroxy acid) microspheres: effects of polymer molecular weight and surface properties. *J. Control. Release*, **1997**, 45 (1), 75-86.

[71] Giteau, A.P., et al., Effect of various additives and polymers on lysozyme release from PLGA microspheres prepared by an s/o/w emulsion technique. *Eur. J. Pharm. Biopharm.,* **2010**, 75,128-136.

[72] Sophocleous, A.M.; Zhang Y.; Schwendeman S. P., A new class of inhibitors of peptide sorption and acylation in PLGA. *J. Control. Release*, **2009**, 137 (3), 179-184.

[73] Houchin, M.; Topp E., Chemical degradation of peptides and proteins in PLGA: A review of reactions and mechanisms. *J. Pharm. Sci.*, **2008**, 97 (7), 2395-2404.

[74] Ghassemi, A.H., et al., Hydrophilic polyester microspheres: effect of molecular weight and copolymer composition on release of BSA. *Pharm. Res.,* **2010**, 27 (9), 2008-2017.

[75] Cristian, V., et al., Microparticles for drug delivery based on functional polycaprolactones with enhanced degradability: loading of hydrophilic and hydrophobic active compounds. *Macromol. Biosci.,* **2010**, 10 (9999), 1-9.

[76] Noga, D.E., et al., Synthesis and Modification of Functional Poly(lactide) Copolymers: Toward Biofunctional Materials. *Biomacromolecules*, **2008**, 9 (7), 2056-2062.

[77] Wang, S.; Cui W.; Bei J., Bulk and surface modifications of polylactide. *Anal. Bioanal. Chem.,* **2005**, 381 (3), 547-556.

[78] Gan, Z., et al., Enzymatic degradation of poly(ε-caprolactone) film in phosphate buffer solution containing lipases. *Polym. Degrad. Stabil.*, **1997**, 56 (2), 209-213.

[79] Seyednejad, H., et al., Preparation and characterization of 3D-printed scaffolds based on functionalized polyesters for bone tissue engineering applications, *Acta Biomater*., **2011**, 7 (5), 1999-2006.

[80] De Smedt S. C.; Demeester J.; Hennink W. E., Cationic polymer based gene delivery systems. *Pharm. Res.,* **2000**, 17 (2), 113-126.

[81] Torchilin, V.P., Cell penetrating peptide-modified pharmaceutical nanocarriers for intracellular drug and gene delivery. *Biopolymers,* **2008**, 90 (5), 604-610.

[82] Bordignon, C., et al., Gene therapy in peripheral blood lymphocytes and bone marrow for ADA- immunodeficient patients. *Science,* **1995**, 270 (5235), 470-475.

[83] Corredor, J.C.; Nagy É., The non-essential left end region of the fowl adenovirus 9 genome is suitable for foreign gene insertion/replacement. *Virus Res.*, **2010**, 149 (2), 167-174.

[84] Ross, P. J.; Kennedy M. A.; Parks R. J., Host cell detection of noncoding stuffer DNA contained in helper-dependent adenovirus vectors leads to epigenetic repression of transgene expression. *J. Virol.*, **2009**, 83 (17), 8409-8417.

[85] Cody, J. J., et al., Arming a replicating adenovirus with osteoprotegerin reduces the tumor burden in a murine model of osteolytic bone metastases of breast cancer. *Cancer Gene Ther.*, **2010**, 17 (12), 893-905.

[86] Cherng, J. Y., et al., Effect of size and serum proteins on transfection efficiency of poly ((2-dimethylamino)ethyl methacrylate)-plasmid nanoparticles. *Pharm. Res.,* **1996**, 13 (7), 1038-1042.

[87] Luten, J., et al., Biodegradable polymers as non-viral carriers for plasmid DNA delivery. J. Control. Release, **2008**, 126 (2), 97-110.

[88] Lim, Y.B., et al., Development of a safe gene delivery system using biodegradable polymer, Poly[α-(4-aminobutyl)-L-glycolic acid]. *J. Am. Chem. Soc.,* **2000**, 122 (27), 6524-6525.

[89] Lim, Y.B., et al., Biodegradable polyester, poly[α-(4-aminobutyl)-L-Glycolic Acid], as a non-toxic gene carrier. *Pharm. Res.*, **2000**, 17 (7), 811-816.

[90] Vroman, B., et al., Copolymers of ε-caprolactone and quaternized ε-caprolactone as gene carriers. *J. Control. Release,* **2007**, 118 (1), 136-144.

[91] Beyerle, A., et al., In vitro cytotoxic and immunomodulatory profiling of low molecular weight polyethylenimines for pulmonary application. *Toxicol. in vitro,* **2009**, 23, 500-508.

[92] Shim, M. S.; Kwon Y. J., Acid-responsive linear polyethylenimine for efficient,specific, and biocompatible siRNA delivery. *Bioconjugate Chem.,* **2009**, 20, 488-499.

[93] Shim, M. S.; Kwon Y. J., Controlled cytoplasmic and nuclear localization of plasmid DNA and siRNA by differentially tailored polyethylenimine. *J. Control. Release,* **2009**, 133, 206-213.

[94] Reul, R.; Nguyen J.; Kissel T., Amine-modified hyperbranched polyesters as non-toxic, biodegradable gene delivery systems. *Biomaterials,* **2009**, 30 (29), 5815-24.

[95] Liu, M., et al., Novel poly(amidoamine)s with pendant primary amines as highly efficient gene delivery vectors. *Macromol. Biosci.,* **2010**, 10 (4), 384-392.

Chapter 3

Synthesis and Characterization of Hydroxyl-Functionalized Polyesters and Their Effect on Adhesion, Proliferation, and Differentiation of Human Mesenchymal Stem Cells

Hajar Seyednejad
Natalja E. Fedorovich
Roel van Eijk
Mies J. van Steenbergen
Wouter J. A. Dhert
Tina Vermonden
Cornelus F. van Nostrum
Wim E. Hennink

Biomacromolecules
2009, 10 (11), 3048- 3054

The aim of this study was to develop new hydrophilic polyesters for tissue engineering applications. In our approach, (poly(benzyloxymethyl glycolide-co-ε-caprolactone), pBMGCL)'s were synthesized through melt copolymerization of ε-caprolactone (CL) and benzyl protected hydroxymethyl glycolide (BMG). Deprotection of the polymers yielded copolymers with pendant hydroxyl groups (poly(hydroxymethylglycolide-co-ε-caprolactone), pHMGCL). The synthesized polymers were characterized by GPC, NMR and DSC techniques. The resulting copolymers consisting up to 10 % of HMG monomer were semi-crystalline with a melting temperature above body temperature. Water contact angles measurements of polymeric films showed that increasing HMG content resulted in higher surface hydrophilicity as evidenced form decrease in receding contact angle from 68° for PCL to 40° for 10%HMGCL. Human mesenchymal stem cells showed good adherence onto pHMGCL films as compared to the more hydrophobic PCL surfaces. The cells survived and were able to differentiate towards osteogenic lineage on pHMGCL surfaces. This study shows that the aforementioned hydrophilic polymers are attractive candidates for the design of scaffolds for tissue engineering applications.

1. Introduction

Tissue engineering is a multidisciplinary field, which combines the principles of engineering and life sciences towards generating replacements for biological tissues and organs which have lost their function due to a disease or an accident.[1, 2] The key elements for the success of tissue regeneration are: cells, scaffold, cell/matrix interactions along with signaling and therapeutic molecules.[3] Scaffolds- those porous, three-dimensional, temporary structures- play an important role in manipulating cell function and guidance of new organ formation.[4] The scaffolds reported so far are mainly based on biodegradable polymers among which aliphatic polyesters such as PLA, PGA, PCL and their copolymers.[1, 5-8]

While the ester groups in the main chain of these polymers ensure biodegradation due to hydrolysis, the absence of pendant functional groups limits the versatility of these materials.[9] Besides, these polymers are mostly hydrophobic materials and their application is limited when cell adhesion is considered. There are different methods to improve the surface characteristics of polymeric scaffolds such as plasma treatment[10-12] , surface entrapment of a second polymer[13-15] and partial surface hydrolysis by acid or base treatment[16] but these methods have some limitations, such as limited amount of penetration into pores of the scaffold or causing the degradation of the aliphatic polyester scaffolds.[17] The introduction of functional groups in these polymers is an important alternative to tailor the physical and chemical properties such as hydrophilicity and degradation rate[18-21] and also opens opportunities for further functionalization with biologically active molecules[22-25] to enhance cell/matrix interaction.

The goal of this study was to develop a new functionalized polymer with appropriate physical properties and controlled cell response. Therefore, we recently introduced a novel functionalized dilactone with protected hydroxyl groups, benzyloxymethyl glycolide.[26] The deprotected homopolymers of this monomer are not suitable for making scaffolds for tissue engineering due to its rapid degradation.[27] Hence, in the present work we synthesized and deprotected random copolymers of benzyl protected hydroxymethyl glycolide (BMG) and ε-caprolactone (CL). CL was chosen because poly(ε-caprolactone) is a biocompatible and biodegradable polymer widely used in biomedical applications. However, poly(ε-caprolactone) degrades very slowly[28] with a degradation rate ranging from 2 to 4 years[29] and the polymer is not favorable for cell adhesion and proliferation due to its intrinsic hydrophobicity and lack of bioactive functional groups.[30, 31] In this study, we investigated the effect of

chemical structure of these functionalized polyesters on their physical properties as well as on adhesion, survival and osteogenic differentiation of human mesenchymal stem cells (hMSCs), which are important parameters to design scaffolds for tissue engineering applications.

2. Materials and methods

2.1. Materials

All chemicals used in this study were purchased from Aldrich and used as received, unless stated otherwise. All solvents were purchased from Biosolve (Valkenswaard, The Netherlands) except acetone (Merck, Darmstadt, Germany), hexane (Antonides-Interchema, Oosterzee, The Netherlands), toluene, and sulfuric acid (Acros, Geel, Belgium). Toluene was distilled from P_2O_5 and stored over 3 Å molecular sieves under argon. Tetrahydrofuran (THF) was distilled from sodium/benzophenone. 3*S*-Benzyloxymethyl-1,4-dioxane-2,5-dione (BMG) was synthesized as described by Leemhuis et al.[26, 32] ε-Caprolactone, 1,4-butanediol, and silica gel (0.035-0.070 mm, 60 Å) were obtained from Acros (Geel, Belgium). ε-Caprolactone (CL) was distilled from CaH_2. *O*-Benzyl-L-serine was supplied by Senn Chemicals (Dielsdorf, Switzerland). Sodium nitrite ($NaNO_2$) and dimethylaminopyridine (DMAP) were purchased from Fluka (Zwijndrecht, The Netherlands). Sodium sulfate (Na_2SO_4), triethylamine, sodium carbonate (Na_2CO_3), and benzyl alcohol (BnOH) were provided by Merck (Darmstadt, Germany). Bromoacetyl bromide, tin(II) 2-ethylhexanoate ($SnOct_2$) and Pd/C (palladium, 10 wt % (dry basis) on activated carbon, wet (50% water w/w), Degussa type E101 NE/W) were obtained from Aldrich (Zwijndrecht, The Netherlands).

Phosphate buffer saline (PBS) was purchased from Braun (The Netherlands). Ethylenediamine tetraacetic acid (EDTA)/trypsin was provided by PAA (Germany). Bovine serum albumin (BSA) was purchased from HyClone (Perbio, The Netherlands). Tissue culture polystyrene plates (TCPS) and non-adhesive cell culture plates were provided by Greiner bio-one (Germany). Human mesenchymal stem cells (hMSCs) were isolated from bone marrow aspirates, obtained from donors with written informed consent, and culture-expanded as described previously.[33] Briefly, aspirates were resuspended by using 20-gauge needles, plated at a density of $5x10^5$ cells per cm^2 and cultured in hMSC expansion medium consisting of αMEM (Invitrogen, Breda, The Netherlands) supplemented with 10% FBS (Lonza, Basel, Switzerland), 0.1 mM ascorbic acid (Sigma-Aldrich, Zwijndrecht, The Netherlands), 2 mM L-glutamine (Glutamax,

Invitrogen), 100 U/ml penicillin, 100 μg/ml streptomycin (Invitrogen), and 1 ng/ml rhFGF-basic (233-FB, R&D Systems). Medium was refreshed twice a week and cells were used for further subculturing or cryopreservation. Cell cultures were maintained in a humidified incubator at 5% CO_2 and 37°C. hMSCs passage 3-6 were used in the study.

2.2. Characterization

2.2.1. NMR Spectroscopy

NMR measurements were performed using a Gemini 300 MHz spectrometer (Varian Associates Inc., NMR Instruments, Palo Alto, CA). Chemical shifts were recorded in ppm with reference to the solvent peak (δ= 7.26 ppm and δ=77.3 ppm for $CDCl_3$ in ^{1}H NMR and ^{13}C NMR, respectively).

2.2.2. Gel Permeation Chromatography (GPC)

The molecular weights of the obtained polymers were measured by means of GPC using a 2695 Waters Aliance system and a Waters 2414 refractive index detector. Two PL-gel 5 μm mixed-D columns fitted with a guard column (Polymer Labs, M_w range 0.2- 400 KDa) were used. The columns were calibrated with polystyrene standards of known molecular weights using HPLC grade chloroform for the protected copolymers and AR grade THF for the deprotected copolymers, eluting at 1 mL/min flow rate at 30 °C. The concentration of samples was 5 mg/mL and the injection volume was 50 μL.

2.2.3. Differential Scanning Calorimetry (DSC)

Thermal properties of the different polymers were evaluated using a TA Instruments DSC Q2000 apparatus. Scans were taken from -80 °C to 100 °C with a heating rate of 10 °C/min and a cooling rate of 0.5 °C/min under nitrogen flow rate of 50 mL/min. The glass transition temperature (T_g) was recorded as the midpoint of heat capacity change in the second heating run. T_m and heat of fusion (ΔH_f) were determined from the onset of endothermic peak position and integration of endothermic area in the second heating run, respectively.

2.2.4. Fourier Transformed Infrared Spectroscopy (FT-IR)

The Fourier transformed infrared spectra of polymers were recorded in transmission mode on a Bio-Rad FTS6000 FT-IR spectrometer with Win-IR Pro software (Cambridge, MA). Spectra were obtained from KBr tablets compressed

at 10 tons with a hydraulic press. Each tablet contained about 10 mg of polymers. Scans (64) were co-added at 2 cm^{-1} resolutions at a scan speed of 0.16 cm/s (5 kHz laser modulation).

2.3. Methods

2.3.1.Synthesis of Poly (ε-caprolactone) (PCL)

Poly(ε-caprolactone) was synthesized via ring opening polymerization, using BnOH and $SnOct_2$ as initiator and catalyst, respectively. Both distilled and non-distilled CL were used to investigate whether as-received monomer can be used without further purification. In a typical procedure with a monomer/initiator ratio of 300/1, CL (324 mg, 2.84 mmol) was added to the dry Schlenk tube under a dry N_2 atmosphere. Initiator (BnOH, 9.46 µmol) and catalyst ($SnOct_2$, 4.7 µmol) were added from stock solutions in toluene. The tube was evacuated for 1 hour, then closed and immersed in an oil bath which was heated at 130 °C. Polymerization was performed overnight and three different monomer/initiator molar ratios were used, namely 100/1, 200/1 and 300/1. The formed polymers were dissolved in chloroform, precipitated in cold methanol and dried overnight under vacuum. The obtained polycaprolactones were characterized by ^{1}H NMR, GPC and DSC.

^{1}H NMR ($CDCl_3$): δ=1.3- 1.5 (m, O- CH_2- CH_2 - C*H_2* - CH_2 - CH_2 –CO), 1.5- 1.7 (m, O- CH_2 - C*H_2* – CH_2 - C*H_2* - CH_2 –CO), 2.2- 2.4 (t, CH_2 - CH_2 - CH_2 - C*H_2* –CO), 4.0 (t, O- C*H_2*)

2.3.2. Synthesis of Random Copolymers of CL and BMG (poly(benzyloxymethyl glycolide-co-ε-caprolactone), pBMGCL)

Synthesis of BMG-caprolactone random copolymers was carried out in a dried Schlenk tube equipped with magnetic stirrer. In a typical procedure, CL (801 mg, 7.01 mmol) and BMG (184 mg, 0.77 mmol) were introduced into the tube under a dry nitrogen atmosphere. Next, initiator (BnOH, 0.025 mmol) and catalyst ($SnOct_2$, 0.012 mmol) from stock solutions in toluene were loaded into the tube. The tube was evacuated for 2 hours, subsequently closed and immersed in an oil bath thermostated at 130 °C. The polymerization was performed overnight and the formed polymers were purified in the same manner as described for poly(ε-caprolactone).

^{1}H NMR ($CDCl_3$): δ= 1.3-1.4 (m, CH_2-CH_2-*CH_2*-CH_2-CH_2), 1.5-1.7 (m, CH_2-*CH_2*-CH_2-*CH_2*-CH_2), 2.3 (t, CH_2-*CH_2*-CO), 2.4 (t, CH_2-*CH_2*-CO), 3.7-4.0 (m, CH-*CH_2*), 4.0 (t, O-*CH_2*-CH_2), 4.0 (t, O-*CH_2*-CH_2), 4.4- 4.9 (m, *CH_2*-Ar, O-*CH_2*-CO), 5.1-5.5 (m, C*H*), 7.2-7.4 (m, C-*H_{Ar}*).

^{13}C NMR ($CDCl_3$): δ= 24.0-24.7 (m, CH_2), 24.9- 25.6 (m, CH_2), 27.8-28.5 (m, CH_2), 33.2-34.3 (m, CH_2), 59.9- 61.5 (m, CH_2), 64.1 (s, CH_2), 64.9-65.7 (m, CH_2), 68.0-68.9 (m, CH_2), 70.4-70.9 (m, CH), 71.2-71.4 (m, CH_2), 71.5-73.1 (m, CH), 73.4 (s, CH_2), 127.4-128.7 (m, CH_{Ar}), 137.1-137.8 (m, C_{Ar}), 166.1-168.0, (m, C=O), 171.8-171.9 (m, C=O), 172.4-172.9 (m, C=O), 173.4 (s, C=O), 173.5 (s, C=O).
IR (KBr): v= 3504 cm^{-1} (-OH), 3032 cm^{-1} (benzyl), 2946, 2868 cm^{-1} (CH_2), 1751 cm^{-1} (C=O), 741, 699 cm^{-1} (benzyl).

2.3.3. Removal of Benzyl Groups of Protected Random Copolymers of CL and BMG to Yield Poly(hydroxymethylglycolide-co-ε-caprolactone), (pHMGCL)

Protecting benzyl groups of pBMGCL were removed in a hydrogenation reaction using Pd/C catalyst essentially as described by Leemhuis et al.[26] In short, pBMGCL (700 mg, 0.059 mmol) was dissolved in dry THF (90 mL) and subsequently the catalyst (43 mg, 0.106 mmol) was added. The flask was filled with hydrogen in three consecutive steps of evacuation, refilling with H_2 and the reaction was done under H_2 pressure overnight. The catalyst was removed afterwards using a glass filter and THF was removed by evaporation. The deprotected polymers were characterized by NMR, DSC and GPC.
^{1}H NMR ($CDCl_3$): δ=1.2-1.4 (m,CH_2-CH_2-C*H*$_2$-CH_2-CH_2), 1.5-1.7 (m, CH_2-C*H*$_2$-CH_2-C*H*$_2$-CH_2, O-CH_2-C*H*$_2$-C*H*$_2$-CH_2-O), 2.3 (t, CH_2-C*H*$_2$-CO), 2.4 (t, J) 6.7 CH_2-C*H*$_2$-CO), 3.7-4.4 (m, CH-C*H*$_2$, O-C*H*$_2$-CH_2), 4.5-5.1 (m, O-C*H*$_2$-CO), 5.0-5.4 (m, C*H*).
IR (KBr): v= 3496 cm^{-1} (-OH), 2948, 2869 cm^{-1} (CH_2), 1744 cm^{-1} (C=O).

2.3.4. Preparation of Polymeric Films by Spin Coating

To prepare uniform polymeric films, the different polymers were dissolved in chloroform (0.2 g/mL) and spin coated (Specialty Coating Systems, Inc. model: P6708D) for 120s at speed of 1800 ~ 2000 rpm on round glass coverslips of 22 mm diameter (Fisher Scientific, The Netherlands). Subsequently, the films were put in a vacuum oven at room temperature for 48 hours to evaporate the solvent.

2.3.5. Water Contact Angle Measurements

The wettability of polymer films was evaluated by measuring advancing and receding water contact angles using sessile drop technique (Data Physics,

OSC50). For advancing contact angle (Adv-CA), a water droplet (10µL) was placed onto the surface of a polymeric film and the contact angle between water and surface was measured immediately by taking pictures of the droplet using an optical microscope and averaging the right and left angles using surface contact angle software (SCA20, DataPhysics). For receding contact angle (Rec-CA), the water droplet was withdrawn slowly and the contact angle was measured after different time points. The reported values are the mean values of at least four measurements on each surface.

2.3.6. Viability analysis

To test cell viability on polymer surfaces, hMSCs from passage 3 were seeded on 8% pHMG-CL and PCL polymer films at 5000 cells/cm^2, cultured in expansion medium and the viability of the cells was analyzed after one and seven days. Cells seeded on tissue culture poly(styrene) **(**TCPS) were used as a control. The viability of the cells was determined by a LIVE/DEAD assay (Molecular Probes MP03224, Eugene, USA) according to the manufacturer's recommendations. At least 250 cells per group were observed and scored using a fluorescence microscope. The excitation/emission filters were set at 488/530 nm to observe living (green) cells and at 530/580 nm to detect dead (red) cells. The cell viability was calculated as the average ratio of vital to total cells in a sample. All values are reported as mean ± standard deviation.

2.3.7. Cell Adhesion

hMSCs from passage 6 were used to investigate their adhesion on polymeric films with graded hydrophilicity. The polymeric films were placed in the wells of a 12-well non-adhesive plate (n = 4). Then 20,000 cells were seeded per well and allowed to adhere onto the polymeric surfaces in expansion medium. At different time intervals (6 hrs and 24 hrs) the plates were washed three times with PBS in order to remove the unattached cells. The adhered cells were detached using trypsin (0.5 mg/mL)/EDTA (0.22 mg/mL) for 10 minutes at 37 °C and resuspended in PBS with 1 % BSA. Finally, the total numbers of cells were counted using a BD FACSCanto™ II Flow Cytometry System. TCPS was used as positive control.

2.3.8. Analysis of osteogenic differentiation

To study osteogenic differentiation, hMSCs from passage 3 were detached from

culture flasks, seeded at 5000 cells/cm^2 on 8% pHMG-CL and PCL films (n=3) and cultured in osteogenic differentiation medium (αMEM (Invitrogen) supplemented with 10% FBS (Lonza), 0.1 mM ascorbic acid 2-phosphate (AsAP; Sigma-Aldrich), 2 mM L-glutamine (Glutamax, Invitrogen), 100 U/ml penicillin, 100 μg/ml streptomycin (Invitrogen), 10^{-8} M dexamethasone (Sigma-Aldrich) and 10 mM β-glycerophosphate (Sigma-Aldrich), for one and two weeks. Cells seeded on tissue culture polystyrene (TCPS) and cultured in osteogenic medium were used as a positive control. hMSCs cultured on TCPS in expansion medium served as negative controls.

Osteogenic differentiation of hMSCs was assessed by alkaline phosphatase staining and collagen type I immunocytochemistry after, respectively, one and two weeks. For the evaluation of alkaline phosphatase activity, the cells were fixed in 4% formalin and permeabilized in 0.2% Triton X-100 in Tris buffered saline for ten minutes. The cells were subsequently stained with Fuchsin Substrate-Chromogen system (DAKO, Carpinteria, USA) according to the manufacturer's protocol. Monolayers were counterstained with hematoxylin and mounted with Aquatex. The presence of alkaline phosphatase positive cells (pink-red) was visualized with an Olympus BX50 light microscope equipped with an Olympus DP 70 camera. For immunocytochemical analysis of collagen type I, the monolayers were fixed for 10 minutes in 4% formalin, permeabilized with 0.2% Triton X-100 in PBS, blocked in 3% (w/v) BSA in PBS for 30 min and incubated with mouse anti-collagen type I antibody (20 µg/ml in 5% (w/v) BSA in PBS, Merck, Japan) for one hour. A biotinylated secondary antibody was applied (1/200 in 5% (w/v) BSA in PBS, biotinylated sheep anti-mouse, GE Healthcare, Diegem, Belgium) for one hour and the staining was enhanced by incubation with streptavidine-peroxidase for one hour (2 µg/ml in 5% (w/v) BSA in PBS, Immunotec, Montreal, Canada). The staining was developed with DAB and counterstained with Mayer's hematoxylin.

3. Results and discussion

3.1. Poly(ε-caprolactone) synthesis

Ring opening polymerization of CL was performed at 130 °C using BnOH and $SnOct_2$ as initiator and catalyst, respectively. The molar ratio between catalyst and initiator was kept constant at 0.5. Both distilled and as-received CL were used to investigate whether the non-purified CL could be used for polymerization reactions. No significant differences were observed for the thermal properties as well as molecular weight of the polymers synthesized with both non-purified and

distilled monomer; hence the as-received monomer was used in the further polymerizations.

3.2. Synthesis of Random Copolymers of CL and BMG

Random copolymers of ε-caprolactone (CL) and benzyl protected hydroxyl methyl glycolide (BMG) were synthesized at 130 °C in an overnight reaction using BnOH and $SnOct_2$ as initiator and catalyst, respectively (Fig. 1).

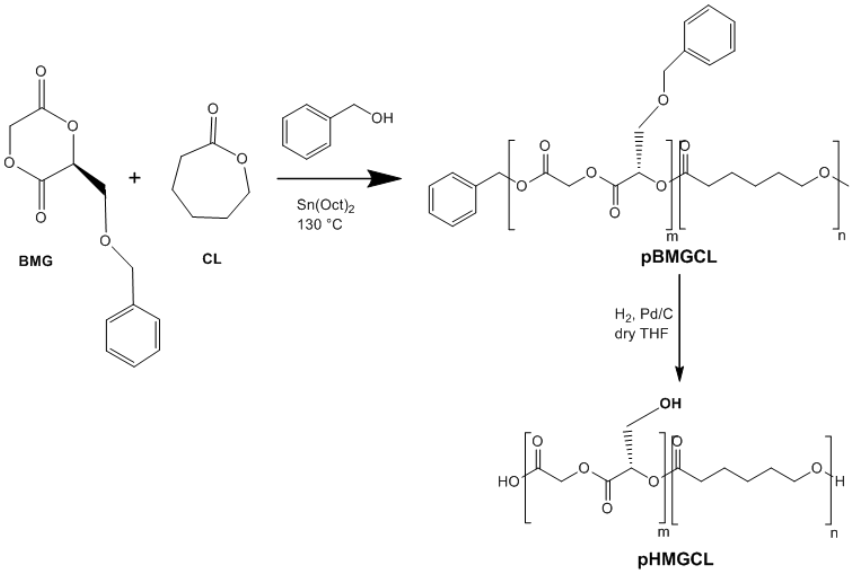

Fig1. Synthesis of BMG-CL and HMG-CL random copolymers

Stannous octoate was used as the catalyst since it is frequently used in ring opening polymerization.[34] The removal of the protecting groups was done in an overnight reaction in dry THF, using H_2 as reducing agent and the formed copolymers were characterized by ^1H NMR. As can be seen in Fig. 2, disappearance of the peak of protective benzyl groups at 7.2 ppm demonstrates full deprotection.

Different amounts of the BMG monomer (from 4 to 10 mol %) were used to synthesize the random copolymers. The copolymer compositions were measured using ^1H NMR by comparison between the integration of CH_2 peak of BMG monomer (at 3.7- 4.0 ppm) to those of CL monomer (the average of peak signals at 1.3- 1.5 ppm, 2.2- 2.4 ppm, 4.0- 4.2 ppm). Table 1 shows that the copolymer compositions are very close to the feed ratio of the monomers.

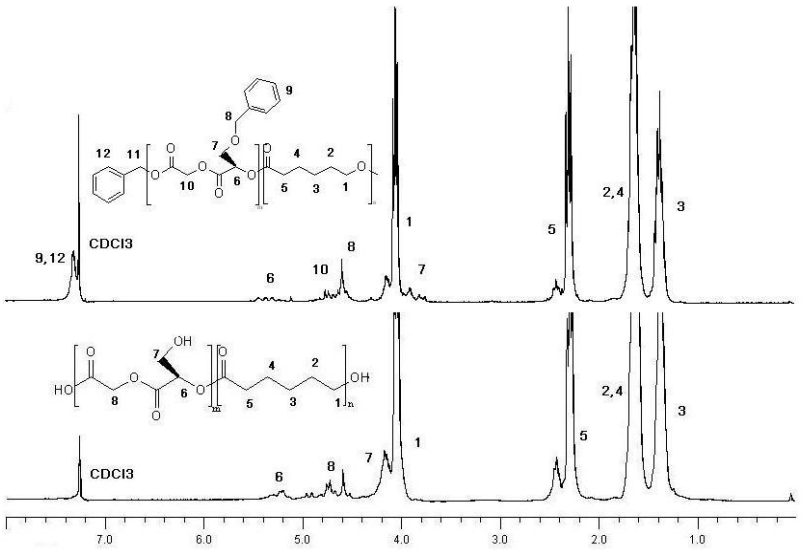

Fig 2. ^{1}H NMR spectra of protected (pBMGCL) (above) and deprotected (pHMGCL) (below) random copolymers dissolved in $CDCl_3$

Analysis of thermal properties of the copolymers before and after deprotection showed that with increasing BMG content in the copolymer, both the melting temperature and the extent of crystallinity (as reflected by ΔH_f) were decreased. For instance, the melting temperatures as well as the heat of fusion decreased from 57 °C and 72 J/g for polycaprolactone to 37 °C and 40 J/g for the protected copolymer with 10 % of BMG (Table 1). Both protected and deprotected copolymers were semi-crystalline, which indicates that the BMG content was not large enough to prevent the PCL segments to crystallize. Furthermore, the melting temperature of the copolymers up to 13 % of HMG monomer was above 37 °C (Table 1), which makes these polymers suitable candidates to make scaffolds for in vivo applications since they are dimensionally stable at body temperature. In addition, the glass transition temperature of the polymers was between -65 °C to -43 °C and only one T_g was observed in the second heating run of these copolymers, which means that the copolymers had a random structure.

Table1. Properties of BMG-CL polymers synthesized with increasing amounts of BMG monomer at M/I molar ratio of 300

BMG/CL Molar Ratio In feed	BMG/CL Molar Ratio In polymer	Yield (%)	pBMGCL					pHMGCL				
			DSC			GPC		DSC			GPC	
			T_m (°C)	ΔH_f (J/g)	T_g (°C)	M_w (kDa)	PDI	T_m (°C)	ΔH_f (J/g)	T_g (°C)	M_w (kDa)	PDI
0/ 100	0/ 100	90	-	-	-	-	-	57	72.6	-60	34.7	2.5
4/ 96	3.5/ 96.5	80	49	56.3	-55	68.3	2.0	50	57.3	-56	57.8	1.9
6/ 94	5.5/ 94.5	89	46	53.6	-52	59.8	1.9	48	56.7	-53	58.4	1.8
8/ 92	10/ 90	88	42	47.2	-49	47.0	2.1	45	54.9	-50	40.0	1.9
10/ 90	13/ 87	86	37	40.6	-44	36.7	2.3	40	51.2	-43	31.7	1.9

Polymerization reactions at 130 °C, overnight.

Table 1 shows that M_w and M_n of the copolymers decreased with increasing amount of BMG monomer. This might be due to trace impurities present in the BMG monomer (e.g. the open ring structure of BMG, (S)-3-(benzyloxy)-2-(2-bromoacetoxy)propanoic acid), which can act as initiator.[35] Table 1 also shows that there was no considerable change in the molecular weight of polymers after deprotection which shows that in accordance with previous observations no chain scission occurred during the deprotection reaction.[26, 36] The slight difference between the molecular weight of protected and deprotected polymers can be attributed to either the loss of benzyl groups after deprotection or the difference in polymer–GPC eluent interaction.

We also investigated the effect of change in the monomer/initiator (M/I) ratio on the molecular weight of random copolymers with 2 % and 10 % of BMG monomer. As can be seen in Table 2, for the copolymers with 2 % BMG, the molecular weight of polymers increased with increasing the monomer to initiator ratio which means that the molecular weight of these copolymers can be controlled by M/I ratio. It turned out that the molecular weights of copolymers synthesized with higher BMG content (e.g. 10 %) were not well tailorable with M/I ratio (results not shown).

Table 2. Effect of M/I ratio on characteristics of BMG-CL random copolymers (2 % BMG)

M/I Molar Ratio	Yield (%)	pBMGCL					pHMGCL				
		DSC			GPC		DSC			GPC	
		T_m (°C)	ΔH_f (J/g)	T_g (°C)	M_w (kDa)	PDI	T_m (°C)	ΔH_f (J/g)	T_g (°C)	M_w (kDa)	PDI
100	92	52	72.2	-55	29.6	2.3	51	64.3	-46	26.3	2.2
200	90	52	66.1	-56	54.9	2.1	52	64.9	-57	37.4	2.3
300	95	51	65.3	-58	63.5	2.1	52	61.5	-56	51.6	2.4
400	96	53	64.8	-56	78.7	2.1	53	61.9	-57	59.0	2.5

3.3. Wettability of polymeric films

Contact angle (CA) measurements were performed to study the copolymer-dependent hydrophilicity of polymer films. Advancing water contact angles (Adv-CA) on the polymer films prepared by spin coating were measured by placing a water droplet on the surface and measuring the contact angles immediately. As it can be seen in Fig. 3, the PCL Adv-CA was 77.7 ± 4.5° which is in agreement with published data.[37] For the copolymers having 4 to 10 % of HMG monomer, the Adv-CA varied from 82.5 ± 0.7° to 73.0 ± 2.6°. The receding CA (Rec-CA) was measured in time. Figure 3 shows that the Rec-CA on PCL slightly decreased in time from 74.7 ± 4.1° to 68.7 ± 6.5°. Importantly, incorporation of HMG in the copolymer film resulted in substantial reduction of Rec-CA. For instance, the Rec-CA for 10% HMG-CL copolymer decreased from 64.0 ± 2.0° to 39.6 ± 5.8° after one minute to 20 minutes of water contact, respectively.

This large difference in Adv-CA and Rec-CA after prolonged exposure to water can be explained as follows. In contact with air, which is a rather hydrophobic medium, the hydroxyl groups will be buried in the bulk of the polymer film. Upon exposure to water, the polymer reorients its polar hydroxyl groups to the surface and thereby hydrophilicity increases.[38, 39] The minimization of the interfacial energy is the driving force for the change in the orientation of the surface molecules in different environments.[40]

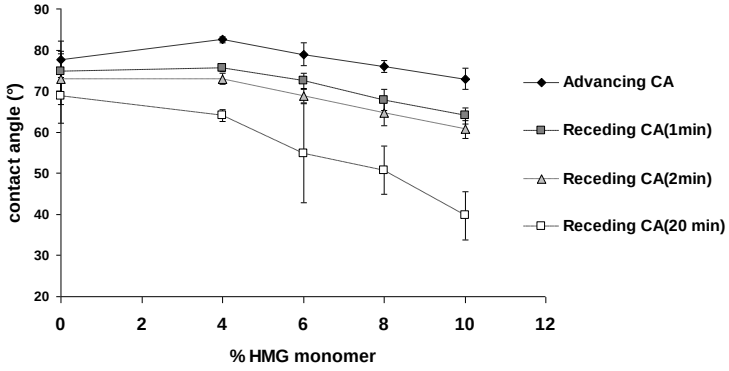

Fig 3. Advancing- receding water contact angles of HMG-CL polymeric films (mean ± SD, n = 4)

3.4. Morphology and viability of human MSCs on polymeric surfaces

To assess to which degree polymer films affect the viability of seeded hMSCs, their survival was studied after one and seven days. A control population of hMSCs in fresh medium on TCPS surfaces was used to determine the relative cell survival. After one and seven days, reduced spreading and survival of hMSCs on PCL films compared to pHMGCL was observed (Fig. 4). Cells attached well on pHMGCL films after one day, while they were less spread out on PCL films and some of the cells exhibited round morphology. After seven days, hMSCs cultured on pHMGCL covered the whole surface of the polymer, resembling the stretched morphology on TCPS surfaces, while hMSCs on PCL films were mostly clustered and hardly spread out on this polymer film (Fig. 4). Viability of cells adhering onto pHMGCL films was 97±1% at day one and 99±1% at day seven on pHMGCL films and comparable with the high viability of cell monolayers on TCPS. On PCL films cell viability was limited to only 69±12% after one day and to 78±7% viable cells after seven days.

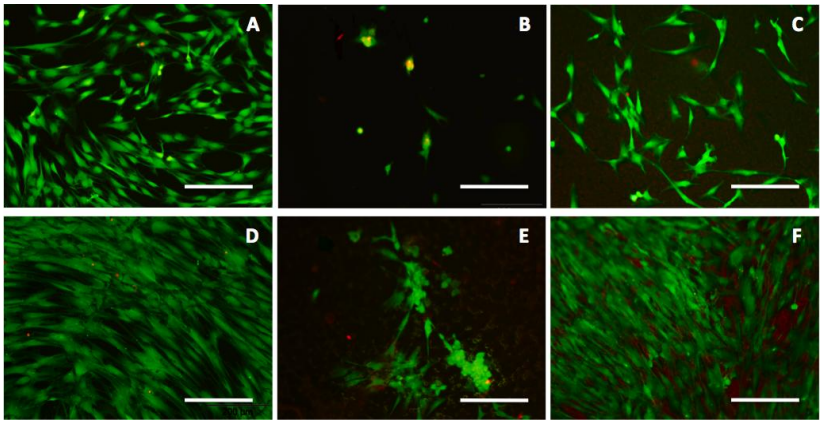

Fig 4. Viability analysis of seeded hMSCs after one (A-C) and seven (D-F) days of culture, viable cells (green), dead cells (red), scale bar is 200 µm; A/D: TCPS; B/E: PCL; C/F: pHMG-CL films.

3.5. Attachment of human MSCs on polymeric surfaces

The adhesion of hMCSs on pHMGCL surfaces was investigated. TCPS, a material routinely used for adhesion of cells with a CA of 62 ± 2° [41] was used as positive control. As shown in Fig. 5, there was no significant difference between the numbers of attached cells on pHMGCL surfaces and on TCPS after 6 hours,

while the number of adhered cells on PCL surface was significantly lower than on TCPS. After 24 hours, the number of adhered cells on polymeric surface with 8% HMG increased, while the change between 6 and 24 hours on other polymeric surfaces was not significantly different. Also, after 24 hours the number of attached cells on PCL was much lower than that on the more hydrophilic surfaces as well as on TCPS.

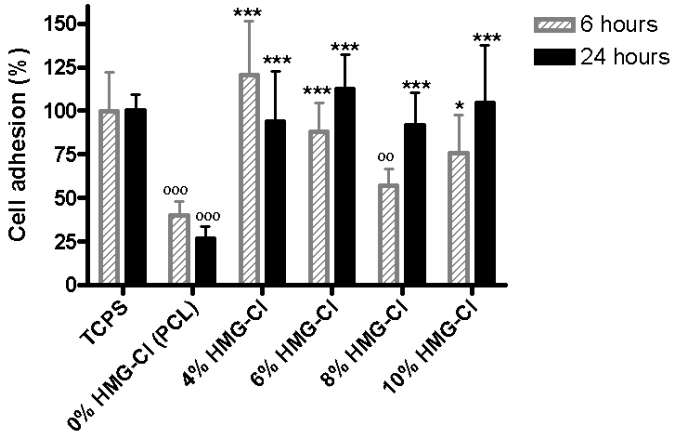

Fig 5. Adhesion of human mesenchymal stem cells onto polymeric films (surface area of 3.7 cm^2) with graded hydrophilicity (mean ± 95% confidence intervals, n = 4). Numbers of adhered cells were normalized to the number of cells adhered on TCPS. Circles indicate (°° p< 0.01, °°° p< 0.001) significantly lower than number of adhered cells on TCPS. Asterisks indicate (* p< 0.05, ** p< 0.01, *** p< 0.001) significantly higher than number of adhered cells on PCL.

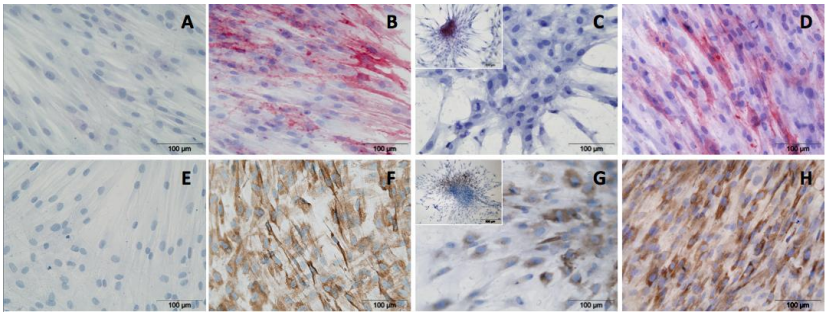

Fig 6. Osteogenic differentiation of hMSCs on polymeric films. ALP staining (red) after one week (A-D); collagen type I staining (brown) after two weeks (E-H), counterstaining with hematoxylin; hMSCs cultured on TCPS in expansion medium (A/E) and in osteogenic medium (B/F); hMSCs on PCL (C/G; inset: cell-clusters) and pHMGCL films (D/H).

Overall, the results show that hMCSs adhered substantially better on more hydrophilic surfaces than on PCL. This is in agreement with the others' findings that cells preferably adhere on moderate hydrophilic surfaces[40] with a contact angle around 55°.[41, 42]

3.6. Osteogenic differentiation of human MSCs on polymeric films

When determining alkaline phosphatase activity (Fig. 6A-D), which is present early during osteogenic differentiation, we observed that after seven days ALP was abundant in cells cultured on pHMGCL films. ALP activity of hMSCs seeded on PCL films was only present in large cell clusters. Immunocytochemical analysis of hMSCs incubated for two weeks in osteogenic medium (Fig. 6E-H) revealed the presence of the late osteogenic marker collagen type I in hMSCs cultured on pHMGCL films. The presence of collagen type I staining on PCL surfaces was much lower and limited to large groups of cells. These findings indicate that hMSCs retain the ability to differentiate along the osteogenic lineage after seeding on pHMGCL polymeric surfaces.

4. Conclusions

Random copolymers of BMG and CL were synthesized by melt polymerization using BnOH and $SnOct_2$ as initiator and catalyst, respectively. The copolymers were fully deprotected to yield copolymers with hydroxyl functional groups in their structure (pHMGCL). The aforementioned copolymers having up to 10 % of HMG monomer were semi-crystalline with a melting temperature above body temperature. This enables the use of these polymers for the design of stable scaffolds in tissue engineering. It was also shown that the wettability of these polymers can be tuned by the percentage of HMG monomer in the copolymer. The increase in the hydrophilicity of the HMG-CL copolymers as compared to PCL resulted in an improved adherence of hMSCs onto polymeric surfaces. Human MSCs were viable on pHMGCL films and differentiated towards osteogenic lineage. In conclusion, we successfully obtained materials with tunable hydrophilicity and cell adhesion properties, which support survival and osteogenic differentiation of human MSCs and thus are interesting candidates for tissue engineering applications.

5. Acknowledgment

The authors wish to acknowledge Mr. Carlos van Kats for his help with spin coating of polymers and the Dutch Program for Tissue Engineering (DPTE) for financial support (project number 6731).

Reference

[1] Langer, R.; Vacanti, J. P. Tissue Engineering. *Science* **1993**, 260, 920-926.

[2] Place, E. S.; George, J. H.; Williams, C. K.; Stevens, M. M. Synthetic polymer scaffolds for tissue engineering. *Chem. Soc. Rev* **2009**, 38, 1139–1151.

[3] Murugan, R.; Ramakrishna, S. Nano-featured scaffolds for tissue engineering: A review of methodologies. *Tissue Eng.* **2006**, 12, 435-447.

[4] Chen, G.; Tateishi, T. U. T. Scaffold design for tissue engineering. *Macromol. Biosci.* **2002**, 2, 67-77.

[5] Freyman, T. M.; Yannas, I. V.; Gibson, L. Cellular materials as porous scaffolds for tissue engineering. *Prog. Mater Sci.* **2001**, 46, 273-282.

[6] Li, W. J.; Tuli, R.; Huang, X.; Laquerriere, P.; Tuan, R. S. Multilineage differentiation of human mesenchymal stem cells in a three-dimensional nanofibrous scaffold. *Biomaterials* **2005**, 26 , 5158-5166.

[7] Reignier, J.; Huneault, M. A. Preparation of interconnected poly(ε-caprolactone) porous scaffolds by a combination of polymer and salt particulate leachin. *Polymer* **2006**, 47, 4703-4717.

[8] Srivastava, R. K.; Albertsson, A. C. Porous scaffolds from high molecular weight polyesters synthesized via enzyme-catalyzed ring-opening polymerization. *Biomacromolecules* **2006**, 7, 2531-2538.

[9] Noga, D. E.; Petrie, T. A.; Kumar, A.; Weck, M.; Garcia, A. J.; Collard, D. M. Synthesis and modification of functional poly(lactide) copolymers: Toward biofunctional materials. *Biomacromolecules* **2008**, 9, 2056-2062.

[10] Pompe, T.; Keller, K.; Mothes, G.; Nitschke, M.; Teese, M.; Zimmermann, R.; Werner, C., Surface modification of poly(hydroxybutyrate) films to control cell-matrix adhesion. *Biomaterials* **2007**, 28, 28-37.

[11] Yang, F.; Qu, X.; Cui, W.; Bei, J.; Yu, F.; Lu, S.; Wang, S., Manufacturing and morphology structure of polylactide-type microtubules orientation-structured scaffolds. *Biomaterials* **2006**, 27, 4923-4933.

[12] Yang, J.; Bei, J.; Wang, S. Enhanced cell affinity of poly (D,L-lactide) by combining plasma treatment with collagen anchorage. *Biomaterials* **2002**, 23, 2607-2614.

[13] Desai, N. P.; Hubbell, J. A. Surface physical interpenetrating networks of poly(ethylene terephthalate) and poly(ethylene oxide) with biomedical applications. *Macromolecules* **1992**, 25, 226-232.

[14] Quirk, R. A.; Davies, M. C.; Tendler, S. J. B.; Chan, W. C.; Shakesheff, K. M. Controlling biological interactions with poly(lactic acid) by surface entrapment modification. *Langmuir* **2001**, 17, 2817-2820.

[15] Zhu, H.; Ji, J.; Lin R.; Gao C.; Feng, L.; Shen, J. Surface engineering of poly(D,L-lactic acid) by entrapment of chitosan-based derivatives for the promotion of chondrogenesis. *J. Biomed. Mater. Res.* **2002**, 62, 532-539.

[16] Lee, S. J., Khang, G., Lee, Y.M., Lee, H.B. Interaction of human chondrocytes and NIH/3T3 fibroblasts on chloric acid-treated biodegradable polymer surfaces. *J. Biomater. Sci., Polym. Ed.* **2002**, 13, 197-212.

[17] Wang, L.; Jia, X.; Chen, Y.; Che, Y.; Yuan, Z. Synthesis, degradability, and cell affinity of poly (DL-lactide-co-RS- hydroxyethyl-β-malolactonate). *J. Biomed. Mater. Res. Part A.* **2008**, 87, 459-469.

[18] Timbart, L.; Amsden, B. G. Functionalizable biodegradable photocrosslinked elastomers based on 2-oxepane-1,5-dione. *J. Polym. Sci., Part A: Polym. Chem.* **2008**, 46, 8191-8199.

[19] Dai, W.; Huang, H.; Du, Z.; Lang, M. Synthesis, characterization and degradability of the novel aliphatic polyester bearing pendant N-isopropylamide functional groups. *Polym. Degrad. Stab.* **2008**, 93, 2089-2095.

[20] Wang, S.; Cui, W.; Bei, J. Bulk and surface modifications of polylactide. *Anal. Bioanal.Chem.* **2005**, 381, 547-556.

[21] Parrish, B.; Breitenkamp, R. B.; Emrick, T. PEG- and peptide-grafted aliphatic polyesters by click chemistry. *J. Am. Chem. Soc.* **2005**, 127, 7404-7410.

[22] Grafahrend, D.; Calvet, J. L.; Klinkhammer, K.; Salber, J.; Dalton, P. D.; Möller, M.; Klee, D. Control of protein adsorption on functionalized electrospun fibers. *Biotechnol. Bioeng.* **2008**, 101, 609-621.

[23] He, B.; Poon, Y. F.; Feng, J.; Chan-Park, M. B. Synthesis and characterization of functionalized biodegradable poly(DL-lactide-co-RS-beta-malic acid). *J. Biomed. Mater. Res. Part A*. **2008**, 87, 254-263.

[24] Amato, I.; Ciapetti, G.; Pagani, S.; Marletta, G.; Satriano, C.; Baldini, N.; Granchi, D. Expression of cell adhesion receptors in human osteoblasts

cultured on biofunctionalized poly-(ε-caprolactone) surfaces. *Biomaterials* **2007**, 28, 3668-3678.

[25] Karakecili, A.; Satriano, C.; Gumusderelioglu, M.; Marletta, G. Relationship between the fibroblastic behaviour and surface properties of RGD-immobilized PCL membranes. *J. Mater. Sci. Mater. Med.* **2007**, 18, 317- 319.

[26] Leemhuis, M.; van Nostrum, C. F.; Kruijtzer, J. A. W.; Zhong, Z. Y.; ten Breteler, M. R.; Dijkstra, P. J.; Feijen, J.; Hennink, W. E. Functionalized poly(α-hydroxy acid)s via ring-opening polymerization: Toward hydrophilic polyesters with pendant hydroxyl groups. *Macromolecules* **2006**, 39, 3500-3508.

[27] Leemhuis, M.; Kruijtzer, J. A. W.; van Nostrum, C. F.; Hennink, W. E. In vitro hydrolytic degradation of hydroxyl-functionalized poly(α-hydroxy acid)s. *Biomacromolecules* **2007**, 8, 2943-2949.

[28] Sun, H.; Mei, L.; Song, C.; Cui, X.; Wang, P. The in vivo degradation, absorption and excretion of PCL-based implant. *Biomaterials* **2006**, 27, 1735-1740.

[29] Liu, S. Q., In *Bioregenerative engineering: principles and applications.* John Wiley and Sons: **2007**; p 474.

[30] Chen, G.; Zhou, P.; Mei, N.; Chen, X.; Shao, Z.; Pan, L.; Wu, C. Silk fibroin modified porous poly(ε-caprolactone) scaffold for human fibroblast culture in vitro. *J. Mater. Sci. Mater. Med.* **2004**, 15, 671-677.

[31] Yildirim, E. D.; Ayan, H.; Vasilets, V. N.; Fridman, A.; Guceri, S.; Sun, W. Effect of dielectric barrier discharge plasma on the attachment and proliferation of osteoblasts cultured over poly(ε-caprolactone) scaffolds. *Plasma Processes Polym.* **2008**, 5, 58-66.

[32] Leemhuis, M.; van Steenis, J. H.; van Uxem, M. J.; van Nostrum, C. F.; Hennink, W. E. A versatile route to functionalized dilactones as monomers for the synthesis of poly(α-hydroxy) acids. *Eur. J. Org. Chem.* **2003**, 17, 3344-3349.

[33] Siddappa, R.; Martens, A.; Doorn, J.; Leusink, A.; Olivo, C.; Licht, R.; van Rijn, L.; Gaspar, C.; Fodde, R.; Janssen, F.; van Blitterswijk, C.; de Boer, J. cAMP/PKA pathway activation in human mesenchymal stem cells in vitro results in robust bone formation in vivo. *Proc. Nat. Acad. Sci. U.S.A.* **2008**, 105, 7281-7286.

[34] Gottschalk, C.; Frey, H. Hyperbranched polylactide copolymers. *Macromolecules* **2006**, 39, 1719-1723.

[35] Zhang, X.; MacDonald, D. A.; Goosen, M. F. A.; McAuley, K. B. Mechanism of lactide polymerization in the presence of stannous octoate: the effect of hydroxy and carboxylic acid substances. *J. Polym. Sci., Part A: Polym. Chem.* **1994**, 32, 2965-2970.

[36] Loontjens, C. A. M.; Vermonden, T.; Leemhuis, M.; van Steenbergen, M. J.; van Nostrum, C. F.; Hennink, W. E. Synthesis and characterization of random and triblock copolymers of ε-caprolactone and (benzylated)hydroxymethyl glycolide. *Macromolecules* **2007**, 40, 7208-7216.

[37] Tiaw, K. S.; Goh, S. W.; Hong, M.; Wang, Z.; Lan, B.; Teoh, S. H. Laser surface modification of poly(ε-caprolactone) (PCL) membrane for tissue engineering applications. *Biomaterials* **2005**, 26, 763-769.

[38] Makal, U.; Wynne, K. J. Water induced hydrophobic surface. *Langmuir* **2005**, 21, 3742-3745.

[39] Ko, Y. C.; Ratner, B. D.; Hoffman, A. S. Characterization of hydrophilic-hydrophobic polymeric surfaces by contact angle measurements. *J. Colloid Interface Sci.* **1981**, 82, 25-37.

[40] Hogt, A. H.; Gregonis, D. E.; Andrade, J. D.; Kim, S. W.; Dankert, J.; Feijen, J. Wettability and ζ potentials of a series of methacrylate polymers and copolymers. *J. Colloid Interface Sci.* **1985**, 106, 289-298.

[41] Woodfield, T. B. F.; Miot, S.; Martin, I.; van Blitterswijk, C. A.; Riesle, J. The regulation of expanded human nasal chondrocyte re-differentiation capacity by substrate composition and gas plasma surface modification. *Biomaterials* **2006**, 27, 1043-1053.

[42] van Wachem, P. B.; Beugeling, T.; Feijen, J.; Bantjes, A.; Detmers, J. P.; van Aken, W. G. Interaction of cultured human endothelial cells with polymeric surfaces of different wettabilities. *Biomaterials* **1985**, 6, 403-408.

[43] Li, B.; Ma, Y.; Wang, S.; Moran, P. M. Influence of carboxyl group density on neuron cell attachment and differentiation behavior: Gradient-guided neurite outgrowth. *Biomaterials* **2005**, 26, 4956-4963.

[44] Lips, P. A. M.; van Luyn, M. J. A.; Chiellini, F.; Brouwer, L. A.; Velthoen, I. W.; Dijkstra, P. J.; Feijen, J. Biocompatibility and degradation of aliphatic segmented poly(ester amide)s: In vitro and in vivo evaluation. *J. Biomed. Mater. Res. Part A*. **2006**, 76, 699-710.

3D Printing

Chapter 4

Preparation and Characterization of a 3D-printed Scaffold Based on a Functionalized Polyester for Bone Tissue Engineering Application

Hajar Seyednejad
Debby Gawlitta
Wouter J. A. Dhert
Cornelus F. van Nostrum
Tina Vermonden
Wim E. Hennink

Acta Biomaterialia
2011, 7(5), 1999- 2006

At present, there is a strong need for suitable scaffolds that meet the requirements for bone tissue engineering applications. The objective of this study was to investigate the suitability of porous scaffolds based on a hydroxyl functionalized polymer (poly(hydroxymethylglycolide-co-ε-caprolactone), pHMGCL) for tissue engineering. In a recent study, this polymer was shown to be a promising material for bone regeneration. The scaffolds consisting of pHMGCL or poly(ε-caprolactone) (PCL) were produced by means of a rapid prototyping technique (3D plotting) and were shown to have a high porosity and an interconnected pore structure. The thermal and mechanical properties of both scaffolds were investigated and human mesenchymal stem cells were seeded onto the scaffolds to evaluate the cell attachment properties, as well as cell viability and differentiation. It was shown that the cells filled the pores of the pHMGCL scaffold within 7 days and displayed increased metabolic activity when compared with cells cultured in PCL scaffolds. Importantly, pHMGCL scaffolds supported osteogenic differentiation. Therefore, scaffolds based on pHMGCL are promising templates for bone tissue engineering applications.

1. Introduction

Tissue engineering combines the principles of engineering and life sciences to provide substitutes that can restore, maintain or augment tissue function [1]. For tissue engineering the availability of a biodegradable and biocompatible scaffolds is needed [2, 3]. These scaffolds serve as a temporary construct and should posses certain surface characteristics, particularly hydrophilicity to promote cell adhesion. Further, scaffolds should have adequate mechanical properties to maintain the 3D structure and gradually degrade when the new tissue and an extracellular matrix is formed. Scaffolds should be highly porous with large interconnected pores to facilitate cell growth and diffusion of nutrients and waste products into and out of the scaffold [4-6].

There are many conventional techniques to make 3D scaffolds for tissue engineering applications such as solvent casting, gas foaming, particulate leaching, and electrospinning [7, 8]. However, these technologies have all some limitations such as the difficulty to yield an interconnected porous structure for cell growth. Among the scaffold fabrication techniques, those based on rapid prototyping (RP) methods, including stereolithography [9], three-dimensional printing [10], selective laser sintering [11], fused deposition modeling [12], and direct wiring [13] are preferred since these methods result in the formation of complex, well-defined and reproducible constructs via a computer-aided design (CAD) model and computer-controlled (CAM) tool handling [4, 14]. Another advantage is that these complex structures can be designed according to the need of individual patients by using their 3D medical scan data [2]. Out of these RP techniques, 3D-printing (melt plotting) is an attractive method to fabricate scaffolds for tissue engineering applications since this technology does not use possibly toxic solvents for production [15, 16].

The preferred polymer used for rapid prototyping techniques is poly(ε-caprolactone) [2, 15, 17, 18]. This aliphatic polyester is a biocompatible and biodegradable polymer with a degradation time ranging from 2 to 4 years [19]. However, its surface characteristics are not favorable for cell adhesion and proliferation due to its intrinsic hydrophobicity and lack of bioactive functional groups [20, 21]. In our group, we have developed a new copolyester based on PCL, i.e. poly(hydroxymethylglycolide-co-ε-caprolactone) (pHMGCL). This copolymer is more hydrophilic than PCL and features a tunable degradation rate, as well as available hydroxyl functional groups for further functionalization with e.g. peptides [22, 23]. We have also shown that human mesenchymal stem cells exhibited good adherence onto pHMGCL films as compared to the more hydrophobic PCL surfaces. The cells survived and differentiated towards

osteogenic lineage on pHMGCL surfaces [23]. In the present study, 3D scaffolds of this novel hydroxyl-functionalized polyester and PCL were fabricated by means of 3D-plotting. Both polymers were synthesized and characterized for structural, thermal, and molecular weight properties and the thermal and mechanical properties of scaffolds based on these polymers were studied. Furthermore, the compatibility of human mesenchymal stem cells with these 3D structures was also evaluated by investigating the attachment, differentiation, and metabolic activity of seeded cells.

2. Materials and Methods

2.1. Materials

All chemicals used in this study were purchased from Aldrich and used as received, unless stated otherwise. All solvents were purchased from Biosolve (Valkenswaard, The Netherlands) except acetone (Merck, Darmstadt, Germany), hexane (Antonides-Interchema, Oosterzee, The Netherlands), toluene, and sulfuric acid (Acros, Geel, Belgium). Toluene was distilled from P_2O_5 and stored over 3 Å molecular sieves under argon. Tetrahydrofuran (THF) was distilled from sodium/benzophenone. 3S-Benzyloxymethyl-1,4-dioxane-2,5-dione (benzyl-protected hydroxymethyl glycolide, BMG) was synthesized as described by Leemhuis et al. [24, 25]. ε-Caprolactone (CL) and silica gel (0.035-0.070 mm, 60 Å) were obtained from Acros (Geel, Belgium). CL was distilled from CaH_2. O-Benzyl-L-serine was supplied by Senn Chemicals (Dielsdorf, Switzerland). Sodium nitrite ($NaNO_2$) and dimethylaminopyridine (DMAP) were purchased from Fluka (Zwijndrecht, The Netherlands). Sodium sulfate (Na_2SO_4), triethylamine, sodium carbonate (Na_2CO_3), and benzyl alcohol (BnOH) were provided by Merck (Darmstadt, Germany). Bromoacetyl bromide, tin(II) 2-ethylhexanoate ($SnOct_2$) and Pd/C (palladium, 10 wt % (dry basis) on activated carbon, wet (50% water w/w), Degussa type E101 NE/W) were obtained from Aldrich (Zwijndrecht, The Netherlands).

Human bone marrow aspirates were obtained during total hip replacement procedures with informed consent and approval of the local medical ethical committee. The mononuclear cell fraction was isolated by centrifuging on Ficoll-paque. Subsequently, the cells were plated in growth medium containing α-MEM (Gibco) supplemented with 0.2 mM L-ascorbic acid 2-phosphate (Sigma), 10% heat-inactivated fetal bovine serum (Invitrogen), 100 units/ml penicillin with 100 µg/ml streptomycin (Invitrogen), and 1 ng/mL rhB-FGF (R&D Systems). Cells were passaged at subconfluence and seeded onto the scaffolds before passage

5. Media were refreshed every 3-4 days during the cell expansion and scaffold cultures.

The isolated cells were characterized for accepted characteristics of human mesenchymal stem cells (hMSCs) such as their multilineage potential and the CD-surface marker profile. Multilineage potential was confirmed by differentiation into the adipogenic, osteogenic and chondrogenic lineages as previously described [26]. Further, the MSCs were FACS-analyzed for the absence or presence of established MSC markers [27]. They were negative for CD31, CD45, and showed >90% positivity for CD73, CD90, and CD105, and thus exhibited a marker profile that agrees with the one described for MSCs.

2.2. Synthesis of Poly(ε-caprolactone)

Poly(ε-caprolactone) was synthesized via ring opening polymerization (ROP) using BnOH and $SnOct_2$ as initiator and catalyst, respectively. In a typical procedure, ε-caprolactone (5.78 mL, 65.9 mmol), BnOH (5.6 mg, 0.052 mmol), and $SnOct_2$ (10.5 mg, 0.026 mmol) were loaded into a dry Schlenk tube under dry N_2 atmosphere. The tube was evacuated for 1 hour, then closed and immersed in an oil bath which was heated at 130 °C. Polymerization was performed overnight and the formed polymer was dissolved in chloroform, precipitated in cold methanol and dried overnight under vacuum. The obtained poly(ε-caprolactone) was characterized by ^{1}H NMR, GPC and DSC.

2.3. Synthesis of Random Copolymer of CL and BHMG (poly (benzyloxymethyl glycolide-co-ε-caprolactone), pBMGCL)

A random copolymer of BMG and ε-caprolactone was synthesized by a ROP method. Briefly, ε-CL (6.54 mL, 59 mmol) and BMG (1.2 g, 5.1 mmol) were introduced into a dry schlenk tube, equipped with magnetic stirrer, under a dry nitrogen atmosphere. Next, BnOH (23.14 mg, 0.214 mmol) and $SnOct_2$ (43.3 mg, 0.107 mmol) were added as initiator and catalyst, respectively. The tube was evacuated for 2 hours, subsequently closed and immersed in an oil bath pre-heated at 130 °C. The polymerization was performed overnight and the formed polymer was purified in the same manner as described for poly(ε-caprolactone). The protected polymer was characterized by ^{1}H NMR, GPC and DSC.

2.4. Removal of Benzyl Groups of pBMGCL to Yield Poly(hydroxymethylglycolide-co-ε-caprolactone), pHMGCL

Protective benzyl groups of pBMGCL were removed in a hydrogenation reaction using Pd/C catalyst essentially as described by Leemhuis et al. [24]. In short, pBMGCL (7.0 g, 4.13 mmol) was dissolved in dry THF (500 mL) and subsequently the Pd/C catalyst (3.0 g, 7.4 mmol) was added. The flask was filled with hydrogen in three consecutive steps of evacuation, refilling with H_2 and the reaction was done under H_2 pressure overnight. The catalyst was removed afterwards using a glass filter and THF was removed by evaporation. The deprotected polymer was characterized by ^{1}H NMR, DSC and GPC.

2.5. Scaffold Preparation

Three-dimensional scaffolds were prepared by means of 3D-printing (melt-plotting) as depicted in Fig. 2. The 3D-printer, a Bioscaffolder (Envisiontec GmbH, Gladbeck, Germany), can create scaffolds with pre-defined geometries, varying in shape, strand thickness, and porosity [10]. PCL or pHMGCL were loaded into the reservoir and heated to 110 °C or 50 °C, respectively. The molten polymers were extruded through a 23G nozzle. Parallel strands were deposited in a layer-by-layer fashion on a cooled collector plate with a speed of 350 mm/min and 500 mm/min for PCL and pHMGCL, respectively. The meandering strand pattern was rotated at 90° angles between layers to create square pores in the constructs. The distance between strands was set to 0.9 mm and the spindle speed was 200 rpm. Scaffold geometry was imaged on a stereo microscope (SZ61/SZ2-ILST, Olympus, The Netherlands).

2.6. Nuclear Magnetic Resonance (NMR)

NMR measurements were performed using a Gemini 300 MHz spectrometer (Varian Associates Inc., NMR Instruments, Palo Alto, CA). Chemical shifts were recorded in ppm with reference to the solvent peak (δ= 7.26 ppm for $CDCl_3$ in ^{1}H NMR).

2.7. Differential Scanning Calorimetry (DSC)

Differential scanning calorimetry (TA Instruments DSC Q2000) was employed to evaluate the thermal properties of the different polymers and scaffolds. For the polymers, scans were taken from -80 °C to 100 °C with a heating rate of 10 °C/min and a cooling rate of 0.5 °C/min under nitrogen flow of 50 mL/min. The

glass transition temperature (T_g) was recorded as the midpoint of heat capacity change in the second heating run. Melting temperature (T_m) and heat of fusion (ΔH_f) were determined from the onset of endothermic peak position and integration of endothermic area in the second heating run, respectively. For scaffolds, the samples were equilibrated at -90 °C and then heated to 100 °C with a heating rate of 10 °C/min. All the thermal transitions were reported for the first heating run.

2.8. Gel Permeation Chromatography (GPC)

The molecular weights of the obtained polymers were measured by means of GPC using a 2695 Waters Aliance system and a Waters 2414 refractive index detector. Two PL-gel 5 µm mixed-D columns fitted with a guard column (Polymer Labs, M_w range 0.2- 400 KDa) were used. The columns were calibrated with polystyrene standards of known molecular weights using AR grade THF, eluting at 1 mL/min flow rate at 30 °C. The concentration of samples was 5 mg/mL and the injection volume was 50 µL.

2.9. Dynamic Mechanical Analysis (DMA)

A DMA instrument (TA instruments DMA 2980) was used to evaluate the viscoelastic properties of the polymers and fabricated scaffolds at room temperature. For each sample, measurements were performed in triplicate. Cylindrical structures were used to measure the compression modulus of the samples. A force of 1N was applied on surface of the samples and it was increased to 18N with a rate of 3N/min. The force and displacement were recorded throughout the compression and converted to stress and strain based on the initial specimen dimensions. The stress-strain curve was plotted and the compression modulus was calculated from the slope of the linear part of this curve.

2.10. Porosity Measurements

The porosity of scaffolds was determined by calculating the bulk density (ρ) of PCL and pHMGCL disks based on crystallinity percentage of these polymers obtained from thermal analysis data [28]. Then, the apparent density (ρ^*) of 3D scaffolds was calculated by measuring the volume and weight of the porous scaffolds and the porosity is defined as [29]:

$$\text{Porosity } (\varepsilon) = (1- \rho^*/\rho) \times 100$$

2.11. Cell Seeding

3D-plotted scaffolds, consisting of PCL or pHMGCL were cut into 5x5x3 mm dimensions for the cell seeding experiments. Subsequently, the scaffolds were sterilized in 70 % ethanol and air-dried. Prior to cell seeding, the scaffolds were soaked in growth medium for several hours. Next, 3.5 x 10^5 hMSCs were dynamically seeded onto each scaffold for two hours on an orbital shaker at 300 rpm and 37 °C. Following seeding, the constructs were cultured statically at 37 °C and 5% CO_2. After allowing cell attachment for 24 hours, three scaffolds of both polymers were harvested to check for cell attachment and metabolic activity. After 7 days, the cells were grown to sufficient confluence, and the medium was changed to osteogenic differentiation medium consisting of α-MEM, 0.2 mM L-ascorbic acid 2-phosphate, 10 % heat-inactivated fetal bovine serum, 100 units/ml penicillin with 100 µg/ml streptomycin, 10 mM β-glycerophosphate (G9891, Sigma) and 10 nM dexamethasone (D8893, Sigma). After 11 days, the remaining cultures were harvested to determine metabolic activity and osteogenic cell differentiation.

2.12. Cell Attachment and Proliferation

Attachment of cells seeded into the scaffolds was visualized by conventional light microscopy. The cell-seeded scaffolds were harvested after 1 and 11 days for additional evaluation of cell attachment, metabolic activity, and proliferation. Following fixation in formalin, the cells were permeabilized with Triton X-100 (Sigma) and their actin cytoskeleton was stained with phalloidin-FITC (Sigma) for 1 hour and nuclei were counterstained with 4′,6-diamidino-2-phenylindole dihydrochloride (DAPI, Sigma). Cell distribution and morphology were inspected on a fluorescence microscope (Olympus).

2.13 Assessment of Metabolic Activity

After 1 and 11 days, the metabolic activity of the cells seeded in the scaffolds was assessed (n=3). For this, scaffolds were incubated in WST-1 reagent (Roche Diagnostics, Germany), according to the manufacturer's protocol. Briefly, WST-1 reagent was added to the culture medium to a final 10x dilution. After a 2-hour incubation at 37 °C, absorbance was measured at 450 nm and corrected for 655 nm background absorption and medium control.

2.14 Osteogenic Differentiation

Cell morphology and differentiation in the cell-seeded scaffolds at day 11 were visualized by fluorescent tri-staining on a fluorescence microscope (Olympus), distinguishing cell nuclei, actin fibers and alkaline phosphatase (ALP). Briefly, the cells were fixed in formalin and permeabilized in 0.2% Triton X-100. Samples (n=3) were then incubated in the working solution of the Vector Red Alkaline Phosphatase Substrate Kit (Vector Laboratories, USA) for 30-60 minutes to detect ALP, an early marker of osteogenesis. FITC-labeled phalloidin was applied to identify the actin fibers and DAPI was used for nuclear staining.

2.15. Statistical Analysis

Metabolic activity data were compared by ANOVA in SPSS 15.0 and significance was attributed according to a Bonferroni's posthoc test. A p-value of 0.05 was considered significant. Data are shown as mean values with standard deviations.

3. Results and Discussion

3.1. Polymer Synthesis and Characterization

PCL and pHMGCL were synthesized via ring opening polymerization, using BnOH and $SnOct_2$ as initiator and catalyst, respectively (Figure 1). The monomer to initiator molar ratio was 300. The molar ratio of BMG to ε-CL monomer for the pBMGCL synthesis was 8/92 and ^1H NMR analysis of the obtained polymer showed that the percentages of these monomers in pBMGCL copolymer were the same as the feed ratio.

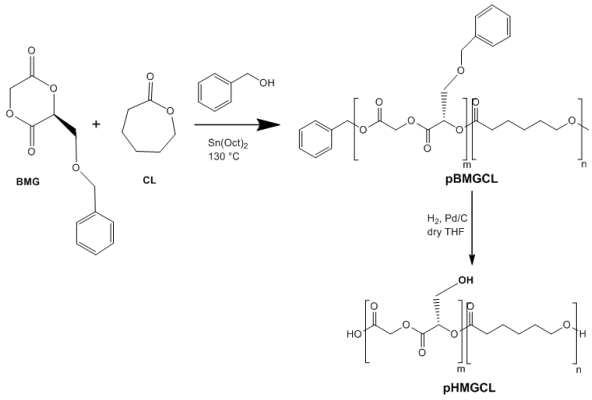

Fig.1. Synthesis of poly (benzyloxymethyl glycolide-co-ε-caprolactone) (pBMGCL) and poly (hydroxymethyl glycolide-co-ε-caprolactone) (pHMGCL) random copolymers.

GPC analysis (Table 1) showed that M_w's of PCL and pBMGCL were 79.1 ± 2.0 kDa and 40.1 ± 2.8 kDa, respectively. Besides, in agreement with previous studies [22, 30], removal of the protecting benzyl groups was not associated with chain scission as the M_w of the polymer hardly decreased after deprotection (Table1).

Table1. Characteristics of polymers and scaffolds

BMG/CL Molar Ratio In feed	BMG/CL Molar Ratio In polymer	Protected polymer				Yield (%)	Deprotected polymer				Scaffolds	
		DSC		GPC			DSC		GPC		DSC	
		T_m (°C)	ΔH_f (J/g)	M_w (kDa)	PDI		T_m (°C)	ΔH_f (J/g)	M_w (kDa)	PDI	T_m (°C)	ΔH_f (J/g)
0/ 100	0/ 100	-	-	-	-	87	54	61	79.1	2.0	54	63
8/ 92	8/ 92	42	47	40.1	2.8	95	43	42	38.1	2.7	40	51

[a]Polydispersity Index (M_w/M_n)

DSC analysis showed that the melting temperature of PCL and pHMGCL was 54 °C and 43 °C, respectively. Thermal properties of PCL were similar to the values reported in the literature [31]. In line with our expectations and previous findings [23], incorporation of HMG monomer in the copolymer structure resulted in a decrease in crystallinity (ΔH decreased from 61 J/g for PCL to 42 J/g for pHMGCL) and melting temperature of the polymer.

3.2. Scaffolds Preparation and Characterization

Three-dimensional scaffolds of PCL and pHMGCL were prepared by means of a 3D-printing (melt-plotting) technique (Figure 2). In order to print these polymers, the parameters in the settings of the Bioscaffolder were varied due to the inherent differences in melting temperature and viscosity of these polymers. These parameters were optimized and the final settings are summarized in Table 2. As PCL was not fluid enough at its melting temperature, it was heated up to 110 °C while the viscosity of pHMGCL was sufficient at 50 °C to run through the extruder. Due to the difference in printing temperature of these polymers, printer settings such as the printing speed were adapted resulting in the different strand heights. However, the pore sizes of the scaffolds were kept constant.

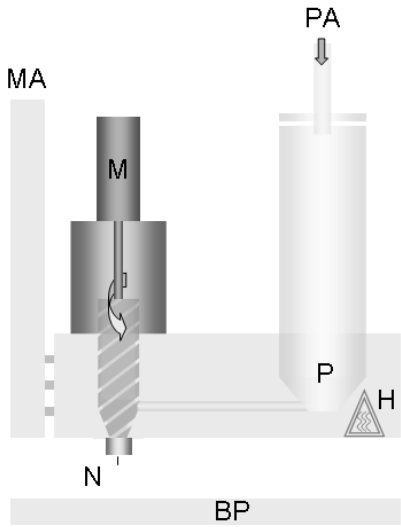

Fig.2. Schematic presentation of the Bioscaffolder polymer printing module. The printing head is attached to the mechanical arm (MA) that is controlled in x,y,z-movements by the computer program, PrimCam. The polymer (P) is loaded into the reservoir that can be heated (H). Once the polymer is molten, it will flow due to application of pressurized air (PA), through the horizontal tube connecting the reservoir with the extruder. The extruder is rotated by the motor (M) and the polymer is printed through the nozzle (N) onto the base plate (BP).

The internal pore structure of scaffolds is an important characteristic which determines the cells, nutrients, and waste products transport into and out of the structure [32]. The porous structure of these scaffolds was visualized by means of stereo microscopy (Figure 3). This figure shows that in the scaffolds channels are present with a length equal to the thickness of the scaffold and a cross section area of less than 1 mm^2 (the distance between the strands is 900 µm). Furthermore, the 3D structures of melt-plotted scaffolds consisted of interconnected pores and open channels, both on the side (Figure 3B) and on the top of scaffolds (Figure 3C). As it can be seen in Figure 4 the pores of printed PCL scaffold have a rectangular shape with 90° angles while the pores of pHMGCL are more rounded rectangular. This can be ascribed to the difference in the intrinsic properties of these polymers such as thermal properties, viscosity and surface characteristics. Although different parameters in the settings of the

Bioscaffolder were varied, the pore shapes of these scaffolds were slightly different.

Table2. Parameters used with the Bioscaffolder to print the polymers into three-dimensional structures.

Parameters	PCL	pHMGCL
Temperature (°C)	110	50
Strand distance (mm)	0.9	0.9
Strand height (µm)	200	150
Spindle speed (rpm)	200	200
Printing speed (mm/min)	350	500

*PCL strands were collected at room temperature and pHMGCL strands were collected on a dry-ice cooled- plate.

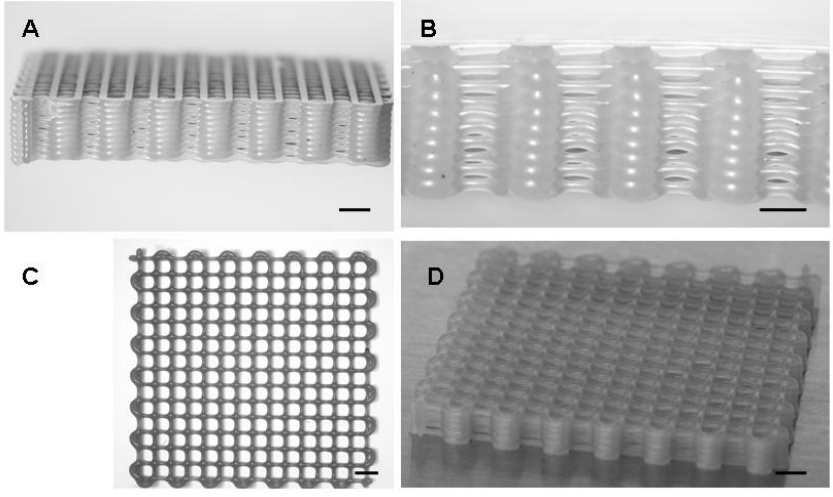

Fig.3. Stereomicroscopic images of 3D-plotted pHMGCL scaffold. A, B) Side views, demonstrating the interconnectivity of the channels. C) Top view, D). Oblique view. Scale bar is 1 mm.

The thermal properties of the scaffolds were also evaluated and it was shown that there were no distinct changes in the crystallinities of the polymers after melt plotting (Table 1). The scaffold based on pHMGCL showed a slightly lower melting temperature than that of the non-extruded polymer obtained after synthesis (Table 1, 40 versus 42 °C). GPC analysis showed that this decrease in

melting temperature is not due to polymer degradation. Most likely, this difference in the melting temperature can be attributed to the difference in procedure to establish the melting points. For pHMGCL obtained after synthesis, the melting temperature is acquired from the second heating cycle (in order to exclude the thermal history of the polymer) whereas for the scaffold, the melting temperature is obtained from the first heating cycle (to get insight into the thermal properties of the scaffold after processing). It should be noted however that the melting temperatures of the scaffolds are well above body temperature (37 °C), and hence they are likely dimensionally stable upon implantation.

Porosity is an important factor of scaffolds for bone tissue formation since the pores allow migration and proliferation of cells as well as vascularization [33]. Importantly, the mechanical interlocking between a porous implant biomaterial and the surrounding natural bone is better than with a non-porous material, which leads to a better mechanical stability at the implant/bone interface [34]. The porosity of the 3D scaffolds was measured by calculating the bulk density and the apparent density of polymeric disks and porous scaffolds, respectively. The bulk density was derived from the % crystallinity, which was calculated based on the relation between the experimental heat of fusion and the reported heat of fusion for 100% crystalline PCL (139.5 J/g [28]). The density of the crystalline and the amorphous PCL is 1.200 and 1.021 g/cm^3, respectively [35]. Therefore, the density of PCL and pHMGCL was calculated to be 1.09 g/cm^3 and 1.07 g/cm^3, respectively. The apparent density (ρ^*) of the scaffolds was calculated by measuring the weight and volume of porous structures. Then the percentages of porosity were defined by using the formula of Salgado et al. [29] and these were calculated to be 69.7 and 72.8 % for PCL and pHMGCL scaffolds, respectively. These values are in the range of porosity values normally used for scaffolds in bone tissue regeneration [34].

The compression modulus of the solid disks as well as porous 3D scaffolds was evaluated. It was observed that the moduli of PCL and pHMGCL disks were 59.0 ± 8.7 MPa and 65.6 ± 11.7 MPa, respectively. These values are in agreement with the values reported for PCL solid disks [18]. The compressive modulus of the 3D-plotted scaffolds was around 10 MPa. This lower compressive modulus can be explained by the porosity of the scaffolds, but the measured compressive modulus of these scaffolds are well in the range of requirements for bone regeneration [34].

3.3. Cell Attachment and Proliferation

After cell seeding, cell clusters were present within the scaffold pores, some of which appeared to be attached to the scaffolds. However, after one day in culture, predominantly single cells were attached to both scaffold types (Figure 4). During subsequent cell proliferation, the MSCs grew to span the scaffold pores of pHMGCL scaffold as detected by light microscopy within 7 days (Figure 4) and 50- 70% of the pores were populated by 11 days. In contrast, the cells only adhered to and grew on the strands of PCL scaffolds and did not fill the pores within 11 days, as shown in Figure 4. This difference in cell adherence can be attributed the higher hydrophilicity of pHMGCL due to its hydroxyl groups that promote cell attachment [23].

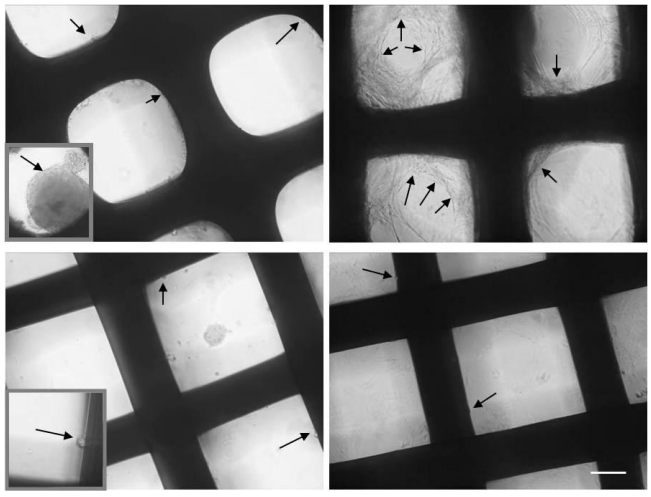

Fig.4. Light microscopic evaluation of MSCs, seeded onto pHMGCL (top) or PCL (bottom) scaffolds after 1 and 11 days (left and right, respectively). The two insets show magnifications of a cell cluster (top inset) and a single cell (bottom inset) attached to the scaffold at day 1 (both images are of comparable scale). Arrows indicate the cells on the black (non-transparent) scaffolds and the scale bar denotes 200 μm.

3.4. Assessment of Metabolic Activity

The total metabolic activity of all cells was determined using the WST-1 assay. A higher metabolic activity of a particular cell culture can reflect both increased cell number and/or increased activity per cell.

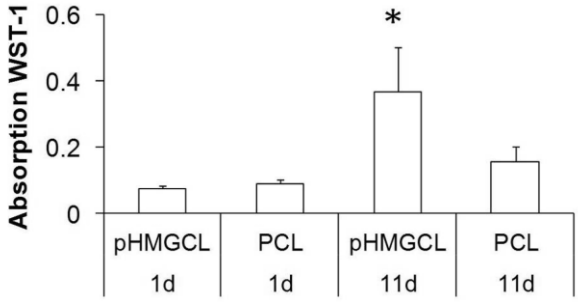

Fig.5. The metabolic activity (WST-1 assay) per scaffold is shown after 1 and 11 days of culturing. The MSCs were either cultured on PCL or pHMGCL scaffolds and exhibited significantly increased activity on the pHMGCL scaffolds at 11 days (*$p<0.05$ compared to all other groups). 3.5 x 10^5 hMSCs were dynamically seeded onto each scaffold.

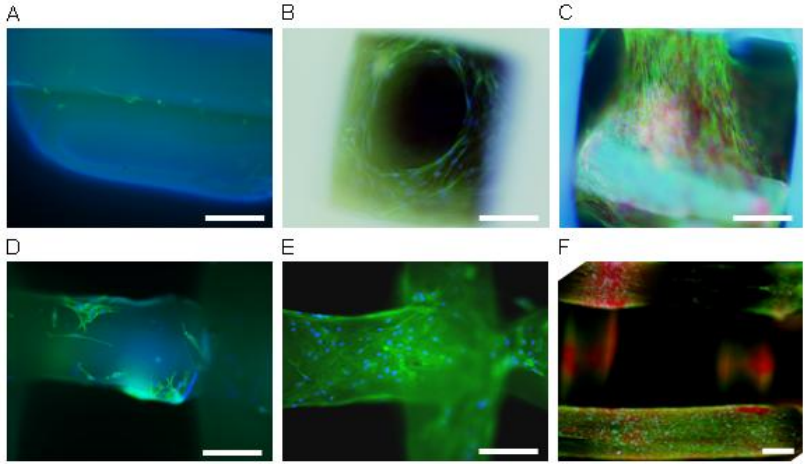

Fig.6. Attachment and differentiation of MSCs in pHMGCL (top) or PCL (bottom) scaffolds. Actin filaments (green) and nuclear staining (blue) show the cell attachment after 1 day (A, D) or 11 days (B,C,E,F). Only a few cells (green) were detected on the strands (bluish autofluorescence) of both scaffold types and only those cells that had attached on the outside of the scaffold could be visualized (A, D). After 11 days of culture in both scaffold types (B, E), cells had divided to completely cover the strands of the PCL scaffolds (E), while in the pHMGCL scaffolds cells had even proliferated to span the scaffold pores (B). Note that the autofluorescence of the pHMGCL strands has increased and interferes with detection of cells on the strands (in B and C). The cellular alkaline phosphatase (red) production (C, F) is showing the osteogenic differentiation potential of MSCs in both scaffold types. Scale bars indicate 200 µm.

The metabolic activity (WST-1) of the cells cultured on the PCL and pHMGCL scaffolds was low and comparable at day 1. However, after culturing for 11 days, a significant twofold increase of the metabolic activity of the cells in the pHMGCL scaffolds compared to those in PCL scaffolds was observed (Figure 5). These quantitative data indicate increased metabolic activity per scaffold in the pHMGCL scaffolds. This confirms the qualitative microscopic observations that show more cells and more differentiation in the pores of the pHMGCL constructs (Figures 4 and 6B, E, the latter of which is discussed below).

3.5. Osteogenic Differentiation

The osteogenic differentiation potential of the hMSCs was investigated in both scaffold types by evaluating the expression of alkaline phosphatase (ALP), an early marker of osteogenesis [26, 36]. After one day in culture with the scaffolds, only a few cells could be detected on both scaffold types (Figure 6A, D). The cells were able to exhibit a spread, attached morphology on both scaffold types and did not show any sign of osteogenic differentiation (ALP) at this point. It should be noted that only cells that attached to the outside of the scaffolds or grew into the pores could be detected by fluorescence microscopy.

After 11 days, the cells had proliferated and were able to not only attach to the strands of the pHMGCL scaffold but to span complete pores. The attachment of the cells to the pHMGCL strands could not be determined from the fluorescent images as the autofluorescence of the scaffold material was too high after culturing for 11 days (Figure 6B). However, cells inside the pores could be distinguished. In addition, the ability of the cells to attach to the pHMGCL scaffold was observed at day 1 when autofluorescence was minimal and also in the light microscopic evaluations.

In contrast, cell proliferation had resulted in complete coverage of the strands of the PCL scaffolds (which did not increase their autofluorescence and therefore allowed visualization of cells on the strands) but none of the PCL scaffold pores was filled with cells (Figure 6E).

It was demonstrated that the cells spanning the pHMGCL scaffold pores were differentiated towards the osteogenic lineage as depicted in Figure 6C. The cells that had proliferated on the PCL scaffold strands also showed ALP expression, but only when they were clustered (Figure 6F). Though ALP expression was not quantified, from the fluorescence microscopic examination, it was evident that more cells were expressing ALP in the pHMGCL scaffolds. As mentioned before, in these scaffolds the majority of pores were filled with cells

that were expressing ALP compared to local expression on the strands of the PCL. This is in agreement with our previous finding [23] where we showed that the increase in hydrophilicity of the pHMGCL polymers as compared to PCL resulted in improved osteogenic differentiation in monolayer cultures.

4. Conclusions

This chapter describes the preparation and characterization of three-dimensional scaffolds for bone tissue regeneration by means of a rapid prototyping technique avoiding the use of organic solvents. The prepared scaffolds made of a hydroxyl functionalized polyester (pHMGCL) meet the requirements for scaffolds in bone tissue engineering applications with respect to physical characteristics such as a melting temperature above body temperature, more than 70% porosity in the form of interconnected pores and a compressive modulus in the range of elastic modulus of the bone. Importantly, human mesenchymal stem cells seeded into this scaffold grew to fill most of the pores within 7 days in culture, while in the PCL scaffolds the cells only adhered to the scaffold strands. The metabolic activity of the cells was significantly enhanced in the pHMGCL scaffolds compared to PCL scaffolds. Finally, cells preferably differentiated in the areas of high cell density, which were mainly present in the pHMGCL scaffolds, rather than PCL scaffolds. Therefore, these results indicate that the three-dimensional, hydroxyl functionalized polyester (pHMGCL) scaffold with good cell adhesion, and differentiation characteristics can be considered as a promising template for bone tissue regeneration and possesses excellent properties in comparison with the commonly used PCL scaffolds.

Acknowledgement

The authors wish to acknowledge the Dutch Program for Tissue Engineering (DPTE) for financial support (project number 6731).

References

[1] Langer R. Perspectives and Challenges in Tissue Engineering and Regenerative Medicine. *Adv. Mater.* **2009**, 21 (32-33), 3235-3236.

[2] Hollister S. J. Porous scaffold design for tissue engineering. *Nat. Mater.* **2005**, 4 (7), 518-524.

[3] Hutmacher D. W. Scaffolds in tissue engineering bone and cartilage. *Biomaterials* **2000**, 21 (24), 2529-2543.

[4] Woodfield T. B. F., Malda J., de Wijn J., Péters F., Riesle J., van Blitterswijk C. A. Design of porous scaffolds for cartilage tissue engineering using a three-dimensional fiber-deposition technique. *Biomaterials* **2004**, 25 (18), 4149-4161.

[5] Shipley R. J., Jones G. W., Dyson R. J., Sengers B. G., Bailey C. L., Catt C. J., et al. Design criteria for a printed tissue engineering construct: A mathematical homogenization approach. *J. Theor. Biol.* **2009**, 259 (3), 489-502.

[6] Ilagan B. G., Amsden B. G. Macroporous photocrosslinked elastomer scaffolds containing microposity: Preparation and in vitro degradation properties. *J. Biomed. Mater. Res. Part A*, **2010**, 93 (1), 211-218.

[7] Chen G., Ushida T., Tateishi T. Scaffold design for tissue engineering. *Macromol. Biosci.* **2002**, 2 (2), 67-77.

[8] Dalton P. D., Woodfield T., Hutmacher D. W. Erratum to: SnapShot: Polymer Scaffolds for Tissue Engineering [Biomaterials 30/4 (2009) 701-702]. *Biomaterials* **2009**, 30 (12), 2421-2423.

[9] Melchels F. P. W., Feijen J., Grijpma D. W. A review on stereolithography and its applications in biomedical engineering. *Biomaterials* **2010**, 31 (24), 6121-6130.

[10] Fedorovich N. E., De Wijn J. R., Verbout A. J., Alblas J., Dhert W. J. A. Three-dimensional fiber deposition of cell-laden, viable, patterned constructs for bone tissue printing. *Tissue Eng. Part A* **2008**, 14 (1), 127-133.

[11] Eosoly S., Brabazon D., Lohfeld S., Looney L. Selective laser sintering of hydroxyapatite/poly-ε-caprolactone scaffolds. *Acta Biomater.* **2010**, 6, 2511- 2517.

[12] Schantz J. T., Brandwood A., Hutmacher D. W., Khor H. L., Bittner K. Osteogenic differentiation of mesenchymal progenitor cells in computer designed fibrin-polymer-ceramic scaffolds manufactured by fused deposition modeling. *J. Mater. Sci. Mater. Med.* **2005**, 16 (9), 807-819.

[13] Gratson G. M., Xu M., Lewis J. A. Microperiodic structures: Direct writing of three-dimensional webs. *Nature* **2004**, 428 (6981), 386-386.

[14] Yang S., Leong K. F., Du Z., Chua C. K. The Design of Scaffolds for Use in Tissue Engineering. Part II. Rapid Prototyping Techniques. *Tissue Eng.* **2002**, 8 (1), 1-11.

[15] Park S., Kim G., Jeon Y., Koh Y., Kim W. 3D polycaprolactone scaffolds with controlled pore structure using a rapid prototyping system. *J. Mater. Sci. Mater. Med.* **2009**, 20 (1), 229-234.

[16] Landers R., Pfister A., Hübner U., John H., Schmelzeisen R., Mülhaupt R. Fabrication of soft tissue engineering scaffolds by means of rapid prototyping techniques. *J. Mater. Sci.* **2002**, 37 (15), 3107-3116.

[17] Dietmar W. H., Thorsten S., Iwan Z., Kee Woei N., Swee Hin T., Kim Cheng T. Mechanical properties and cell cultural response of polycaprolactone scaffolds designed and fabricated via fused deposition modeling. *J. Biomed. Mater. Res.* **2001**, 55 (2), 203-216.

[18] Williams J. M., Adewunmi A., Schek R. M., Flanagan C. L., Krebsbach P. H., Feinberg S. E., et al. Bone tissue engineering using polycaprolactone scaffolds fabricated via selective laser sintering. *Biomaterials* **2005**, 26 (23), 4817-4827.

[19] Sun H., Mei L., Song C., Cui X., Wang P. The in vivo degradation, absorption and excretion of PCL-based implant. *Biomaterials* **2006**, 27 (9), 1735-1740.

[20] Chen G., Zhou P., Mei N., Chen X., Shao Z., Pan L., et al. Silk fibroin modified porous poly(ε-caprolactone) scaffold for human fibroblast culture in vitro. *J. Mater. Sci. Mater. Med.* **2004**, 15 (6), 671-677.

[21] Yildirim E. D., Ayan H., Vasilets V. N., Fridman A., Guceri S., Sun W. Effect of dielectric barrier discharge plasma on the attachment and proliferation of osteoblasts cultured over poly(ε-caprolactone) scaffolds. *Plasma Processes. Polym.* **2008**, 5 (1), 58-66.

[22] Loontjens C. A. M., Vermonden T., Leemhuis M., Van Steenbergen M. J., Van Nostrum C. F., Hennink W. E. Synthesis and characterization of random and triblock copolymers of ε-caprolactone and (benzylated)hydroxymethyl glycolide. *Macromolecules* **2007**, 40 (20), 7208-7216.

[23] Seyednejad H., Vermonden T., Fedorovich N. E., Van Eijk R., Van Steenbergen M. J., Dhert W. J. A., et al. Synthesis and characterization of hydroxyl-functionalized caprolactone copolymers and their effect on

adhesion, proliferation, and differentiation of human mesenchymal stem cells. *Biomacromolecules* **2009**, 10 (11), 3048-3054.

[24] Leemhuis M., Van Nostrum C. F., Kruijtzer J. A. W., Zhong Z. Y., Ten Breteler M. R., Dijkstra P. J., et al. Functionalized poly(α-hydroxy acid)s via ring-opening polymerization: Toward hydrophilic polyesters with pendant hydroxyl groups. *Macromolecules* **2006**, 39 (10), 3500-3508.

[25] Leemhuis M., Van Steenis J. H., Van Uxem M. J., van Nostrum C. F., Hennink W. E. A versatile route to functionalized dilactones as monomers for the synthesis of poly(α-hydroxy) acids. *Eur. J. Org. Chem.* **2003** (17), 3344-3349.

[26] Pittenger M. F., Mackay A. M., Beck S. C., Jaiswal R. K., Douglas R., Mosca J. D., et al. Multilineage Potential of Adult Human Mesenchymal Stem Cells. *Science* **1999**, 284 (5411), 143-147.

[27] Dominici M., Le Blanc K., Mueller I., Slaper-Cortenbach I., Marini F., Krause D., et al. Minimal criteria for defining multipotent mesenchymal stromal cells. The International Society for Cellular Therapy position statement. *Cytotherapy* **2006**, 8 (4), 315-317.

[28] Más Estellés J., Vidaurre A., Meseguer Dueñas J., Castilla Cortázar I. Physical characterization of polycaprolactone scaffolds. *J. Mater. Sci. Mater. Med.* **2008**, 19 (1), 189-195.

[29] Salgado A. J., Gomes M. E., Chou A., Coutinho O. P., Reis R. L., Hutmacher D. W. Preliminary study on the adhesion and proliferation of human osteoblasts on starch-based scaffolds. *Mater. Sci. Eng. Part C.* **2002**, 20 (1-2), 27-33.

[30] Ghassemi A. H., van Steenbergen M. J., Talsma H., van Nostrum C. F., Jiskoot W., Crommelin D. J. A., et al. Preparation and characterization of protein loaded microspheres based on a hydroxylated aliphatic polyester, poly(lactic-co-hydroxymethyl glycolic acid). *J. Controlled Release* **2009**, 138 (1), 57-63.

[31] Ciardelli G., Chiono V., Vozzi G., Pracella M., Ahluwalia A., Barbani N., et al. Blends of poly-(ε-caprolactone) and polysaccharides in tissue engineering applications. *Biomacromolecules* **2005**, 6 (4), 1961-1976.

[32] Saito E., Kang H., Taboas J., Diggs A., Flanagan C., Hollister S. Experimental and computational characterization of designed and fabricated 50:50 PLGA porous scaffolds for human trabecular bone applications. *J. Mater. Sci. Mater. Med.* **2010**; Article in Press.

[33] Kuboki Y., Takita H., Kobayashi D., Tsuruga E., Inoue M., Murata M., et al. BMP-induced osteogenesis on the surface of hydroxyapatite with

geometrically feasible and nonfeasible structures: Topology of osteogenesis. *J. Biomed. Mater. Res.* **1998**, 39 (2), 190-199.

[34] Karageorgiou V., Kaplan D. Porosity of 3D biomaterial scaffolds and osteogenesis. *Biomaterials* **2005**, 26 (27), 5474-5491.

[35] Lebourg M., Sabater Serra R., Más Estellés J., Hernández Sánchez F., Gómez Ribelles J., Suay Antón J. Biodegradable polycaprolactone scaffold with controlled porosity obtained by modified particle-leaching technique. *J. Mater. Sci. Mater. Med.* **2008**, 19 (5), 2047-2053.

[36] Hoemann C. D., El-Gabalawy H., McKee M. D. In vitro osteogenesis assays: Influence of the primary cell source on alkaline phosphatase activity and mineralization. *Pathol. Biol.* **2009**, 57 (4), 318-323.

Chapter 5

In vivo Biocompatiblity and Biodegradation of 3D-printed Scaffolds Based on a Hydroxyl-Functionalized Poly(ε-caprolactone)

Hajar Seyednejad
Debby Gawlitta
Raoul V. Kuiper
Alain De Bruin
Cornelus F. van Nostrum
Tina Vermonden
Wouter J. A. Dhert
Wim E. Hennink

Manuscript Submitted

The aim of this study was to evaluate the *in vivo* biodegradation and biocompatibility of three-dimensional (3D) scaffolds based on a hydroxyl-functionalized polyester (poly(hydroxymethylglycolide-co-ε-caprolactone), PHMGCL), which has enhanced hydrophilicity, increased degradation rate, and improved cell-material interactions as compared to its counterpart poly(ε-caprolactone), PCL. In this study, 3D scaffolds based on this polymer (PHMGCL, HMG:CL 8:92) were prepared by means of fiber deposition (melt-plotting). The biodegradation and tissue biocompatibility of PHMGCL and PCL scaffolds after subcutaneous implantation in Balb/c mice were investigated. At 4 and 12 weeks post implantation, the scaffolds were retrieved and evaluated for extent of degradation by measuring the residual weight of the scaffolds, thermal properties (DSC), and morphology (SEM) whereas the polymer was analyzed for both its composition (^{1}H NMR) and molecular weight (GPC). The scaffolds with infiltrated tissues were harvested, fixed, stained, and histologically analyzed. The *in vitro* enzymatic degradation of these scaffolds was also investigated in lipase solutions. It was shown that PHMGCL 3D-scaffolds lost more than 60% of their weight within 3 months of implantation while PCL scaffolds showed no weight loss in this time frame. The molecular weight (M_w) of PHMGCL decreased from 46.9 kDa before implantation to 23.2 kDa after 3 months of implantation, while the molecular weight of PCL was unchanged in this period. ^{1}H NMR analysis showed that the degradation of PHMGCL was characterized by a loss of HMG units. *In vitro* enzymatic degradation showed that PHMGCL scaffolds were degraded within 50 hours, while the degradation time for PCL scaffolds of similar structure was 72 hours. A normal foreign body response to both scaffold types characterized by the presence of mononuclear inflammatory cells and fibrosis was observed with a more rapid onset in PHMGCL scaffolds. The extent of tissue-scaffold interactions as well as vascularization was shown to be higher for PHMGCL scaffolds compared to PCL ones. Therefore, the fast degradable, biocompatible PHMGCL scaffold is a promising biomaterial for tissue engineering applications.

1. Introduction

One of the main challenges in tissue engineering is designing suitable scaffolds that meet the crucial requirements for application in regenerative medicine. Both natural and synthetic polymers have been used for this purpose, however, the ability to adjust material properties and tailor their performance in terms of tissue response and biodegradation time makes synthetic biocompatible polymers more attractive than natural polymers. The proper choice of polymer needs thoughtful considerations about the polymer's physical and chemical properties, degradation rate, and the ability to promote specific events at the cellular and tissue level[1]. Moreover, the polymeric scaffold should be biocompatible, which, as defined by Williams[2], means that it should be able to "perform as a substrate that will support the appropriate cellular activity, including the facilitation of molecular and mechanical signaling systems, in order to optimize tissue regeneration, without eliciting any undesirable local or systemic response in the eventual host". Besides biocompatibility, the physical architecture of the scaffold is also of great importance. Designing a three-dimensional structure comprising open-cells and interconnected pores[3] that allow facile communication between the biological cells dispersed within the scaffold[4] and promote migration, proliferation, differentiation, and vascularization as well as in and out diffusion of nutrients and metabolic waste products is preferred[5]. Several studies on ceramic, metal, and polymeric implants demonstrated enhanced osteogenesis of porous versus solid implants, both at macroscopic and microscopic levels[5]. Hulbert et al.[6] showed already in 1970 that the minimum pore size of synthetic materials required for bone regeneration is approximately 100 µm and subsequent studies demonstrated that larger pore sizes (more than 300 µm) promote bone ingrowth[5].

There are several techniques to design scaffolds for TE applications. In the last decade, especially solid freeform fabrication (SFF) methods have gained wide attention. SFF refers to the fabrication of a structure based on a computer-designed model with rapid prototyping (RP) as the most commonly used technique[7]. In a typical RP method (i.e. melt-plotting or fiber deposition), a 3D model of the scaffold is created using a computer and in the next step the dispensing material is loaded into the 3-axis robot arm and the material is extruded in a layer-by-layer fashion enabling formation of a well-defined structure with respect to external shape as well as internal morphology[8, 9]. The most commonly used polymer for this technology is poly(ε-caprolactone) PCL[10-14], which despite its good biocompatibility and processability, is rather hydrophobic leading to limited cell-scaffold interactions. Further, PCL is semi-crystalline which together with its hydrophobicity and low water absorbing capacity, resulted in very

slow degradation kinetics (2 to 4 years)[15]. Recently, we have developed a functionalized aliphatic polyester based on PCL, namely poly(hydroxymethylglycolide-co-ε-caprolactone), PHMGCL, which possesses significantly higher hydrophilicity due to its hydroxyl groups attached to the backbone[16], resulting in a significant increase in human mesenchymal stem cells adhesion, proliferation, and differentiation as compared to PCL[16, 17]. We have also shown the possibility of designing three-dimensional (3D) PHMGCL structures by means of a melt-plotting technique[17] at considerably lower temperature than used for PCL (50 °C vs. 110 °C, respectively). Furthermore, we demonstrated that PHMGCL scaffolds degrade much faster than PCL scaffolds *in vitro*[18].

The main function of scaffolds in tissue engineering approaches is to provide a substrate for cell adhesion and proliferation and thus facilitate the formation of new tissue. Ideally, the degradation rate of the scaffolds should match the rate at which the new tissue is formed. Therefore, it is important to evaluate how the newly formed tissue integrates with the synthetic scaffold and to what extent the implanted scaffold causes a foreign body reaction. Thus, in the current study, to continue our investigations on the characteristics of scaffolds based on this functionalized polyester, the biocompatibility and biodegradation of 3D-melt plotted porous structures based on PHMGCL or PCL after subcutaneous implantation in balb/c mice are investigated. The changes in the physical and chemical properties of the harvested PHMGCL and PCL scaffolds after 1 and 3 months of implantation were investigated. We also evaluated the tissue response to the aforementioned scaffolds in this time frame. Generally, macrophages represent an important component of the cellular infiltrate after implantation of a foreign material. Macrophages secrete several enzymes including lipase[19], an enzyme that is known for its ability to catalyze the degradation of PCL[20]. Therefore, also the *in vitro* degradation of the synthetic scaffolds in the presence of lipase was investigated.

2. Materials and Methods

2.1. Materials

The chemicals used in this study were purchased from Sigma-Aldrich and used as received, unless stated otherwise. The solvents were purchased from Biosolve (Valkenswaard, The Netherlands) except acetone (Merck, Darmstadt, Germany), hexane (Antonides-Interchema, Oosterzee, The Netherlands), toluene, and sulfuric acid (Acros, Geel, Belgium). Toluene was distilled from P_2O_5 and stored over 3 Å molecular sieves under argon. 3S-Benzyloxymethyl-1,4-dioxane-2,5-

dione (benzyl-protected hydroxymethyl glycolide, BMG) was synthesized as described by Leemhuis et al. [21, 22]. ε-Caprolactone (CL) and silica gel (0.035-0.070 mm, 60 Å) were obtained from Acros (Geel, Belgium). O-Benzyl-L-serine was supplied by Senn Chemicals (Dielsdorf, Switzerland). Sodium nitrite ($NaNO_2$) and dimethylaminopyridine (DMAP) were purchased from Fluka (Zwijndrecht, The Netherlands). Sodium sulfate (Na_2SO_4), triethylamine, sodium carbonate (Na_2CO_3), and benzyl alcohol (BnOH) were provided by Merck (Darmstadt, Germany). Bromoacetyl bromide, tin(II) 2-ethylhexanoate ($SnOct_2$) and Pd/C (palladium, 10 wt % (dry basis) on activated carbon, wet (50% water w/w), Degussa type E101 NE/W) were obtained from Aldrich (Zwijndrecht, The Netherlands). Lipase (from *Pseudomonas cepacia,* 30 units/mg) was purchased from Sigma-Aldrich (Germany) and used as received.

2.2. Methods

2.2.1. Polymer Synthesis

Poly(hydroxymethylglycolide-co-ε-caprolactone) was synthesized as described before[17]. In short, [poly(benzyloxymethylglycolide-co-ε-caprolactone), PBMGCL] was synthesized by loading ε-CL (6.54 mL, 59 mmol) and BMG (1.2 g, 5.1 mmol), initiator (BnOH, 23.14 mg, 0.214 mmol), and catalyst ($SnOct_2$, 43.3 mg, 0.107 mmol) into a dry schlenk tube. The tube was evacuated for 2 hours, subsequently closed and immersed into an oil bath pre-heated at 130 °C. The polymerization was performed overnight and the formed polymer was purified by dissolution in chloroform and precipitation in methanol. Next, the protective benzyl groups of pBHMGCL were removed in a hydrogenation reaction using Pd/C catalyst essentially as described by Leemhuis et al[21] to yield PHMGCL. Both PBMGCL and PHMGCL were characterized by ^{1}H NMR, DSC, and GPC. Poly(ε-caprolactone) was synthesized as described before[17] using monomer/initiator/catalyst ratio of 300/1/0.5 in a ring opening polymerization at 130 °C for 16 hours.

2.2.2. Polymer Characterization

The copolymer compositions were determined by proton nuclear magnetic resonance (^{1}H NMR) spectroscopy (Gemini 300 MHz, Varian Associates Inc., NMR Instruments, Palo Alto, CA). Chemical shifts were recorded in ppm with reference to the solvent peak (δ= 7.26 ppm for $CDCl_3$ in ^{1}H NMR).

Thermal properties of polymers were determined using differential scanning calorimetry (DSC, TA Instruments Q2000). Samples of approximately 5

mg were loaded into aluminum pans and scanned from -80 °C to 100 °C with a heating rate of 10 °C/min and a cooling rate of 0.5 °C/min under nitrogen flow of 50 mL/min. The glass transition temperature (T_g) was recorded as the midpoint of heat capacity change in the second heating run. Melting temperature (T_m) and heat of fusion (ΔH_f) were determined from the onset of the endothermic peak position and integration of endothermic area in the second heating run, respectively. For scaffolds, the samples were equilibrated at -90 °C and then heated to 100 °C with a heating rate of 10 °C/min and the thermal transitions were reported for the first heating run.

The molecular weight (M_w and M_n) of the obtained polymers was measured using gel permeation chromatography (GPC) with a 2695 Waters Aliance system and a Waters 2414 refractive index detector. Two PL-gel 5 µm mixed-D columns fitted with a guard column (Polymer Labs, M_w range 0.2- 400 KDa) were used. The columns were calibrated with polystyrene standards of known molecular weights using AR grade THF, eluting at 1 mL/min flow rate at 30 °C. The concentration of the polymers was 5 mg/mL and the injection volume was 50 µL.

2.2.3. Scaffold Preparation and Characterization

Three-dimensional scaffolds were prepared using 3D-printing (melt-plotting) as described before[17]. Briefly, PCL and PHMGCL were loaded into the Bioscaffolder reservoir and heated to 110 or 50 °C, respectively. The molten polymers were then extruded via a 23G nozzle by means of compressed air pressure, resulting in parallel strands, which were deposited in a layer-by-layer fashion at a speed of 350 or 500 mm/min for PCL and PHMGCL, respectively. Square pores were created in the scaffolds by rotating the meandering strand pattern over a 90° angle. The distance between strands was set to 0.9 mm and the spindle speed was 200 rpm. The scaffold geometry was imaged on a stereo microscope (SZ61/SZ2-ILST, Olympus, The Netherlands). The morphology of the strands of harvested scaffolds after implantation (explants) was studied by scanning electron microscopy (SEM, Phenom™, FEI Company, The Netherlands). Parts of the scaffolds were glued onto a 12 mm diameter aluminum sample holder using conductive carbon paint (Agar scientific Ltd., England) and coated with palladium under vacuum using an ion coater.

2.2.4. *In vitro* Degradation of Scaffolds

To prepare scaffolds for the *in vitro* degradation study, first a block of scaffold (dimension of 1cm χ 1cm) was melt-plotted and subsequently small, round scaffolds (diameter of 0.5 cm) were punched out of this block, using a biopsy puncher. The obtained samples (20 mg) were immersed in 5 mL PBS (pH 7.4, 0.033 M NaH_2PO_4, 0.066 M Na_2HPO_4, 0.056 M NaCl) containing 0.5% sodium azide as bacterial growth inhibitor and 0.1% lipase at 37 °C on a shaker. The buffer was refreshed every 24 hours, as described before[20, 23]. At different time intervals, triplicate scaffolds were withdrawn, washed twice with de-ionized water and dried in vacuum at room temperature for three days. The dry weight of each scaffold was measured at the start of the experiment (W_0) and at the sampling time point (W_t). The percentage mass loss was calculated according to the following equation:

$$\%\text{-mass loss} = (W_0 - W_t)/W_0 \chi\ 100\ \%$$

The scaffolds were also characterized for thermal properties (DSC) and the molecular weight of polymer was determined using GPC, as described in section 2.2.2.

2.2.5. Sterilization of scaffolds

The printed scaffolds were sterilized by submersion in 70% ethanol on a roller bench for 60 minutes. Subsequently, the scaffolds were allowed to dry in the flow of a laminar air flow (LAF) cabinet and transferred into sterile wells plates and stored until use.

2.2.6. *In vivo* Implantation studies

Ten Balb/c mice (female, 6-8 weeks, Charles River, Brussels, Belgium) were anaesthetized with 1.5% isoflurane. Four approximately 8 mm dorsal incisions were made on each mouse to create subcutaneous pockets. The scaffolds were transferred into the separate pockets of each mouse and the skin was closed using Vicryl 5.0 sutures. Peroperatively and postoperatively, the animals received 0.05 mg/kg buprenorphine subcutaneously (Temgesic, Schering-Plough/Merck, USA). The mice were housed together at the Central Laboratory Animal Institute of Utrecht University. The experiments were approved by the local Ethics Committee for Animal Experimentation and in compliance with the Institutional Guidelines on the Use of Laboratory Animals. After 1 and 3 months, the animals

were sacrificed, and the scaffolds were further processed into two groups; to investigate either the polymer degradation (n=7 per scaffold type per time point) by removing the adhered tissue from the explanted scaffolds as described in section 2.2.7, or to investigate the tissue reaction (n=3 per scaffold type per time point) by analyzing the ingrown tissue into the pores of scaffolds (infiltrated tissue), and the adjacent tissue to the scaffolds as described in section 2.2.8.

2.2.7. Explant Tissue Digestion Protocol

The extent of degradation of the explanted scaffolds was investigated by measuring the weight loss and observing morphology (SEM), as well as by measuring the polymer properties using ^{1}H NMR, DSC, and GPC analysis. Since tissue grew into the pores of the implanted scaffolds, an oxidizing agent was employed to remove the adhered tissue[24]. Briefly, the scaffolds were treated with 10 mL of sodium hypochlorite (NaOCl) solution in water (concentration of 5.25%) for 20 min. This duration was sufficient to remove the adhered tissue from the PCL scaffolds. However, due to high extent of tissue-PHMGCL scaffold interaction, the tissue adhered to these scaffolds was not completely removed. Therefore, a number of these scaffolds (n=3 per time point) was retrieved by dissolution in dichloromethane (DCM) and subsequent filtration to remove non-soluble tissue fragments. Next, DCM was evaporated and the weight of dry polymer was measured and considered as W_t of the scaffolds.

2.2.8. Histological Examination

The retrieved scaffolds (n=3 per scaffold per time point) together with the ingrown tissues were fixed in formalin. The fixed implants were dehydrated through a graded series of alcohol solutions and then transferred into xylene. This procedure resulted in dissolution of the remaining scaffolds present in the tissue. The fixed tissues were subsequently embedded in paraffin. The obtained paraffin blocks were then cut into 5 µm thick sections, deparaffinizied in xylene and rehydrated in graded series of alcohol prior to staining. The sections were stained with Mayer's hematoxylin (Merck, 1.09249.0500, 10 seconds) and 0.2% eosin (in 50% ethanol, 20 seconds) (H & E). The different samples were scored using light microscopy by two independent observers (blinded) for signs of inflammation. The number of infiltrated cells: mononuclear and multinucleated giant cells, as well as the extent of fibrosis were scored (-, +/-, +, ++) on an ordinal scale.

Vascular invasion of the scaffolds was studied in detail using αSMA immunohistochemistry. Antigen retrieval was accomplished by boiling the

sections in 10 mM citrate buffer for 15 minutes. Sections were blocked in 0.3% H_2O_2 and 3% bovine serum albumin. Incubation with the ALP-conjugated primary antibody (1:300, monoclonal mouse, A5691, Sigma) was performed for one hour at room temperature. Negative control sections were stained with concentration-matched mouse IgG1 (X0931, Dako). Staining was then detected with the VECTOR Red Alkaline Phosphatase Substrate Kit (SK-5100, Vector Laboratories). The nuclei were lightly counterstained with 50% Mayer's hematoxylin.

2.2.9 Statistics

Statistical analysis of the data was done using a one-way analysis of variance (ANOVA) with a post hoc Tukey-Kramer multiple comparison test using GraphPad Instat software (version 3.05; San Diego, CA)[25]. A p-value<0.05 was considered statistically significant.

3. Results

3.1. Scaffold Preparation and Characterization

PHMGCL and PCL were synthesized via ring opening polymerization, using BnOH and $SnOct_2$ as initiator and catalyst, respectively. The monomer to initiator molar ratio was 300/1 and the catalyst/ initiator ratio was 0.5/1. The molar ratio of BMG/ ε-CL in feed was 8/92 and ^{1}H NMR analysis of the obtained PBMGCL showed that copolymer composition matched that of feed (Table 1). GPC analysis showed that M_w's of PCL and PHMGCL were 79.1 kDa (PDI= 2.0) and 47.1 kDa (PDI=1.9), respectively (Table 1). DSC analysis showed that the melting temperatures of PCL and PHMGCL were 54 °C and 43 °C, respectively (Table 1).

Table1. Characteristics of the polymers used in this study.

BMG/CL Molar Ratio In feed	BMG/CL Molar Ratio In polymer	pBMGCL DSC T_m (°C)	pBMGCL DSC ΔH_f (J/g)	pBMGCL GPC M_w (kDa)	pBMGCL GPC PDI	Yield (%)	pHMGCL DSC T_m (°C)	pHMGCL DSC ΔH_f (J/g)	pHMGCL GPC M_w (kDa)	pHMGCL GPC PDI
0/ 100	0/ 100	-	-	-	-	87	54	61	79.1	2.0
8/ 92	8/ 92	42	47	49.2	2.4	95	43	42	47.1	1.9

[a]polydispersity Index (=M_w/M_n)

Three-dimensional, porous scaffolds of PHMGCL and PCL were prepared using 3D-plotting[17]. The physical properties of the scaffolds are listed in Table 2. It can be seen that the characteristics (molecular weight and thermal properties) of

these polymers were not changed after melt-plotting process. Macroscopic observations of the scaffolds showed that they possessed a well-defined, porous structure in three dimensions comprising interconnected pores, with a pore size of approximately 900 µm in one direction (Fig.1 A&B) and smaller pores (around 100 µm) in the other two directions (Fig.1 C&D). The porosity of scaffolds was approximately 70% as calculated based on the bulk density of polymers and apparent density of the scaffolds[17].

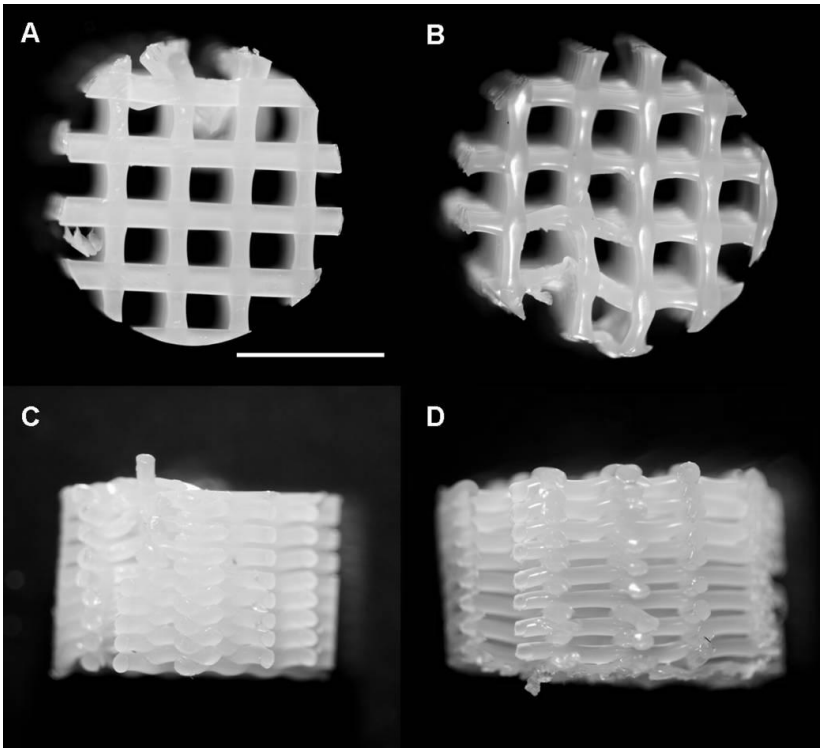

Fig.1. Macroscopic images of 3D-printed scaffolds before implantation. Top view of A) PCL and B) PHMGCL scaffolds. Side view of C) PCL and D) PHMGCL scaffold. Scale bar is 2.5 mm.

3.2. Enzymatic Degradation of scaffolds

The *in vitro* enzymatic degradation kinetics of 3D-printed scaffolds based on PCL and PHMGCL were investigated in aqueous solutions of lipase, an enzyme secreted by macrophages[19]. The weight of scaffolds in 0.1 mg/mL of lipase solutions decreased in time. PHMGCL and PCL scaffolds were completely

degraded within 50 and 72 hours, respectively (Fig.2). DSC analysis of both scaffolds exposed to lipase for different times showed no change in melting temperature and melting enthalpy during degradation (supplementary data). GPC analysis showed that molecular weight of PHMGCL and PCL had not changed (supplementary data). The degradation of PCL and PHMGCL scaffolds in lipase solution of 0.5 mg/mL was also investigated and the degradation rate was found to be much faster than the hydrolysis in low concentrated enzyme solution (0.1 mg/mL) as both scaffold types were completely degraded in 24 hours. Moreover, the rate of lipase-catalyzed degradation of both scaffold types was found to be much higher at higher enzyme concentration (0.5 vs. 0.1 mg/mL), indicating that the rate of enzymatic degradation of these polyester scaffolds is dependent on the enzyme content, as also shown by others[20].

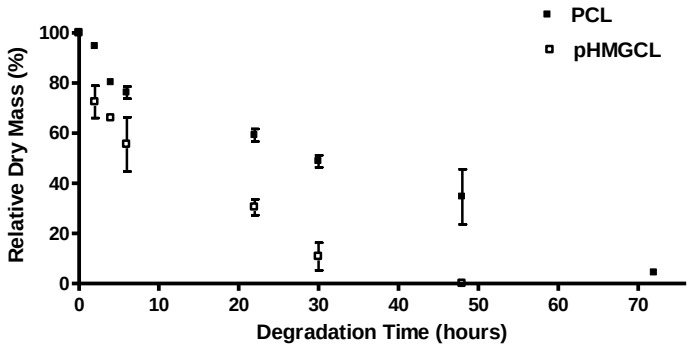

Fig.2. Weight loss of PCL and PHMGCL scaffolds (n=3 ± SD) in PBS (pH=7.4) containing lipase (0.1 mg/mL) at 37 °C.

3.3. *In vivo* Biodegradation of Scaffolds

The *in vivo* degradation of polymeric scaffolds which were subcutaneously implanted in mice was investigated. At one and three months post implantation, the scaffolds were retrieved from the animals as a block (containing surrounding and infiltrated tissue) and were treated as described in section 2.2.7 and characterized for weight loss as well as changes in chemical and physical properties. Figure 3 shows that the PCL scaffolds did not undergo any mass loss during 3 months of implantation, while mass loss of PHMGCL scaffolds after 1 and 3 month of subcutaneous implantation was 39.8 ± 11.7% and 63.2 ± 4.9%, respectively.

The composition of PHMGCL in the remaining but partially degraded scaffolds was established using ^{1}H NMR (Fig. 4). Comparing the integrals of

peaks corresponding to HMG units (5.0-5.4 ppm) to those of CL units (1.2-1.8 ppm) showed that after one month of implantation, there was a decrease in HMG units and the polymer became consequently richer in CL units (Fig. 4B). However, after 3 months, there were some additional peaks at 5.0-5.4 ppm, 2.7-2.9 ppm, 1.8-2.1 ppm, and 0.8-1.0 ppm observed in the NMR spectrum of PHMGCL (as well as PCL, supplementary data). After 3 months of implantation, the peak related to glycolic acid units at 4.6-4.8 ppm was absent, indicating that these units were completely degraded within this time frame.

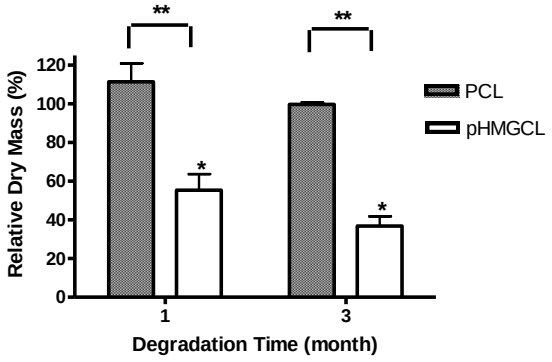

Fig.3. Weight loss of PCL and PHMGCL scaffolds (n=3 ± SD) upon subcutaneous implantation in mice. *P<0.05, **p<0.001.

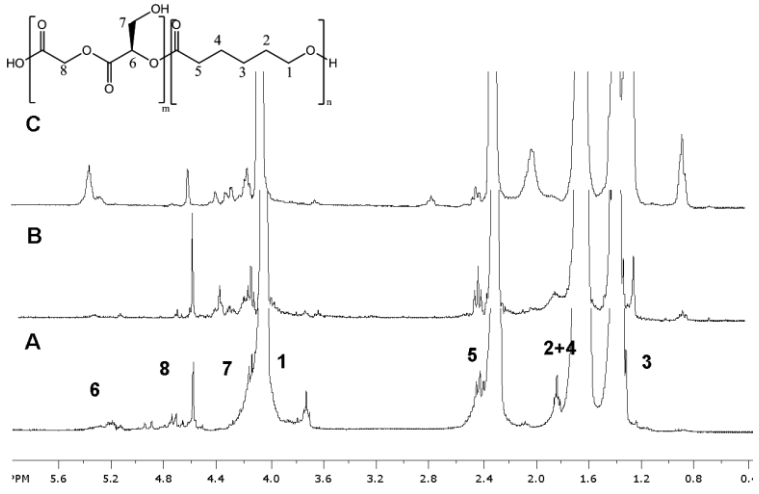

Fig.4. ^{1}H NMR spectra of PHMGCL dissolved in $CDCl_3$ (A) before implantation, (B) after 1 month and (C) 3 months subcutaneous implantation of scaffolds in mice.

SEM analysis was employed to determine changes in surface morphology of the scaffolds. As can be seen in Figure 5, the fibers of the PCL scaffold after one month of implantation had a smooth surface (Fig. 5A) while those of the PHMGCL fibers were roughened (Fig. 5B) and showed an arborizing morphology. The thermal properties of the scaffolds were evaluated using DSC (Table 2). The melting temperature of the PCL scaffolds was slightly decreased after implantation (from 54.8 °C before implantation to 54.6 ± 0.2 after 1 months of implantation) and was unchanged afterwards. The heat of fusion for these scaffolds was decreased from 67.6 J/g to 61.6 ± 2.7 J/g after one month and then increased to 65.7 ± 1.2 J/g after three months. The T_m of PHMGCL scaffolds increased from 40.4 °C to 42.9 ± 0.1 °C after one month and was unchanged afterwards (Table 2). The melting enthalpy (ΔH) of PHMGCL first decreased from 51.2 J/g to 40.0 ± 2.2 J/g after one month and then increased to 49.8 ± 5.5 J/g after three months of implantation. The molecular weight of the polymers before and after implantation was determined using of GPC analysis (Table 2). The M_w of PCL hardly changed during three months of implantation, however, the M_w of PHMGCL decreased from 46.9 kDa before implantation to 34.7 ± 1.3 kDa after one month and 23.2 ± 2.7 kDa after three months of implantation.

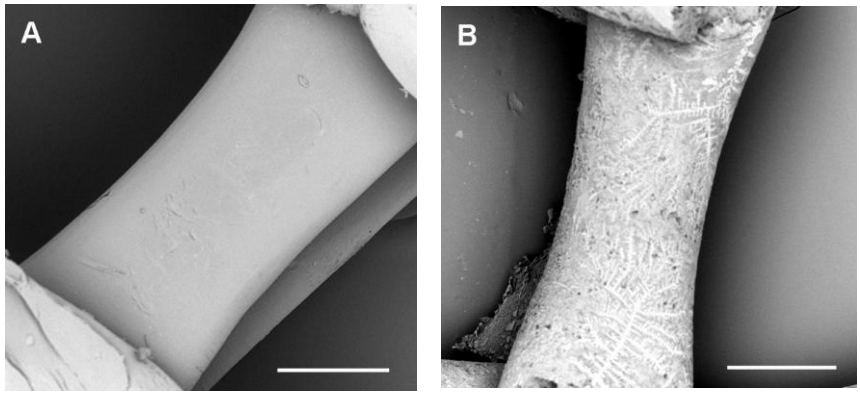

Fig.5. Scanning electron microscopy images of scaffolds' strands of (A) PCL and (B) PHMGCL after one month of subcutaneous implantation in mice. Scale bar is 200 µm. The roughened surface of PHMGCL might be due to degradation of amorphous regions by enzymes, yielding crystalline structures ('spherulites') at the surface.

Table2. Physical characteristics of PCL and PHMGCL scaffolds before and after subcutaneous implantation in mice.

Scaffolds	Before Implantation				One month implantation				Three months implantation			
	T_m (°C)	ΔH_f (J/g)	M_w (kDa)	PDI	T_m (°C)	ΔH_f (J/g)	M_w (kDa)	PDI	T_m (°C)	ΔH_f (J/g)	M_w (kDa)	PDI
PCL	54.8	67.6	76.6	1.8	54.6 ± 0.2	61.5 ± 2.6	73.2 ± 2.1	1.9 ± 0.1	54.3 ± 0.2	65.6 ± 1.2	75.0 ± 1.2	1.9 ± 0.1
PHMGCL	40.3	51.2	46.9	2.1	42.9 ± 0.1	40.0 ± 2.2	34.7 ± 1.3	1.9 ± 0.1	42.7 ± 0.1	49.8 ± 5.4	23.2 ± 2.7	1.8 ± 0.2

3.4. Biocompatibility of the Scaffolds

The *in vivo* cellular response to PHMGCL and PCL scaffolds was studied. The gross observation after one month of implantation showed that newly formed tissue invaded the pores of PHMGCL and PCL scaffolds. This ingrown tissue was very difficult to remove particularly from PHMGCL scaffolds after explantation (see section 2.2.7), indicating a strong tissue-material interaction.

Figure 6 represents the cellular responses to PHMGCL (Fig. 6A-B) and PCL (Fig. 6C-D) scaffolds after one month of implantation. It should be mentioned that during tissue processing, the polymer was dissolved in xylene and the dissolved strands are visible in the tissue sections as pores in the ingrown tissue, consistent with the preserved structural integrity of the scaffolds one month after implantation.

The pores of both scaffold types were infiltrated by adipose and loose connective tissue. Further, the presence of inflammatory cells (i.e. monocytes) is more obvious in the infiltrating tissue surrounding PHMGCL than the PCL scaffolds. Variable numbers of multinucleated giant cells (fused macrophages) surrounded the cavities of PHMGCL scaffold where the polymer fibers were present (inserts in Figure 6). Several giant cells exhibited a stretched morphology that is typical for osteoclasts (Figure 6A-insert). Semiquantitative scoring of the host tissue responses and infiltration is presented in Table 3 and shows that a higher number of mononuclear inflammatory cells was observed in the tissues grown into the PHMGCL scaffolds than in tissue grown into PCL. This difference is consistent with the faster biodegradation kinetics and the arborizing surface roughening (in the form of branches, Figure 5) of the PHMGCL scaffolds. In addition to mononuclear cell invasion, the strands on the outside of the PHMGCL scaffolds were surrounded by a denser layer of a more mature fibrous tissue (fibrosis) in comparison with PCL scaffolds.

After 3 months of implantation, the number of mononuclear cells (i.e., predominantly macrophages) in the tissue infiltrating the PHMGCL scaffolds had decreased, however, the presence of multinucleated giant cells (i.e., fused macrophages, typical for a foreign body reaction) further increased (Table 3) and these cells were present inside the scaffold pores (Figure 7, A-B).

Table3. Median histological scores for inflammatory cell outcome and vascularization of the infiltrated and surrounding tissue of the implanted scaffolds. The number of infiltrating cells (mononuclear and giant cells) as well as the extent of fibrosis and vascularization is scored on an ordinal scale (raging from -, +/-, +, ++, to +++)

.

Time Point	Scaffold	Inflammatory cell outcome			Vascularization	
		Mononuclear cells	Multinucleated giant cells	Fibrosis	Center of scaffold	Periphery of scaffold
One Month	PHMGCL	+	++	++	+	++
	PCL	+	+/-	+	+	+
Three Months	PHMGCL	+/-	+++	+++	++	++
	PCL	++	+	++	+	+

Fibrosis was further advanced to the center of PHMGCL scaffolds as compared to the fibrosis observed after 1 month of implantation. However, the fibrous layer inside the scaffold was remarkably thinner than the fibrous layer observed on the periphery of scaffolds. Furthermore, the overall structure of these scaffolds remained intact also 3 months after subcutaneous implantation. Importantly, after 3 months PHMGCL scaffolds showed an increased number of blood vessels per cross-sectional area in the inner parts of the scaffold when compared to number of blood vessels after one month of implantation (Table 3), also emphasizing the more mature nature of the newly formed connective tissue. The inflammatory response to the PCL scaffolds is presented in Figure 7 (C-D).

After one month, the presence of mononuclear and giant cells throughout the (surrounding and infiltrated) tissue is less prominent than for PHMGCL scaffolds. However, the incidence of these cells was increased after 3 months, indicating a milder tissue response in PCL scaffolds as compared to PHMGCL scaffolds. At one month after implantation, fibrosis was virtually absent in PCL scaffolds and a minimal number of blood vessels was observed in the loose connective tissue surrounding the more central scaffold pores.

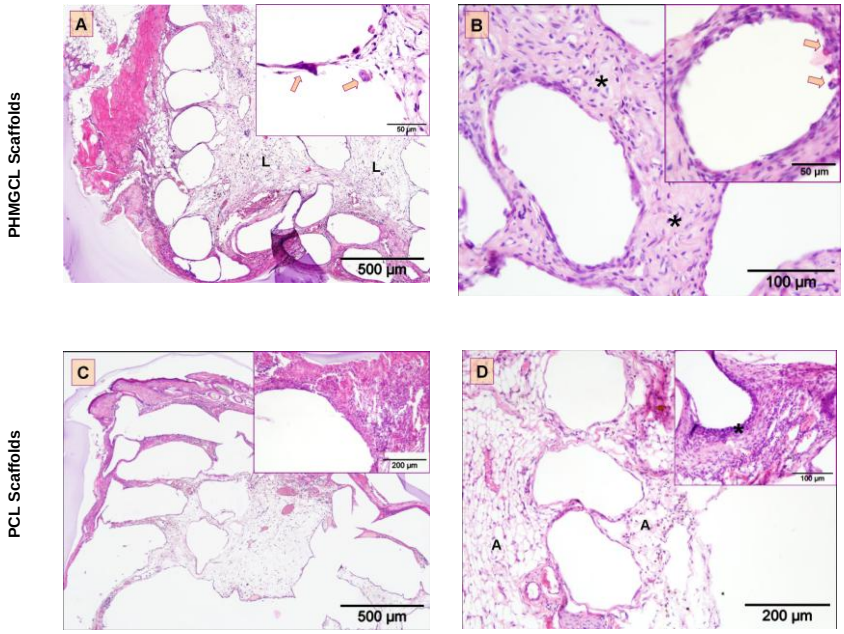

Fig.6. Representative Hematoxylin and Eosin (H&E) images after one month of implantation. (A-B) PHMGCL scaffold, (C-D) PCL scaffold. The empty spaces in the tissues represent the places where scaffold strands were present and washed away during processing steps. Infiltrated tissue of PHMGCL scaffold is mainly filled with loose connective tissue (marked “L” in A) while this tissue in PCL scaffolds is mainly composed of adipose tissue (marked “A” in D). High magnification images show the presence of multinucleated giant cells (arrows in A-B) and more advanced fibrosis (asterisks) in PHMGCL scaffolds, and more extensive mononuclear inflammatory cell infiltration in PCL scaffolds (marked by asterisk in D).

There was no increase in the number of blood vessels in the infiltrated tissue in PCL scaffolds after 3 months. Overall, vascularization remains lower in PCL than in PHMGCL scaffolds in the time frame studied.

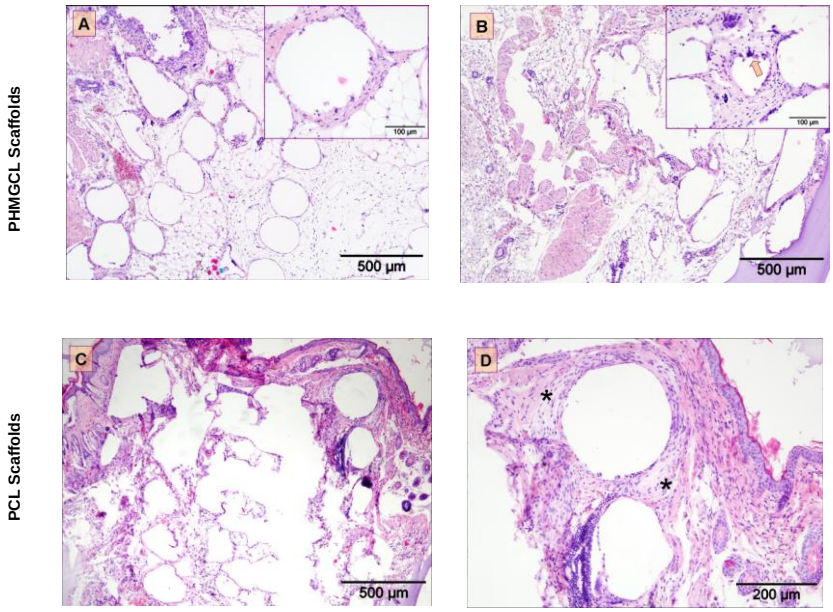

Fig.7. Representative Hematoxylin and Eosin (H&E) images after three months of implantation. (A-B) PHMGCL scaffold, (C-D) PCL scaffold. The empty spaces in the tissues show polymer strands and the scaffold pores are filled with the tissue infiltrate. The porous structure of the scaffolds is preserved after 3 months of implantation and the infiltrating tissue filled the scaffold pores. The presence of mononuclear inflammatory cells is subsided in the infiltrating tissue of PHMGCL scaffolds (A-B) and giant cells in this tissue can be observed (B-insert). The number of mononuclear cells in the tissue that surrounds pHMGCL scaffolds is still higher than that of PCL scaffolds and fibrosis has further advanced (asterisks) in the infiltrated tissue of PCL scaffolds (C-D).

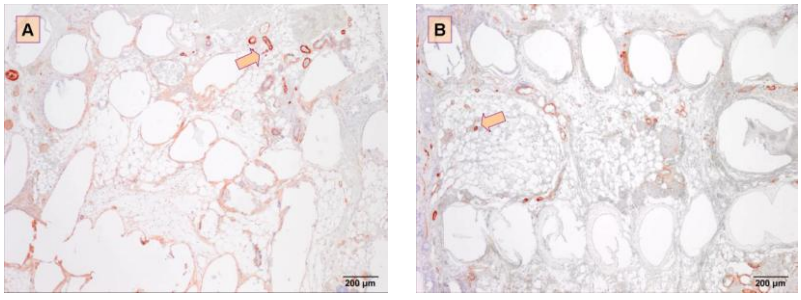

Fig.8. Representative αSMA (in red) images for (A) PHMGCL and (B) PCL after 3 month of subcutaneous implantation. SMA is present in the smooth muscle cells of the vascular walls[48]. The arrows indicate the circular and ellipsoid cross section of the vascular structures present in the infiltrating tissues.

4. Discussion

PCL and PHMGCL were synthesized by ring opening polymerization in the melt and it was shown that the thermal properties of PCL (T_m and ΔH of 54 °C and 61 J/g) were similar to values reported in the literature[15]. Further, the crystallinity of the copolymer decreased (as reflected by decrease in ΔH and T_m from 61 J/g and 54 °C for PCL to 42 J/g and 42 °C for PHMGCL, Table 1), which is in agreement with our previous findings[16]. These polymers were further processed into 3D, porous scaffolds, containing large, interconnected pores, which allow ingrowth of tissue after *in vivo* implantation.

PCL and PHMGCL scaffolds exposed to PBS solutions containing lipase showed a decrease in their mass (Figure 3), while the bulk properties were unchanged. These observations point to surface erosion of the scaffolds mediated by the enzyme. Indeed, lipase catalyzed degradation of polymeric implants starts with adsorption of the enzyme onto the polymer substrate, followed by formation of a transition complex between the polymer and enzyme, and finally chain scission of the polymer[26]. Because the degradation occurs only at the material surface, the bulk properties of the polymer are unchanged[27, 28] which is in line with our observations. Interestingly, Figure 2 shows that the degradation rate of the PHMGCL scaffold was faster than the PCL ones. This can be attributed to the fact that HMG units are more hydrated than CL units, which in turn probably results in an easier and thus enhanced enzymatically catalyzed hydrolysis of ester bonds in PHMGCL. Lendlein et al.[20] also showed that the enzymatic degradation rate of a series of multiblock copolymers consisting of PCL and poly(p-dioxanone) segments increased with increasing content of the more hydrophilic poly(p-dioxanone) units. Moreover, it is well accepted that crystalline regions are more difficult to degrade by enzymes than the amorphous regions[29]. This is due to the fact that the catalytic center of lipase is located inside this protein and amorphous polymer chains have higher mobility when compared to crystalline chains and thus have better access to these centers[30, 31]. Indeed, PHMGCL has lower crystallinity when compared to PCL (as reflected by lower T_m and ΔH_f, Table 1) and is therefore more prone to enzymatic degradation in comparison with PCL surface.

The *in vivo* biodegradation of PCL and PHMGCL was elucidated by characterizing the properties of harvested implants after 1 and 3 months. The absence of weight loss of PCL scaffolds in combination with the stable thermal properties as well as molecular weights of this polymer (Table 1) imply that these scaffolds did not undergo degradation in the time frame studied. The slight increase in the weight of PCL scaffolds at both time points (Figure 3) is likely

related to traces of ingrown tissue which were difficult to remove from the internal pores of the scaffolds. It is well known that PCL is a hydrophobic, slowly degrading polyester with a degradation time ranging from 2 to 4 years[15]. Sun et al.[32] showed in a rat study that PCL capsules remained intact for 2 years, the M_w decreased from 66 kDa to 15 kDa and the capsules finally fragmented after 30 months when M_w reached 8 kDa. Pitt et al.[33] showed that degradation of PCL particles is characterized by a two stage pattern. First, a decrease in molecular weight is observed without mass loss and second, when the molecular weight dropped to 5 kDa, mass loss and loss of particles integrity were observed. We have also shown previously[18] that PCL films incubated in PBS (pH 7.4) at 37 °C for a duration of 70 weeks hardly showed any mass loss while the M_n slightly decreased from 40 kDa to 30 kDa. Although we observed that these scaffolds degrade *in vitro* in 72 hours in the presence of lipase (0.1 mg/mL), no degradation was observed for PCL implants *in vivo* in the time frame studied. This difference might be attributed to the fact that the concentration of PCL degrading enzymes *in vivo* is too low to be effective. In line with our findings, Lam et al.[24] also showed that up to 6 months, cellular mechanisms (e.g. enzymatic degradation) do not play a role in degradation of PCL scaffolds.

In contrast to PCL scaffolds, a substantial mass decrease of PHMGCL scaffolds after one month of subcutaneous implantation was observed, which can be attributed to the presence of hydroxyl groups in the polymer backbone, which results in an increased hydrolysis rate of this polymer compared to PCL. This degradation was confirmed by ^{1}H NMR analysis, as it was shown that HMG units were preferentially removed from the degrading polymer after one month of implantation (the HMG:CL ratio dropped from 8:92 to 6.5:93.5). There were some extra peaks in the NMR spectra of both PHMGCL and PCL after 3 months of implantation, which might be attributed to the traces of tissue (e.g., lipids) originating from incompletely digested infiltrated tissue that was still attached to the PHMGCL scaffolds, upon solublization in deuterated chloroform. Therefore, it was not possible to accurately calculate the ratio of HMG:CL units at this time point.

Nonetheless, the mass reduction of implanted PHMGCL scaffolds is greater than that of PHMGCL films of the same composition degraded *in vitro*[18] (63 and 20% mass loss in 3 months, respectively). Although the rate of *in vivo* mass loss is significantly higher than *in vitro*, the decrease in molecular weight of PHMGCL *in vivo* is about the same as *in vitro*: the M_n of this polymer decreased from 22.3 kDa to 17.3 kDa and 12.8 kDa, after one and three months of subcutaneous implantation, respectively; upon incubation of PHMGCL films in

PBS at 37 °C, the number-average molecular weight (M_n) of PHMGCL decreased from 21 kDa to 11 kDa within one month and decreased to 7 kDa within 3 months of incubation. The observed fast *in vivo* degradation rate is most likely due to cellular and enzymatic activities on PHMGCL surfaces, as cellular responses are triggered upon implantation of a biodegradable material[34]. The protein adsorption and subsequent cell adhesion onto surfaces is a competitive process, which is affected by the surface composition, hydrophilicity/hydrophobicity, and roughness[35, 36]. Therefore, the surface properties of a biomaterial largely influence and direct cell behavior[37]. The difference in wettability of PHMGCL surface as compared to PCL surface (as shown before[16]) might result in adsorption of a different array of proteins which in turn increase cell binding (including mononuclear cells and macrophages). Macrophages that attach and recognize a foreign material, secrete inflammatory cytokines, enzymes with esterase activity, and also display high phagocytic activity[34]. It has been shown that macrophages are able to phagocytose particles up to a size of 5 µm[38], while if the objects are bigger, these cells will fuse to produce giant cells which have the ability to digest the foreign materials. But if these giant cells do not succeed in phagocytosis of the material, they will remain at the biomaterial-tissue interface and secrete enzymes such as lipase at the biomaterial surface[34]. One of the first signs of surface erosion is the change in surface morphology such as the appearance of cracks (for poly(anhydride) surfaces)[39], surface roughening (for poly(ortho esters))[39], and crystalline spherulitic skeleton (for poly(3-hydroxybutyrate))[40]. In this study, one month after implantation we observed surface roughening on PHMGCL surfaces, which in combination with the presence of giant cells might be attributed to the release of enzymes from these cells resulting in an enhanced degradation rate. On the surface of the degraded PHMGCL scaffolds, spherulites are seen (SEM analysis, Figure 5), which points that the enzymatic degradation preferentially occurs at the amorphous regions of the material. Taken together, the weight loss of PHMGCL scaffolds in combination with the change in the bulk properties (thermal properties and molecular weight) as well as the surface morphological changes implies that the *in vivo* degradation of these scaffolds occurs via a combination of surface (likely catalyzed by enzymes secreted by activated macrophages/giant cells) and bulk erosion.

Inevitably, biomaterial implantation is always accompanied by injury through the surgical procedure and introducing a foreign material into the body, which both initiate an inflammatory response (known as the foreign body reaction). This response is followed by the formation of a provisional matrix[41]

which releases bioactive agents (such as chemoattractants, growth factors, etc.) to control the wound healing process[42]. The tissue reaction to implanted biomaterial is further advanced by an acute inflammatory response, which is normally resolved in less than a week[41]. Following acute inflammation, a chronic inflammation occurs, which is characterized by the infiltration of mononuclear cells (e.g. monocytes), macrophages, and giant cells in the tissue that surrounds the material[41]. This chronic inflammation further progresses into the formation of granulation tissue which is characterized by the presence of macrophages, infiltrated fibroblasts, and neovascularization in the newly formed tissue[41] and finally leads to the formation of a fibrous capsule. This tissue response to biomaterials depends on a variety of factors, including the physico-chemical properties of the implant[43], reactivity (bioactive or inert), surface texture, biodegradability/bioresorbability, as well as the duration and site of implantation[44]. We showed previously that PHMGCL surfaces are more hydrophilic than PCL ones[16], and this increased hydrophilicity resulted in an enhanced *in vitro* adhesion of human mesenchymal stem cells (hMCSs)[16, 17] and chondrocytes[18] when compared to PCL surfaces. Interestingly, both scaffold types after one month of implantation triggered a foreign body reaction (as demonstrated by the presence of mononuclear inflammatory cells), which progressed to a mild chronic inflammatory response (as indicated by the presence of giant cells and progressing fibrosis) after three months of implantation. However, the extent of tissue response to PHMGCL scaffolds was higher as compared to PCL scaffolds. This is likely due to differences in the surface properties of PHMGCL and PCL, which in turn resulted in adsorption of different proteins onto these surfaces, and further increased cells adhesion (including mononuclear cells and macrophages) to the surface of PHMGCL scaffolds.

Our observations are in line with previous studies in which it was shown that no severe inflammation response was observed upon subcutaneous implantation of PCL scaffolds in rats for 28 days[45] and in rabbits for 6 months[24] and the scaffolds were filled with adipose tissue after 3 months of implantation, while this tissue was replaced by fibrous tissue after 6 months. A study by Schantz et al.[46] showed that upon implantation of 3D PCL scaffolds subcutaneously in mice for 17 weeks, fibrous tissue was predominantly formed within the scaffolds whereas vascularization was more apparent at the adjacent tissue but not in the infiltrated tissue.

Vascularization is another essential factor for tissue engineered constructs as it determines the extent of blood, oxygen, nutrients and waste products exchange within the host tissue that infiltrated into the scaffold.

Angiogenesis (neo-vascularization) associated with implanted biomaterials is at least dependent on three factors: the bioactive nature of the scaffold, the extent of porosity, pore interconnectivity, and the metabolic activity of the infiltrating host tissue[44]. Besides, an increase in macrophage population/activity has been reported to increase vascularization[47]. The scaffolds prepared in this study, comprised of a highly porous structure, with well-defined interconnectivity and it was observed that the internal porous structure of both scaffolds was preserved during 3 months of implantation which in turn allowed infiltration of newly formed tissue into the scaffolds. Importantly, more vascularization in the infiltrated tissue in PHMGCL scaffolds was observed than in PCL scaffolds after one and three months of implantation, which indicates a faster integration of PHMGCL scaffolds with newly formed tissue as compared to PCL scaffolds.

5. Conclusions

This study shows that PHMGCL scaffolds have a faster biodegradation rate compared to PCL scaffolds, induce a more intense tissue-biomaterial interaction, and demonstrate a good biocompatibility when implanted subcutaneously in mice. These relatively fast degrading biomaterials might be considered as interesting scaffolds for application in tissue engineering.

References

[1] Causa, F.; Netti, P. A.; Ambrosio, L., A multi-functional scaffold for tissue regeneration: The need to engineer a tissue analogue. *Biomaterials* **2007,** 28, (34), 5093-5099.

[2] Williams, D. F., On the mechanisms of biocompatibility. *Biomaterials* **2008,** 29, (20), 2941-2953.

[3] Jones, A. C.; Arns, C. H.; Hutmacher, D. W.; Milthorpe, B. K.; Sheppard, A. P.; Knackstedt, M. A., The correlation of pore morphology, interconnectivity and physical properties of 3D ceramic scaffolds with bone ingrowth. *Biomaterials* **2009,** 30, (7), 1440-1451.

[4] Shoichet, M. S., Polymer Scaffolds for Biomaterials Applications. *Macromolecules* **2009,** 43, (2), 581-591.

[5] Karageorgiou, V.; Kaplan, D., Porosity of 3D biomaterial scaffolds and osteogenesis. *Biomaterials* **2005,** 26, (27), 5474-5491.

[6] Hulbert, S. F.; Young, F. A.; Mathews, R. S.; Klawitter, J. J.; Talbert, C. D.; Stelling, F. H., Potential of ceramic materials as permanently implantable skeletal prostheses. *Journal of Biomedical Materials Research* **1970,** 4, (3), 433-456.

[7] Ameddah, H.; Assas, M., Bio-CAD reverse engineering of free-form surfaces by planar contours. *Computer-Aided Design and Applications* **2011,** 8, (1), 37-42.

[8] Fedorovich, N. E.; Alblas, J.; Hennink, W. E.; Oner, F. C.; Dhert, W. J. A., Organ printing: the future of bone regeneration? *Trends in Biotechnology* **2011,** 29 (12), 601-606.

[9] Yeong, W. Y.; Chua, C. K.; Leong, K. F.; Chandrasekaran, M., Rapid prototyping in tissue engineering: challenges and potential. *Trends in Biotechnology* **2004,** 22, (12), 643-652.

[10] Park, S. A.; Lee, S. H.; Kim, W. D., Fabrication of porous polycaprolactone/hydroxyapatite (PCL/HA) blend scaffolds using a 3D plotting system for bone tissue engineering. *Bioprocess and Biosystems Engineering* **2011,** 34, (4), 505-513.

[11] Park, S. A.; Kim, H. J.; Lee, S. H.; Lee, J. H.; Kim, H. K.; Yoon, T. R.; Kim, W., Fabrication of nano/microfiber scaffolds using a combination of rapid prototyping and electrospinning systems. *Polymer Engineering and Science* **2011,** 51(9), 1883-1890.

[12] Sobral, J. M.; Caridade, S. G.; Sousa, R. A.; Mano, J. F.; Reis, R. L., Three-dimensional plotted scaffolds with controlled pore size gradients:

Effect of scaffold geometry on mechanical performance and cell seeding efficiency. *Acta Biomaterialia* **2011,** 7, (3), 1009-1018.

[13] Yoon, H.; Kim, G. H.; Koh, Y. H., A micro-scale surface-structured PCL scaffold fabricated by a 3D plotter and a chemical blowing agent. *Journal of Biomaterials Science, Polymer Edition* **2010,** 21, (2), 159-170.

[14] Hoque, M. E.; San, W. Y.; Wei, F.; Li, S.; Huang, M. H.; Vert, M.; Hutmacher, D. W., Processing of polycaprolactone and polycaprolactone-based copolymers into 3D scaffolds, and their cellular responses. *Tissue Engineering - Part A* **2009,** 15, (10), 3013-3024.

[15] Woodruff, M. A.; Hutmacher, D. W., The return of a forgotten polymer - Polycaprolactone in the 21st century. *Progress in Polymer Science (Oxford)* **2010,** 35, (10), 1217-1256.

[16] Seyednejad, H.; Vermonden, T.; Fedorovich, N. E.; Van Eijk, R.; Van Steenbergen, M. J.; Dhert, W. J. A.; Van Nostrum, C. F.; Hennink, W. E., Synthesis and characterization of hydroxyl-functionalized caprolactone copolymers and their effect on adhesion, proliferation, and differentiation of human mesenchymal stem cells. *Biomacromolecules* **2009,** 10, (11), 3048-3054.

[17] Seyednejad, H.; Gawlitta, D.; Dhert, W. J. A.; Van Nostrum, C. F.; Vermonden, T.; Hennink, W. E., Preparation and characterization of a three-dimensional printed scaffold based on a functionalized polyester for bone tissue engineering applications. *Acta Biomaterialia* **2011,** 7, (5), 1999-2006.

[18] Seyednejad, H.; Ji, W.; Schuurman, W.; Dhert, W. J. A.; Malda, J.; Yang, F.; Jansen, J. A.; van Nostrum, C.; Vermonden, T.; Hennink, W. E., An Electrospun Degradable Scaffold Based on a Novel Hydrophilic Polyester for Tissue-Engineering Applications. Macromolecular Bioscience, **2011,** 11, 1684-1692.

[19] Takemura, R.; Werb, Z., Secretory products of macrophages and their physiological functions. *American Journal of Physiology - Cell Physiology* **1984,** 15, (1), C1-C9.

[20] Kulkarni, A.; Reiche, J.; Hartmann, J.; Kratz, K.; Lendlein, A., Selective enzymatic degradation of poly(ε-caprolactone) containing multiblock copolymers. *European Journal of Pharmaceutics and Biopharmaceutics* **2008,** 68, (1), 46-56.

[21] Leemhuis, M.; Van Nostrum, C. F.; Kruijtzer, J. A. W.; Zhong, Z. Y.; Ten Breteler, M. R.; Dijkstra, P. J.; Feijen, J.; Hennink, W. E., Functionalized poly(α-hydroxy acid)s via ring-opening polymerization: Toward

hydrophilic polyesters with pendant hydroxyl groups. *Macromolecules* **2006,** 39, (10), 3500-3508.

[22] Mark Leemhuis, Jan H. van S., Michelle J van Uxem, Cornelus F van Nostrum, Wim E Hennink, *Eur. J. Org. Chem.* **2003,** 2003, (17), 3344-3349.

[23] Li, S.; Liu, L.; Garreau, H.; Vert, M., Lipase-catalyzed biodegradation of poly(ε-caprolactone) blended with various polylactide-based polymers. *Biomacromolecules* **2003,** 4, (2), 372-377.

[24] Lam, C. X. F.; Hutmacher, D. W.; Schantz, J.-T.; Woodruff, M. A.; Teoh, S. H., Evaluation of polycaprolactone scaffold degradation for 6 months in vitro and in vivo. *Journal of Biomedical Materials Research Part A* **2009,** 90A, (3), 906-919.

[25] Ji, W.; Yang, F.; van den Beucken, J. J. J. P.; Bian, Z.; Fan, M.; Chen, Z.; Jansen, J. A., Fibrous scaffolds loaded with protein prepared by blend or coaxial electrospinning. *Acta Biomaterialia* **2011,** 6, (11), 4199-4207.

[26] Sivalingam, G.; Chattopadhyay, S.; Madras, G., Enzymatic degradation of poly (ε-caprolactone), poly (vinyl acetate) and their blends by lipases. *Chemical Engineering Science* **2003,** 58, (13), 2911-2919.

[27] Zeng, J.; Chen, X.; Liang, Q.; Xu, X.; Jing, X., Enzymatic degradation of poly(L-lactide) and poly(ε-caprolactone) electrospun fibers. *Macromolecular Bioscience* **2004,** 4, (12), 1118-1125.

[28] Gan, Z.; Yu, D.; Zhong, Z.; Liang, Q.; Jing, X., Enzymatic degradation of poly(ε-caprolactone)/poly(DL-lactide) blends in phosphate buffer solution. *Polymer* **1999,** 40, (10), 2859-2862.

[29] Ahola, S.; Turon, X.; Österberg, M.; Laine, J.; Rojas, O. J., Enzymatic hydrolysis of native cellulose nanofibrils and other cellulose model films: Effect of surface structure. *Langmuir* **2008,** 24, (20), 11592-11599.

[30] Herzog, K.; Müller, R. J.; Deckwer, W. D., Mechanism and kinetics of the enzymatic hydrolysis of polyester nanoparticles by lipases. *Polymer Degradation and Stability* **2006,** 91, (10), 2486-2498.

[31] Mochizuki, M.; Hirami, M., Structural effects on the biodegradation of aliphatic polyesters. *Polymers for Advanced Technologies* **1997,** 8, (4), 203-209.

[32] Sun, H.; Mei, L.; Song, C.; Cui, X.; Wang, P., The in vivo degradation, absorption and excretion of PCL-based implant. *Biomaterials* **2006,** 27, (9), 1735-1740.

[33] Pitt, C. G.; Chasalow, F. I.; Hibionada, Y. M.; Klimas, D. M.; Schindler, A., Aliphatic polyestres-1. The degradation of poly(epsilon-caprolactone) in vivo. *Journal of Applied Polymer Science* **1981,** 26, (11), 3779-3787.

[34] Franz, S.; Rammelt, S.; Scharnweber, D.; Simon, J. C., Immune responses to implants - A review of the implications for the design of immunomodulatory biomaterials. *Biomaterials* **2011,** 32, (28), 6692-6709.

[35] Alves, C. M.; Reis, R. L.; Hunt, J. A., The competitive adsorption of human proteins onto natural-based biomaterials. *Journal of the Royal Society Interface* **2010,** 7, (50), 1367-1377.

[36] Cunliffe, D.; Smart, C. A.; Alexander, C.; Vulfson, E. N., Bacterial adhesion at synthetic surfaces. *Applied and Environmental Microbiology* **1999,** 65, (11), 4995-5002.

[37] Hallab, N. J.; Bundy, K. J.; O'Connor, K.; Moses, R. L.; Jacobs, J. J., Evaluation of metallic and polymeric biomaterial surface energy and surface roughness characteristics for directed cell adhesion. *Tissue Engineering* **2001,** 7, (1), 55-70.

[38] Xia, Z.; Triffitt, J. T., A review on macrophage responses to biomaterials. *Biomedical Materials* **2006,** 1, (1), R1-R9.

[39] Achim, G. p., Mechanisms of polymer degradation and erosion. *Biomaterials* **1996,** 17, (2), 103-114.

[40] Gopferich, A.; Langer, R., Influence of microstructure and monomer properties on the erosion mechanism of a class of polyanhydrides. *Journal of Polymer Science, Part A: Polymer Chemistry* **1993,** 31, (10), 2445-2458.

[41] Anderson, J. M.; Rodriguez, A.; Chang, D. T., Foreign body reaction to biomaterials. *Seminars in Immunology* **2008,** 20, (2), 86-100.

[42] Chen, S.; Jones, J. A.; Xu, Y.; Low, H.-Y.; Anderson, J. M.; Leong, K. W., Characterization of topographical effects on macrophage behavior in a foreign body response model. *Biomaterials* ***2010,*** 31, (13), 3479-3491.

[43] Pieper, J. S.; van Wachem, P. B.; van Luyn, M. J. A.; Brouwer, L. A.; Hafmans, T.; Veerkamp, J. H.; van Kuppevelt, T. H., Attachment of glycosaminoglycans to collagenous matrices modulates the tissue response in rats. *Biomaterials* **2000,** 21, (16), 1689-1699.

[44] Burugapalli, K.; Pandit, A., Characterization of tissue response and in vivo degradation of cholecyst-derived extracellular matrix. *Biomacromolecules* **2007,** 8, (11), 3439-3451.

[45] Byers, B. A.; Guldberg, R. E.; Hutmacher, D. W.; Garcia, A. J., Effects of Runx2 genetic engineering and in vitro maturation of tissue-engineered constructs on the repair of critical size bone defects. *Journal of Biomedical Materials Research - Part A* **2006,** 76, (3), 646-655.

[46] Schantz, J.-T.; Ng, M. M.-L.; Netto, P.; Chong Lai Ming, J.; Wong, K. M.; Hutmacher, D. W.; Teoh, S. H., Application of an X-ray microscopy technique to evaluate tissue-engineered bone-scaffold constructs. *Materials Science and Engineering: C* **2002,** 20, (1-2), 9-17.

[47] Censi, R.; Van Putten, S.; Vermonden, T.; Di Martino, P.; Van Nostrum, C. F.; Harmsen, M. C.; Bank, R. A.; Hennink, W. E., The tissue response to photopolymerized PEG-p(HPMAm-lactate)-based hydrogels. *Journal of Biomedical Materials Research - Part A* **2011,** 97 A, (3), 219-229.

[48] Meaney Murray, M.; Spector, M., The migration of cells from the ruptured human anterior cruciate ligament into collagen-glycosaminoglycan regeneration templates in vitro. *Biomaterials* **2001,** 22, (17), 2393-2402.

Electro Spinning

Chapter 6

Electrospun Degradable Scaffold Based on a Hydrophilic Polyester for Tissue engineering Applications

Hajar Seyednejad
Wei Ji
Wouter Schuurman
Wouter J. A. Dhert
Jos Malda
Fang Yang
John A. Jansen
Cornelus F. van Nostrum
Tina Vermonden
Wim E. Hennink

Macromolecular Bioscience
2011, 11, 1684- 1692

Electrospun nanofibrous scaffolds have gained widespread attention in the field of tissue engineering due to their high morphological resemblance to the native extracellular matrix. The purpose of this study was to prepare and characterize electrospun scaffolds based on a novel functionalized polyester, (poly(hydroxymethylglycolide-co-ε-caprolactone), pHMGCL). This polymer has been shown to be more hydrophilic than its counterpart, (poly(ε-caprolactone), PCL), which in turn resulted in higher cell adhesion, proliferation, and differentiation both on 2D and 3D matrices. In this study, *in vitro* degradation of pHMGCL films (composed of 10 mol% of HMG) showed considerable mass loss and molecular weight reduction within 70 weeks, while no mass loss and changes in molecular weight of PCL occurred in this period. pHMGCL fibers obtained by electrospinning were characterized for morphological and physical properties and the possibility to obtain uniform fibers by varying the polymer solution (type of solvent and concentration) was shown. Scaffolds composed of fibers with uniform diameter (~ 900 nm) and possessing melting temperatures higher than body temperature were prepared. As an indication for the feasibility of this material for regenerative medicine approaches, articular chondrocytes were seeded onto electrospun pHMGCL scaffolds. Chondrocytes attached to the fibers and re-differentiated as was demonstrated by the production of glycosaminoglycans (GAG) and collagen type II within four weeks of *in vitro* culture. Thus, our results indicate that degradable, hydrophilic pHMGCL electrospun scaffolds can be used for tissue engineering applications with respect to physical, morphological, and cell-biomaterial interactions.

1. Introduction

Biomaterials used in the field of tissue engineering to assist developing functional substitutes for damaged organs and tissues, should be biodegradable and biocompatible[1, 2]. Biomaterials are often an integral part of the engineered tissue constructs, i.e. scaffolds, providing physical support for cell attachment, growth, and differentiation[3] by providing a three-dimensional environment for the seeded cells and enabling them to produce essential components of the tissue. In an ideal situation, the degradation rate of the biomaterial matches the deposition rate of the newly-formed extracellular matrix (ECM) and the formed degradation products are non-toxic and are either metabolized or eliminated from the body by the kidneys[4]. The polymers which have frequently been investigated for the preparation of scaffolds for tissue engineering applications include the well-known aliphatic polyesters such as polylactic acid (PLA)[5-7], and poly(ε-caprolactone) (PCL)[8-11]. However, the major drawbacks of these polymers are the lack of functional groups and their slow degradation rate. So far, considerable efforts have been made to prepare polyesters with functional groups[12], nevertheless, the number of investigated functionalized aliphatic polyesters with application in tissue engineering is limited. We have recently developed a hydroxyl-functionalized polyester, poly(hydroxymethyl glycolide-co-ε-caprolactone) pHMGCL[13], that is more hydrophilic than poly(ε-caprolactone) PCL[14], and has shown to support human mesenchymal stem cells adhesion, proliferation, and differentiation in two dimensional (2D)[14] and 3D[15] environments. In this paper, we present the hydrolytic degradation kinetics of this functionalized polyester *in vitro* over a period of 70 weeks and compare it with that of PCL. Furthermore, we demonstrate the possibility of fabricating fibrous scaffolds based on this polymer by means of solution electrospinning. It has been hypothesized that in order to promote the essential intercellular reactions and native intracellular responses, the ECM must be mimicked. In this regard, fiber-based scaffolds are very attractive candidates for tissue engineering as they mimic the morphological properties of the ECM[16-18]. Electrospinning is a facile technique with the ability to prepare fibers with diameters ranging from a few nanometers to several micrometers for a wide range of applications in tissue engineering[19-23]. The most commonly used polyester in electrospinning to fabricate scaffolds for tissue engineering applications is PCL[24-28]. This polymer is widely used because of its biocompatibility, ease of processability, and abundant availability[29]. However, as mentioned, PCL is a very hydrophobic polymer that lacks functional groups and degrades very slowly[11, 30] which makes this polymer more suitable for long-term drug delivery devices rather than tissue engineering scaffolds. Additionally it has

been shown that PCL is hydrophobic for cells to adhere and several approaches have been investigated to modify the surface of PCL implants to render it more favorable for cell adhesion[19, 31-34]. However, these attempts only result in better cell-scaffold interactions and do not improve the degradation rate of this polymer. To address these problems, in this study we prepared fibrous scaffolds based on hydroxyl-functionalized PCL (i.e. pHMGCL) by solution electropinning and compared their properties with its counterpart, PCL electrospun scaffolds. The different scaffolds were characterized for their physical and morphological properties. Finally, an exploratory cell culture study was performed using expanded articular chondrocytes. These cells were seeded onto the electrospun pHMGCL and PCL scaffolds and the production of GAG and collagen II was monitored to get an indication of the suitability of these scaffolds for cartilage tissue engineering applications.

2. Experimental Part

2.1. Materials

All chemicals used in this study were purchased from Sigma-Aldrich (Zwijndrecht, The Netherlands) and used as received, unless stated otherwise. All solvents were purchased from Biosolve (Valkenswaard, The Netherlands). Toluene was distilled from P_2O_5 and stored over 3 Å molecular sieves under argon. Tetrahydrofuran (THF) was distilled from sodium/benzophenone. 3S-Benzyloxymethyl-1,4-dioxane-2,5-dione (benzyl-protected hydroxymethyl glycolide, BHMG) was synthesized as described by Leemhuis et al.[13, 35] ε-Caprolactone (CL) and silica gel (0.035-0.070 mm, 60 Å) were obtained from Acros (Geel, Belgium), and benzyl alcohol (BnOH) was provided by Merck (Darmstadt, Germany), tin(II) 2-ethylhexanoate ($SnOct_2$) and Pd/C (palladium, 10 wt % (dry basis) on activated carbon, wet (50% water w/w), Degussa type E101 NE/W) were obtained from Sigma-Aldrich (Zwijndrecht, The Netherlands).

2.2. Methods

2.2.1. Synthesis of poly (ε-caprolactone) and poly (hydroxymethylglycolide-co-ε-caprolactone)

Poly(ε-caprolactone) (PCL) was synthesized via ring opening polymerization (ROP) using BnOH and $SnOct_2$ as initiator and catalyst, respectively. In a typical procedure, ε-caprolactone (5.78 mL, 65.9 mmol), BnOH (5.6 mg, 0.052 mmol), and $SnOct_2$ (10.5 mg, 0.026 mmol) were loaded into a dry Schlenk tube under a dry N_2 atmosphere. The tube was evacuated for 2 hours, then closed and

immersed into an oil bath which was heated at 130 °C. Polymerization was performed overnight and the formed polymer was dissolved in chloroform, precipitated in cold methanol and dried overnight under vacuum. The obtained poly(ε-caprolactone) was characterized by ^{1}H NMR, GPC and DSC.

Poly(benzyloxymethylglycolide–co-ε-caprolactone) (pBMGCL) was synthesized in the same manner as PCL, using BMG (1.11 g, 4.7 mmol), ε-caprolactone (4.8 g, 42.4 mmol), BnOH (16.9 mg, 0.16 mmol), and $SnOct_2$ (32.6 mg, 0.085 mmol). Protecting benzyl groups of the polymer were removed in a hydrogenation reaction using Pd/C catalyst essentially as described by Leemhuis et al.[13] In short, pBMGCL (5 g) was dissolved in dry THF (300 mL) and subsequently the Pd/C catalyst (2.3 g) was added. The flask was filled with hydrogen in three consecutive steps of evacuation, refilling with H_2 and the reaction was performed under H_2 atmosphere overnight. The formed polymer (pHMGCL) was obtained by removing the catalyst via filtration and evaporation of THF. Both protected and deprotected polymers were characterized by ^{1}H NMR, DSC and GPC as described in detail in characterization section.

2.2.2. Scaffold fabrication

Polymer solutions for electrospinning were prepared by overnight stirring at room temperature in the selected solvents. For pHMGCL, two solutions with 30 and 40 w/v % concentration in 2,2,2-trifluoroethanol (TFE) and acetone were prepared. PCL solutions were prepared by dissolving 20 w/v % of polymer in acetone. These solutions were then loaded into a syringe (equipped with a needle) and the flow rate was controlled using a syringe pump. A high voltage generator was used to create an electrostatic field and a metallic plate covered by aluminum foil was used as collector. The polymer solution was pushed through the syringe with a constant rate to bring the polymer droplet to the tip of needle. When the electrostatic field strength overcame the surface tension of the liquid droplet at the tip of the needle, the droplet was stretched into fibers and deposited onto the collector. Different parameters in this procedure were varied until optimal conditions for fiber formation were identified. These parameters including voltage (18 kV), feed rate (3 mL/hr), and the distance between tip of needle and collector (20 cm) were further kept constant throughout the experiments. The formulation parameters including solvent type and solution concentration were varied to obtain optimal fiber morphology, as mentioned in results and discussion part.

2.3. Characterization

2.3.1. Nuclear Magnetic Resonance (NMR)

^{1}H NMR spectra of polymers were obtained using a Gemini 300 MHz spectrometer (Varian Associates Inc., NMR Instruments, Palo Alto, CA). Chemical shifts were recorded in ppm with reference to the solvent peak (δ= 7.26 ppm for $CDCl_3$ in ^{1}H NMR).

2.3.2. Differential Scanning Calorimetry (DSC)

The thermal properties of polymers and scaffolds were determined using differential scanning calorimetry (TA Instruments DSC Q2000). For the polymers, scans were taken from -80 °C to 100 °C with a heating rate of 10 °C/min and a cooling rate of 0.5 °C/min under a nitrogen flow of 50 mL/min. The glass transition temperature (T_g) was recorded as the midpoint of heat capacity change in the second heating run. Melting temperature (T_m) and heat of fusion (ΔH_f) were determined from the onset of endothermic peak position and integration of endothermic area in the second heating run, respectively. For scaffolds, the samples were equilibrated at -90 °C and thermal transitions were reported for the first heating run when heated to 100 °C with a heating rate of 10 °C/min.

2.3.3. Gel Permeation Chromatography (GPC)

The molecular weights of the synthesized polymers were measured by means of GPC using a 2695 Waters Aliance system and a Waters 2414 refractive index detector. Two PL-gel 5 μm mixed-D columns fitted with a guard column (Polymer Labs, M_w range 0.2-400 KDa) were used. The columns were calibrated with polystyrene standards of known molecular weights using AR grade THF, eluting at 1 mL/min flow rate at 30 °C.

2.3.4. Scanning Electron Microscopy (SEM)

The morphology of obtained fibers was investigated using light microscopy (Leica Microsystems, Wetzlar, Germany) and scanning electron microscopy (JEOL JSM-6310). For SEM analysis, electrospun fibrous scaffolds were mounted on metal stubs and sputter coated with gold.

2.3.5. *In vitro* Degradation

Polymeric films of PCL and pHMGCL were made by solvent casting method. Polymer solutions were prepared using chloroform as solvent and the solvent was evaporated slowly at room temperature to obtain uniform films from which disks of 1 cm in diameter and around 2 mm thickness were punched out. Degradation of the films was done in phosphate buffered saline (PBS; 0.033 M NaH_2PO_4, 0.066 M Na_2HPO_4, 0.056 M NaCl) at pH 7.4 containing 0.5% sodium azide to prevent bacterial growth. The films were submerged in 10 mL PBS, in individual tubes with the screw caps tightened and maintained at 37 °C. The pH of buffer was monitored regularly and the buffer was refreshed every 2-3 days. At specific time intervals, three films were removed, rinsed thoroughly with de-ionized water, and dried in vacuum for three days at room temperature.

The dry weight of each film was measured at the start of the experiment (W_0) and at the sampling time point (W_t). The percentage mass loss was calculated according to the following equation:

$$\% \text{ mass loss} = (W_t - W_0)/W_0 \chi\ 100$$

The percentage crystallinity and melting temperature of degraded samples was determined using DSC. The molecular weights of degraded polymers were measured by GPC, as described in the previous section.

2.3.6. Cell attachment and differentiation

Full thickness healthy articular cartilage was obtained from the femoropatellar joints of a fresh equine cadaver (age: 6 years) under aseptic conditions. Cartilage was digested overnight using 0.15% collagenase type II (Worthington Biochemical Corporation, Lakewood, NJ, USA) at 37 °C. The cell suspension was filtered through a 100 µm cell strainer and washed with PBS. Cells were resuspended in chondrocyte expansion medium (DMEM, Invitrogen, Carlsbad, CA, USA), supplemented with 10% fetal bovine serum (FBS, Biowhittaker, Walkersville, MD, USA), 100 U ml^{-1} penicillin, 100 µg ml^{-1} streptomycin (both Sigma-Aldrich) and 10 ng ml^{-1} βFGF (R&D Systems, Minneapolis, MN, USA). Cells were then counted and seeded in 175 cm^2 culture flasks at a density of 5000 cells/cm^2 in expansion medium and maintained in a humidified incubator (37 °C, 5% CO_2). After one passage (t = 10 days), the chondrocytes were detached using 0.25% trypsin (Invitrogen), resuspended in differentiation medium (DMEM supplemented with 0.2 mM ascorbic acid 2-phosphate (Sigma-Aldrich), 0.5% human serum albumin (Cealb, Sanquin, Utrecht, The Netherlands), 1x ITS-X (Invitrogen), 100 units/mL penicillin and 100 unit/mL streptomycin, and 5 ng/mL

TGF-b2 (R&D Systems). Electrospun PCL or pHMGCL scaffolds were sterilized using 70% ethanol solution and the cells were seeded onto these scaffolds at a density of 1.0×10^6 cells/cm^2. Samples were cultured for 4 weeks. Differentiation medium was replaced every 2–3 days.

To observe the morphology of the cells attached to fibers, the cellular constructs were harvested, washed with PBS to remove non-adherent cells and then fixed with 4% glutaraldehyde (Sigma, Zwijndrecht, The Netherlands) for 1 hour at room temperature, dehydrated through a series of graded ethanol solutions, and then air-dried overnight. Dry cellular constructs were sputter coated with gold and observed with SEM.

For the evaluation of cellular differentiation, samples were dehydrated through graded ethanol series, cleared in xylene, embedded in paraffin, and were sectioned to yield 5 µm sections. For histology, sections were stained using a triple stain of haematoxylin (Klinipath, Duiven, the Netherlands), fast green FCF (0.001% w/v) and safranin O (0.1% w/v) (both Merck, Darmstadt, Germany). For immunolocalization of collagen type II, sections were rehydrated, endogenous peroxidase activity was inactivated using a 0.3% H_2O_2 solution for 10 min. Next, the samples were washed with PBS/Tween 20 (0.1%) for 5 min, blocked with 5% bovine serum albumin (BSA, Invitrogen) in PBS for 30 min and incubated overnight with anti-collagen type II antibody (1:100, II-6B3II, Developmental Studies Hybridoma Bank, Iowa City, IA, USA). Samples were then incubated for 60 min with the secondary HRP-conjugated goat anti-mouse antibody (1:200, Dako, Glostrup, Denmark). Staining was visualized using DAB solution for 10 min, counterstaining was performed with hematoxylin. Isotype controls were performed by using mouse isotype IgG1 monoclonal antibody (1:200, Dako) at concentrations similar to those used for the staining. The sections were examined using a light microscope (Olympus BX5, Hamburg, Germany) and photomicrographs taken with an Olympus DP70 camera.

For biochemical analysis, samples (n=3) were digested overnight at 56 °C in a solution containing 250 µg/mL papain (Sigma-Aldrich). Quantification of total DNA was performed by Quant-iT PicoGreen dsDNA kit (Molecular Probes, Invitrogen) using a spectrofluorometer (Bio-Rad, Hercules, California). The amount of GAG was determined spectrophotometrically[36] after reaction with dimethylmethylene blue dye (Sigma-Aldrich) at pH 3.0. Intensity of color change was quantified immediately in a microplate reader (Bio-Rad) by measuring absorbance at 540 and 595 nm. Calibration was done with a standard of chondroitin sulphate C (Sigma-Aldrich). The amount of GAGs was calculated

using a standard of chondroitin sulphate C (Sigma-Aldrich) and by calculating the ratio of absorbances.

3. Results and Discussions

3.1. *In vitro* Degradation

PCL and pHMGCL were synthesized via ring opening polymerization using BnOH and $SnOct_2$, as initiator and catalyst, respectively, as described previously[13-15] (Figure 1). The monomer-to-initiator ratio was 300/1 for both polymers. Thermal and molecular weight characteristics of the obtained polymers are shown in Table 1. The feed ratio of BMG/CL used to synthesize pBMGCL was 10/90 and ^{1}H NMR analysis showed that the copolymer composition was close to that of the feed, which is expected since the polymerization yield was high (> 90%).

In vitro hydrolytic degradation of films of PCL and hydroxyl-functionalized PCL (pHMGCL) was investigated in PBS at 37 °C for 70 weeks. Polymer degradation was monitored by weight loss measurements, DSC, GPC, and ^{1}H NMR analysis of films. During this period, hardly any mass loss was observed for PCL films (Figure 2).

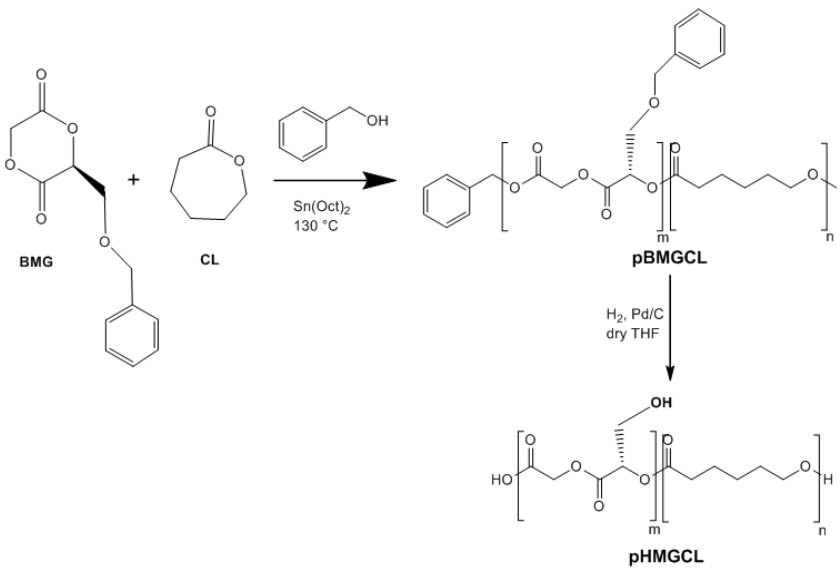

Fig.1. Synthesis of poly(hydroxymethylglycolide-co-ε-caprolactone) (pHMGCL), composed of 5 mol% HMG, 5 mol% GA, and 90 mol% CL.

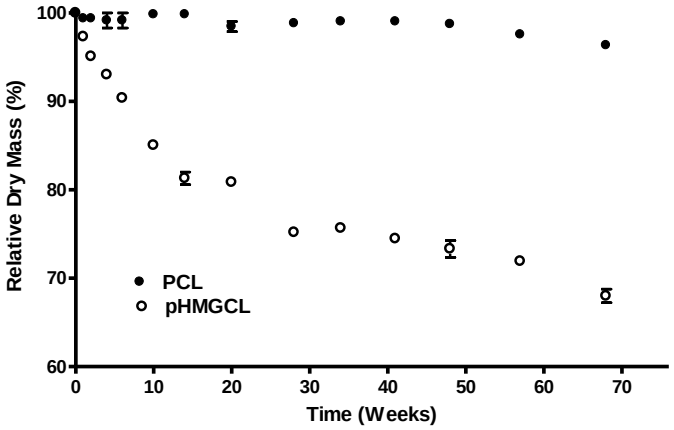

Fig.2. Weight loss of PCL and pHMGCL films (n= 3 ± SD) upon incubation in PBS (pH = 7.4) at 37 °C.

GPC analysis showed that the M_n of PCL decreased from 40 kDa to around 30 kDa (Figure 3) during the 70 weeks of degradation. Besides, there was hardly any change in the melting temperature while the percentage crystallinity of PCL, calculated from the melting enthalpy of 100% crystalline PCL[37], was constant during the first 14 weeks of incubation in PBS and thereafter slightly increased from 45% to around 60% (Figure 4).

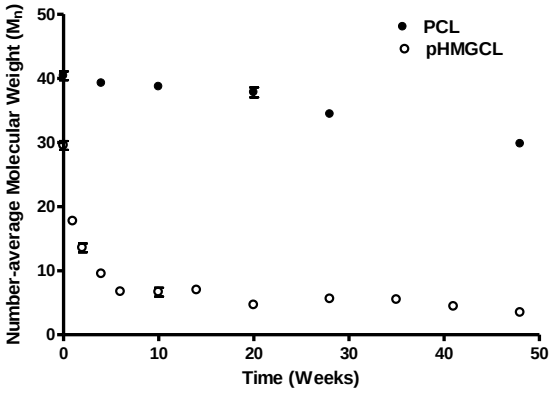

Fig.3. Number average molecular weight (M_n) of PCL and pHMGCL (n=3 ± SD) upon incubation of films of these polymers in PBS (pH=7.4) at 37 °C.

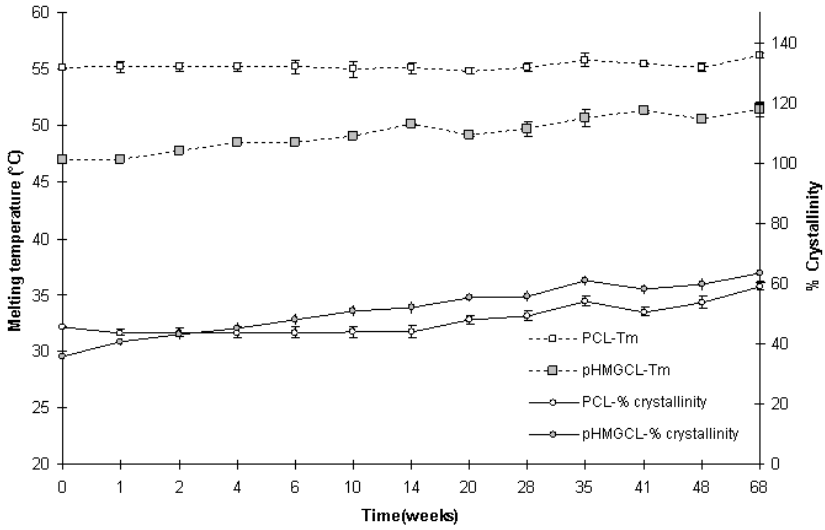

Fig.4. Thermal properties of films of PCL and pHMGCL (n = 3 ± SD) upon incubation in PBS at 37 °C. The percentage crystallinity of samples was calculated based on the enthalpy of fusion value of 139.5 J/g for 100% crystalline PCL[37].

These data are in agreement with literature data [38] where it was shown that that PCL scaffolds need more than 5 years to degrade. This means that although the degradation is not complete in the time frame investigated and in agreement with literature data[4] the degradation of PCL occurs via bulk erosion. The increase in crystallinty has also been observed previously[39] and is ascribed to preferential hydrolytic chain scission in the amorphous domains of PCL films resulting in recrystallization. Figure 2 shows that pHMGCL lost around 32% of their weight upon incubation for 70 weeks. A relatively fast weight loss was observed during the first 10 weeks (up to 20%), followed by a slower gradual weight loss up to 30% during the next 50 weeks. It was further shown that the molecular weight of pHMGCL underwent a rapid decrease during the first 6 weeks of degradation (M_n decreased from 30 to 6 kDa), thereafter the M_n decreased with a slower rate, reaching less than 3 kDa after 70 weeks (Figure 3). Determination of thermal properties of these polymeric films (Figure 4) showed that there was a slight increase in the melting temperature of the degraded pHMGCL films (47 °C to 51 °C after 70 weeks). The change in the dry mass of this polymer can be attributed to the presence of monomer units with hydroxyl groups which likely results in a higher water-absorbing capacity as compared to hydrophobic PCL films, leading to faster hydrolysis of the ester bonds in the pHMGCL polymer chains.

Additionally, there is a considerable decrease in the molecular weight of this polymer within the degradation period which in combination with the mass loss data demonstrates that degradation of pHMGCL mainly proceeds via a combination of bulk and surface erosion. Moreover, it can be assumed that after 70 weeks incubation in PBS, low molecular weight pHMGCL (M_n=3 kDa) undergoes fragmentation and phagocytosis, as observed for low molecular weight PCL in the *in vivo* conditions[40]. Investigating the thermal properties of the degraded pHMGCL samples (Figure 4) showed that the melting temperature of the pHMGCL films slightly increased which was associated with an increase in the crystallinity of pHMGCL in time. Since degradation preferentially occurs in the amorphous regions of semi-crystalline materials in earlier stages of degradation[41], an increase in the crystallinity of the remaining material occurs, but also re-crystallization of part of the degraded amorphous regions might contribute to this phenomenon[37].

Degraded pHMGCL polymer films were also analyzed by ^{1}H NMR. Comparing the integration of protons corresponding to HMG units (peak at 4.1-4.3 ppm) to those of glycolic acid units (peak at 4.6-4.8 ppm) showed that this ratio decreased gradually (Table 2). However, after 70 weeks, the peaks corresponding to HMG units disappeared completely (Figure 5) and it is shown that the polymer contains only glycolic acid and caprolactone units at this time. Based on these results, it can be concluded that the hydrolysis of pHMGCL preferentially occurred at hydroxyl enriched units, likely due to increased hydration at these sites[42, 43].

Table 2. Structural analysis of degraded pHMGCL films based on ^{1}H NMR.

Degradation time (weeks)	CL units (%)	Glycolic acid (GA) units (%)	HMG units (%)
0	90	5	5
10	92	4.4	3.5
20	95	2.9	2.1
48	98	1.6	0.3
70	98	2	0

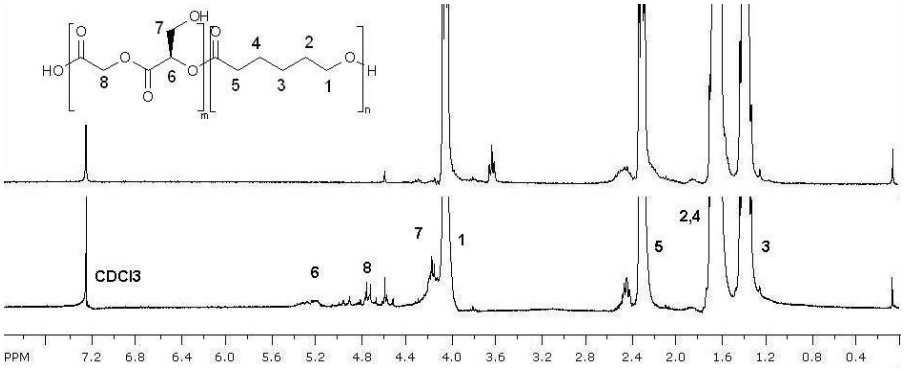

Fig.5. ^{1}H NMR spectra of pHMGCL (below) and degraded pHMGCL after 70 weeks incubation in PBS at 37 °C (above) in $CDCl_3$.

3.2. Scaffold Preparation

Fibrous scaffolds of PCL (20 w/v % in acetone) and pHMGCL (30 w/v % in TFE and 40 w/v % in TFE and acetone) were prepared by solution electrospinning. For the 30 w/v % pHMGCL solution in TFE, electrospnning resulted in formation of some irregularly shaped fibers together with beads as depicted in light microscopy images (Figure 6A). However, when the concentration was raised to 40 w/v%, the amount of beads decreased substantially but the fibers had a varying diameter (Figure 6B).

To avoid the formation of beads in the scaffold, the polymer was dissolved in acetone and electrospinning of a solution with 40 w/v % concentration resulted in a uniform fibrous structure (fiber diameter around 900 µm) as depicted in Figure 6C. There are several factors in electrospinning procedure including processing parameters such as applied voltage, flow rate, and capillary-collector distance and solution properties such as viscosity, solvent volatility, and solution conductivity which affect the morphology of polymeric fibers as well as their diameter[44].

In this study, we varied the processing parameters until we obtained fibers of good quality (absence of beads and uniform diameter) and subsequently these parameters were further kept constant throughout the procedure. However, the solution properties needed to be optimized as well. The polymer solution concentration is one of the factors that determines the spinability of a solution as it affects both viscosity and surface tension of the solution and it should neither be too diluted nor too concentrated[45]. Electrospinning of pHMGCL solution in TFE (30 w/v %) because of its low viscosity resulted that the polymer fibers broke up

into droplets before reaching the collector due to the surface tension, leading to a beaded structure (Figure 6A).

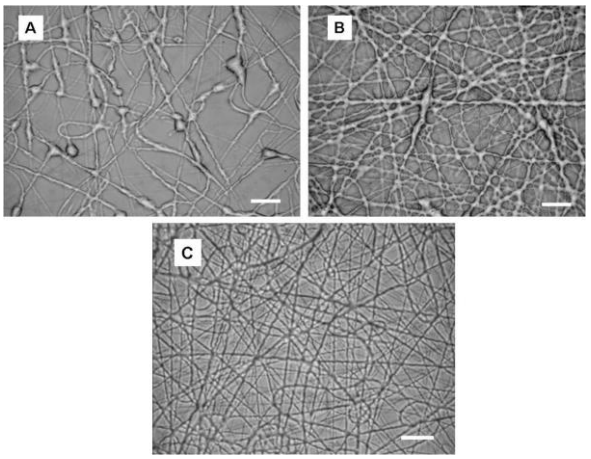

Fig.6. Light microscopy images of pHMGCL fibers prepared using different electrospinning conditions. Top: morphology of fibers obtained from TFE solution (A) 30 wt/v%, (B) 40 wt/v%. Bottom (C) morphology of fibers obtained from 40 wt/v % in acetone solution. (Scale bar is 10 μm).

When the concentration of this solution was increased to 40 w/v %, the beads disappeared, however, the fibers were not uniform in diameter and looked wet, likely because not all solvent evaporated during the fiber deposition (Figure 6B). Consequently, the choice of solvent is a crucial factor determining fiber forming capability of a solution. In order to have sufficient solvent evaporation between the capillary tip and the collector, a volatile solvent has to be used[45]. Indeed, when the solvent was changed from TFE to acetone (boiling temperature of 78 and 56 °C, respectively) beadless fibers were formed (Figure 6C).

The thermal properties of scaffolds were determined by means of DSC and the results showed that both pHMGCL and PCL scaffolds have a melting temperature above body temperature (Table 1), which ensures dimensional stability of scaffolds in actual *in vivo* conditions. The T_m of the scaffolds was slightly lower than the T_m of the polymers before electrospinning which might be due to the fast solidification of polymers during fiber deposition. This fast solidification can also explain the lower extent of crystallinity as shown by enthalpy of fusion (Table 1).

Table1. Characteristics of the polymers and scaffolds used in this study.

Polymer	BMG/CL molar ratio in feed	HMG/CL molar ratio in protected polymer[a]	HMG/GA/CL molar ratio in deprotected polymer [a]	T_m (°C)[b]	ΔH_f (J/g)[b]	M_w (kDa)[c]	PDI[c]	$T_{m,scaffold}$ (°C)[b]	$\Delta H_{f,scaffold}$ (J/g)[b]
PCL	0/ 100	0/ 100	-	55.1	63.7	72.5	2.5	54.6	61.9
pHMGCL	10/ 90	10/ 90	5/ 5/ 90	47.2	50.9	59.1	2.8	45.4	48.5

[a]Determined by ^{1}H NMR

[b]Measured by DSC

[c]Determined by GPC, PDI=Polydispersity Index (M_w/M_n)

3.3. Cell Morphology and Differentiation

Chondrocytes were seeded onto electrospun pHMGCL and PCL fibrous scaffolds and their morphology and attachment were evaluated by SEM after 24 hours and two weeks (Figure 7).

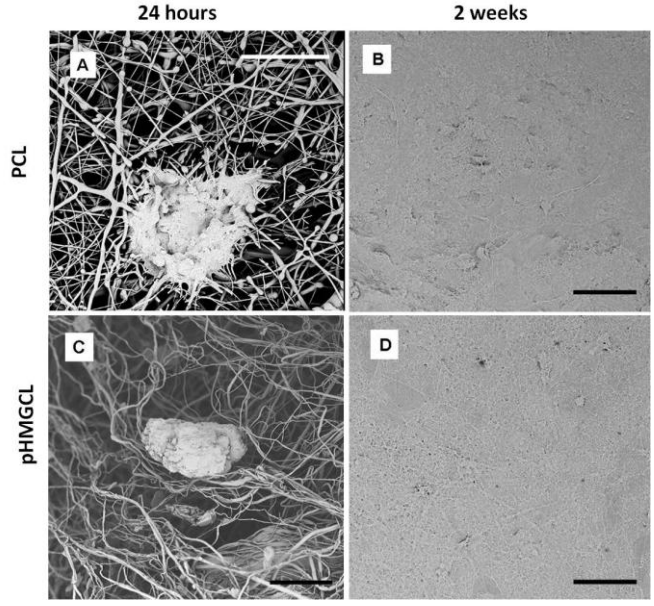

Fig.7. Morphology of the chondrocytes after 24 hours (A and C) and two weeks (B and D) culture on pHMGCL scaffold (above) and PCL scaffold (bottom) as examined by SEM. (A and C) cell clusters adhered to the fibers. (B and D) coverage of the scaffold surface with cells and ECM. Scale bar is 40 µm.

Chondrocytes were attached to the fibers and many cells had a round morphology, similar to native chondrocytes[46]. In our previous studies, human mesenchymal stem cells (hMSCs) were seeded onto 2D[14] films or in 3D[15] scaffolds fabricated by three-dimensional printing. Distinct differences between cell adhesion, proliferation, and differentiation of hMSCs with respect to polymer surface composition were observed. These differences are attributed to the increased hydrophilicity of pHMGCL scaffold upon exposure to water, which in turn makes the surface more favorable for cells. However, in the present study no distinct difference was observed between cell adhesion on the pHMGCL and PCL electrospun scaffolds, which might be due to the type of cells that was used.

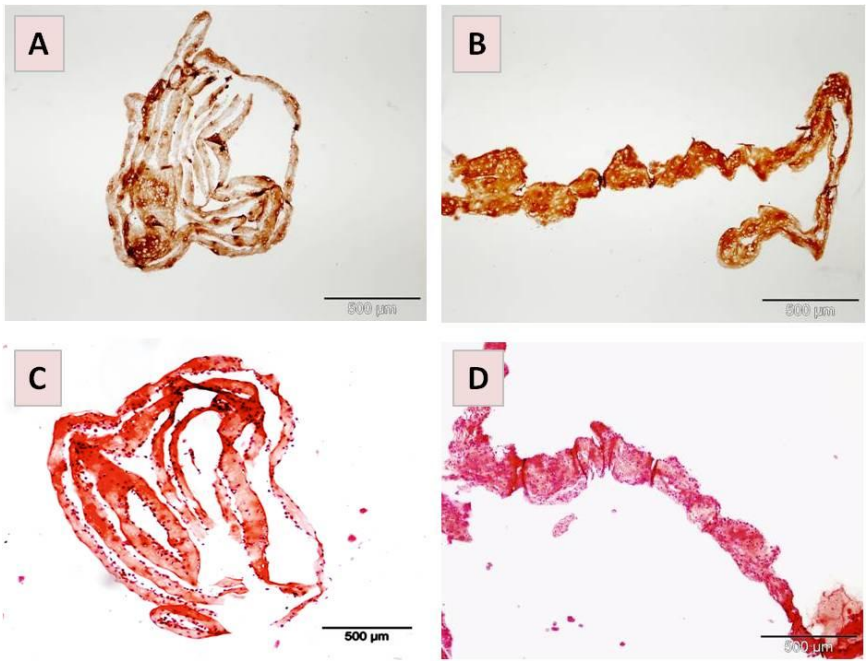

Fig.8. Histological images (cross-section) of cartilaginous tissue formed on pHMGCL scaffolds after 2 weeks (A and C) and 4 weeks (B and D). Immunolocalization of collagen type II (A and B) and Safranin O staining (C and D). Scale bar is 500 µm.

The presence of GAG and collagen type II in the scaffolds was investigated as markers of differentiation. Using (immuno)histochemistry, deposition of collagen type II and GAGs evidenced for both the pHMGCL scaffolds (Figure 8) and PCL scaffolds (data not shown). The quantitative measurement of GAG per scaffold showed that the amounts of GAGs were similar (around 1 µg/construct) for both

PCL and pHMGCL scaffolds. In addition, the ratio of GAG/DNA measured on both scaffold types was similar and equal to 5. These introductory data show that these two scaffold types demonstrate good cell biocompatibility and similar chondrocytes behavior in terms of growth and differentiation.

4. Conclusions

This chapter describes the preparation and characterization of fibrous scaffolds based on a novel hydroxyl-functionalized polyester, pHMGCL, by means of solution electrospinning. The degradation of solvent-cast films made of pHMGCL and its counterpart, PCL, were evaluated *in vitro*. It was shown that pHMGCL degrades much faster than PCL likely due to its higher hydrophilicity and hence faster hydrolysis. The melting temperature of this scaffold (45 °C) ensures its dimensional stability once implanted in the body and its fibrous structure mimics the fibrous collagen part of tissue. To get an indication of feasibility of these scaffolds for tissue engineering applications, articular chondrocytes were seeded onto electrospun pHMGCL and PCL scaffolds. The SEM images showed that chondrocytes adhered to the fibers. Importantly, chondrocytes were able to differentiate and produced glycosaminoglycans and collagen II within four weeks, regardless of scaffold composition. Therefore, these degradable fibrous pHMGCL scaffolds posses excellent properties in terms of degradation kinetics, processability via electrospinning, cell adhesion and differentiation. These results establish the basis for further implementation of this material in the field of cartilage tissue engineering.

References

[1] Dvir T., Timko B. P., Kohane D. S., Langer R. Nanotechnological strategies for engineering complex tissues. *Nat. Nano.*, **2011**, 6, 13-22.

[2] O'Brien F. J. Biomaterials & scaffolds for tissue engineering. *Mater. Today*, **2011**, 14, 88.

[3] Levenberg S., Langer R., Gerald P. S. Advances in Tissue Engineering. In Current Topics in Developmental Biology, Academic Press, **2004**, 61, 113.

[4] Hutmacher D. W. Scaffolds in tissue engineering bone and cartilage. *Biomaterials*, **2000**, 21, 2529.

[5] Kim S. H., Oh S. A., Lee W. K., Shin U. S., Kim H. W. Poly(lactic acid) porous scaffold with calcium phosphate mineralized surface and bone marrow mesenchymal stem cell growth and differentiation. *Mater. Sci. Eng. C.* **2011**, 31, 612.

[6] Van Der Pol U., Mathieu L., Zeiter S., Bourban P. E., Zambelli P. Y., Pearce S. G., Bouré L. P., Pioletti D. P., Augmentation of bone defect healing using a new biocomposite scaffold: An in vivo study in sheep. *Acta Biomater.* **2010**, 6, 3755-3762.

[7] Kanczler J. M., Ginty P. J., Barry J. J. A., Clarke N. M. P., Howdle S. M., Shakesheff K. M., Oreffo R. O. C., The effect of mesenchymal populations and vascular endothelial growth factor delivered from biodegradable polymer scaffolds on bone formation. *Biomaterials*, **2008**, 29, 1892.

[8] Liao J., Guo X., Grande-Allen K. J., Kasper F. K., Mikos A. G. Bioactive polymer/extracellular matrix scaffolds fabricated with a flow perfusion bioreactor for cartilage tissue engineering. *Biomaterials*, **2010**, 31, 8911-8920.

[9] Zhang H., Migneco F., Lin C. Y., Hollister S. J. Chemically-conjugated bone morphogenetic protein-2 on three-dimensional polycaprolactone scaffolds stimulates osteogenic activity in bone marrow stromal cells. *Tissue Eng. A.* **2010**, 16, 3441-3448.

[10] Liao J., Guo X., Nelson D., Kasper F. K., Mikos A. G. Modulation of osteogenic properties of biodegradable polymer/extracellular matrix scaffolds generated with a flow perfusion bioreactor. *Acta Biomater.* **2010**, 6, 2386-2398.

[11] Woodruff M. A., Hutmacher D. W. The return of a forgotten polymer - Polycaprolactone in the 21st century. *Prog. Polym. Sci.* **2010**, 35, 1217-1256.

[12] Seyednejad H., Ghassemi A. H., van Nostrum C. F., Vermonden T., Hennink W. E. Functional aliphatic polyesters for biomedical and pharmaceutical applications. *J. Controlled Release*, **2011**, 152, 168-176.

[13] Loontjens C. A. M., Vermonden T., Leemhuis M., Van Steenbergen M. J., Van Nostrum C. F., Hennink W. E. Synthesis and characterization of random and triblock copolymers of ε-caprolactone and (benzylated)hydroxymethyl glycolide. *Macromolecules*, **2007**, 40, 7208-7216.

[14] Seyednejad H., Vermonden T., Fedorovich N. E., Van Eijk R., Van Steenbergen M. J., Dhert W. J. A., Van Nostrum C. F., Hennink W. E. Synthesis and characterization of hydroxyl-functionalized caprolactone copolymers and their effect on adhesion, proliferation, and differentiation of human mesenchymal stem cells. *Biomacromolecules*, **2009**, 10, 3048-3054.

[15] Seyednejad H., Gawlitta D., Dhert W. J. A., van Nostrum C. F., Vermonden T., Hennink W. E. Preparation and characterization of a three-dimensional printed scaffold based on a functionalized polyester for bone tissue engineering applications. *Acta Biomater.* **2011**, 7, 1999-2006.

[16] Meng D., Erol M., Boccaccini A. R. The influence of tetracycline loading on the surface morphology and biocompatibility of films made from p(3hb) microspheres. *Adv. Eng. Mater.* **2010**, 12, B467-B268.

[17] Agarwal S., Greimer A., Wendorff J. H. Electrospinning of manmade and biopolymer nanofibers- Progress in techniques, materials, and applications. *Adv. Funct. Mater.* **2009**, 19, 2863-2879.

[18] Ji W., Sun Y., Yang F., van den Beucken J. J. J. P., Fan M., Chen Z., Jansen J. A., Bioactive electrospun scaffolds delivering growth factors and genes for tissue engineering applications. *Pharm. Res.* **2010**, 28 (6), 1259-1272.

[19] Yoo H. S., Kim T. G., Park T. G. Surface-functionalized electrospun nanofibers for tissue engineering and drug delivery. *Adv. Drug Delivery Rev.* **2009**, 61, 1033-1042.

[20] Cao H., Liu T., Chew S. Y. The application of nanofibrous scaffolds in neural tissue engineering. *Adv. Drug Delivery Rev.* **2009**, 61, 1055-1064.

[21] Jang J. H., Castano O., Kim H. W. Electrospun materials as potential platforms for bone tissue engineering. *Adv. Drug Delivery Rev.* **2009**, 61, 1065-1083.

[22] Lim S. H., Mao H. Q. Electrospun scaffolds for stem cell engineering, *Adv. Drug Delivery Rev.* **2009**, 61, 1084-1096.

[23] Baker B. M., Handorf A. M., Ionescu L. C., Li W. J., Mauck R. L. New directions in nanofibrous scaffolds for soft tissue engineering and regeneration. *Expert Rev. Med. Dev.* **2009**, 6, 515-532.

[24] Wang C. Y., Zhang K. H., Fan C. Y., Mo X. M., Ruan H. J., Li F. F. Aligned natural-synthetic polyblend nanofibers for peripheral nerve regeneration. *Acta Biomater.* **2011**, 7, 634-643.

[25] Ladd M. R., Lee S. J., Stitzel J. D., Atala A., Yoo J. J. Co-electrospun dual scaffolding system with potential for muscle-tendon junction tissue engineering. *Biomaterials*, **2011**, 32, 1549-1559.

[26] Valmikinathan C. M., Hoffman J., Yu X. Impact of scaffold micro and macro architecture on Schwann cell proliferation under dynamic conditions in a rotating wall vessel bioreactor. *Mater. Sci. Eng. C*. **2011**, 31, 22.

[27] Ji W., Yang F., Van Den Beucken J. J. J. P., Bian Z., Fan M., Chen Z., Jansen J. A. Fibrous scaffolds loaded with protein prepared by blend or coaxial electrospinning. *Acta Biomater.* **2010**, 6, 4199-4207.

[28] Ruckh T. T., Kumar K., Kipper M. J., Popat K. C. Osteogenic differentiation of bone marrow stromal cells on poly(ε-caprolactone) nanofiber scaffolds. *Acta Biomater.* **2010**, 6, 2949.

[29] Erisken C., Kalyon D. M., Wang H., Örnek-Ballanco C., Xu J. Osteochondral tissue formation through adipose-derived stromal cell differentiation on biomimetic polycaprolactone nanofibrous scaffolds with graded insulin and beta-glycerophosphate concentrations. *Tissue Eng. A*, **2011**, 17, 1239-1252.

[30] Sun H., Mei L., Song C., Cui X., Wang P. The in vivo degradation, absorption, and excretion of PCL-based implant. *Biomaterials*, **2006**, 27, 1735-1740.

[31] Chang K. Y., Hung L. H., Chu I. M., Ko C. S., Lee Y. D. The application of type II collagen and chondroitin sulfate grafted PCL porous scaffold in cartilage tissue engineering. *J. Biomed. Mater. Res. A.* **2010**, 92, 712-723.

[32] Chen J. P., Su C. H. Surface modification of electrospun PLLA nanofibers by plasma treatment and cationized gelatin immobilization for cartilage tissue engineering. *Acta Biomater.* **2011**, 7, 234-243.

[33] Yildirim E. D., Besunder R., Pappas D., Allen F., Güceri S., Sun W. Accelerated differentiation of osteoblast cells on polycaprolactone

scaffolds driven by a combined effect of protein coating and plasma modification. *Biofabrication*, **2010**, 2, 014109.

[34] Zhang H., Lin C. Y., Hollister S. J. The interaction between bone marrow stromal cells and RGD-modified three-dimensional porous polycaprolactone scaffolds. *Biomaterials*, **2009**, 30, 4063-4069.

[35] Leemhuis M., Hein van Steenis J., van Uxem M. J., van Nostrum C. F., Hennink W. E. A versatile route to functionalized dilactones as monomers for the synthesis of poly(α-hydroxy) acids. *Eur. J. Org. Chem.* **2003**, 17, 3344.

[36] Farndale R. W., Buttle D. J., Barrett A. J. Improved quantitation and discrimination of sulphate glycosaminoglycans by use of dimethylmethylene blue. *Biochim. Biophys. Acta* **1986**, 883, 173-177.

[37] Lam C. X. F., Teoh S. H., Hutmacher D. W. Comparison of the degradation of polycaprolactone and polycaprolactone-(β-tricalcium phosphate) scaffolds in alkaline medium. *Polym. Int*. **2007**, 56, 718-728.

[38] Lam C. X. F., Savalani M. M., Teoh S. H., Hutmacher D. W. Dynamics of in vitro polymer degradation of polycaprolactone-based scaffolds: Accelerated versus simulated physiological conditions. *Biomed. Mater.* **2008**, 3, 034108.

[39] Htay A. S., Teoh S. H., Hutmacher D. W. J. Development of perforated microthin poly(ε-caprolactone) films as matrices for membrane tissue engineering. *Biomat. Sci. Polym. Ed.* **2004**, 15, 683-700.

[40] Woodward S. C., Brewer P. S., Moatamed F. The intracellular degradation of poly(ε-caprolactone). *J. Biomed. Mater. Res.* **1985**, 19, 437-444.

[41] Gopferich A. Mechanisms of polymer degradation and erosion, *Biomaterials*, **1996**, 17, 103-114.

[42] Ghassemi A. H., van Steenbergen M. J., Talsma H., van Nostrum C. F., Jiskoot W., Crommelin D. J. A., Hennink W. E. Preparation and characterization of protein loaded microspheres based on a hydroxylated aliphatic polyester, poly(lactic-co-hydroxymethyl glycolic acid). *J. Controlled Release*, **2009**, 138, 57-63.

[43] Leemhuis M., Kruijtzer J. A. W., van Nostrum C. F., Hennink W. E. In vitro hydrolytic degradation of hydroxyl-functionalized poly(α-hydroxy acid)s. *Biomacromolecules*, **2007**, 8, 2943.

[44] Pham Q. P., Sharma U., Mikos A. G. Electrospinning of polymeric nanofibers for tissue engineering applications: A review. *Tissue Eng.* **2006**, 12, 1197-1211.

[45] Sill T. J., von Recum H. A. Electrospinning: Applications in drug delivery and tissue engineering. *Biomaterials*, **2008**, 29, 1989-2006.

[46] Lin Z., Willers C., Xu J., Zheng M. H. The chondrocyte: Biology and clinical application. *Tissue Eng.* **2006**, 12, 1971-1984.

Chapter 7

Coaxially Electrospun Scaffolds Based on Hydroxyl-functionalized Poly(ε-caprolactone) and Loaded with VEGF for Tissue Engineering Applications

Hajar Seyednejad
Wei Ji
Fang Yang
Cornelus F. van Nostrum
Tina Vermonden
Wouter J. A. Dhert
Wim E. Hennink
John A. Jansen

Manuscript in preparation

The aim of this study was to fabricate nanofibrous scaffolds based on blends of a hydroxyl functionalized polyester (poly(hydroxymethylglycolide-co-ε-caprolactone), pHMGCL) and poly(ε-caprolactone) (PCL), loaded with bovine serum albumin (BSA) as protein stabilizer and vascular endothelial growth factor (VEFG) as potent angiogenic factor by means of a coaxial electrospinning technique. The scaffolds were characterized by scanning electron microscopy (SEM), fluorescence microscopy (FM), and differential scanning calorimetry (DSC). The scaffolds displayed a uniform fibrous structure with a fiber diameter around 700 nm. The release of BSA from the core of the fibers was studied by high performance liquid chromatography (HPLC) and it was shown that the coaxial scaffolds composed of blends of pHMGCL and PCL exhibited faster release than the comparative PCL scaffolds likely because of a faster degradation of pHMGCL compared to PCL. VEGF was also incorporated in the core of the scaffolds and the effect of the released protein on the attachment and proliferation of endothelial cells was investigated. It was shown that the incorporated protein preserved its biological activity and resulted in initial higher number of adhered cells. Thus, these bioactive scaffolds based on blends of pHMGCL/PCL loaded with VEGF can be considered as a promising candidate for tissue engineering applications.

1. Introduction

Suitable scaffolds for tissue engineering applications are structures based on biodegradable and biocompatible materials, which can support cell attachment and proliferation, deliver biochemical factors (i.e. growth factors), and enable diffusion of vital cell nutrients/ metabolic products into/out of the scaffold, respectively[1]. In fact, the success of tissue engineering approaches depends on the integration of all these factors in an implantable device. Therefore, development of biocompatible scaffolds, which are capable to deliver biologically active proteins (e.g. growth factors) at the desired site with a sufficient local dose for a specific time frame and that support cell adhesion and preserve cell function is of great importance[2]. There are essentially two methods of incorporating proteins in polymeric matrices: chemical bonding of protein of interest to the polymer matrix or physical encapsulation of the protein inside the polymer matrix[3, 4]. The latter approach is preferred due to its simplicity and it also minimizes exposure of growth factor to the harsh conditions required to covalently link the proteins of interest on the scaffold surface (as in chemical bonding)[5]. One of the methods based on the physical incorporation of protein to obtain bioactive scaffolds, among others[6], is electrospinning which is a versatile and simple method to produce ultrafine fibrous structures from polymer solutions that mimic the fibrous structure of the extracellular matrix (ECM)[7, 8]. The diameter of the fibers obtained using this technique ranges from several nanometers to a few microns[9]. Several researchers have developed electrospun nanofibers based on both natural polymers such as chitosan[10], alginate[11], gelatin[12], and synthetic polymers including poly(ε-caprolactone) (PCL)[13], poly(lactic-co-glycolic acid)[14-18], and poly(L-lactide-co-caprolactone)[19-22].

Coaxial electrospinning is an advanced technique comprising of two concentric needles rendering the possibility to make fiber mesh scaffolds with core/sheath morphology prepared from an immiscible organic polymer solution and an aqueous protein solution[23]. As a result, the obtained scaffolds are loaded with growth factors that after release promote cell adhesion and growth. The most frequently used polymer for coaxial electrospinning is PCL[24-28] due to its ease of processing into fibers. However, PCL is a slowly degrading polyester that is eliminated from the body only after 2 to 4 years[29], is intrinsically hydrophobic and lacks functional groups to promote cell adhesion[30, 31].

We have recently developed a novel polyester, poly(hydroxymethylglycolide-co-ε-caprolactone) (pHMGCL)[32], which is based on PCL and features a tunable degradation rate[33], and has hydroxyl groups for further functionalization[34] with e.g. peptides. Previously, we have shown that the

scaffolds made of this polymer exhibit superior human mesenchymal stem cells adhesion, proliferation, and differentiation properties as compared to PCL matrices, both in 2D[35] and 3D[36] forms. In the present study, we aimed to improve the properties of coaxially electrospun PCL scaffolds with respect to hydrophilicity, degradation rate, protein release rate, and cell adhesion/proliferation by incorporating pHMGCL into these structures. Therefore, we prepared scaffolds using pHMGCL/PCL solutions as shell and an aqueous solution of bovine serum albumin (BSA) as model protein and protein stabilizer as well as vascular endothelial growth factor (VEGF) as a potent angiogenic factor[37] in the core. The release of protein from different scaffolds was investigated and to demonstrate that the bioactivity of released VEGF was preserved, the effect of released VEGF on attachment and proliferation of endothelial cells seeded on these scaffolds was demonstrated.

2. Materials and Methods

2.1. Materials

All chemicals used in this study were purchased from Sigma-Aldrich and used as received, unless stated otherwise. All solvents were purchased from Biosolve (Valkenswaard, The Netherlands). Toluene was distilled from P_2O_5 and stored over 3 Å molecular sieves under argon. Tetrahydrofuran (THF) was distilled from sodium/benzophenone. 3*S*-Benzyloxymethyl-1,4-dioxane-2,5-dione (benzyl-protected hydroxymethyl glycolide, BMG) was synthesized as described by Leemhuis et al. [38, 39]. ε-Caprolactone (CL) and silica gel (0.035-0.070 mm, 60 Å) were obtained from Acros (Geel, Belgium), and benzyl alcohol (BnOH) was provided by Merck (Darmstadt, Germany), Pd/C (palladium, 10 wt % (dry basis) on activated carbon, wet (50% water w/w), Degussa type E101 NE/W) were obtained from Aldrich (Zwijndrecht, The Netherlands). Recombinant human VEGF 165 was purchased from R&D Systems (Netherlands). Endothelial medium (EM, containing basal medium 200, low serum growth supplements (LSGS) kit containing 2% fetal bovine serum (FBS), 10 ng/ml epidermal growth factor, 3 ng/ml basic fibroblast growth factor (bFGF), 10 mg/ml heparin, 0.2 mg/ml bovine serum albumin (BSA), 1 mg/ml hydrocortisone, and 0.2% gentamicin/amphotericin B) was purchased from Cascade Biologics (Oregon, USA) and assay medium (AM, containing minimal essential medium (α-MEM), 10% FBS, 50 µg/gentamycin) was purchased from Gibco-BRL.

2.2. Synthesis of PCL

PCL was synthesized via ring opening polymerization of ε-caprolactone (CL) using BnOH and $SnOct_2$ as initiator and catalyst, respectively, according to a previously described method[35]. The molar ratio of CL/BnOH was 1000/1 in the feed. The obtained PCL was characterized by ^{1}H NMR, GPC and DSC.

2.3. Synthesis of Poly(hydroxymethylglycolide-co-ε-caprolactone), (pHMGCL)

A random copolymer of benzyl protected hydroxymethylglycolide (BMG) and ε-caprolactone (p(BMGCL)) was synthesized, using monomer to initiator molar ratio of 300/1, by ring opening polymerization method as described before[36]. Briefly, ε-CL (2.29 mL, 0.02 mol), BMG (1.6 g, 0.007 mol), BnOH (9.94 mg, 0.09 mmol), and $SnOct_2$ (18.61 mg, 0.04 mmol) were loaded into a dry schlenk tube, equipped with a magnetic stirrer, under a dry nitrogen atmosphere. Following 2 hours of evacuation, the tube was subsequently closed and immersed in an oil bath pre-heated at 130 °C. The polymerization was performed overnight and the formed polymer was precipitated in methanol, filtrated, and dried in vacuum overnight. The protective benzyl groups of pBMGCL were removed in a hydrogenation reaction using Pd/C catalyst essentially as described by Leemhuis et al. [38]. In short, pBHMGCL (4.0 g, 8.5 mmol) was dissolved in dry THF (400 mL) and subsequently the Pd/C catalyst (3.0 g, 7.4 mmol) was added. The flask was filled with hydrogen in three consecutive steps of evacuation, refilling with H_2 and the reaction was done at room temperature under an H_2 pressure overnight. The catalyst was removed afterwards using a glass filter and THF by evaporation. pBMGCL and pHMGCL were characterized by ^{1}H NMR, DSC, and GPC.

2.4. Fabrication of Coaxial Electrospun Scaffolds

Different types of scaffolds were prepared by coaxial electrospinning. The processing parameters used to obtain these scaffold are presented in Table 1. In general, coaxial electrospinning was performed using a nozzle which delivered the core and shell solutions to the inner and outer needles, respectively (Fig.1). The diameters of the inner and outer needles were 0.5 and 0.8 mm, respectively. The electrospun fibers were collected on a stationary plate covered with an aluminum foil and the scaffolds were freeze-dried for three days before further characterization.

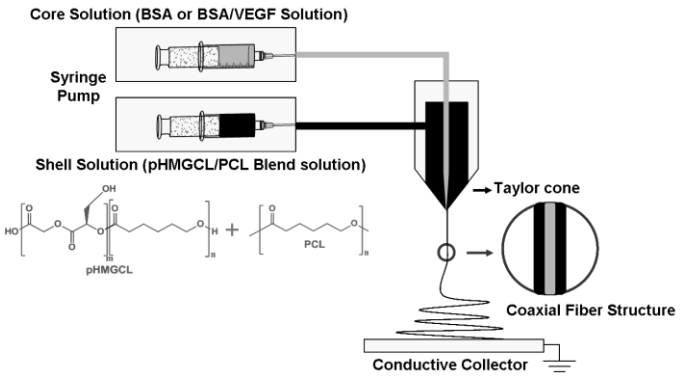

Fig.1. Coaxial electrospinning setup.

2.5. Scanning Electron Microscopy (SEM)

The morphology of the prepared fibrous scaffolds was studied by SEM. Scaffolds were mounted on metal stubs using conductive double-sided tapes and subsequently sputter-coated with platinum. The morphology of the fibers was examined by SEM (JEOL JSM-3010) at an accelerating voltage of 3.0kV. Fiber diameters were measured by ImageJ software and more than 100 counts were used for each scaffold.

2.6. Fluorescence Microscopy (FM)

In order to visualize the presence and distribution of proteins inside the coaxial fibers, samples for fluorescent microscopy were prepared using FITC-BSA, which was dissolved in the core solution (Table1, Groups 5-7). A thin layer of electrospun fibers was collected on a glass slide and observed using an automated fluorescence microscope (Axio Imager Microscope Z1; Carl Zeiss Micro imaging GmbH, Gottingen, Germany). The excitation wavelength and emission wavelength for FITC-BSA were 488 and 525 nm, respectively, and images were captured with a 40X/ 0.75 objective.

2.7. Nuclear Magnetic Resonance (NMR)

NMR measurements of the polymers were performed using a Gemini 300 MHz spectrometer (Varian Associates Inc., NMR Instruments, Palo Alto, CA). Chemical shifts were recorded in ppm with reference to the solvent peak (δ= 7.26 ppm for $CDCl_3$ in ^1H NMR).

Table1. Experimental groups of coaxial electrospun scaffolds used in this study. The flow rate of core and shell solutions (1.8 and 0.6 mL hr^{-1}, respectively) and the collection distance (18 cm) was constant for all the groups.

Sample code	Solutions	Voltage (kV)	Analysis
Group 1	20% PCL/ TFE + 0.2% BSA/ MilliQ	10	Characterization (SEM, DSC, Loading efficiency) & protein release
Group 2	20% PCL/pHMGCL(1:1)/ TFE + 0.2% BSA/ MilliQ	11	Characterization (SEM, DSC, Loading efficiency) & protein release
Group 3	20% PCL/pHMGCL(1:2)/ TFE + 0.2% BSA/ MilliQ	13	Characterization (SEM, DSC, Loading efficiency) & protein release, endothelial cell proliferation
Group 4	20% PCL/pHMGCL(1:2)/ TFE + 0.2% BSA+ 5µg VEGF/ MilliQ	12	Endothelial cell proliferation
Group 5	20% PCL/ TFE + 0.2% FITC-BSA/ MilliQ	10	FM
Group 6	20% PCL/pHMGCL(1:1)/ TFE + 0.2% FITC-BSA/ MilliQ	11	FM
Group 7	20% PCL/pHMGCL(1:2)/ TFE + 0.2% FITC-BSA/ MilliQ	13	FM

2.8. Differential Scanning Calorimetry (DSC)

The thermal properties of polymers and scaffolds were evaluated by differential scanning calorimetry (DSC). For the polymers, scans were taken from -80 °C to 100 °C with a heating rate of 10 °C/min and a cooling rate of 0.5 °C/min under a nitrogen flow of 50 mL/min. The glass transition temperature (T_g) was recorded as the midpoint of heat capacity change in the second heating run. Melting temperature (T_m) and heat of fusion (ΔH_f) were determined from the onset of endothermic peak position and integration of endothermic area in the second heating run, respectively. For scaffolds, the samples were equilibrated at -90 °C and then heated to 100 °C with a heating rate of 10 °C/min. The thermal transitions of the scaffolds were reported for the first and second heating runs.

2.9. Gel Permeation Chromatography (GPC)

The molecular weights of the polymers were measured by means of GPC using a 2695 Waters Aliance system and a Waters 2414 refractive index detector. Two PL-gel 5 µm mixed-D columns fitted with a guard column (Polymer Labs, M_w range 0.2- 400 KDa) were used. The columns were calibrated with polystyrene standards of known molecular weights using AR grade THF, eluting at 1 mL/min flow rate at 30 °C. The concentration of the polymers was approximately 5 mg/mL and the injection volume was 50 µL.

2.10. Water Contact Angle Measurements (CA)

The wettability of polymer films was evaluated by measuring advancing and receding water contact angles using sessile drop technique (Data Physics, OSC50). Uniform polymeric films were prepared by means of spin coating method (Specialty Coating Systems, Inc., model P6708D) using polymer solutions in chloroform (0.2 g/mL) and spin coated for 120 s at a speed of 1800-2000 rpm on round glass cover slips (Fisher Scientific, The Netherlands). Subsequently, the films were put in a vacuum oven at room temperature for 48 h to evaporate the solvent.

For advancing contact angle (Adv-CA), a water droplet (10 µL) was placed onto the surface of a polymeric film and the contact angle between water and surface was measured immediately by taking pictures of the droplet using an optical microscope and averaging the right and left angles using surface contact angle software (SCA20, Data Physics). For the receding contact angle (Rec-CA), the water droplet was withdrawn slowly and the contact angle was measured after different time points. The reported values are mean values of at least four measurements.

2.11. Protein Loading Efficiency (LE)

The protein loading efficiency of the scaffolds was determined according to the method described by Ji et al.[25] Briefly, round pieces (diameter of 1 cm, weighing approximately 20 mg) of freeze-dried scaffolds (n=3) were incubated in 2 mL of dimethylsulfoxide for 1h. Subsequently, 4 mL of 0.2 M NaOH aqueous solution containing 0.5% sodium dodecyl sulfate was added and the obtained solution was incubated for 1 hour at room temperature. Next, the protein concentration in this solution was measured by Micro-BCA™ assay (Pierce, Rockford, IL). Results are presented as the “loading efficiency” of scaffolds, which is defined as the percentage of protein loaded in the scaffolds with respect to the total amount of protein used in the process.

2.12. *In vitro* Release Study

The release of BSA from the different fibrous scaffolds was investigated as described by Ji et al[25]. In short, round BSA-loaded scaffolds punched out of the electrospun mat (diameter of 1cm, thickness of approximately 2 mm, weighing approximately 20 mg) were introduced in MilliQ water (1.5 mL) at 37 °C. The vials were placed on a shaker (speed of 100 rpm) and at t = 0.5, 1.0, 2.0, 4.0 and 24 h, sample volumes of 200 µL and thereafter 500 µL were taken up to 35 days and

the release medium was adjusted each time to 1.5 mL. Release experiments were performed in triplicate. The BSA concentration in the samples was determined by high performance liquid chromatography (HPLC) using a HPLC column (Hypersil Gold, Thermo Scientific, USA) connected to a L2130 HPLC pump and a L-2400 UV detector set at 280 nm (Hitachi Corp., Tokyo, Japan). A 40/60 mixture of acetonitrile/water containing 0.1% (w/v) formic acid was used as the mobile phase with a flow rate of 0.4 ml min^{-1}. The results are presented as cumulative release as a function of time according to the following equation:

$$\text{Cumulative release (\%)} = 100 \times M_t / M_\infty$$

where M_t is the amount of protein released at time t and M_∞ is the amount of protein loaded in the scaffold. BSA standards (1.8 - 180 µg/mL) were used for calibration.

2.13. VEGF bioactivity assay

An *in vitro* cell-based assay was used to investigate the biological activity of VEGF released from the scaffolds. A scaffold based on PCL/pHMGCL 1:2 (Group 4, Table 2) with VEGF loading was selected for this assay because of its attractive BSA release properties. Human umbilical vein endothelial cells (HUVECs; BD, Franklin Lakes, USA) were expanded in endothelial medium (EM) at 37 °C in a humid atmosphere with 5% CO_2 according to the guidelines provided by BD (Becton, Dickinson, and company, Franklin Lakes, USA). The medium was changed twice a week, and cells from passage 8 were used in the release experiment.

Scaffolds were punched into disc shape with diameter of 15 mm, and freeze dried for 2 days followed by 4 minutes of argon plasma treatment for sterilization[40]. Next, the scaffolds were placed in 24-well plates and incubated for 1 hour at 37°C in assay medium (AM). Then, cells were seeded at a density of 40×10^3 cells/cm^2, and cultured in AM. As a control, the same number of cells was seeded in a well plate as well as on scaffolds containing only BSA in the core (Group 3) and cultured in AM. The medium was refreshed at day 1 after cell seeding, and thereafter 3 times per week.

HUVECs growth, as measured by total cellular DNA content, was assessed by Quant-iT™ Picogreen® dsDNA assay kit (Molecular Probes, Eugene, USA) according to the instructions of the manufacturer. At selected time points (1, 4, and 7 days post-seeding), samples (n=3) were prepared by washing

the cell layers twice with PBS and adding 1mL of MilliQ to each well to lyse the cells. After that, the scaffolds containing attached cells were treated by repetitive freezing (-80°C) and thawing (37°C) cycles and 10 minutes of sonication. For the standard curve, serial dilutions of dsDNA stock were prepared (concentrations ranging from 0–2000 ng/ml). Next, 100 µL of either sample or dsDNA was added to the wells, followed by 100 µL of working solution. After 2-5 minutes of incubation in the dark, DNA was measured on a fluorescence cuvette reader (microplate fluorescence reader, Bio-Tek, Winooski, USA) with a 485 nm excitation filter and a 530 nm emission filter. Data were normalized to control group and expressed as fold of DNA content.

The morphology of HUVECs cultured on the scaffolds was also examined. Two samples for each type of scaffold at each time point were seeded with HUVECs at a density of 40×10^3 cells/cm^2 and incubated in AM for 4 and 10 days. After these culture periods, cell layers were rinsed twice with PBS, fixed with 2% glutaraldehyde in cacodylate buffer [$Na(CH_3)_2AsO_2.3H_2O$, pH=5.0-7.4] for 5 min and dehydrated in a graded series of ethanol. Finally, cell layers were dried using tetramethylsilane (TMS), sputter coated with gold, and the cells were examined morphologically using a scanning electron microscope (JEOL, SEM 6340F).

2.14. Statistical analysis

Statistical analysis of the data was done using a one-way analysis of variance (ANOVA) with a post hoc Tukey-Kramer multiple comparison test[25] for cell growth at individual time points using GraphPad Instat software (version 3.05; San Diego, CA). A *p*-value<0.05 was considered statistically significant.

3. Results and Discussion

3.1. Polymer Synthesis and Characterization

PCL and pHMGCL were synthesized via ring opening polymerization (ROP) at 130 °C for 16 hours using BnOH and $SnOct_2$ as initiator and catalyst, respectively, as described before[35, 36]. The BMG/CL monomer molar ratio in the feed was 25/75 and the obtained pBMGCL was subsequently deprotected by removal of the benzyl groups to yield pHMGCL. ^{1}H NMR analysis showed that the HMG/CL monomer molar ratio in the polymer was very close to that of the feed (Table 2). DSC analysis showed that the melting temperature of PCL and pHMGCL was 54 and 37 °C, respectively. The crystallinity of pHMGCL was substantially lower than PCL as indicated by the heat of fusion (ΔH) which was 65

and 31 J/g for PCL and pHMGCL, respectively. GPC analysis showed that the molecular weights (M_n) of PCL and pHMGCL were 71.1 and 17.3 kDa, respectively. The polydispersities were around 2 and in agreement with values generally obtained for polymers synthesized using ROP[41].

Table 2. Characteristics of the polymers used in this study.

Polymer	Monomer/initiator Molar ratio	BMG/CL Molar ratio In feed	HMG/CL Molar ratio In polymer[a]	Yield (%)	DSC			GPC	
					T_g (°C)[b]	T_m (°C)[b]	ΔH (J/g)[b]	M_w (kDa)[c]	PDI[c]
PCL	1000	0/ 100	-	98	-60.8	53.7	65.4	128	1.8
pHMGCL	300	25/ 75	23/ 77	93	-53.1	37.1	31.6	35	2.0

Measured by [a] ^{1}H NMR, [b] DSC, and [c] GPC.

3.2. Scaffolds Preparation and Characterization

BSA-loaded PCL scaffolds were prepared by coaxially electrospinning a PCL solution in TFE (20 w/v %) and a BSA solution in MilliQ water (0.2 w/v %), as shell and core solutions, respectively (Group 1, Table 1). Scaffolds with a uniform fibrous structure and with a fiber diameter of 0.7 ± 0.1 µm were formed (Figure 2A). However, preparation of scaffolds of acceptable quality composed of only pHMGCL as shell forming polymer was not possible likely due to the low molecular weight of this polymer as compared to PCL (M_w of 35 versus 128 kDa) and hence low viscosity of the 20 w/v% polymer solution. The viscosity of pHMGCL solution was raised by increasing the concentration from 20 w/v % up to 40 w/v %. However, the resulting solution was sticky and not electrospinnable due to the blockage of nozzle. An attempt to increase the molecular weight of pHMGCL by increasing M/I ratio in polymerization did not yield significantly longer polymer chains likely because of traces of impurities present in the synthesized monomer[35]. In order to increase the hydrophilicity of the scaffolds, pHMGCL was blended with PCL in different weight ratios (Group 2 and 3 scaffolds, Table 1). SEM analysis of these scaffolds showed absence of beads and a uniform structure (Fig. 2 B and C) composed of fibers with the same diameters as the fibers of the PCL scaffold. In our approach, using solutions of pHMGCL and PCL resulted in good electrospinning conditions (e.g. stable Taylor cone and continuous jet ejecting during process). According to other reports[25, 42] the formation of uniform fibers is affected by the feed rate ratio between the core and the shell solutions. The flow rate ratio (core: shell) of between 1:3 and 1:6 allows the formation of stable core/shell Taylor cones that subsequently after evaporation of the solvents yields uniform core/shell fibers. Therefore, an

inner/outer solution flow rate of 1:3 was chosen. Sharp boundaries between the core and shell layers can be clearly observed in Figure 3 and are attributed to the immiscibility of core/ shell solutions.

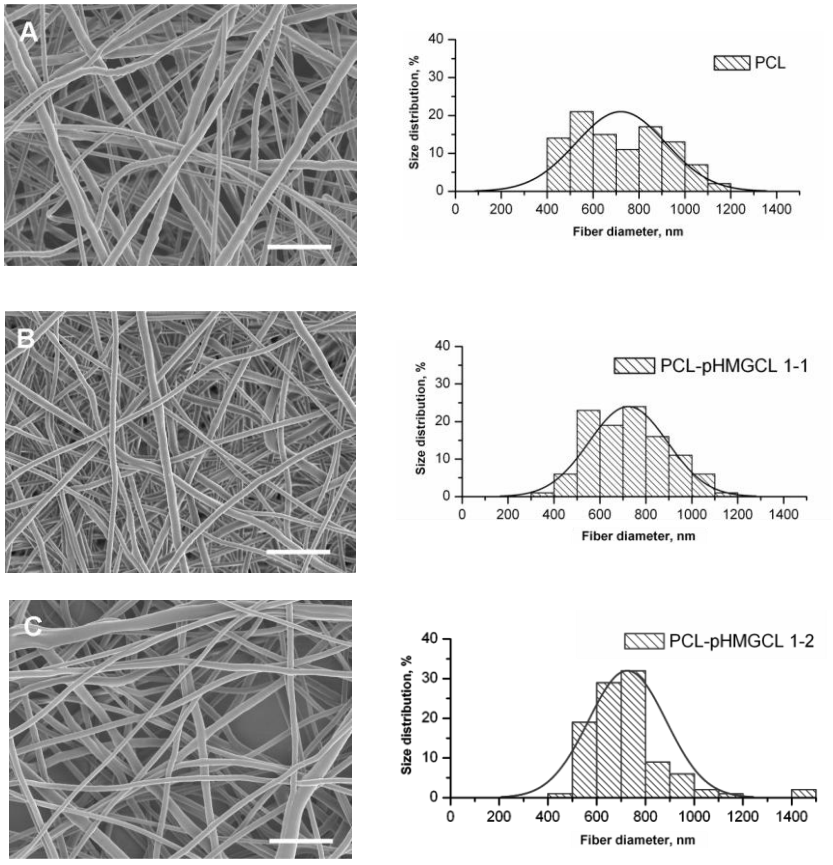

Fig.2. Left: Scanning electron microscopy images of fibrous scaffolds (A) PCL, (B) PCL/pHMGCL 1:1, and (C) PCL/pHMGCL 1:2 (scale bar is 5 µm). Right: Fiber size distribution of electrospun coaxial scaffolds obtained using ImageJ software and considering more than 100 counts per scaffold.

The successful loading of FITC-BSA inside the nanofibers was shown by means of fluorescence microscopy (FM) and Figure 3 demonstrates a uniform distribution of protein (indicated by green stain) in the fibers. The fibrous bead-free morphology observed in these images is also consistent with SEM images shown in Figure 2.

Contact angle (CA) measurements on spun-coated films of the same composition as the electrospun scaffolds were performed to study the blend composition-dependent surface hydrophilicity of scaffolds. Figure 4 shows that the advancing contact angle (Adv-CA) for a PCL film was 77.7 ± 4.5°. For the PCL/pHMGCL blends of 1:1 and 1:2 weight ratios, the Adv-CA was 76.8 ± 3.4° and 75.8 ± 1.4° (Fig. 4A), respectively. The receding CA's (Rec-CA) were measured in time and Figure 4 shows that they slightly decreased for PCL films from 74.7 ± 4.1° to 68.7 ± 6.5° within 20 minutes. Interestingly, for films prepared of PCL/pHMGCL 1:1 blend, the Rec-CA decreased from 70.4 ± 2.1° to 55.1 ± 3.3° within 10 minutes whereas for films of PCL/pHMGCL 1:2 blend, the Rec-CA decreased even more from 68.4 ± 1.9° to 47.7 ± 1.2° in 10 minutes. It was not possible to measure the Rec-CA further due to almost full spreading of the water droplets on the surface (Fig. 4B). The considerable decrease in Rec-CA in time can be attributed to the reorientation of the polar hydroxyl groups of pHMGCL on the surface of the polymeric film upon exposure to water. This is in agreement with our previous findings[35] where we showed that receding contact angles on polymeric films of pHMGCL decrease substantially with increasing the percentage of hydrophilic units in this copolymer and also decrease in time. However, the full water-spreading as we observed for the blends was not observed on the film containing only pHMGCL with maximum 10 molar% of HMG units[35].

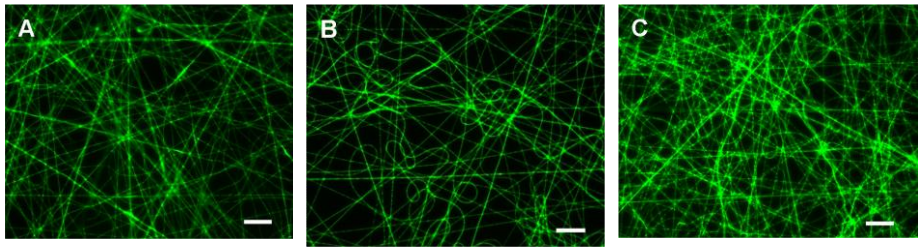

Fig.3. Fluorescent microscopy images of FITC-BSA loaded in coaxial fibrous scaffolds (A) PCL, (B) PCL/pHMGCL 1:1, and (C) PCL/pHMGCL 1:2. Scale bar is 20 µm.

The thermal properties of the scaffolds were analyzed using DSC. As shown in Table 3, a single melting peak was observed for scaffolds with PCL/pHMGCL blends as the shell (Table 1, Groups 2 and 3). The heat of fusion of these scaffolds (in the first heating run) decreased from 73 to 54 J/g with increasing pHMGCL content in the blend from 0 % in PCL scaffolds to 67 % in PCL/pHMGCL 1:2 scaffolds. However, ΔH values measured at the second heating run were slightly lower than the ΔH values obtained at the first heating

cycles most probably due to the thermal history of the samples. Further, ΔH values (second heating run) were in good agreement with the calculated ΔH values (Table 3). The glass transition temperatures (T_g) of the scaffolds were -58.6 °C, -55.2 °C, and -47.4 °C for PCL, PCL/pHMGCL 1:1, and PCL/pHMGCL 1:2, respectively. Table 3 shows that the experimental T_g's are in good agreement with those calculated by Fox equation[43]:

$$\frac{1}{T_g} = \frac{W_1}{T_{g,1}} + \frac{W_2}{T_{g,2}}$$

in which W_1 and W_2 are the weight fractions and $T_{g,1}$ and $T_{g,2}$ are the glass transition temperatures of the components in a blend.

Based on these results, it can be concluded that electrospun scaffolds of pHMGCL and PCL consist of a miscible blend of the two polymers.

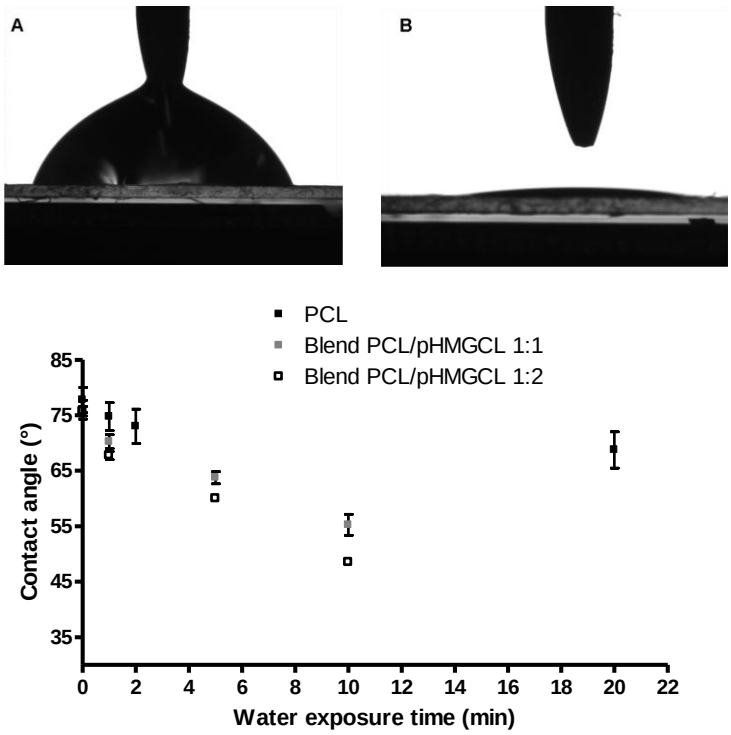

Fig.4. TOP: (A) Advancing contact angle and (B) receding contact angle after 20 minutes water exposure on film of PCL/pHMGCL 1:2. BOTTOM: Advancing and the time-dependent receding contact angles on polymeric films of different compositions (n=3 ± SD).

Table 3. Thermal properties of coaxial electrospun scaffolds before and after release.

Scaffold	Theoretical values		Before release					After release	
			First heating run			Second heating run		Second heating run	
	T_g (°C)*	ΔH (J/g)**	T_g (°C)	T_m (°C)	ΔH (J/g)	T_m (°C)	ΔH (J/g)	T_m (°C)	ΔH (J/g)
PCL	N.A.	N.A.	-58.6	55.9	73.2	55.1	63.6	55.2	61.2
PCL/ pHMGCL (1:1)	-57.5	48.5	-55.2	54.6	63.6	55.5	50.6	49.0	72.3
PCL/ pHMGCL (1:2)	-55.8	42.7	-47.4	53.6	54.3	55.8	40.7	48.6	78.2

* based on Fox equation, ** based on weight percentage of caprolactone in the blends.

3.3. BSA Loading Efficiency and *in-vitro* Release

BSA was chosen as a model protein for VEGF in this study due to similarities in their molecular weight ($M_{w,\ BSA}$= 67 kDa, $M_{w,VEGF}$=45 kDa)[44-46] and hydrodynamic radius ($R_{h,BSA}$=3.5 nm[47], $R_{h,VEGF}$= 3 nm[48]). The measured protein loading was 93 %. The BSA release profiles of the different scaffolds are shown in Figure 5. This figure shows that in the release profiles three stages can be distinguished; up to 4 hours an initial release ('burst' phase) followed by a gradual sustained release up to 10 days (phase 1) and a slow release up to 35 days (phase 2) (Table 4). The burst release was 21.0 ± 1.2 %, 34.9 ± 1.3 %, and 27.2 ± 0.8 % for PCL, PCL/pHMGCL 1:1, and PCL/pHMGCL 1:2 scaffolds, respectively. This burst release of protein is most likely due to either the presence of some non-uniformities (such as cracks, open ends, etc.) in the fibers structure and/or partial mixing of core and shell solutions during electrospinning which might lead to presence of the protein on the surface of fibers instead in the core. After this burst release, the protein was released in a sustained manner reaching 40.2 ± 1.8 %, 61.7 ± 2.1 %, and 70.1 ± 6.8 % for PCL, PCL/pHMGCL 1:1, and PCL/pHMGCL 1:2 scaffolds after 10 days. After this phase, a very small amount of BSA was released in the next phase for all scaffolds up to 35 days and reached 46.8 ± 2.1, 70.1 ± 2.3, and 77.5 ± 5.1 for PCL, PCL/pHMGCL 1:1, and PCL/pHMGCL 1:2 scaffolds, respectively.

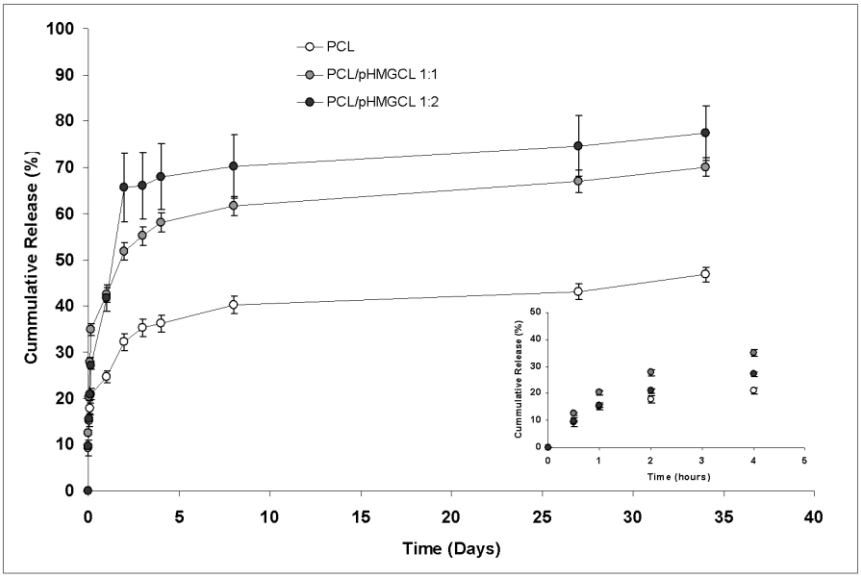

Fig.5. BSA release profiles of coaxial electrospun scaffolds (Group 1, 2 and 3) loaded with 0.2% BSA (n=3). Results are shown as mean ± SD. The cumulative release is reported based on the amount of protein loaded in each scaffold. The insert shows the burst release of BSA up to 4 hours.

Table 4. Percentage of BSA released from coaxial scaffolds as burst (0-4 hrs), phase 1 (4 hrs-10 days), and phase 2 (10-35 days). Data are presented as means ± standard deviations (n=3 samples from the same scaffold).

	Burst Release (0-4 hrs)	Phase 1 (4hrs- 10 days)	Phase 2 (10- 35 days)
Group 1	21.0 ± 1.2	19.2 ± 1.8	2.1 ± 2.1
Group 2	34.9 ± 1.3	26.8 ± 2.1	8.4 ± 2.3
Group 3	27.2 ± 0.8	42.9 ± 6.8	7.4 ± 5.1

It has been reported that several parameters among which shell thickness, surface area, defects, permeability, and solubility of the drug in the polymer shell control the rate of drug release from coaxial fibrous scaffolds[28]. For the coaxial fibers of the present study, it is most likely that the protein release is due to diffusion across nanopores in the polymeric shell, degradation of polymeric shell, and/ or a combination of these factors[49]. Degradation does not likely play a role in the mechanism of BSA release from PCL scaffolds because this polymer undergoes a very slow hydrolytic degradation which takes more than 2 years[33, 50, 51]. However, in our previous degradation study of pHMGCL with 10% HMG

content[33], we showed that this polymer degrades much faster than PCL and undergoes more than 10% weight loss within 35 days while the M_n drops from 30 kDa to less than 8 kDa. Based on those results it can be assumed that the pHMGCL used in the present study (containing > 20 molar % of hydrophilic HMG units) degrades even faster, as we also observed for related copolymers of HMG with lactide (pLHMGA)[52]. Indeed, measuring the dry weight of post-release scaffolds and comparing that with the initial weight of scaffolds, showed that PCL, PCL/pHMGCL (1:1), and PCL/pHMGCL (1:2) scaffolds lost 0.3 ± 0.4, 17.5 ± 4.5, and 26.0 ± 4.0 percent of their initial weight. Since the weight of incorporated protein (BSA) is negligible compared to the weight of scaffolds, this mass loss can not be related to the protein release and is therefore indicative of polymer degradation. SEM images of post-release scaffolds confirmed that PCL fibers were intact after 35 days (Fig. 6 A and B), while fibers of scaffolds containing pHMGCL in the shell showed signs of degradation as observed by fibers fragmentation (Fig. 6 C-F). Investigating the thermal properties of scaffolds after 35 days of protein release showed that crystallinity of scaffolds composed of pHMGCL/PCL (as reflected by ΔH) was notably increased while the crystallinity of PCL scaffolds was unchanged (Table 3). This increase in ΔH can be attributed to the preferential hydrolytic degradation of amorphous regions in the pHMGCL structure, resulting in crystallization of CL segments of the pHMGCL/PCL blend that were initially present in amorphous regions of the material.

Increasing the weight fraction of hydrophilic pHMGCL in the fibers shell from 0% in PCL scaffold to 50 and 67 % in PCL/pHMGCL scaffolds (1:1 and 1:2, respectively) resulted in a significant increase in amount of released protein after 10 days (PCL vs. 1:1 and 1:2 blend: $p<0.05$ and $p<0.001$, respectively) and after 35 days (PCL vs. 1:1 and 1:2 blend: $p<0.05$ and $p<0.01$, respectively). In addition, increasing the pHMGCL weight fraction in the blend from 50% in 1:1 scaffold to 67% in 1:2 scaffold, resulted in a significantly increased release of protein after 10 days ($p<0.05$), however, the cumulative release after 35 days was not significantly different ($p>0.05$).

Overall, based on these results it can be concluded that the protein release from PCL scaffolds is likely governed by diffusion via nanopores in the fibers shell, which have a size (slightly) bigger than the hydrodynamic diameter of BSA (less than 5 nm)[47], while the protein release from pHMGCL/PCL scaffolds is likely controlled by a combination of diffusion and shell degradation.

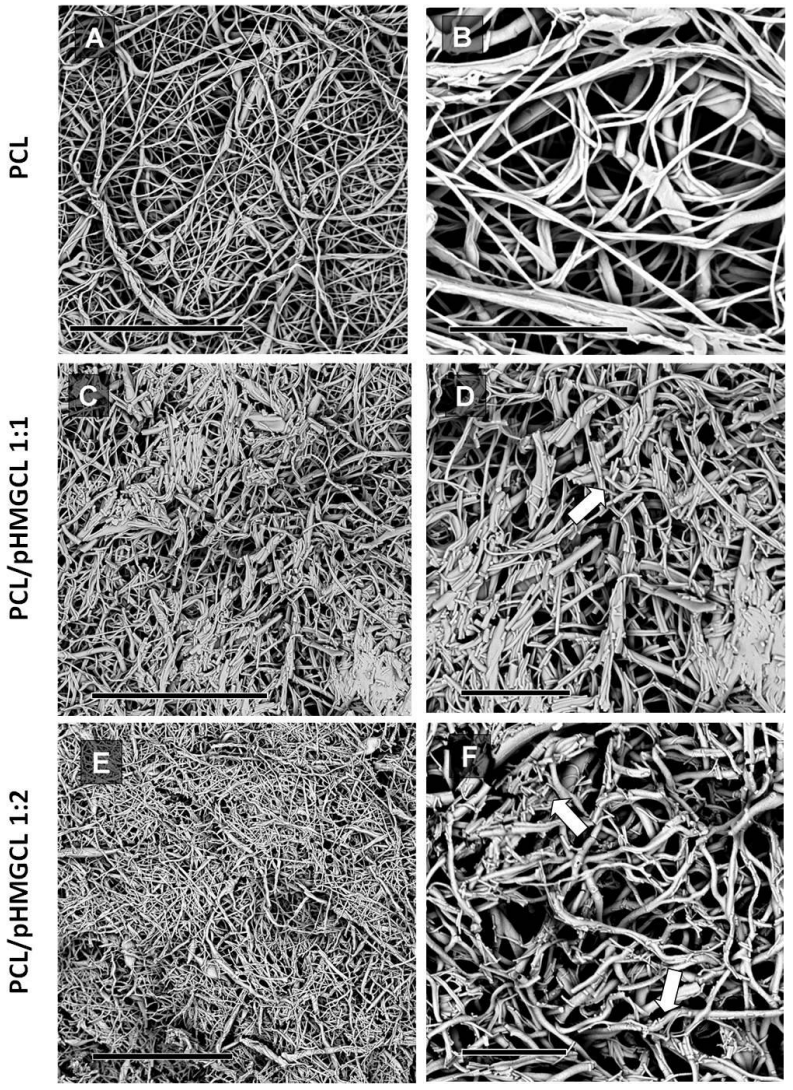

Fig.6. SEM images of BSA-loaded nanofibrous scaffolds after 35 days incubation in MilliQ-water at 37 °C. Scale bar is 30 µm (left) and 10 µm (right). White arrows show degraded fibers.

3.4. VEGF Bioactivity

As the biological half-life of VEGF is very short (30 min)[5], administration of this growth factor intravenously requires high doses and/ or multiple injections[5, 53]. However, administration of large amounts of VEGF in the body should be avoided

as it results in catastrophic pathological vessel formation at non-targeted sites[5]. Therefore, in tissue engineering approaches (e.g. bone regeneration) a polymeric matrix capable of releasing this protein at the defect site is vital. In this study, we prepared VEGF loaded nanofibrous scaffolds from PCL/pHMGCL 1:2 solution, (containing BSA in the core as protein stabilizer[54]). This type of scaffold was chosen based on the *in vitro* results obtained for BSA as its release profile showed faster and higher overall release of the protein (Figure 5), while one can assume that the loading efficiency and release profile of VEGF is comparable to that of BSA due to their similarity in size[45]. The growth of HUVECs on VEGF-loaded as well as bare (BSA-loaded) scaffolds was evaluated and is presented as the DNA content of cells seeded onto these scaffolds relative to the same value on tissue culture poly(styrene) (TCPS) (Figure 7).

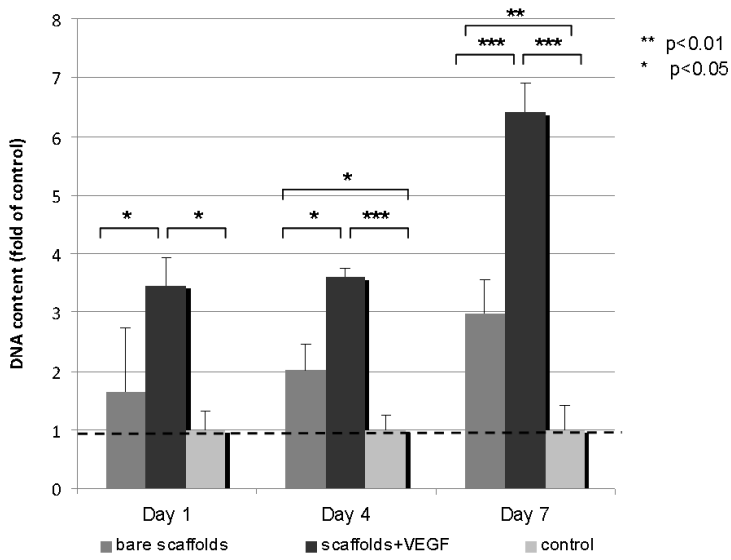

Fig.7. Relative DNA content of human umbilical vein endothelial cells (HUVECs) seeded onto scaffolds of PCL/pHMGCL 1:2 (with/without VEGF) as compared to control group (TCPS) and expressed as fold of DNA content (n=3 ± SD).

This figure shows that at day 1, 4, and 7, the relative DNA content on VEGF-releasing scaffolds was 3.5, 3.6, and 6.5 fold higher than TCPS control, respectively, and 2.3, 1.8, and 2.2 folds higher than on bare scaffolds, respectively. Since the DNA content is positively correlated with the number of viable cells, it can be concluded that the VEGF-releasing scaffolds showed more

viable HUVECs growth compared to those seeded onto bare scaffolds up to 7 days. The culture medium of VEGF-releasing scaffolds was refreshed after 1 day and subsequently once every 3 days, therefore the cell proliferation on these scaffolds at day 4, 7, and 10 can be related to the released VEGF at later time points after the burst release. The cell proliferation was also confirmed by observing the morphology of cells seeded onto VEGF-releasing scaffolds and comparing that to the cell morphology on bare scaffolds by means of SEM. As demonstrated in Figure 8, on day 4 the cells covered the surface of bare scaffolds only partially (Fig. 8A) while the surface of VEGF-releasing scaffolds was almost fully covered with cells (Fig. 8D). Taken together, the results indicate that the pro-angiogenic factor (VEGF) released from coaxial fibers remained biologically active to support HUVECs proliferation on scaffolds up to 7 days.

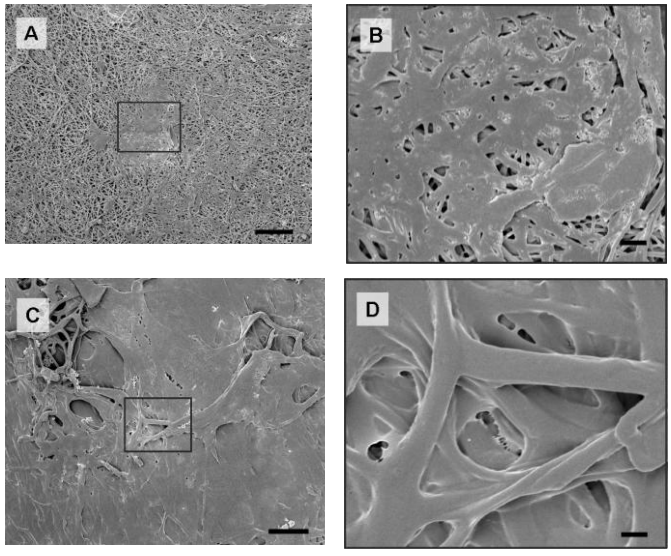

Fig.8. Morphology of human umbilical vein endothelial cells (HUVECs) seeded on bare scaffolds (A-B) and VEGF-loaded scaffolds (C-D) of PCL/pHMGCL 1:2 after 4 days. Scale bar is 10 µm (except B and D which are magnifications of squared sections of A and C; scale bar 1 µm). Cells cover partially (A) and fully (C) surface of scaffolds.

As HUVECs cannot survive under conditions without growth supplements (e.g. VEGF), therefore, the number of cells cultured in the assay medium decreased in time. Therefore, on day 10, the absolute DNA content was too low to report the relative fold of cell growth on the scaffolds. However, we noticed that there was no significant difference between the absolute DNA content of the cells cultured

on the VEGF-releasing scaffolds and the bare scaffolds (data not shown). A possible reason might be the low amount of VEGF released from day 7 to 10, as the release profile is expected to reach a plateau at ~ day 8 based on BSA release results *in vitro* (Figure 5). The estimated concentration of VEGF in the assay medium from day 7 to 10 is around 2 ng/ml, while a previous study revealed that VEGF promotes HUVEC proliferation at concentrations of 12.5-100 ng/ml[55]. Further experiments are directed to increase the VEGF loading in the scaffolds to see whether also long term cellular response can be observed.

4. Conclusions

This chapter describes the preparation and characterization of VEGF-loaded nanofibrous electrospun scaffolds based on blends of a hydroxyl-functionalized polyester (pHMGCL) and PCL by means of coaxial electrospinning. DSC analysis showed that these two polymers are miscible at a molecular level. It was shown by contact angle measurements that scaffolds containing pHMGCL exhibited significantly higher surface hydrophilicity when exposed to water compared to those based on PCL only. BSA as a model protein was loaded into these fibers and it was shown that *in vitro* release of this protein is likely governed by combination of diffusion and degradation. Scaffolds composed of pHMGCL showed an enhanced protein release as compared to PCL scaffolds, likely due to enhanced hydrolysis rate of pHMGCL/PCL blend while PCL scaffolds did not degrade in the time frame investigated. It has shown previously that the increased hydrophilicity of pHMGCL scaffolds results in a considerable increase in adhesion of human mesenchymal stem cells seeded onto these scaffolds comparing to their counterpart PCL scaffolds. In the present study, it was demonstrated that loaded VEGF in pHMGCL containing scaffolds preserved its bioactivity and resulted in enhanced initial cell adhesion and proliferation. Therefore, these bioactive electrospun scaffolds based on blends of pHMGCL and PCL are capable of releasing VEGF in a sustained manner and can be considered as a suitable scaffold for tissue engineering applications.

References

[1] Dvir, T.; Timko, B. P.; Kohane, D. S.; Langer, R., Nanotechnological strategies for engineering complex tissues. *Nature Nanotechnology* **2011,** 6, (1), 13-22.

[2] Mouriño, V.; Boccaccini, A. R., Bone tissue engineering therapeutics: Controlled drug delivery in three-dimensional scaffolds. *Journal of the Royal Society Interface* **2010,** 7, (43), 209-227.

[3] Chen, R. R.; Mooney, D. J., Polymeric growth factor delivery strategies for tissue engineering. *Pharmaceutical Research* **2003,** 20, (8), 1103-1112.

[4] Richardson, T. P.; Peters, M. C.; Ennett, A. B.; Mooney, D. J., Polymeric system for dual growth factor delivery. *Nature Biotechnology* **2001,** 19, (11), 1029-1034.

[5] Lee, K.; Silva, E. A.; Mooney, D. J., Growth factor delivery-based tissue engineering: General approaches and a review of recent developments. *Journal of the Royal Society Interface* **2011,** 8, (55), 153-170.

[6] Levenberg, S.; Langer, R., Advances in Tissue Engineering. In *Current Topics in Developmental Biology*, **2004,** 61, 113-134.

[7] Gan, Z.; Yu, D.; Zhong, Z.; Liang, Q.; Jing, X., Enzymatic degradation of poly(ε-caprolactone)/poly(DL-lactide) blends in phosphate buffer solution. *Polymer* **1999,** 40, (10), 2859-2862.

[8] Sill, T. J.; von Recum, H. A., Electrospinning: Applications in drug delivery and tissue engineering. *Biomaterials* **2008,** 29, (13), 1989-2006.

[9] Huang, Z. M.; Zhang, Y. Z.; Kotaki, M.; Ramakrishna, S., A review on polymer nanofibers by electrospinning and their applications in nanocomposites. *Composites Science and Technology* **2003,** 63, (15), 2223-2253.

[10] Sasmazel, H. T., Novel hybrid scaffolds for the cultivation of osteoblast cells. *International Journal of Biological Macromolecules* **2011,** 49, (4), 838-846.

[11] Jeong, S. I.; Krebs, M. D.; Bonino, C. A.; Samorezov, J. E.; Khan, S. A.; Alsberg, E., Electrospun chitosan-alginate nanofibers with in situ polyelectrolyte complexation for use as tissue engineering scaffolds. *Tissue Engineering - Part A* **2011,** 17, (1-2), 59-70.

[12] Gluck, J. M.; Rahgozar, P.; Ingle, N. P.; Rofail, F.; Petrosian, A.; Cline, M. G.; Jordan, M. C.; Roos, K. P.; MacLellan, W. R.; Shemin, R. J.; Heydarkhan-Hagvall, S., Hybrid coaxial electrospun nanofibrous scaffolds with limited immunological response created for tissue

engineering. *Journal of Biomedical Materials Research - Part B Applied Biomaterials* **2011,** 99 B, (1), 180-190.

[13] Cipitria, A.; Skelton, A.; Dargaville, T. R.; Dalton, P. D.; Hutmacher, D. W., Design, fabrication and characterization of PCL electrospun scaffolds-a review. *Journal of Materials Chemistry* **2011,** 21, (26), 9419-9453.

[14] Meng, Z. X.; Xu, X. X.; Zheng, W.; Zhou, H. M.; Li, L.; Zheng, Y. F.; Lou, X., Preparation and characterization of electrospun PLGA/gelatin nanofibers as a potential drug delivery system. *Colloids and Surfaces B: Biointerfaces* **2011,** 84, (1), 97-102.

[15] Meng, Z. X.; Zheng, W.; Li, L.; Zheng, Y. F., Fabrication, characterization and in vitro drug release behavior of electrospun PLGA/chitosan nanofibrous scaffold. *Materials Chemistry and Physics* **2011,** 125, (3), 606-611.

[16] Han, J.; Lazarovici, P.; Pomerantz, C.; Chen, X.; Wei, Y.; Lelkes, P. I., Co-electrospun blends of PLGA, gelatin, and elastin as potential nonthrombogenic scaffolds for vascular tissue engineering. *Biomacromolecules* **2011,** 12, (2), 399-408.

[17] Sahoo, S.; Toh, S. L.; Goh, J. C. H., A bFGF-releasing silk/PLGA-based biohybrid scaffold for ligament/tendon tissue engineering using mesenchymal progenitor cells. *Biomaterials* **2010,** 31, (11), 2990-2998.

[18] Lee, J. Y.; Bashur, C. A.; Goldstein, A. S.; Schmidt, C. E., Polypyrrole-coated electrospun PLGA nanofibers for neural tissue applications. *Biomaterials* **2009,** 30, (26), 4325-4335.

[19] Yan, S.; Xiaoqiang, L.; Lianjiang, T.; Chen, H.; Xiumei, M., Poly(l-lactide-co-ε-caprolactone) electrospun nanofibers for encapsulating and sustained releasing proteins. *Polymer* **2009,** 50, (17), 4212-4219.

[20] Lee, J.; Tae, G.; Kim, Y. H.; Park, I. S.; Kim, S. H.; Kim, S. H., The effect of gelatin incorporation into electrospun poly(l-lactide-co-ε-caprolactone) fibers on mechanical properties and cytocompatibility. *Biomaterials* **2008,** 29, (12), 1872-1879.

[21] Zhu, Y.; Leong, M. F.; Ong, W. F.; Chan-Park, M. B.; Chian, K. S., Esophageal epithelium regeneration on fibronectin grafted poly(l-lactide-co-caprolactone) (PLLC) nanofiber scaffold. *Biomaterials* **2007,** 28, (5), 861-868.

[22] Inoguchi, H.; Kwon, I. K.; Inoue, E.; Takamizawa, K.; Maehara, Y.; Matsuda, T., Mechanical responses of a compliant electrospun poly(L-

lactide-co-ε-caprolactone) small-diameter vascular graft. *Biomaterials* **2006,** 27, (8), 1470-1478.

[23] Ji, W.; Sun, Y.; Yang, F.; Van Den Beucken, J. J. J. P.; Fan, M.; Chen, Z.; Jansen, J. A., Bioactive electrospun scaffolds delivering growth factors and genes for tissue engineering applications. *Pharmaceutical Research* **2011,** 28, (6), 1259-1272.

[24] Drexler, J. W.; Powell, H. M., Regulation of electrospun scaffold stiffness via coaxial core diameter. *Acta Biomaterialia* **2011,** 7, (3), 1133-1139.

[25] Ji, W.; Yang, F.; Van Den Beucken, J. J. J. P.; Bian, Z.; Fan, M.; Chen, Z.; Jansen, J. A., Fibrous scaffolds loaded with protein prepared by blend or coaxial electrospinning. *Acta Biomaterialia* **2010,** 6, (11), 4199-4207.

[26] Saraf, A.; Baggett, L. S.; Raphael, R. M.; Kasper, F. K.; Mikos, A. G., Regulated non-viral gene delivery from coaxial electrospun fiber mesh scaffolds. *Journal of Controlled Release* **2010***,* 143, (1), 95-103.

[27] Liao, I. C.; Chen, S.; Liu, J. B.; Leong, K. W., Sustained viral gene delivery through core-shell fibers. *Journal of Controlled Release* **2009,** 139, (1), 48-55.

[28] Zhang, Y. Z.; Wang, X.; Feng, Y.; Li, J.; Lim, C. T.; Ramakrishna, S., Coaxial electrospinning of (fluorescein isothiocyanate-conjugated bovine serum albumin)-encapsulated poly(ε-caprolactone) nanofibers for sustained release. *Biomacromolecules* **2006,** 7, (4), 1049-1057.

[29] Li, S.; Liu, L.; Garreau, H.; Vert, M., Lipase-catalyzed biodegradation of poly(ε-caprolactone) blended with various polylactide-based polymers. *Biomacromolecules* **2003,** 4, (2), 372-377.

[30] Zeng, J.; Chen, X.; Liang, Q.; Xu, X.; Jing, X., Enzymatic degradation of poly(L-lactide) and poly(ε-caprolactone) electrospun fibers. *Macromolecular Bioscience* **2004,** 4, (12), 1118-1125.

[31] Yildirim, E. D.; Ayan, H.; Vasilets, V. N.; Fridman, A.; Guceri, S.; Sun, W., Effect of dielectric barrier discharge plasma on the attachment and proliferation of osteoblasts cultured over poly(ε-caprolactone) scaffolds. *Plasma Processes and Polymers* **2008,** 5, (1), 58-66.

[32] Loontjens, C. A. M.; Vermonden, T.; Leemhuis, M.; Van Steenbergen, M. J.; Van Nostrum, C. F.; Hennink, W. E., Synthesis and characterization of random and triblock copolymers of ε-caprolactone and (benzylated)hydroxymethyl glycolide. *Macromolecules* **2007,** 40, (20), 7208-7216.

[33] Hajar Seyednejad, W. J., Wouter Schuurman, Wouter JA Dhert, Jos Malda, Fang Yang, John A. Jansen, Cornelus van Nostrum, Tina Vermonden, Wim E. Hennink, Electrospun Degradable Scaffold Based on a Novel Hydrophilic Polyester for Tissue Engineering Applications. Macromolecular Bioscience **2011**, 11, 1684-1692.

[34] Seyednejad, H.; Ghassemi, A. H.; Van Nostrum, C. F.; Vermonden, T.; Hennink, W. E., Functional aliphatic polyesters for biomedical and pharmaceutical applications. *Journal of Controlled Release* **2011,** 152, (1), 168-176.

[35] Seyednejad, H.; Vermonden, T.; Fedorovich, N. E.; Van Eijk, R.; Van Steenbergen, M. J.; Dhert, W. J. A.; Van Nostrum, C. F.; Hennink, W. E., Synthesis and characterization of hydroxyl-functionalized caprolactone copolymers and their effect on adhesion, proliferation, and differentiation of human mesenchymal stem cells. *Biomacromolecules* **2009,** 10, (11), 3048-3054.

[36] Seyednejad, H.; Gawlitta, D.; Dhert, W. J. A.; Van Nostrum, C. F.; Vermonden, T.; Hennink, W. E., Preparation and characterization of a three-dimensional printed scaffold based on a functionalized polyester for bone tissue engineering applications. *Acta Biomaterialia* **2011,** 7, (5), 1999-2006.

[37] Patel, Z. S.; Young, S.; Tabata, Y.; Jansen, J. A.; Wong, M. E. K.; Mikos, A. G., Dual delivery of an angiogenic and an osteogenic growth factor for bone regeneration in a critical size defect model. *Bone* **2008,** 43, (5), 931-940.

[38] Leemhuis, M.; Van Nostrum, C. F.; Kruijtzer, J. A. W.; Zhong, Z. Y.; Ten Breteler, M. R.; Dijkstra, P. J.; Feijen, J.; Hennink, W. E., Functionalized poly(α-hydroxy acid)s via ring-opening polymerization: Toward hydrophilic polyesters with pendant hydroxyl groups. *Macromolecules* **2006,** 39, (10), 3500-3508.

[39] Mark Leemhuis, Jan H. van S., Michelle J van Uxem, Cornelus F van Nostrum, Wim E Hennink, *Eur. J. Org. Chem.* **2003,** 2003, (17), 3344-3349.

[40] Holy, C. E.; Cheng, C.; Davies, J. E.; Shoichet, M. S., Optimizing the sterilization of PLGA scaffolds for use in tissue engineering. *Biomaterials* **2000,** 22, (1), 25-31.

[41] Philippe Dubois, O. C., Jean-Marie Raquez Handbook of ring-opening polymerization. **2009**, 21-23.

[42] Chakraborty, S.; Liao, I. C.; Adler, A.; Leong, K. W., Electrohydrodynamics: A facile technique to fabricate drug delivery systems. *Advanced Drug Delivery Reviews* **2009,** 61, (12), 1043-1054.

[43] Parashar, P.; Ramakrishna, K.; Ramaprasad, A. T., A study on compatibility of polymer blends of polystyrene/poly(4-vinylpyridine). *Journal of Applied Polymer Science* **2010,** 120, (3), 1729-1735.

[44] Censi, R.; Vermonden, T.; van Steenbergen, M. J.; Deschout, H.; Braeckmans, K.; De Smedt, S. C.; van Nostrum, C. F.; di Martino, P.; Hennink, W. E., Photopolymerized thermosensitive hydrogels for tailorable diffusion-controlled protein delivery. *Journal of Controlled Release* **2009,** 140, (3), 230-236.

[45] Oredein-Mccoy, O.; Krogman, N. R.; Weikel, A. L.; Hindenlang, M. D.; Allcock, H. R.; Laurencin, C. T., Novel factor-loaded polyphosphazene matrices: Potential for driving angiogenesis. *Journal of Microencapsulation* **2009,** 26, (6), 544-555.

[46] Stefanini, M. O.; Wu, F. T. H.; Mac Gabhann, F.; Popel, A. S., A compartment model of VEGF distribution in blood, healthy and diseased tissues. *BMC Systems Biology* **2008,** 2.

[47] Hulse, W.; Forbes, R., A Taylor dispersion analysis method for the sizing of therapeutic proteins and their aggregates using nanolitre sample quantities. *International Journal of Pharmaceutics* **2011,** 416, (1), 394-397.

[48] Kisko, K.; Brozzo, M. S.; Missimer, J.; Schleier, T.; Menzel, A.; LeppanÌˆen, V. M.; Alitalo, K.; Walzthoeni, T.; Aebersold, R.; Ballmer-Hofer, K., Structural analysis of vascular endothelial growth factor receptor-2/ligand complexes by small-angle X-ray solution scattering. *FASEB Journal* **2011,** 25, (9), 2980-2986.

[49] Sahoo, S.; Ang, L. T.; Goh, J. C. H.; Toh, S. L., Growth factor delivery through electrospun nanofibers in scaffolds for tissue engineering applications. *Journal of Biomedical Materials Research - Part A* **2010,** 93, (4), 1539-1550.

[50] Sun, H.; Mei, L.; Song, C.; Cui, X.; Wang, P., The in vivo degradation, absorption and excretion of PCL-based implant. *Biomaterials* **2006,** 27, (9), 1735-1740.

[51] Woodruff, M. A.; Hutmacher, D. W., The return of a forgotten polymer: Polycaprolactone in the 21st century. *Progress in Polymer Science* 35, (10), 1217-1256.

[52] Leemhuis, M.; Kruijtzer, J. A. W.; van Nostrum, C. F.; Hennick, W. E., In vitro hydrolytic degradation of hydroxyl-functionalized poly(α-hydroxy acid)s. *Biomacromolecules* **2007,** 8, (9), 2943-2949.

[53] Fischbach, C.; Mooney, D.; Werner, C., Polymeric Systems for Bioinspired Delivery of Angiogenic Molecules Polymers for Regenerative Medicine. In Springer Berlin / Heidelberg: **2006**, 203, 191-221.

[54] Valmikinathan, C. M.; Defroda, S.; Yu, X., Polycaprolactone and bovine serum albumin based nanofibers for controlled release of nerve growth factor. *Biomacromolecules* **2009,** 10, (5), 1084-1089.

[55] Geutjes, P. J.; Nillesen, S. T. M.; Lammers, G.; Daamen, W. F.; van Kuppevelt, T. H., Cloning, large-scale production, and purification of active dimeric rat vascular endothelial growth factor (rrVEGF-164). *Protein Expression and Purification* **2010,** 69, (1), 76-82.

Chapter 8

Summary, Discussion, & Perspectives

Hajar Seyednejad

1. Summary

Tissue Engineering (TE) is an emerging, alternative approach for organ transplantation which was introduced in 1993 by Langer and Vacanti, and defined by them as an “interdisciplinary field that applies the principles of engineering and life sciences toward the development of biological substitutes that restore, maintain, or improve tissue function or a whole organ”. TE is essentially based on three major components: cells, scaffolds, and bioactive agents (e.g., growth factors). The main function of scaffolds in TE approaches is to provide a substrate for cell adhesion and proliferation and thus facilitate the formation of new tissue. Ideally, scaffolds should be biocompatible and biodegradable, and their degradation rate should match the rate at which the new tissue is formed. The aim of this thesis was to develop synthetic scaffolds based on functionalized polyesters particularly copolymers based on hydroxymethyl glycolide (HMG) and ε-caprolactone (CL) for TE applications. It is assumed that upon introducing HMG units into the copolymer structure, the crystallinity will be decreased. Besides, the hydrophilicity of these copolymers is expected to be higher when compared to PCL, which in turn can result in faster hydrolysis, and higher cell-scaffold interactions.

There are several techniques to make scaffolds for TE applications. These methods fall into two main categories: conventional and advanced techniques. The former consist of methods which mainly utilize a mould to prepare scaffolds. These techniques include solvent casting/particulate leaching, melt molding, gas foaming, emulsification/freeze drying, and phase separation. Also electrospinning, which employs high electrical voltage to produce fibrous scaffolds is considered as a conventional scaffolding method. The latter category (advanced techniques) comprises methods based on solid freeform fabrication (SFF) techniques. Exploiting these techniques, scaffolds are built by selectively adding material in a layer-by-layer fashion which is controlled by a computer program. One of the potential benefits of SFF technology is the ability to create parts with highly reproducible architectures and compositional variations. The advanced techniques can be divided into three main groups: a) methods based on laser technology, that either photopolymerize a liquid resin (i.e., stereolithography (SLA)) or sinter powdered materials (i.e., selective laser sintering), b) systems based on print technology including printing a chemical binder onto a powdered material (3D-printing) or directly printing wax (wax printing), and c) systems based on extrusion (also defined as nozzle-based systems). In **Chapter 1**, advantages and drawbacks of these techniques are discussed.

Despite the variety of techniques employed in TE to prepare scaffolds, the materials used for scaffolding are mostly limited to conventional materials, such as common polyesters, ceramics, and metals. The most frequently used polyesters for scaffolding are poly(lactic acid) PLA, poly(ε-caprolactone) (PCL), and their copolymers. These polyesters, regardless of their biocompatibility and long history of application in the biomedical field, have certain disadvantages such as hydrophobicity, and long degradation rates. These properties are recognized as drawback when cell-material interactions and tunable degradation rates are considered. Therefore, there is a growing need to introduce new materials into the world of TE, as explained in detail in **Chapter 2** of this thesis. This chapter summarizes a variety of functionalized biodegradable polymers with many possibilities to tune physico-chemical properties such as hydrophilicity, possibilities for further chemical modifications, and degradation rate. The different methods to synthesize these functionalized polyesters via polycondensation polymerization, ring opening polymerization, and enzymatic polymerization are discussed. Also some examples for application of these novel polyesters in a variety of biomedical fields including protein/gene delivery, and tissue engineering are provided. However, despite a wide range of functionalized polyesters developed by different research groups, the application of these polymers in the biomedical field is very limited. Further, only a few studies reported on the *in vitro*/ *in vivo* performance of these polymers, but the results obtained so far encourage further investigations.

In **Chapter 3**, a new hydrophilic polyester with different compositions for tissue engineering applications was synthesized through melt copolymerization of ε-caprolactone (CL) and benzyl protected hydroxymethyl glycolide (BMG). Deprotection of the polymers yielded copolymers with pendant hydroxyl groups poly(hydroxymethylglycolide-co-ε-caprolactone), (pHMGCL). The synthesized polymers were characterized by GPC, NMR and DSC techniques. The resulting copolymers consisting up to 10 % of HMG monomer were semi-crystalline with a melting temperature above body temperature which ensures dimensional stability upon implantation of scaffolds based on these polymers. Water contact angles measurements of polymeric films showed that increasing the HMG content resulted in higher surface hydrophilicity as evidenced from a decrease in receding contact angle from 68° for 0% HMG (=PCL) to 40° for a copolymer with 10% HMG. Human mesenchymal stem cells showed good adherence onto pHMGCL films as compared to the more hydrophobic PCL surfaces. The cells were also proliferated and differentiated toward osteogenic lineage which is another indicative of cytocompatibility of these polymers. This chapter shows that the

aforementioned hydrophilic polymers are attractive candidates to design scaffolds for tissue engineering applications.

In a subsequent study presented in **Chapter 4**, the suitability of three-dimensional, porous scaffolds from this hydroxyl functionalized polymer (pHMGCL, HMG:CL 8:92), for potential tissue engineering applications was investigated. Scaffolds consisting of pHMGCL or PCL were produced by means of a rapid prototyping technique (3D melt-plotting) and were shown to have a high porosity and an interconnected pore structure. The thermal and mechanical properties of both scaffolds were investigated and human mesenchymal stem cells were seeded onto the scaffolds to evaluate their cell attachment properties, as well as cell viability and differentiation of the adhered cells. It was shown that the cells filled the pores of the pHMGCL scaffold within 7 days and displayed increased metabolic activity when compared with cells cultured in PCL scaffolds. Importantly, pHMGCL scaffolds supported osteogenic differentiation.

As it is important to evaluate how the newly formed tissue integrates with the synthetic scaffold and to what extent the implanted scaffold induce a foreign body reaction, we investigated the *in vivo* biodegradation and biocompatibility of three-dimensional (3D) scaffolds based on pHMGCL in **Chapter 5**. Three-dimensional scaffolds based on pHMGCL (HMG:CL 8:92) were prepared by means of fiber deposition (melt-plotting). The biodegradation and tissue biocompatibility of pHMGCL and PCL scaffolds after subcutaneous implantation in Balb/c mice were investigated. At 4 and 12 weeks post implantation, the scaffolds were retrieved and evaluated for extent of degradation by measuring the residual weight of the scaffolds, thermal properties (DSC), and morphology (SEM), whereas the remaining partially degraded polymer was analyzed for both its composition (^{1}H NMR) and molecular weight (GPC). The scaffolds with infiltrated and adjacent tissues were harvested, fixed, stained and histologically analyzed.

In vitro lipase-catalyzed degradation showed that pHMGCL scaffolds were degraded within 50 hours, while the degradation time for PCL scaffolds of similar structure at the same enzyme concentration was 72 hours. This faster degradation is ascribed to the degradation of more hydrated HMG units in pHMGCL as compared to hydrophobic PCL, as well as preferential hydrolysis of the more amorphous pHMGCL compared to PCL. *In vivo*, it was shown that pHMGCL 3D-scaffolds lost more than 60% of their weight within 3 months of implantation while PCL scaffolds showed no significant weight loss in this time frame. This faster *in vivo* degradation of pHMGCL scaffolds compared to their *in vitro* degradation (**chapter 6**) is likely caused by enzymes with esterase activity,

which are released from macrophages and giant cells that adhere to pHMGCL surface. The molecular weight (M_w) of pHMGCL decreased from 46.9 kDa before implantation to 23.2 kDa after 3 months of implantation, while the molecular weight of PCL was unchanged in this period. ^{1}H NMR analysis showed that hydrolysis of pHMGCL occurred mainly at the sites of the hydrophilic HMG units resulting in a decrease in the ratio of HMG:CL in the copolymer structure. A normal foreign body response to both scaffold types characterized by the presence of mononuclear inflammatory cells and fibrosis was observed with a more rapid onset in pHMGCL scaffolds. Importantly, the extent of tissue-scaffold interactions as well as vascularization was shown to be higher for pHMGCL scaffolds compared to PCL ones.

In **Chapter 6**, we showed that pHMGCL can be used to prepare scaffolds also by another scaffolding technique; electrospinning. The pHMGCL fibers obtained by electrospinning were characterized for their morphological and physical properties and the possibility to obtain uniform fibers by varying the polymer solution (type of solvent and concentration) was shown. Scaffolds composed of fibers with uniform diameter (~ 900 nm) and possessing melting temperatures higher than body temperature were prepared. As verification for the feasibility of this material for regenerative medicine approaches, articular chondrocytes were seeded onto electrospun pHMGCL scaffolds. Chondrocytes attached to the fibers and re-differentiated as was demonstrated by the production of glycosaminoglycans (GAG) and collagen type II within four weeks of *in vitro* culture. In addition, degradation of pHMGCL (composed of 10 mol% of HMG) and PCL films prepared by solvent casting method was studied *in vitro* in PBS (pH 7.4) at 37 °C. It was shown that pHMGCL films went through considerable mass loss and molecular weight reduction within 70 weeks, while no mass loss and changes in molecular weight of PCL occurred in this period.

To prepare bioactive scaffolds for TE application, a variation of electrospinning method, namely coaxial electrospinning, was utilized in **Chapter 7**. In this chapter, nanofibrous scaffolds based on blends of pHMGCL (HMG:CL 25:75) and poly(ε-caprolactone) (PCL), loaded with bovine serum albumin (BSA) as protein stabilizer and vascular endothelial growth factor (VEFG) as potent angiogenic factor were prepared by means of a coaxial electrospinning technique. The scaffolds were characterized by scanning electron microscopy (SEM), fluorescence microscopy (FM), and differential scanning calorimetry (DSC). The scaffolds displayed a uniform fibrous structure with a fiber diameter around 700 nm. Release of BSA from the core of the fibers was studied by high performance liquid chromatography (HPLC) and it was shown that the coaxial scaffolds

containing higher ratios of hydroxyl functionalized polyester exhibited faster release than the comparative PCL scaffolds, likely because of a faster hydrolysis rate of pHMGCL compared to PCL. VEGF was also incorporated in the core of the scaffolds and the effect of released protein on endothelial cells attachment and proliferation was investigated. It was shown that the incorporated protein preserved its biological activity and resulted in enhanced initial cell proliferation.

2. Discussion and Perspectives

A key feature of tissue engineering is that biologics such as cells and proteins are delivered via a degradable material, termed a scaffold, to the site of injury in the body and provide support for regeneration of the lost/ damaged tissue[1]. In the early 1990s, Langer and Vacanti[2] and their colleagues from MIT and Harvard[3-6] introduced the term of tissue engineering. At that time, the total annual health care costs of Americans suffering from tissue loss or end-stage organ failure was estimated to be over $400 billion[2]. This value has increased tremendously over the last decades by the aging society, and for that reason encouraged scientists in multidisciplinary fields to investigate better means to help these patients and explore different aspects of an ideal tissue engineered construct. Along this way, different approaches have been investigated and improvements have been made from scaffolding techniques to cell seeding steps. It has become clear that a detailed knowledge on the structure and function of the tissue of interest is required and in particular three-dimensional microenvironment of the cells plays a key role in the tissue regeneration.

The main theme of this thesis is based on application of new materials, i.e. functionalized polyesters, to prepare scaffolds for tissue engineering applications. These functionalized polyesters (pHMGCL)s were characterized for physical, chemical, mechanical properties (chapters 3 and 4), and their processability for process into different scaffold types was investigated (chapters 4, 6, and 7). The cell-scaffold interaction of these scaffolds was assessed in a variety of *in vitro* cell seeding experiments (chapters 3, 4, 6, and 7). Degradation of the scaffolds *in vitro* (chapter 6) and *in vivo* (chapter 5) was also evaluated and their biocompatibility in an *in vivo* subcutaneous model (chapter 5) was investigated. Nevertheless, there are several aspects of the developed scaffolds that need to be improved, optimized, and evaluated for final successful application of these materials in clinic.

2.1. Mechanical properties

The mechanical properties of scaffolds developed in this thesis were evaluated in compressive mode at room temperature, as described in chapter 4. It was shown that the compressive modulus of solid disks of pHMGCL (HMG:CL 8:92) was around 65 MPa. This value for 3D-melt plotted, porous scaffolds of pHMGCL (with more than 70% porosity) decreased to around 10 MPa. Although the melting temperatures of both polymers are above body temperature, the mechanical properties of these scaffolds at the application temperature (37 °C) need to be evaluated.

The scaffolds studied in this thesis were designed for bone and cartilage tissue engineering applications. Virtually all natural materials are composites and they consist of a relatively small number of polymeric and ceramic components or building blocks[7]. The best way to illustrate how the structure can affect the mechanical performance of a material is to take tendon, ligament, skin, cartilage, and bone as examples. These structures all share the same polymeric components (i.e., collagen and elastin) but the fractions and structure of each component in the material vary distinctively, resulting in a wide range of characteristics which fit the requirements for the specific application of those materials. Bone, for instance, is a sophisticated composite of different hierarchical levels. From a structural perspective, bone tissue consists of two main parts; a compact shell called cortical bone and a porous core called trabecular bone. The combination of a dense shear stress-resisting shell and a cellular inner structure with a typical relative density of between 0.05 and 0.3, prevents buckling and results in excellent bending resistance[8]. Bone can be basically described as a composite consisting of 70% calcium phosphate crystals and 20-30% collagen matrix with some water. The approximate modulus of (subchondral) bone is 5 GPa[9].

Figure 1 illustrates the extraordinary mechanical properties of bone in contrast to engineered bulk materials used for medical purposes. In this figure, the Young modulus is plotted against fracture toughness, which is a measure of a material to crack propagation. The graph depicts the relation between elasticity of a material and its toughness. It reveals that up to now, no artificial bulk material is able to mimic bone and serve as an ideal material for scaffold engineering. One of the best approaches to overcome the shortage of suitable materials for bone tissue engineering is to develop composites, based on biodegradable polymers reinforced with ceramics[10]. Composite materials are promising since they capture the benefits and compensate the drawbacks of each individual component.

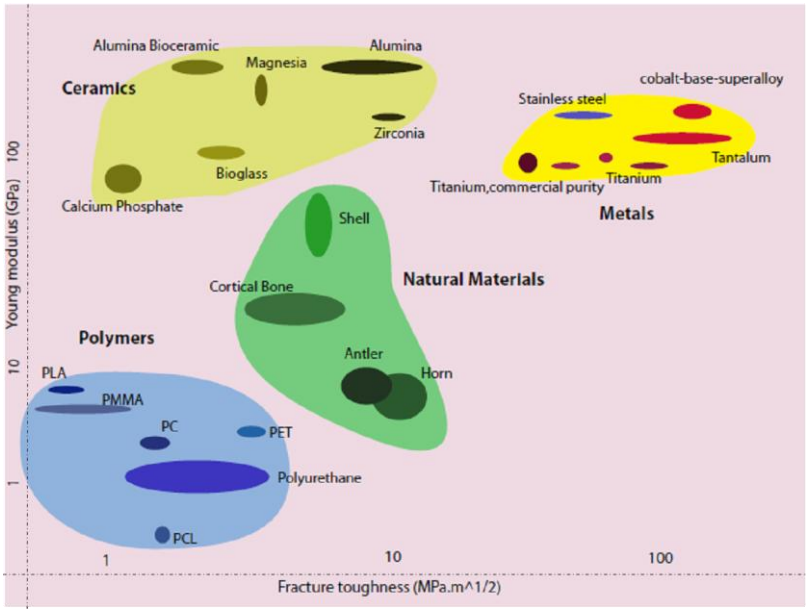

Figure 1. Mechanical properties of natural materials in comparison with engineered materials for medical purposes. Reproduced from Ref[8].

Cartilage, on the other hand, has a structure that is more complex. Hyaline cartilage, for instance, is built up from three layers. The superficial layer contains up to 90% dry weight of collagen fibers which are arranged in a network parallel to the surface. The middle layer has a lower collagen content of 60% dry weight, and the collagen fibers are arranged at an angle of about 45° with respect to a line normal to the cartilage surface. In the third layer, which joints cartilage and bone, the collagen fibrils are oriented perpendicular to the bone surface and the collagen content is the lowest (less than 60%)[7]. Figure 2 represents the zonal structure of collagen. This tissue is mainly composed of water, chondrocytes, type II collagen, and the proteoglycan aggrecan[9]. The composition of each zone is defined by the specific organization of cells and ECM molecules and this variation results in approximate moduli of 0.08 to 320 MPa[9].

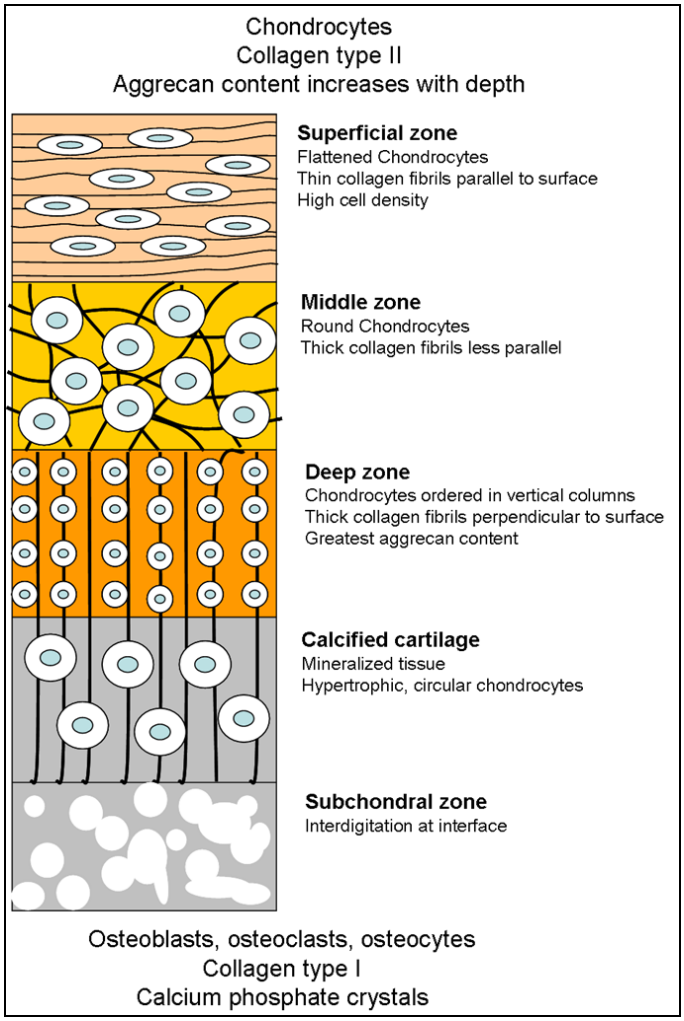

Figure 2. Schematic presentation of cartilage-bone interface. Orange indicates aggrecan concentration, light blue indicates collagen fibers, while dark blue shows mineralized tissue. Adopted from Ref[9].

Therefore, the modulus of pHMGCL (10 MPa) is insufficient for bone and (most of) cartilage tissue engineering constructs. Increasing the mechanical properties of pHMGCL scaffolds can be achieved by developing composite scaffolds based on this functionalized polyester and ceramics (such as hydroxyapatite (HA), tricalcium phosphate (TCP), and bioglasses). This approach is expected to result in improved toughness as well as enhanced formation of new tissue, as the

calcium phosphate materials are well known to stimulate bone formation and exhibit good osteoconductivity[11].

2.2. Diverse functionality

One of the main advantages of (pHMGCL)s developed in this thesis over conventional polyesters is the hydroxyl functionality on the backbone of these polymers. This functionality can be further used to develop new polyesters with improved properties for tissue engineering applications. For instance, the OH groups can be converted into acrylate or methacrylate groups to develop unsaturated polyesters, which can be used in a variety of biomedical applications such as dental restorative materials[12-16], bone cements[17-19], and photopolymerizable resins for stereolithography[20-22]. The (meth)acrylate-functionalized (pHMGCL)s can be further functionalized with adhesion peptides (e.g., RGD) to improve the cell adhesion properties of scaffolds based on these polymers even further. This can be achieved via Michael Addition reaction[23-25] using thiol-functionalized RGD peptides and (meth)acrylate-functionalized pHMGCL. Initial experiments showed that methacrylate moieties attached to pHMGCL could be photopolymerized yielding a strong network.

In another approach, carboxylated (pHMGCL)s can be developed via modifying hydroxyl-functionalized pHMGCL with succinic anhydride according to the conditions reported by others[26-28]. These carboxylated polyesters can be further functionalized with peptides[29].

2.3. Growth factors

Three essential elements are involved in regeneration of bone: (1) osteoconduction, (2) osteogenesis, and (3) osteoinduction [30]. Osteoconduction means the ability of a material to allow bone growth on its surface, or down into its pores and channels[31] and can be achieved by the right choice of materials used for scaffolding, as described in section 2.1. Osteogenesis is based on the capability of living osteoprogenitor cells which can be differentiated toward osteogenic lineage[31]. Osteoinduction, however, is the stimulation of mesenchymal stem cells, which are not committed to the osteogenic lineage to differentiate toward osteoprogenitor cells and bone forming osteoblasts[32]. This process is initiated by the 'osteoinductive' growth factors such as bone morphogenetic proteins (BMPs). To induce bone formation *in vivo*, the injection of a growth factor (GF) solution is not a relevant option, since the *in vivo* half-lives of these proteins are very short and their retention at the target site is minimal[33, 34]. Therefore, a

delivery system is needed to retain growth factors for sufficient time at the defect site and allow migration of osteoprogenitor cells to this location. This role can be performed by the biocompatible and biodegradable scaffold. In our approach in chapter 7, we demonstrated the possibility of loading bovine serum albumin (BSA) into pHMGCL fibers prepared via coaxial electrospinning and it was shown that this protein was released for more than 30 days. It was further demonstrated that vascular endothelial growth factor (VEGF) loaded into these fibers, retained its bioactivity after being released. Further investigations are needed into incorporation of other relevant growth factors into these scaffolds and assess the release effect on the osteogenesis of mesenchymal stem cells.

Furthermore, the growth factor (GF) release from 3D scaffolds of pHMGCL needs to be investigated as well. This can be achieved via either combination of electrospinning and 3D-melt plotting to produce biphasic scaffolds[35, 36] capable of delivering GF at the site of implantation, or incorporation of GF-releasing microspheres into the 3D scaffolds[37, 38]. The latter can be accomplished by incorporating microspheres based on functionalized polyesters (pLHMGA), which have been developed in our group recently[39] and were shown to have tunable release profiles for a variety of drugs[40], proteins[41, 42], and peptides[43].

3. Cells: with or without?

As described in the Introduction chapter of this thesis, several approaches have been sought to prepare grafts for tissue regeneration. These strategies generally fall into two major categories: (a) acellular, and (b) cellular matrices[44]. In the first approach, the matrices are either prepared without cells and implanted as such *in vivo*, or are seeded with cells *in vitro* and the cellular components are removed before implantation to produce collagen-rich matrices[45]. These matrices are degraded slowly *in vivo* and are generally replaced by the extracellular matrix (ECM) proteins that are secreted by the ingrowing cells. In the second approach (cellular matrices), a small piece of donor tissue is dissociated into individual cells and these cells are either seeded into the host or expanded *in vitro* onto the scaffold and then implanted into the host[44]. The source of donor tissue can be heterologous (such as bovine), allogenic (same species, different individual), or autologous. The most preferred cells are autologous cells which are obtained from a tissue biopsy of the host (e.g., bone marrow aspirate in case of mesenchymal stem cells), expanded *in vitro*, and explanted into the same host.

In this thesis we demonstrated the superior cell adhesion properties of pHMGCL scaffolds over conventional PCL scaffolds. However, the main limitation

of applying cell-based tissue engineered constructs is the inherent difficulty of growing specific cell types in large quantity[44]. Therefore, acellular approaches are considered as an interesting route to develop artificial grafts for tissue regeneration[46-48]. Therefore, it might be interesting to develop acellular constructs based on pHMGCL electrospun scaffolds, specifically for cartilage tissue engineering. This can be achieved by *in vitro* chondrocytes seeding into electrospun scaffolds using bioreactors that will result in deposition of growth factor-rich ECM into the scaffolds. Upon decellularization, a chondrogenic ECM/polymer matrix can be produced and its efficacy to form cartilaginous tissue *in vivo* can be assessed.

Another interesting approach to incorporate cells into the scaffolds developed in this thesis is to print a cell-laden hydrogel with PHMGCL simultaneously. The possibility of incorporating cells into thermosensitive hydrogels have been shown in our group recently[49]. However, in order to improve the mechanical properties of hydrogels, one approach would be to reinforce these cell-laden scaffolds with polymer fibers. To this end, PHMGCL might be considered as a very good candidate since it can be printed at relatively low temperatures comparing to common polyesters (50 versus 120 °C, for PHMGCL and PCL, respectively). Printing these two components in a layer-by-layer fashion, will result in a scaffold composed of adjacent fibers of hydrogel and polymer.

4. *In vivo* tissue regeneration

Throughout this thesis, we evaluated the cell-scaffold interactions of pHMGCL construct using a variety of cell sources, including hMSCs (chapter 3 and 4) and chondrocytes (chapter 6). The differentiation of these cells into osteogenic and chondrogenic lineages *in vitro* have been shown promising, however, what remains to be done is to study the performance of these scaffolds in a relevant *in vivo* bone/cartilage defect model. It is important to investigate the optimum conditions to prepare osteoconductive and chondrogenic scaffolds *in vitro* based on the conditions described in the previous sections, and to investigate whether these scaffolds are capable of performing their role in the *in vivo* conditions. Many models have been developed to proof the feasibility of bone grafts *in vivo*. These models can be divided into several groups: bone augmentation models (e.g., posterior spinal fusion[50]), nonweight-bearing defect models (e.g., critical-sized calvarial defects[51]), segmental defect models (e.g., femur cavity defect model[52, 53]), and functional joint models (e.g., full-thickness knee defects[54] and

osteochondral defects[55-57]). These models are normally evaluated in relatively large animals (e.g., rabbit, sheep, goat, etc.). An advantage of any model is the potential to evaluate multiple (different) samples in the same animal. It is normally preferable to use critical size defects, meaning that the defect will not heal spontaneously[58]. The use of these models will lead to the conclusion that, in case of success, the bone graft healed a defect instead of only enhancing its spontaneous healing[58]. Total joint models are reletively new models, which combine bone and cartilage tissue engineering to create functional joints[9, 59, 60].

5. Surface characterizations

Our *in vivo* implantation study showed that the biodegradation of PHMGCL scaffolds *in vivo* follows a different pattern as compared to its *in vitro* degradation. We hypothesized that protein adsorption, cell binding (including mononuclear cells and macrophages) and subsequent cytokine and enzyme secretion by these cells play an important role in the biodegradation of pHMGCL *in vivo*. Whether the type of proteins that adsorb onto these surfaces are beneficial for final application in tissue engineering is still unknown. Therefore, it is recommended to study (e.g., using proteomics techniques) the proteins that adsorb from extracellular matrices onto pHMGCL surfaces and compare that with PCL surfaces. The obtained insight will provide an opportunity to tune the surface properties according to the desired protein adsorption for specific applications.

6. Scale-up

6.1. Monomer

One of the main challenges for further development of pHMGCL scaffolds that needs additional investigations is optimization of BMG monomer synthesis. The synthesis route of this monomer is very labor-intensive and contains several steps which result in relatively low overall yields. Moreover, the purification of the monomer by flash column chromatography and subsequent crystallization steps remains challenging. This high purity is demanded to obtain high molecular weight polymers, which is an important issue when processability of obtained polymers into scaffolds is considered.

6.2. Polymer

pHMGCL polymers developed in this thesis have been synthesized via ring opening polymerization (ROP) methods, followed by hydrogenation. The yield of

ROP reactions is quite high (more than 90%), however, the yield of hydrogenation reaction varies from batch to batch. Moreover, removal of the Pd/C catalyst employed in this reaction has been challenging in some batches. In order to avoid batch-to-batch variances in polymer characteristics, new methods should be investigated to produce pHMGCL polymers at large scales.

7. Valley of death

The subsequent two decades following the introduction of tissue engineering concept in the early 1990s, showed enormous advances that have been made in this field and despite the challenges still remain to solve, regenerative medicine has undoubtedly a very bright future[61]. However, in spite of tremendous efforts that have been made to develop new tissue engineered constructs, the number of tissue engineering products resulting from this vast research on the market is limited so far[62]. The fundamental question that remains is: "why does such a gap exists between research and clinical translation?". Indeed, the gap between research and commercialization is universal and is termed the "Valley of Death"[63] due to the large number of investments that 'die' between technology development at the bench and actual commercialization, especially in the biotech field, due to lack of funds for large pre-clinical and clinical studies to gain regulatory approval.

Overall, this thesis clearly highlights the advantages of applying functionalized polyesters over the use of conventional polyesters to prepare scaffolds for TE applications. It is demonstrated that by introducing hydroxyl functionality into one of the most commonly used polyesters in the TE field, PCL, the overall properties of this polymer, including degradation rate and even more importantly cell-material interactions in terms of cell adhesion, proliferation, and differentiation, are significantly improved. The cumulative results presented in this thesis open doors to numerous opportunities to employ these scaffolds in the TE field.

Having said that, I finish this thesis with a hope that development of these functionalized polyesters with improved properties in comparison with common polyesters does not 'die' at this stage and further investigations into development of optimal scaffolds based on these polymers for tissue engineering applications would be performed in future to find a way into clinics.

References

[1] Hollister, S. J., Scaffold design and manufacturing: From concept to clinic. *Advanced Materials* **2009,** 21, (32-33), 3330-3342.

[2] Langer, R.; Vacanti, J. P., Tissue engineering. *Science* **1993,** 260, (5110), 920-926.

[3] Mooney, D. J.; Organ, G.; Vacanti, J. P.; Langer, R., Design and fabrication of biodegradable polymer devices to engineer tubular tissues. *Cell Transplantation* **1994,** 3, (2), 203-210.

[4] Cohen, S.; Bano, M. C.; Cima, L. G.; Allcock, H. R.; Vacanti, J. P.; Vacanti, C. A.; Langer, R., Design of synthetic polymeric structures for cell transplantation and tissue engineering. *Clinical Materials* **1993,** 13, (1-4), 3-10.

[5] Wald, H. L.; Sarakinos, G.; Lyman, M. D.; Mikos, A. G.; Vacanti, J. P.; Langer, R., Cell seeding in porous transplantation devices. *Biomaterials* **1993,** 14, (4), 270-278.

[6] Gilbert, J. C.; Takada, T.; Stein, J. E.; Langer, R.; Vacanti, J. P., Cell transplantation of genetically altered cells on biodegradable polymer scaffolds in syngeneic rats. *Transplantation* **1993,** 56, (2), 423-427.

[7] Wegst, U. G. K.; Ashby, M. F., The mechanical efficiency of natural materials. *Philosophical Magazine* **2004,** 84, (21), 2167-2181.

[8] Butscher, A.; Bohner, M.; Hofmann, S.; Gauckler, L.; Müller, R., Structural and material approaches to bone tissue engineering in powder-based three-dimensional printing. *Acta Biomaterialia* **2011,** 7, (3), 907-920.

[9] Yang, P. J.; Temenoff, J. S., Engineering orthopedic tissue interfaces. *Tissue Engineering - Part B: Reviews* **2009,** 15, (2), 127-141.

[10] Tanner, K. E., Bioactive composites for bone tissue engineering. *Proceedings of the Institution of Mechanical Engineers. Part H, Journal of engineering in medicine* **2010,** 224, (12), 1359-1372.

[11] Zheng, L.; Yang, F.; Shen, H.; Hu, X.; Mochizuki, C.; Sato, M.; Wang, S.; Zhang, Y., The effect of composition of calcium phosphate composite scaffolds on the formation of tooth tissue from human dental pulp stem cells. Biomaterials 2011, 32, (29), 7053-7059.

[12] Naoum, S. J.; Ellakwa, A.; Morgan, L.; White, K.; Martin, F. E.; Lee, I. B., Polymerization profile analysis of resin composite dental restorative materials in real time. Journal of Dentistry **2011,** DOI:10.1016/j.jdent.2011.10.006.

[13] Boulden, J. E.; Cramer, N. B.; Schreck, K. M.; Couch, C. L.; Bracho-Troconis, C.; Stansbury, J. W.; Bowman, C. N., Thiol-ene-methacrylate composites as dental restorative materials. *Dental Materials* **2011,** 27, (3), 267-272.

[14] Park, H. Y.; Kloxin, C. J.; Scott, T. F.; Bowman, C. N., Covalent adaptable networks as dental restorative resins: Stress relaxation by addition-fragmentation chain transfer in allyl sulfide-containing resins. *Dental Materials* **2010,** 26, (10), 1010-1016.

[15] Cramer, N. B.; Couch, C. L.; Schreck, K. M.; Boulden, J. E.; Wydra, R.; Stansbury, J. W.; Bowman, C. N., Properties of methacrylate-thiol-ene formulations as dental restorative materials. *Dental Materials* **2010,** 26, (8), 799-806.

[16] Kim, L. U.; Kim, J. W.; Kim, C. K., Effects of molecular structure of the resins on the volumetric shrinkage and the mechanical strength of dental restorative composites. *Biomacromolecules* **2006,** 7, (9), 2680-2687.

[17] Shen, S. C.; Ng, W. K.; Shi, Z.; Chia, L.; Neoh, K. G.; Tan, R. B. H., Mesoporous silica nanoparticle-functionalized poly(methyl methacrylate)-based bone cement for effective antibiotics delivery. *Journal of Materials Science: Materials in Medicine* **2011**, 22(10), 2283-2292.

[18] Lam, W. M.; Pan, H. B.; Fong, M. K.; Cheung, W. S.; Wong, K. L.; Li, Z. Y.; Luk, K. D. K.; Chan, W. K.; Wong, C. T.; Yang, C.; Lu, W. W., In Vitro characterization of low modulus linoleic acid coated strontium-substituted hydroxyapatite containing PMMA bone cement. *Journal of Biomedical Materials Research - Part B Applied Biomaterials* **2011,** 96 B, (1), 76-83.

[19] Wang, J.; Liu, C.; Liu, Y.; Zhang, S., Double-network interpenetrating bone cement via in situ hybridization protocol. *Advanced Functional Materials* **2010,** 20, (22), 3997-4011.

[20] Elomaa, L.; Teixeira, S.; Hakala, R.; Korhonen, H.; Grijpma, D. W.; Seppälä, J. V., Preparation of poly(ε-caprolactone)-based tissue engineering scaffolds by stereolithography. *Acta Biomaterialia* **2011,** 7, (11), 3850-3856.

[21] Seck, T. M.; Melchels, F. P. W.; Feijen, J.; Grijpma, D. W., Designed biodegradable hydrogel structures prepared by stereolithography using poly(ethylene glycol)/poly(d,l-lactide)-based resins. *Journal of Controlled Release* **2010,** 148, (1), 34-41.

[22] Melchels, F. P. W.; Feijen, J.; Grijpma, D. W., A poly(d,l-lactide) resin for the preparation of tissue engineering scaffolds by stereolithography. *Biomaterials* **2009,** 30, (23-24), 3801-3809.

[23] Yu, Y.; Deng, C.; Meng, F.; Shi, Q.; Feijen, J.; Zhong, Z., Novel injectable biodegradable glycol chitosan-based hydrogels crosslinked by Michael-type addition reaction with oligo(acryloyl carbonate)-b-poly(ethylene glycol)-b-oligo(acryloyl carbonate) copolymers. *Journal of Biomedical Materials Research - Part A* **2011,** 99 A, (2), 316-326.

[24] Censi, R.; Fieten, P. J.; Di Martino, P.; Hennink, W. E.; Vermonden, T., In situ forming hydrogels by tandem thermal gelling and Michael addition reaction between thermosensitive triblock copolymers and thiolated hyaluronan. *Macromolecules* **2010,** 43, (13), 5771-5778.

[25] Chen, W.; Yang, H.; Wang, R.; Cheng, R.; Meng, F.; Wei, W.; Zhong, Z., Versatile synthesis of functional biodegradable polymers by combining ring-opening polymerization and postpolymerization modification via michael-type addition reaction. *Macromolecules* **2010,** 43, (1), 201-207.

[26] Noga, D. E.; Petrie, T. A.; Kumar, A.; Weck, M.; Garcia, A. J.; Collard, D. M., Synthesis and modification of functional poly(lactide) copolymers: Toward biofunctional materials. *Biomacromolecules* **2008,** 9, (7), 2056-2062.

[27] Xie, Z.; Lu, T.; Chen, X.; Lu, C.; Zheng, Y.; Jing, X., Triblock poly(lactic acid)-b-poly(ethylene glycol)-b-poly (lactic acid)/paclitaxel conjugates: Synthesis, micellization, and cytotoxicity. *Journal of Applied Polymer Science* **2007,** 105, (4), 2271-2279.

[28] Van de Manakker, F.; Van der Pot, M.; Vermonden, T.; Van Nostrum, C. F.; Hennink, W. E., Self-assembling hydrogels based on ß-cyclodextrin/cholesterol inclusion complexes. *Macromolecules* **2008,** 41, (5), 1766-1773.

[29] Kim, J. E.; Noh, K. T.; Yu, H. S.; Lee, H. Y.; Jang, J. H.; Kim, H. W., A fibronectin peptide-coupled biopolymer nanofibrous matrix to speed up initial cellular events. *Advanced Engineering Materials* **2010,** 12, (4), B94-B100.

[30] Cypher, T. J.; Grossman, J. P., Biological principles of bone graft healing. *Journal of Foot and Ankle Surgery* **1996,** 35, (5), 413-417.

[31] Albrektsson, T.; Johansson, C., Osteoinduction, osteoconduction and osseointegration. *European Spine Journal* **2001,** 10, (SUPPL. 2), S96-S101.

[32] Kempen, D. H. R., Bone regeneration based on growth factor releasing polymer composites. *PhD thesis* **2011**, 20.

[33] Hosseinkhani, H.; Hosseinkhani, M.; Khademhosseini, A.; Kobayashi, H., Bone regeneration through controlled release of bone morphogenetic protein-2 from 3-D tissue engineered nano-scaffold. *Journal of Controlled Release* **2007,** 117, (3), 380-386.

[34] Lee, K.; Silva, E. A.; Mooney, D. J., Growth factor delivery-based tissue engineering: General approaches and a review of recent developments. *Journal of the Royal Society Interface* **2011,** 8, (55), 153-170.

[35] Park, S. A.; Kim, H. J.; Lee, S. H.; Lee, J. H.; Kim, H. K.; Yoon, T. R.; Kim, W., Fabrication of nano/microfiber scaffolds using a combination of rapid prototyping and electrospinning systems. *Polymer Engineering and Science* **2011,** 51, (9), 1883-1890.

[36] Yeo, M.; Lee, H.; Kim, G., Three-dimensional hierarchical composite scaffolds consisting of polycaprolactone, ß-tricalcium phosphate, and collagen nanofibers: Fabrication, physical properties, and in vitro cell activity for bone tissue regeneration. *Biomacromolecules* **2011,** 12, (2), 502-510.

[37] Miranda, E. S.; Silva, T. H.; Reis, R. L.; Mano, J. F., Nanostructured natural-based polyelectrolyte multilayers to agglomerate chitosan particles into scaffolds for tissue engineering. *Tissue Engineering - Part A* **2011,** 17, (21-22), 2663-2674.

[38] Francis, L.; Meng, D.; Knowles, J. C.; Roy, I.; Boccaccini, A. R., Multi-functional P(3HB) microsphere/45S5 Bioglass®-based composite scaffolds for bone tissue engineering. *Acta Biomaterialia* **2010,** 6, (7), 2773-2786.

[39] Ghassemi, A. H.; van Steenbergen, M. J.; Talsma, H.; van Nostrum, C. F.; Jiskoot, W.; Crommelin, D. J. A.; Hennink, W. E., Preparation and characterization of protein loaded microspheres based on a hydroxylated aliphatic polyester, poly(lactic-co-hydroxymethyl glycolic acid). *Journal of Controlled Release* **2009,** 138, (1), 57-63.

[40] Chaisri, W.; Ghassemi, A. H.; Hennink, W. E.; Okonogi, S., Enhanced gentamicin loading and release of PLGA and PLHMGA microspheres by varying the formulation parameters. *Colloids and Surfaces B: Biointerfaces* **2011,** 84, (2), 508-514.

[41] Ghassemi, A. H.; van Steenbergen, M. J.; Talsma, H.; van Nostrum, C. F.; Jiskoot, W.; Crommelin, D. J.; Hennink, W. E., Microspheres of hydrophilic PLGA highly attractive for protein delivery. *Journal of*

controlled release : official journal of the Controlled Release Society **2010,** 148, (1), e39-40.

[42] Ghassemi, A. H.; Van Steenbergen, M. J.; Talsma, H.; Van Nostrum, C. F.; Crommelin, D. J. A.; Hennink, W. E., Hydrophilic polyester microspheres: Effect of molecular weight and copolymer composition on release of BSA. *Pharmaceutical Research* **2010,** 27, (9), 2008-2017.

[43] Ghassemi, A. H.; van Steenbergen, M. J.; Barendregt, A.; Talsma, H.; Kok, R. J.; van Nostrum, C. F.; Crommelin, D. J. A.; Hennink, W. E., Controlled Release of Octreotide and Assessment of Peptide Acylation from Poly(D,L-lactide-co-hydroxymethyl glycolide) Compared to PLGA Microspheres. *Pharmaceutical Research*, **2011,** DOI: 10.1007/s11095-011-0517-3.

[44] Koh, C. J.; Atala, A., Tissue Engineering, Stem Cells, and Cloning: Opportunities for Regenerative Medicine. *Journal of the American Society of Nephrology* **2004,** 15, (5), 1113-1125.

[45] Liao, J.; Guo, X.; Grande-Allen, K. J.; Kasper, F. K.; Mikos, A. G., Bioactive polymer/extracellular matrix scaffolds fabricated with a flow perfusion bioreactor for cartilage tissue engineering. *Biomaterials* **2010,** 31, (34), 8911-8920.

[46] Perniconi, B.; Costa, A.; Aulino, P.; Teodori, L.; Adamo, S.; Coletti, D., The pro-myogenic environment provided by whole organ scale acellular scaffolds from skeletal muscle. *Biomaterials* **2011,** 32, (31), 7870-7882.

[47] Hui, W.; Xiong-sheng, C.; Sheng-yuan, Z.; Jun-jun, H.; Tao-yi, C., Biocompatibility and superiority of lyophilized acellular ligament scaffolds. *Journal of Clinical Rehabilitative Tissue Engineering Research* **2011,** 15, (29), 5334-5338.

[48] Du, L.; Wu, X., Development and characterization of a full-thickness acellular porcine cornea matrix for tissue engineering. *Artificial Organs* **2011,** 35, (7), 691-705.

[49] Censi, R.; Schuurman, W.; Malda, J.; Di Dato, G.; Burgisser, P. E.; Dhert, W. J. A.; Van Nostrum, C. F.; Di Martino, P.; Vermonden, T.; Hennink, W. E., A printable photopolymerizable thermosensitive p(HPMAm-lactate)-PEG hydrogel for tissue engineering. *Advanced Functional Materials* **2011,** 21, (10), 1833-1842.

[50] Hui, C. F. F.; Chan, C. W.; Yeung, H. Y.; Lee, K. M.; Qin, L.; Li, G.; Leung, K. S.; Hu, Y. Y.; Cheng, J. C. Y., Low-intensity pulsed ultrasound enhances posterior spinal fusion implanted with mesenchymal stem

cells-calcium phosphate composite without bone grafting. *Spine* **2011,** 36, (13), 1010-1016.

[51] Zou, D.; Zhang, Z.; He, J.; Zhu, S.; Wang, S.; Zhang, W.; Zhou, J.; Xu, Y.; Huang, Y.; Wang, Y.; Han, W.; Zhou, Y.; Wang, S.; You, S.; Jiang, X.; Huang, Y., Repairing critical-sized calvarial defects with BMSCs modified by a constitutively active form of hypoxia-inducible factor-1α and a phosphate cement scaffold. *Biomaterials* **2011,** 32, (36), 9707-9718.

[52] Dai, C.; Guo, H.; Lu, J.; Shi, J.; Wei, J.; Liu, C., Osteogenic evaluation of calcium/magnesium-doped mesoporous silica scaffold with incorporation of rhBMP-2 by synchrotron radiation-based μCT. *Biomaterials* **2011,** 32, (33), 8506-8517.

[53] Brown, K. V.; Li, B.; Guda, T.; Perrien, D. S.; Guelcher, S. A.; Wenke, J. C., Improving bone formation in a rat femur segmental defect by controlling bone morphogenetic protein-2 release. *Tissue Engineering - Part A* **2011,** 17, (13-14), 1735-1746.

[54] Mimura, T.; Imai, S.; Okumura, N.; Li, L.; Nishizawa, K.; Araki, S.; Ueba, H.; Kubo, M.; Mori, K.; Matsusue, Y., Spatiotemporal control of proliferation and differentiation of bone marrow-derived mesenchymal stem cells recruited using collagen hydrogel for repair of articular cartilage defects. *Journal of Biomedical Materials Research - Part B Applied Biomaterials* **2011,** 98 B, (2), 360-368.

[55] Chen, J.; Chen, H.; Li, P.; Diao, H.; Zhu, S.; Dong, L.; Wang, R.; Guo, T.; Zhao, J.; Zhang, J., Simultaneous regeneration of articular cartilage and subchondral bone in vivo using MSCs induced by a spatially controlled gene delivery system in bilayered integrated scaffolds. *Biomaterials* **2011,** 32, (21), 4793-4805.

[56] Holland, T. A.; Bodde, E. W. H.; Cuijpers, V. M. J. I.; Baggett, L. S.; Tabata, Y.; Mikos, A. G.; Jansen, J. A., Degradable hydrogel scaffolds for in vivo delivery of single and dual growth factors in cartilage repair. *Osteoarthritis and Cartilage* **2007,** 15, (2), 187-197.

[57] Holland, T. A.; Bodde, E. W. H.; Baggett, L. S.; Tabata, Y.; Mikos, A. G.; Jansen, J. A., Osteochondral repair in the rabbit model utilizing bilayered, degradable oligo(poly(ethylene glycol) fumarate) hydrogel scaffolds. *Journal of Biomedical Materials Research - Part A* **2005,** 75, (1), 156-167.

[58] Blitterswijk, C. v., Tissue engineering. **2008**, (Ed.1), 585.

[59] Seidi, A.; Ramalingam, M.; Elloumi-Hannachi, I.; Ostrovidov, S.; Khademhosseini, A., Gradient biomaterials for soft-to-hard interface tissue engineering. *Acta Biomaterialia* **2011,** 7, (4), 1441-1451.

[60] Dormer, N. H.; Berkland, C. J.; Detamore, M. S., Emerging techniques in stratified designs and continuous gradients for tissue engineering of interfaces. *Annals of Biomedical Engineering* **2010,** 38, (6), 2121-2141.

[61] Langer, R., Perspectives and challenges in tissue engineering and regenerative medicine. *Advanced Materials* **2009,** 21, (32-33), 3235-3236.

[62] Place, E. S.; Evans, N. D.; Stevens, M. M., Complexity in biomaterials for tissue engineering. *Nature Materials* **2009,** 8, (6), 457-470.

[63] Hollister, S. J., Scaffold engineering: A bridge to where? *Biofabrication* **2009,** 1, (1).

"Now this is **not** the end.
It is not even the beginning of the end.
But it is, perhaps, the end of the beginning."

Winston Churchill
1874-1965

Appendices

Appendix A

Supporting information Chapter 5

A1. Thermal properties of degraded PHMGCL (Fig.1) and PCL (Fig.2) in lipase solution (0.1 mg/mL) showed that the bulk properties of these scaffolds were unchanged in time.

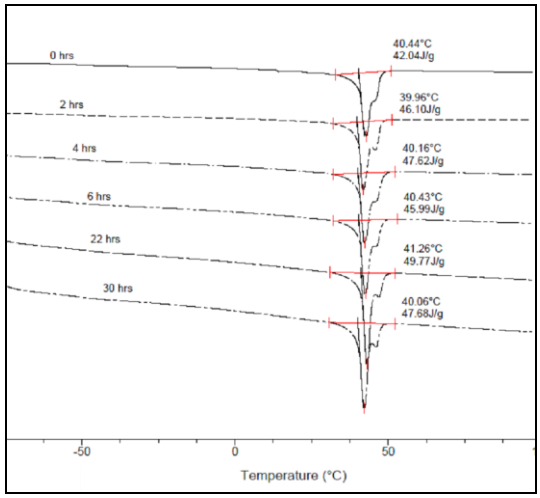

Fig.1. DSC thermograms of PHMGCL scaffolds before and during enzymatic degradation by lipase (0.1 mg/mL) in PBS (pH 7.4) at 37 °C.

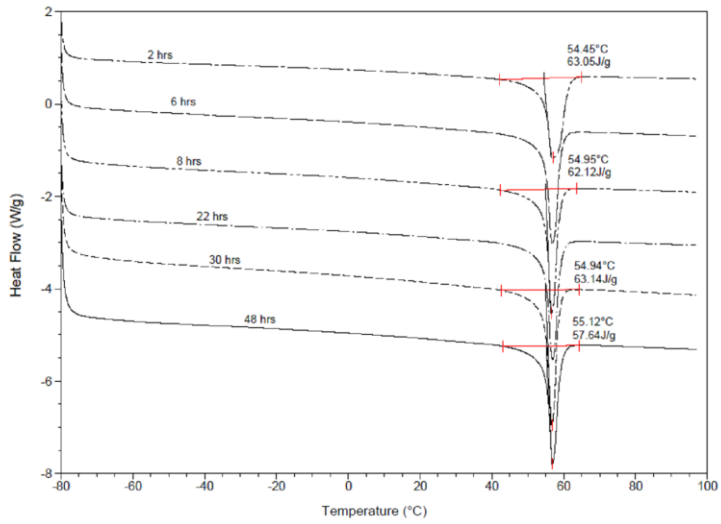

Fig.2. DCS thermograms of PCL scaffolds during enzymatic degradation by lipase (0.1 mg/mL) in PBS (pH 7.4) at 37 °C.

A2. Investigating the molecular weight of degraded PHMGCL and PCL in lipase solution (0.1 mg/mL) showed that the bulk properties of these scaffolds were unchanged in time.

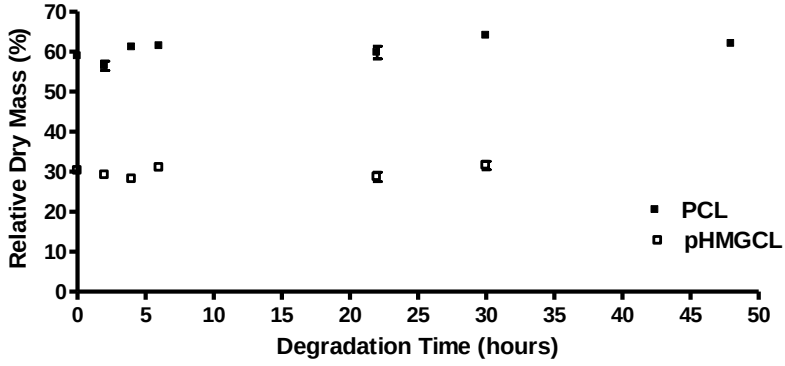

Fig.3. Weight average molecular weight of PCL scaffolds during enzymatic degradation by lipase (0.1 mg/mL) in PBS (pH 7.4) at 37 °C.

A3. The composition of PCL in the explanted scaffolds was established using ^{1}H NMR (Fig.4) and the results showed the composition of this polymer was not changed within 3 months of implantation *in vivo*.

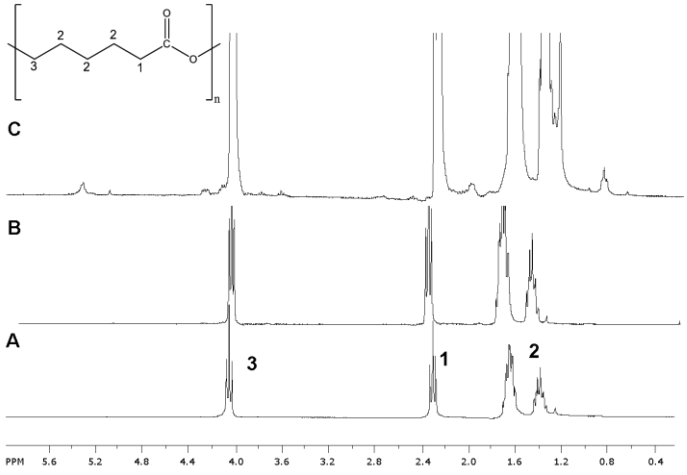

Fig.4. ^{1}H NMR spectra of PCL dissolved in $CDCl_3$ (A) before implantation, (B) after 1 month and (C) 3 months subcutaneous implantation of scaffolds in mice.

Appendix B

Samenvatting in het Netherlands

Tissue engineering (T.E.) is een innovatieve techniek die mogelijk een alternatief biedt voor orgaantransplantaties. Deze techniek is geïntroduceerd door Langer and Vacanti in 1993 met de volgende definitie: tissue engineering is het interdisciplinaire gebied dat de principes van engineering en levenswetenschappen combineert voor de ontwikkeling van biologische materialen die in staat zijn om orgaanfuncties te regenereren, behouden of te verbeteren. Cellen, materialen en bioactieve stoffen zijn hiervoor de basiselementen . De belangrijkste functie van de materialen is het leveren van een stevig substraat om celadhesie en celgroei te mogelijk te maken. Daarvoor moeten deze materialen, ook wel scaffolds genoemd, biocompatibel en biodegradeerbaar zijn. Het doel van dit proefschrift is het ontwikkelen van synthetische scaffolds gebaseerd op gefunctionaliseerde polyesters voor T.E. toepassingen.

In **hoofdstuk 1** worden verschillende technieken samengevat die gebruikt worden om scaffolds te fabriceren. Er is een overzicht gegeven van conventionele en geavanceerde technieken. Tevens zijn hiervan de voor- en nadelen beschreven.

Hoofdstuk 2 concentreert zich op de polymeren die gebruikt kunnen worden als materialen voor biomedische toepassingen. Met name polyesters zoals polymelkzuur (PLA), polycaprolacton (PCL) en hun copolymeren worden veel gebruikt voor het maken van scaffolds. Belangrijke nadelen van deze polymeren zijn hun hydrofobiciteit en langzame degradatie. Vanwege deze eigenschappen is er een grote vraag naar meer geavanceerdere polymeren waarbij de hydrofiliciteit en degradatiesnelheid gevarieerd kan worden. In dit hoofdstuk worden de tot nu toe gerapporteerde gefunctionaliseerde polyesters samengevat alsmede hun syntheseroutes.

Hoofdstuk 3 beschrijft de synthese van een hydrofiele polyester gebaseerd op caprolacton (CL) en hydroxymethylglycolide (HMG). Copolymeren die tot 10% HMG bevatten waren semi-kristallijn met een smeltpunt boven de lichaamstemperatuur. Een toename in HMG gehalte in de polymeren resulteerde in een hydrofieler oppervlak van polymeerfilms. Celadhesie en groei van humane stamcellen op deze pHMGCL films waren significant beter dan op meer hydrofobe pCL films.

Daarna zijn deze polymeren gebruikt voor het creëren van 3D poreuze scaffolds met behulp van een “rapid prototyping” techniek zoals beschreven in

hoofdstuk 4. De thermische en mechanische eigenschappen van scaffolds gebaseerd op pHMGCL en pCL zijn onderzocht. Humane stamcellen zijn gezaaid in deze scaffolds en de poriën van pHMGCL scaffolds waren volledig met cellen volgroeid binnen 7 dagen. Ook lieten deze cellen een verhoogde metabolische activiteit zien in vergelijking met de cellen gezaaid op pCL scaffolds.

Naast in vitro studies is het uiteraard van belang te onderzoeken hoe nieuwgevormd weefsel kan integreren met een synthetische scaffold in vivo. **Hoofdstuk 5** laat een studie zien waarin 3D geprintte scaffolds van pHMGCL en pCL zijn geïmplanteerd in Balb/c muizen. Na 4 of 12 weken zijn de scaffolds verwijderd en geëvalueerd op hun overgebleven gewicht en weefselingroei. Hoewel de pCL scaffolds nauwelijks degradeerden in 3 maanden, waren de pHMGCL scaffolds ruim 60% van hun oorspronkelijke gewicht verloren. NMR analyse liet zien dat met name de HMG groepen preferentieel uit het materiaal waren verwijderd. Verder lieten beide soorten scaffolds een normaal vreemd lichaam reactie zien. Zowel de mate van weefsel-scaffold interacties als de mate van vascularisatie was groter in pHMGCL dan in pCL scaffolds.

Naast 3D printing zijn pHMGCL polymeren ook verwerkt met een andere scaffolding techniek, namelijk electrospinning. **Hoofdstuk 6** beschrijft de karakterisering van pHMGCL vezels verkregen door electrospinning. De vezels hadden een uniforme diameter van ongeveer 900 nm en chondrocyten waren in staat om te re-differentiëren op deze scaffolds in vitro binnen een tijdsbestek van 4 weken, zoals aangetoond door hun productie van glycosaminoglycanen en collageen type II.

Electrospinning biedt de mogelijkheid om holle vezels te creëren die beladen kunnen worden met bioactieve componenten. Deze techniek, coaxial electrospinning, is gebruikt in **hoofdstuk 7**. Scaffolds gebaseerd op pHMGCL beladen met eiwitten (BSA en/of VEGF) zijn gesynthetiseerd. Deze scaffolds beschikten over uniforme vezels met een diameter van 700 nm zoals bleek uit scanning electronen microscopie (SEM). Fluorescent gelabelde eiwitten konden worden gevisualiseerd in de kern van de vezels met fluorescentie microscopie (FM). De afgiftesnelheid van BSA uit de vezels was sneller naar mate het HMG gehalte in de polymeren groter was. Het effect van afgegeven VEGF is bestudeerd door te kijken naar het hechten van endotheelcellen aan de scaffolds en hun proliferatie.

Hieruit bleek dat VEGF zijn bioactiviteit had behouden en dat de afgifte leidde tot een initieel verhoogde celproliferatie.

Dit proefschrift laat duidelijk de voordelen zien van het gebruik van gefunctionaliseerde polyesters in vergelijking met conventionele polyesters voor tissue engineering toepassingen. De introductie van hydroxylgroepen in de meest gebruikte polyesters leidt tot verbeterde eigenschappen van de biomaterialen zoals een variabele degradatiesnelheid en minstens zo belangrijk verbeterde cel-materiaal interacties.

پیوست سوم

چکیده فارسی

مهندسی بافت روش نوینی برای پیوند عضو و بازسازی اعضای آسیب دیده می باشد. این روش که در سال ۱۹۲۳ توسط لانگر و وکانتی معرفی شده است مبتنی بر بکارگیری علوم بین رشته ای شامل مهندسی و علوم زیستی برای جایگزین کردن، ترمیم و بهبود بخشیدن عملکرد بافت یا ارگان آسیب دیده می باشد.

مهندسی بافت بر پایه سه اصل اساسی : سلول، داربست، و عوامل رشد می باشد. عملکرد اصلی داربست در مهندسی بافت فراهم کردن بستری برای چسبیدن و تکثیر سلول ها و بنابراین تسهیل کردن تشکیل بافت جدید می باشد. یک داربست ایده آل باید زیست سازگار و زیست تخریب پذیر بوده و همچنین نرخ تخریب آن باید متناسب با نرخ تشکیل بافت جدید باشد.

هدف این پایان نامه بررسی و توسعه داربست های سنتزی بر اساس پلی استرهای عامل دار شده بویژه پلی استرهایی بر پایه کوپلیمر هیدروکسی تیل گلیکولاید و کاپرولاکتون برای کاربردهای مهندسی بافت بوده است. به علت وجود گروه های هیدروکسیل در ساختار مونومر هیدروکسی تیل گلیکولاید، این مونومر در مقایسه با مونومر کاپرولاکتون آبدوستی بیشتری دارد و بر این اساس وارد کردن این مونومر در زنجیره کوپلیمر کاپرولاکتونی باعث افزایش آبدوستی کوپلیمر و همچنین کاهش درصد کریستالینیتی آن در مقایسه با پلی کاپرولاکتون خالص شده است. این خصوصیات باعث افزایش نرخ هیدرولیز و چسبندگی بیشتر سلولی این داربست می شود.

روش های متفاوتی برای تهیه داربست ها در مهندسی بافت وجود دارد و این روش ها را می توان به دو دسته روش های متداول و پیشرفته طبقه بندی کرد. دسته اول شامل روش هایی نظیر ریخته گری محلولی، ذره شویی، قالب گیری مذاب، تخلخل زایی بوسیله گاز، خشک کردن انجمادی، جدایی فاز، و الکتروریسی می باشد. دسته دوم شامل روش هایی بر اساس نمونه سازی سریع نظیر چاپ کردن سه بعدی می باشد.

در بخش اول این پایان نامه مزایا و معایب این روش ها بررسی شده است. بر خلاف تنوع زیاد روش های ساخت داربست برای مهندسی بافت ، مواد بکاررفته در ساخت داربست ها از تنوع زیادی برخوردار نیستند. این مواد عموما شامل پلی استرها ، سرامیک ها ، فلزات ، و همچنین کامپوزیت این مواد می باشد. عمده پلیمرهای بکاربرده شده در مهندسی بافت شامل پلی لاکتیدها ، پلی کاپرولاکتون ، و کوپلیمرهای آنها می باشد. علیرغم زیست سازگاری بالا و سابقه طولانی کاربرد در مصارف پزشکی ، این پلیمرها به علت آبگریز بودن و همچنین نرخ پایین تخریب در مواردی با محدودیت کاربرد روبرو هستند. بویژه هنگام واکنش مواد با سلول ها ،خصوصیات فیزیکی پلیمر نظیر جذب آب ، زاویه تماس ، و همچنین نرخ تخریب آن از عوامل حیاتی تعیین کننده می باشد.

به منظور سنتز و تهیه پلیمرهایی با خواص فیزیکوشیمیایی متناسب با عملکرد سلول ها احتیاج به ساخت و معرفی مواد جدید در مهندسی بافت است. در بخش دوم این پایان نامه پلیمرهای تخریب پذیر عامل دار شده به طور گسترده ای مورد بررسی قرار گرفته اند. در این بخش ، روش های مختلف سنتز این مواد از جمله پلیمریزاسیون تراکمی ، پلیمریزاسیون حلقه گشا و همچنین پلیمریزاسیون آنزیمی به همراه خصوصیات فیزیکی و شیمیایی آنها مورد بحث و بررسی قرار گرفته است.

در بخش سوم این پایان نامه ، سنتز و بررسی خصوصیات یک پلی استر آبدوست نوین بر مبنای مونومر کاپرولاکتون و مونومر هیدروکسی تیل گلیکولاید مورد بررسی قرار گرفته است. سنتز و ساختار این پلیمر با روش های طیف سنجی متداول ، همچنین کروماتوگرافی مورد ارزیابی قرار گرفته است. داربست های ساخته شده بر مبنای این پلی استر نوین ، دمای ذوبی بالاتر از دمای بدن داشته که پایداری ابعادی آن را هنگام کاشت در بدن تضمین می کند. همچنین زاویه تماس آبی کوپلیمری شامل ۱۰ درصد مونومر آبدوست هیدروکسی تیل گلیکولاید

حدود ۴۰ درجه بوده است که میزان ۲۸ درجه کمتر از زاویه تماس آبی پلی کاپرولاکتون خالص می باشد. سلول های مزنکیمال چسبندگی بسیار خوبی بر روی سطح این داربست ها نشان داده و قابلیت تمایز یافتن به سلول های استخوانی را از خود نشان داده اند.

در بخش بعدی این پایان نامه ، بخش چهارم ، داربست های سه بعدی و متخلخل بر پایه پلی استرهای کاپرولاکتون و هیدروکسی تیل گلیکولاید (۸ درصد) بوسیله روش نمونه سازی سریع تهیه شده اند. این داربست ها دارای تخلخل بالا و حفرات بهم پیوسته بوده و سلول های بنیادی کشت شده در داخل این داربست ها ، چسبندگی بالایی به این داربست نشان داده و حفرات داخلی این داربست را طی زمان ۷ روز پر کرده اند.

به منظور بررسی میزان و نحوه رشد بافت به داخل داربست و بررسی میزان واکنش جسم خارجی ، تخریب و زیست سازگاری این داربست های سه بعدی به صورت in vivo در بخش پنجم این پایان نامه بررسی شده است. تخریب پذیری و زیست سازگاری بافتی داربست های سه بعدی ساخته شده بر مبنای کوپلیمر کاپرولاکتون و هیدروکسی تیل گلیکولاید (۸ درصد) در مدل موش به صورت زیر پوستی برای مدت ۱۲ هفته مورد بررسی قرار گرفته است. پس از ۴ و ۱۲ هفته ، داربست ها از موش خارج شده و خواص فیزیکی و شیمیایی نظیر جرم مولکولی ، خواص حرارتی ، مورفولوژی سطح ، و ترکیب شیمیایی مورد بررسی قرار گرفته است. همچنین اثر داربست ها بر روی بافت های مجاور توسط بررسی هیستولوژیک این بافت مورد ارزیابی قرار گرفته است.

نتایج بدست آمده نشان داده است که داربست های ساخته شده از کوپلیمر کاپرولاکتون و هیدروکسی تیل گلیکولاید در طی زمان ۱۲ هفته ، ۶۰ درصد کاهش وزن داشته اند در حالیکه داربست های کاپرولاکتونی در این بازه زمانی هیچگونه تغییر وزنی نداشته اند. تخریب این داربست

ها در شرایط in vivo نسبت به شرایط in vitro بسیار سریعتر بوده و و این افزایش سرعت تخریب احتمالا ناشی از تخریب آنزیمی توسط این ماکروفاژها و سلول های غول پیکر چسبیده به سطح داربست های کوپلیمری می باشد.

در بخش ششم این پایان نامه ، روش دیگری جهت تهیه داربست های کوپلیمری استفاده شده است. در این روش (الکتروریسی) پارامترهای مختلفی نظیر غلظت محلول پلیمری ، و نوع حلال بکار رفته در این محلول تغییر داده شده تا الیاف یکنواختی با قطر ۹۰۰ نانومتر بدست آید. جهت بررسی امکان استفاده از این الیاف در مهندسی بافت ، سلول های غضروفی در این داربست ها کشت شده و میزان تولید ماتریس خارج سلولی (گلیکوزآمینوگلیکان و کلاژن) پس از زمان ۴ هفته بررسی شده است. علاوه بر این، تخریب داربست های کوپلیمری در شرایط in vitro (محلول فسفات بافر pH=7.4) به مدت زمان ۷۰ هفته مورد بررسی قرار گرفته است.

به منظور تهیه داربست های زیست فعال جهت کاربرد های مهندسی بافت ، در بخش هفتم این پایان نامه ، نوع دیگری از روش الکتروریسی (به صورت هم محور) به منظور تولید الیاف بارگذاری شده با پروتئین استفاده شده است. قطر الیاف بدست آمده در این روش حدود ۷۰۰ نانومتر بوده و رهایش پروتئین بارگذاری شده در این الیاف در طی زمان ۳۰ روز در شرایط آزمایشگاهی بررسی شده است. علاوه بر این فاکتور رشد عروقی نیز در این الیاف بارگذاری شده و اثر رهایش این پروتئین بر چسبندگی و رشد سلول های اندوتلیال انسانی مورد بررسی قرار گرفته است.

بخش نهایی این پایان نامه ، بخش هشتم ، نتایج بدست آمده در این پایان نامه را مورد جمع بندی قرار داده و دورنمایی از کاربرد داربست های تهیه شده در این پایان نامه را جهت کاربرد های گوناگون مهندسی بافت مورد بررسی قرار داده است.

Appendix D

List of abbreviations

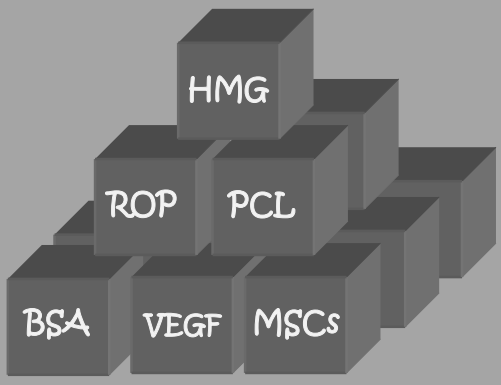

3D-plotting	Three-dimensional plotting
Adv-CA	Advancing Contact Angle
AIBN	Azobisisobutyronitrile
$Al(O^iPr)_3$	Aluminium isopropoxide
ALP	Alkaline Phosphatase
ATRP	Atom Transfer Radical Polymerization
bis-MPA	2,2'-bis(hydroxymethyl)propionic acid
BMG	Benzyl-protected hydroxyl methyl glycolide
BnOH	Benzyl alcohol
BSA	Bovine Serum Albumin
CA	Contact Angle
CAD	Computer-aided Design
$CDCl_3$	Deuterated Chloroform
CMC	Critical Micelle Concentration
DHO	6,7-dihydro-2(5H)-oxepinone
DMA	Dynamic Mechanical Analysis
DNA	Deoxyribonucleic acid
DPTE	Dutch Program for Tissue Engineering
DSC	Differential Scanning Calorimetry
DXO	1,5-dioxepan-2-one
ECM	Extra Cellular Matrix
EDTA	Ethylenediaminetetraacetic acid
EM	Essential Medium
ESB	European Society for Biomaterials
FBS	Fetal Bovine Serum
FDA	Food and Drug Administration
FITC-BSA	Fluorescein isothiocyanate labelled bovine serum albumin
FM	Fluorescence Microscopy
FTIR	Fourier Transform Infrared Spectroscopy
GA	Glycolic Acid
GAG	Glycosaminoglycan
GF	Growth Factor
GPC	Gel Permeation Chromatography
H&E	Hematoxylin and Eosin

HMG	Hydroxymethylglycolide
hMSCs	Human Mesenchymal Stem Cells
HPLC	High Performance Liquid Chromatography
HUVECs	Human Umbilical Vein Endothelial Cells
LA	Lactic Acid
LDA	lithium diisopropyl amide
mCPBA	m-chloroperoxy benzoic acid
M_n	Number-average Molecular Weight
M_w	Weight-average Molecular Weight
NMR	Nuclear Magnetic Resonance
PAGA	Poly(α-(4-aminobutyl)-L-glycolic acid)
PBMGCL	Poly(benzyloxymethylglycolide-co-ε-caprolactone)
PBS	Phosphate Buffered Saline
PCL	Poly(ε-caprolactone)
PDI	Polydispersity Index
PEG	Poly(ethylene glycol)
PEO	Poly(ethylene oxide)
PGA	Poly(glycolic caid)
PHMGCL	Poly(hydroxymethylglycolide-co-ε-caprolactone)
PLA	Poly(lactic acid)
PLAL	poly(lactic acid-co-lysine)
PLGA	poly(lactic-co-glycolic acid)
Rec-CA	Receding Contact Angle
RGD	Arginine-glycine-aspartic acid
ROP	Ring Opening Polymerization
RP	Rapid Prototyping
SCPL	Solvent Casting Particulate Leaching
SCVP	Self-Condensing Vinyl Polymerization
SEM	Scanning Electron Microscopy
SFF	Solid Freeform Fabrication
SLA	Stereolithography
$SnOct_2$	Stannous Octoate
TBD	1,5,7-triazabicyclo[4.4.0]dec-5-ene
TCPS	Tissue Culture Polystyrene

TE	Tissue Engineering
TFE	2,2,2-Trifluoroethanol
T_g	Glass Transition Temperature
TGF	Transforming Growth Factor
THF	Tetrahydrofuran
T_m	Melting Temperature
TMC	Trimethylene Carbonate
UV	Ultra Violet
VEGF	Vascular Endothelial Growth Factor
αMEM	Minimum Essential Medium
αSMA	Smooth Muscle Actin
β-BL	β-butyrolactone
βFGF	Fibroblast Growth Factor
γBrCL	γ-bromo-ε-caprolactone
ΔH_f	Heat of Fusion

Appendix E

List of Publications

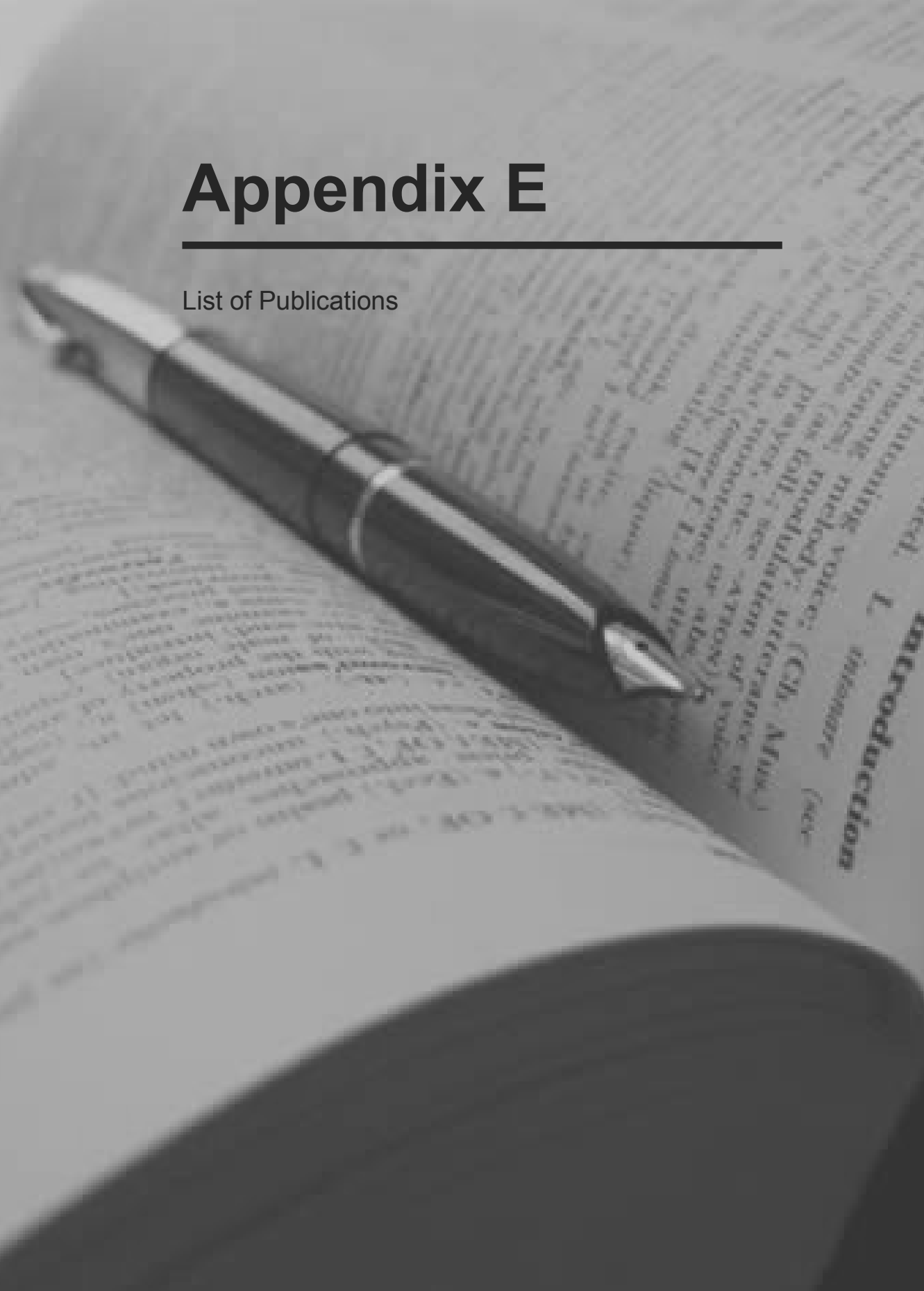

Peer-reviewed Journals

Seyednejad H., Vermonden T., Fedorovich N.E., Van Eijk R., Van Steenbergen M.J., Dhert W.J.A., Van Nostrum C.F., Hennink W.E.
Synthesis and Characterization of Hydroxyl-functionalized Caprolactone Copolymers and Their Effect on Adhesion, Proliferation, and Differentiation of Human Mesenchymal Stem Cells
Biomacromolecules, 2009, 10 (11): 3048- 3054.

Seyednejad H., Gawlitta D., Dhert W.J.A., Van Nostrum C.F., Vermonden T., Hennink W.E.
Preparation and Characterization of a Three-dimensional Printed Scaffold Based on a Functionalized Polyester for Bone Tissue Engineering Applications
Acta Biomaterialia, 2011, 7 (5), 1999- 2006.

Seyednejad H., Ghassemi A.H., Van Nostrum C.F., Vermonden T., Hennink W.E.
Functional Aliphatic Polyesters for Biomedical and Pharmaceutical Applications
Journal of Controlled Release, 2011, 152 (1), 168- 176.

Seyednejad H., Ji W., Schuurman W., Dhert W.J.A., Malda J., Yang F., Jansen J.A., van Nostrum C.F., Vermonden T., Hennink W.E.
Electrospun Degradable Scaffold Based on a Novel Hydrophilic Polyester for Tissue Engineering Applications
Macromolecular Bioscience, 2011, 11 (12), 1684- 1692.

Seyednejad H., Gawlitta D., Kuiper R.V., de Bruin A., van Nostrum C.F., Vermonden T., Dhert W.J.A., Hennink W.E.
In vivo Biocompatibility and Biodegradation of 3D-Printed Porous Scaffolds Based on a Novel Functionalized Polyester.
2011, Submitted.

Seyednejad H., Ji W., Yang F., van Nostrum C.F., Dhert W.J.A., Vermonden T., Hennink W.E., Jansen J.
Coaxially Electrospun Scaffolds Based on Hydroxyl-Functionalized Poly(ε-caprolactone) and Loaded with VEGF for Tissue Engineering Applications.
2011, In preparation.

Seyednejad H., Imani M., Jamieson T., Seifalian A. M.
Topical Hemostatic Agents: A Review
British Journal of Surgery, 2008, 95: 1197- 1225.

Abstracts

Hajar Seyednejad, Debby Gawlitta, Wouter J.A. Dhert, Cornelus F. van Nostrum, Tina Vermonden, Wim E. Hennink
Preparation and Characterization of a 3D-printed Scaffold Based on a Functionalized Polyester for Bone Tissue Engineering Applications. *(Best Lecture Award)*
Dutch Polymer Days, Veldhoven, The Netherlands, March 2011.

Hajar Seyednejad, Sima Rahimian, Cornelus F. van Nostrum, Tina Vermonden, Wim E. Hennink
Synthesis and Characterization of Methacrylated Hydrophilic Polyesters for Tissue Engineering Applications.
Biomaterials and Tissue Engineering, Lunteren, The Netherlands, Dec. 2010.

Hajar Seyednejad, Wouter Schuurman, Wei Ji, Jos Malda, Fang Yang, Cornelus F. van Nostrum, Tina Vermonden, Wim E. Hennink
Electrospun Degradable Scaffolds Based on a Novel Hydrophilic Polyester for Tissue Engineering Applications.
Advanced Functional Polymers for Medicine, Twente, The Netherlands, 15-17 June, 2011.

Wei Ji, Fang Yang, **Hajar Seyednejad**, Jeroen J.J.J.P. van den Beucken, John A. Jansen
The Effect of Nanoapatite (nAp) on Degradation Behavior and Inflammatory Response of PLGA- based Electrospun Scaffolds.
4th International Conference on Tissue Engineering, Crete, Greece May 31 - June 5, 2011.

Hajar Seyednejad, Tina Vermonden, Natalja E. Federovich, Wouter J.A. Dhert, Cornelus F. van Nostrum, Wim E. Hennink
Enhanced Human Mesenchymal Stem Cells Affinity of Modified Poly(ε-caprolactone) Scaffolds by Introducing Hydrophilic Monomers.
Dutch Polymer Days, Plenary Lecture, Veldhoven, The Netherlands, Feb. 2010.

Hajar Seyednejad, Tina Vermonden, Natalja E. Fedorovich, Mies J. van Steenbergen, Wouter J.A. Dhert, Cornelus F. van Nostrum, Wim E. Hennink
Human Mesenchymal Stem Cells Adhere and Proliferate onto Films of Poly(ε-caprolactone) with Hydroxylic Functional Groups. *(Travel Award)*
TERMIS, Galway, Ireland, June 2010.

Hajar Seyednejad, Debby Gawlitta, Wouter J.A. Dhert, Cornelus F. van Nostrum, Tina Vermonden, Wim E. Hennink
Preparation and Characterization of a 3D-printed Scaffold Based on a Functionalized Polyester for Bone Tissue Engineering Applications. *(Best Lecture Award)*
Biomaterials and Tissue Engineering, Lunteren, The Netherlands, Dec. 2010.

Hajar Seyednejad, Tina Vermonden, Natalja E. Fedorovich, Roel van Eijk, Mies J. van Steenbergen, Wouter J.A. Dhert, Cornelus F. van Nostrum, Wim E. Hennink
Synthesis and Characterization of a Novel Hydrophilic Polyester for Tissue Engineering.
Biomaterials and Tissue Engineering, Lunteren, The Netherlands, Dec. 2009.

Hajar Seyednejad, M. Imani, SH. Hojjati, H. Mirzadeh
Preparation of Chemically Crosslinked Microporous Dextran Hydrogels as Wound Dressing Agents.
Polymers for Advanced Technologies, Shanghai, China, Oct. 2007.